

AD-A129 885

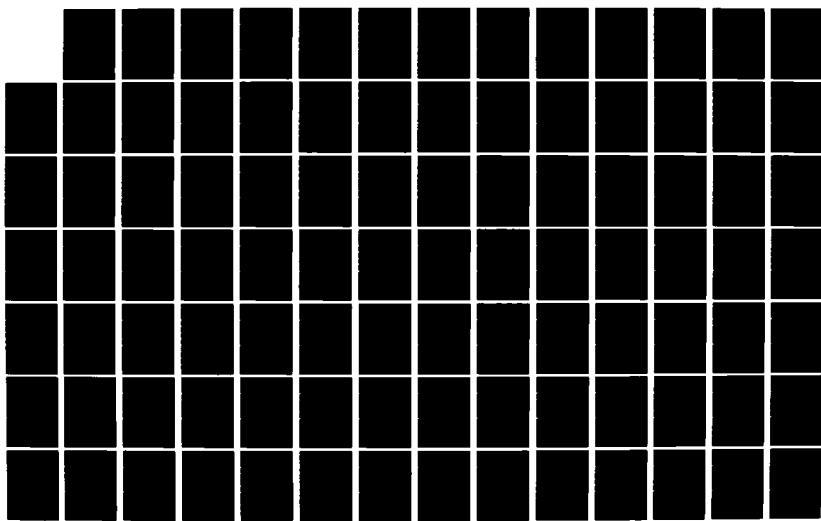
OPTIMUM MULTISENSOR MULTITARGET LOCALIZATION AND
TRACKING(U) NAVAL UNDERWATER SYSTEMS CENTER NEW LONDON
CT NEW LONDON LAB L C NG 07 JUN 83 NUSC-TR-6931

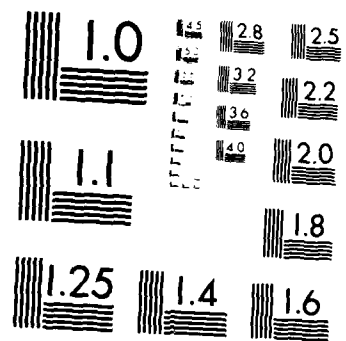
1/4

UNCLASSIFIED

F/G 12/1

NL





MICROCOPY RESOLUTION TEST CHART
NATIONAL BUREAU OF STANDARDS 1963 A

NUSC Technical Report 6931
7 June 1983

12

ADA 1 29805

Optimum Multisensor, Multitarget Localization and Tracking

Lawrence C. Ng
Submarine Sonar Department

DTIC FILE COPY



Naval Underwater Systems Center
Newport, Rhode Island / New London, Connecticut

DTIC

JUN 27 1983

A

Approved for public release; distribution unlimited.

83 06 27 051

Preface

This study was prepared as a dissertation in partial fulfillment of the requirements for the degree Doctor of Philosophy in Electrical Engineering and Computer Science at the University of Connecticut. The work was done under NUSC Project No. A75210, "Time Delay Estimation and Tracking," Principal Investigator, Lawrence C. Ng (Code 3213), Program Principal, CAPT Newcomb, Naval Material Command (NAVMAT-05B); and NUSC Project No. A47002, "SUBACS A/B," Principal Investigator, Lawrence C. Ng, Program Principal, Mike Roberts (NAVSEA PMS-409).

The author acknowledges the contributions of those individuals who supported the completion of this research. Specifically, he acknowledges the assistance of the following groups and individuals:

From the University of Connecticut - the members of the control and communications section of the Department of Electrical Engineering and Computer Science for their constructive comments throughout the course of this study: Professors C. H. Knapp and C. L. Nikias for reviewing portions of the manuscript and serving on his advisory committee; Professor Y. Bar-Shalom for the significant assistance, guidance, time and effort devoted to this entire research project.

From the Naval Underwater Systems Center - the managers and members of the Long Term Training Committee: Drs. F. J. Kingsbury, W. A. Von Winkle and E. Eby for providing the financial and administrative supports; colleagues and supervisors: Drs. G. C. Carter, N. L. Owsley, J. Ianniello and J. Hassab, Messrs. R. Garber, S. Kessler, J. Dlubac and G. Drury for providing numerous consultations and comments.

Reviewed and Approved: 7 June 1983



F. J. Kingsbury
Head, Submarine Sonar Department



W. A. Von Winkle
Associate Technical Director
for Technology

The author of this report is located at the
New London Laboratory, Naval Underwater Systems Center,
New London, Connecticut 06320.

REPORT DOCUMENTATION PAGE		READ INSTRUCTIONS BEFORE COMPLETING FORM
1. REPORT NUMBER TR 6931	2. GOVT ACCESSION NO.	3. RECIPIENT'S CATALOG NUMBER
4. TITLE (and Subtitle) OPTIMUM MULTISENSOR, MULTITARGET LOCALIZATION AND TRACKING		5. TYPE OF REPORT & PERIOD COVERED
7. AUTHOR(s) Lawrence C. Ng		6. PERFORMING ORG. REPORT NUMBER
9. PERFORMING ORGANIZATION NAME AND ADDRESS Naval Underwater Systems Center New London Laboratory New London, Connecticut 06320		10. PROGRAM ELEMENT, PROJECT, TASK AREA & WORK UNIT NUMBERS A75210 A47002
11. CONTROLLING OFFICE NAME AND ADDRESS		12. REPORT DATE 7 June 1983
14. MONITORING AGENCY NAME & ADDRESS (if different from Controlling Office)		13. NUMBER OF PAGES
		15. SECURITY CLASS. (of this report) UNCLASSIFIED
		16a. DECLASSIFICATION/DOWNGRADING SCHEDULE
16. DISTRIBUTION STATEMENT (of this Report) Approved for public release; distribution unlimited.		
17. DISTRIBUTION STATEMENT (of the abstract entered in Block 20, if different from Report)		
18. SUPPLEMENTARY NOTES		
19. KEY WORDS (Continue on reverse side if necessary and identify by block number) Acoustic Signal Processing Multitarget Cramer - Lower Bound Interference Rejection Processing Time Delay Estimation Multisensor, Multitarget Localization and Tracking		
20. ABSTRACT (Continue on reverse side if necessary and identify by block number) The optimum methodology of estimating and tracking target location parameters (e.g., range and bearing) in a passive multisensor, multitarget environment is investigated. Results of this study show that the localization parameters are best obtained via a two-step procedure. First estimate the time delay vector using the optimum multisensor multitarget time delay processor. Next obtain the localization parameter estimates from the time delay vector measurements via geometric mappings between targets and sensors.		

20. (Cont'd)

The optimum multisensor, multitarget time delay processor was studied in detail. The optimum processor was first derived assuming that the observed random waveforms (consist of coherent Gaussian broadband signal waveforms in additive incoherent Gaussian, broadband noise) can be considered as Stationary Parameter Long Observation Time Process. Here the observed waveforms can be reduced to a finite dimensional, complex Gaussian observation vector. A Maximum Likelihood multisensor, multitarget time delay processor is obtained by reducing and solving the resulting vector likelihood equation.

The performance of the optimum processor is analyzed in terms of the Cramer-Rao Lower Bound. Analytical closed form expressions are obtained for the two-targets, two-sensors, and one-target, M-sensors (for any M) cases. In addition, relation between time delay estimation and localization parameter estimation is explored. Comparison between optimum and suboptimum implementation is considered. A joint time delay and spectral estimation processor is presented. A method for improved time delay estimation using a post correlator matched filter approach is also investigated.

To account for the moving target environment, a variable multisensor, multitarget time delay processor is derived. The basic derivation is obtained by partitioning the observation interval into smaller subinterval. It was shown that the length of each partitioned time interval must satisfy certain constraint related to time delay doppler and signal bandwidth. The variable time delay is modeled by a finite order polynomial over the whole observation time interval. By estimating the time delay and delay rate at any given point in time, the corresponding localization parameters and the target motion parameters can be derived through a zero memory geometric transformation. This is the integrated approach to multitarget signal/data processing.

TABLE OF CONTENTS

	<u>Page</u>
LIST OF FIGURES	v
LIST OF SYMBOLS AND ABBREVIATIONS	vii
1. INTRODUCTION	1
1.1 Background	6
1.2 Technical Objectives	9
1.3 Previous Work	9
1.4 Technical Approach and Organization	12
1.5 Statements of Contribution and Summary	13
2. PROBLEM FORMULATION	21
2.1 Introduction	21
2.2 Description of Observables	21
2.3 Statement of the Problem	29
3. OPTIMUM MULTITARGET PARAMETER ESTIMATION	33
3.1 Introduction	33
3.2 The Likelihood Equation	34
3.3 Multiple Parameter Estimation	41
3.4 Estimator Performance Evaluation	44
3.5 Multisensor, Multitarget Parameter Estimation	49
3.5.1 Time Delay Estimation	49
3.5.1.1 Case 1: One Target and Two Sensors ($J = 1$, $M = 2$)	60
3.5.1.2 Case 2: Two Targets and Two Sensors ($J = 2$, $M = 2$)	65
3.5.1.3 Case 3: One Target and M Sensors ($J = 1$, $M = M$)	79
3.5.2 Localization Parameter Estimation	83
3.5.3 Power Spectral Estimation	106

TABLE OF CONTENTS (Cont'd)

	<u>Page</u>
3.5.3.1 Case 1: One Target, M Sensors ($J = 1, M = M$)	110
3.5.3.2 Case 2: Two Targets, M Sensors ($J = 2, M = M$)	110
3.5.3.3 Case 1: Power Spectral Estimation with Known Time Delay	114
3.5.3.4 Case 2: Joint Time Delay and Spectral Estimation	118
4. SUBOPTIMUM REALIZATION OF MULTISENSOR, MULTITARGET TIME DELAY PROCESSOR	123
4.1 Introduction	123
4.2 Weak Signal in Noise Suboptimum Processor Realization	123
4.3 A Single Target Assumption Suboptimum Processor	127
4.4 GCC Performance in the Presence of Interference ...	134
5. IMPROVED MULTITARGET PARAMETER RESOLUTION	140
5.1 Introduction	140
5.2 Post GCC Multitarget Processor	141
5.3 Estimator Performance Evaluation	146
5.4 Simulation	148
5.4.1 Simulation Procedure	148
5.4.2 Discussion of Results	150
6. OPTIMUM VARIABLE TIME DELAY ESTIMATION AND TRACKING	154
6.1 Introduction	154
6.2 The Likelihood Equation	156
6.3 Variable Time Delay Estimation	163
6.4 Performance Bound and Estimator Realization	169
6.4.1 Variable Time Delay Performance Bound	170
6.4.2 Estimator Realization	171

TABLE OF CONTENTS (Cont'd)

	<u>Page</u>
6.4.2.1 Case 1: One Target and Two Sensors with Delay Rate ($J = 1, M = 2,$ $P = 1, N > 2$)	171
6.4.2.2 Case 2: One Target and Two Sensors with Variable Time Delay ($J = 1, M = 2,$ $P = P, N > 2$)	182
6.4.2.3 Case 3: One Target and Three Sensors with Variable Time Delay ($J = 1, M = 3,$ $P = P, N \geq 2$)	190
6.5 Variable Time Delay Tracking	203
6.5.1 Sequential Fixed-interval Time Delay Tracking	204
7. OPTIMUM VARIABLE LOCALIZATION PARAMETER ESTIMATION AND TRACKING	214
7.1 Introduction	214
7.2 Variable Localization Parameter Estimation	217
7.3 Variable Localization Parameter Tracking	226
7.4 Target State Estimation and Tracking	227
7.4.1 Target State Estimation	230
7.4.2 Target State Tracking	234
8. SUMMARY, CONCLUSIONS, AND RECOMMENDATIONS	236
APPENDIX A DEFINITION OF COMPLEX GAUSSIAN PROBABILITY DENSITY FUNCTION (pdf)	244
APPENDIX B CALCULATION OF CRAMER-RAO LOWER BOUND FOR TWO-SENSOR, TWO-TARGET CASE	247
APPENDIX C CRAMER-RAO LOWER BOUND OF TIME DELAY ESTIMATION FROM MULTISENSOR ARRAY	262
APPENDIX D FUNCTIONAL RELATIONSHIPS BETWEEN TARGET LOCATION VECTOR AND MEASURED TIME DELAY VECTOR	273

TABLE OF CONTENTS (Cont'd)

	<u>Page</u>
APPENDIX E STATISTICAL CORRELATION BETWEEN TIME DELAY ESTIMATES WITH COMMON INPUT CHANNEL	281
APPENDIX F DERIVATION OF EQUATION (3.5.2-7a)	292
APPENDIX G CALCULATION OF LOCALIZATION UNCERTAINTY FROM THREE-SENSOR ARRAYS	295
APPENDIX H GCC STATISTICAL PERFORMANCE IN THE PRESENCE OF INTERFERENCE	301
APPENDIX I CALCULATION OF MULTITARGET GENERALIZED CROSS-CORRELATION COVARIANCE	313
APPENDIX J FOURIER REPRESENTATION OF A TIME- COMPRESSED WAVEFORM	320
APPENDIX K VARIABLE TIME DELAY CRAMER-RAO LOWER BOUND FOR TWO-SENSOR, ONE-TARGET CASE	324
REFERENCES	331

LIST OF FIGURES

<u>Figure</u>		
	<u>Page</u>	
1-1 Passive Multisensor, Multitarget Processing	4	
2-1 Description of Passive Sensor Observation	22	
2-2 Target-to-Sensor Geometry	24	
3-1 A Multisensor, Multitarget Time Delay Processing Channel	59	
3-2 Optimum Two-Sensor, One-Target Time Delay Processor	62	
3-3 Optimum Two-Sensor, Two-Target Time Delay Processor	69	
3-4 Frequency Response of the Function $Y_1(\omega)$ at Different Interference-to-Signal Ratios (SNR = 0 dB)	76	
3-5 Frequency Response of the Function $Y_{12}(\omega)$ at Different Interference-to-Signal Ratios (SNR = 0 dB)	77	
3-6 Two-Sensor, Two-Target Cramer-Rao Lower Bound Degradation Ratio Versus Time Delay Separation (SNR = 0 dB)	78	
3-7 Two-Sensor, Two-Target CRLB Degradation Ratio Versus Time Delay Separation and Interference Spectrum (SNR = 0 dB, INR = 0 dB)	80	
3-8 Two-Sensor, Two-Target CRLB Degradation Ratio Versus Time Delay Separation and Interference Spectrum (SNR = 0 dB, INR = 0 dB)	81	
3-9 A Three-Sensor Array System	84	
3-10 Optimum Range and Bearing Estimation from Three-Sensor Arrays (Focused Beamformer)	90	
3-11 Optimum Range and Bearing Estimation from Three-Sensor Arrays Using Two Correlators	94	
3-12 Conventional Range and Bearing Estimation from Three-Sensor Arrays Using Two Correlators	97	
3-13 Optimum One-Target, Multisensor Spectral Estimator	111	
3-14 Optimum Two-Target Power Spectral Estimator	115	
4-1 Suboptimum Two-Sensor, Two-Target Time Delay Processor	128	
4-2 Multitarget Time Delay Interference (SNR = 10 dB, INR = 7 dB)	135	

LIST OF FIGURES (Cont'd)

<u>Figure</u>		<u>Page</u>
4-3	Multitarget Time Delay Interference as a Function of Time Delay Separation (SNR = 10 dB, INR = 7 dB)	136
4-4	GCC Bias in the Presence of Interference (SNR = 10 dB, INR = 7 dB)	137
4-5	Normalized GCC Variance in the Presence of Interference (SNR = 10 dB, INR = 7 dB)	138
5-1	Post GCC Multitarget Processor Simulation	149
5-2	GCC Bias Versus Time Delay Separation (SNR = 0 dB, INR = -1 dB)	151
5-3	Degradation Ratio Versus Time Delay Separation (SNR = 0 dB, INR = -1 dB, S = 0 → B, I = 0 → B, N = 0 → B)	152
5-4	Degradation Ratio Versus Time Delay Separation (SNR = 0 dB, INR = -1 dB, S = 0 → B, I = B/2 → B, N = 0 → B)	153
6-1	Polynomial Model of Variable Time Delay	158
6-2	Two-Sensor, One-Target Time Delay Doppler Processor	176
6-3	Doppler Degradation Ratio for Variable Delay Model and Stationary Delay Model	183
6-4	Two-Sensor, One-Target Variable Time Delay Processor	186
6-5	Sequential Fixed-Interval Time Delay Tracking	205
7-1	Single Target, Three-Sensor Array Variable Localization Parameter Estimation	219
7-2	Geometry of Target State Estimation	230
D-1	A General Three-Sensor Passive Ranging Array System	273
E-1	Generalized Cross Correlator Pair with Common Input Channel	282

LIST OF SYMBOLS AND ABBREVIATIONS

Symbols

a_{ij}	signal attenuation from target j to sensor i
$\text{Arg}()$	Argument of
b_i^j	bias correction for optimum estimate of sensor time delay i of target j.
B	highest frequency of either the signal or noise power spectrum
c	propagation speed of the medium
$\text{COV}()$	statistical covariance
D_{ij}	propagation delay from target j to sensor i
\underline{D}	time delay vector
D	time delay matrix
$\text{diag}()$	a diagonal matrix
$E()$	statistical expectation
$\exp()$	exponential function
G_{kj}	effective array gain at frequency ω_k of target j
$ \tilde{h}_{kj} ^2$	multisensor, multitarget spectral shaping filter
J	number of target
J_{ij}	ij element of Fisher Information Matrix
k	discrete frequency index
$\underline{\lambda}_i$	location vector of sensor i
$\log()$	natural logarithm of
M	number of sensor
M_{12}	mutual dependence
$\text{MAX}()$	maximum of

LIST OF SYMBOLS AND ABBREVIATIONS (Cont'd)

Symbols

$n_i(t)$	noise waveform at sensor i
N_k	discrete noise power spectrum at frequency ω_k
\tilde{N}_k	multitarget equivalent noise discrete power spectrum
$\underline{0}$	a zero vector
$p(\cdot)$	probability density function of
P_{kj}	outer product of multitarget steering vector \underline{v}_{kj}
Q_k	normalized discrete spatial noise covariance matrix at frequency ω_k
\tilde{Q}_k	equivalent noise covariance matrix
$\tilde{Q}^{-1}(w)$	multitarget spatial whitening matrix
\underline{r}_j	target j location vector
R_k	observation covariance matrix at frequency ω_k
$R_{12}(\tau)$	generalized cross correlation between channels 1 and 2
$ R_k $	determinant of matrix R_k
$ r $	absolute value of a scalar r
S_k	discrete signal power spectral level at frequency ω_k
t	time variable
T	basic waveform observation interval
$(\cdot)^T$	transpose of
$tr(\cdot)$	trace of a matrix
$(\cdot)^{-1}$	inverse of
$(\cdot)^*$	complex conjugate transpose of
\underline{v}_{kj}	multisensor, multitarget steering vector of target j at frequency ω_k

LIST OF SYMBOLS AND ABBREVIATIONS (Cont'd)

Symbols

V_{kj}	multisensor, multitarget steering matrix
$\text{VAR}(\cdot)$	statistical variance
W_k	propagation delay matrix
$y(t, \underline{\ell}_i)$	observed waveform at sensor i
α_k	Fourier coefficient vector of multisensor, multitarget observation at frequency ω_k
β_k	Fourier coefficient vector of multitarget waveform
η_k	Fourier coefficient vector of multisensor noise waveform
ϵ	element of the set
ω_k	discrete frequency at $\omega = 2\pi k/T$
$\underline{\theta}$	unknown parameter vector
∇	gradient operator
τ_i	intersensor time delay between sensor $i + 1$ and i
ρ_{ij}	correlation coefficient between τ_i and τ_j
$\rho(\tau)$	normalized correlation function
Π	series product
Σ	series sum
$\Lambda(\cdot)$	log-likelihood function
$\frac{\partial}{\partial \theta_i} (\cdot)$	partial derivative w.r.t. θ_i

Abbreviations

ARMA	Auto-Regressive Moving Average
BLT	B is signal bandwidth, L is array effective length, and T is duration of time domain integration.
CRLB	Cramer-Rao Lower Bound

LIST OF SYMBOLS AND ABBREVIATIONS (Cont'd)

Abbreviations

dB	decibel
EKF	Extended Kalman Filter
FIR	Finite Impulse Response
FFT	Fast Fourier Transform
GCC	Generalized Cross Correlation
INR	Interference-to-Noise Ratio
ISR	Interference-to-Signal Ratio
JPDAF	Joint Probability Data Association Filter
LMS	Least Mean Square
LOS	Line of Sound
MAP	Maximum A Posterior
ML	Maximum Likelihood
MLE	Maximum Likelihood Estimator
MSC	Magnitude Square Coherence
OMP	Optimum Multitarget Processor
pdf	Probability Density Function
RMS	Root Mean Square
SIR	Signal-to-Interference Ratio
SNR	Signal-to-Noise Ratio
SONAR	Sound Navigation and Ranging
SPOINT	Stationary Parameter Long Observation Time
TDOA	Time Difference of Arrival
w.r.t.	with respect to

OPTIMUM MULTISENSOR, MULTITARGET LOCALIZATION AND TRACKING

CHAPTER 1 INTRODUCTION

If you want to hear anything more from me, give and take reason ... Nothing is surer than reason ... nothing is falser than the senses. -- ADELARD OF BATH

We are concerned with the general problem of estimating the target location parameters and the subsequent tracking of these parameters based on a passive observation of target signal waveforms from multiple sensor arrays. The physical situations which motivate our discussions are those arising in underwater sonar (Sound Navigation and Ranging) signal processing. A target in our discussion represents simply an acoustic source of interest. A sensor array consists of one or more hydrophone elements. By localization we mean defining the target position vector (range and bearing) w.r.t. a known reference point; e.g., the acoustic phase center of an array. By tracking we mean defining the target position vector as a function of time. We are interested in the optimum passive localization and tracking algorithm (or processor) operating in a multiple sensor and multiple target environment. We

assume that each target emits a noise-like signal and that each sensor observes a noise-corrupted version of the signal waveform.

In all our discussion we emphasize the study on optimum signal processing from the passive rather than active mode. A major difference between passive and active signal processing is that in the passive case the signal processor designer has no direct control and knowledge of the actual received signal characteristics. Thus, many advanced design techniques which are based on the optimum design of signal waveforms (e.g., methods of pulse compression) used routinely in the active systems are not applicable. This lack of precise knowledge of the reference signal waveforms in the passive case results in a greater uncertainty in the estimated target parameters. Despite the fact that passive processing suffers a greater uncertainty in the resulting estimates, many situations do arise where passive processing is either the only choice or is the preferred approach.

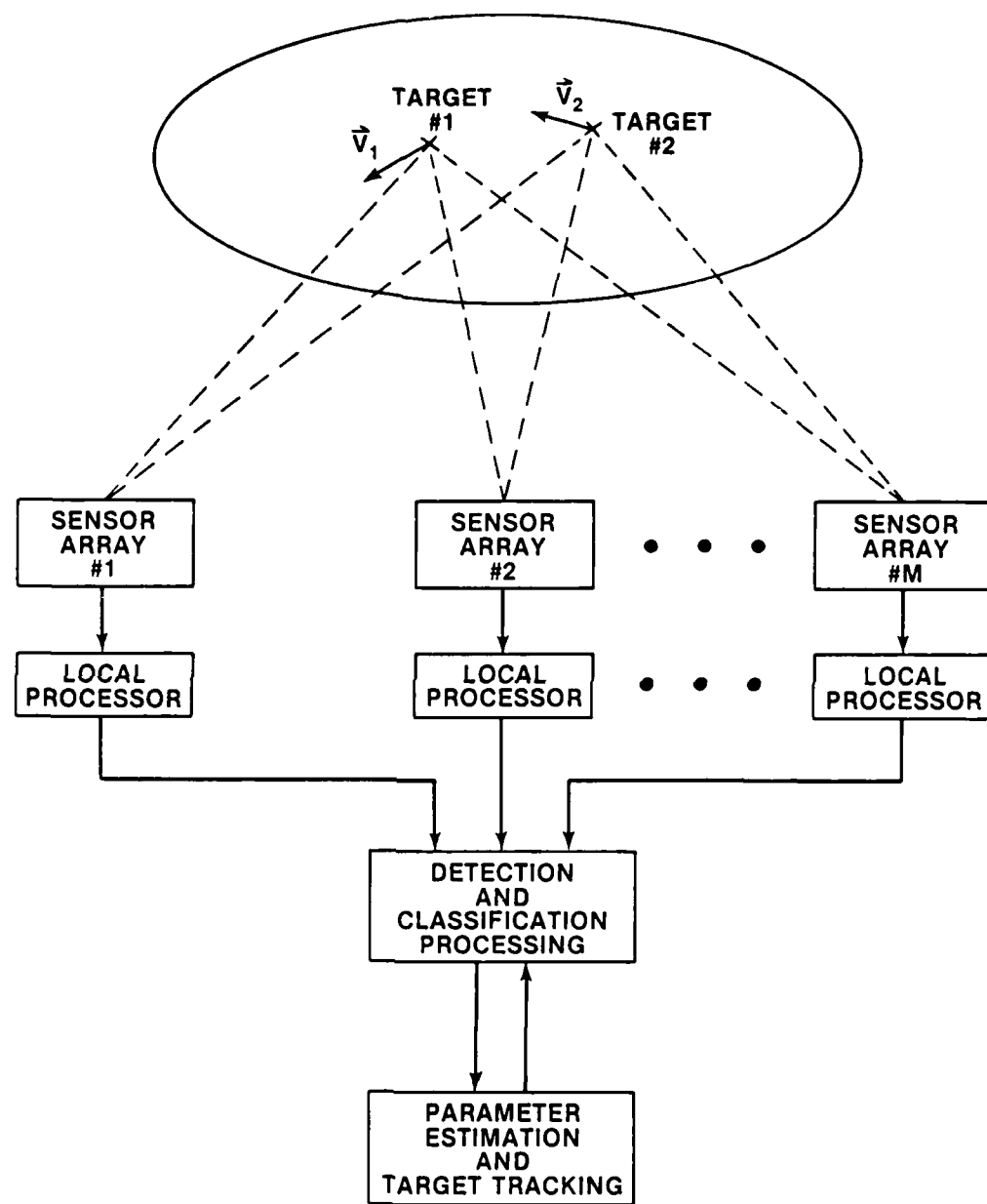
Consider the case of locating the epicenter of an earthquake. Since we have no prior knowledge of the location and the time of occurrence of an earthquake, one must rely on the passive observation of the signal (pressure wave) as it arrives at each of the seismic stations. Now consider the problem of localization and tracking of underwater acoustic sources using sonar. If the objective of the processor is to detect, localize, and track an acoustic source with minimum counterdetection probability, then

passive processing is mandatory. Furthermore, in the absence of noise, the received waveforms contain the true target signature and this could be a valuable aid in target classification. Perhaps a situation which exemplifies this usage is the simple procedure used by a physician in diagnosing a patient's health by listening at various locations of the body using a passive receiver; i.e., a stethoscope.

A more detailed explanation about the subject matter of our study is given below. As shown in Figure 1-1, there are five major elements in our investigation.

1. Multitarget Environment: We assume in our study that there are J targets present within the operating environment of our sensors. We are particularly interested in the case where $J > 1$; i.e., more than one target is present. However, because of the general formulation of the problem, the single target case (a subject of intense study in the literature) can be obtained by letting $J = 1$ in our general J target solution.

We assume that each target emits a known signal spectrum for the purpose of our study. Of course, in reality, the target signal spectrum must be estimated through a priori knowledge or using on-line spectral estimation techniques.



021.610

Figure 1-1. Passive Multisensor, Multitarget Processing

The assumption of a multitarget environment is warranted and justified for the following reasons: (a) improved sensor sensitivity due to advanced new sensor technology greatly increases the operating range of a sonar system; thus by virtue of the expanded coverage, the existence of a multitarget environment is more likely than ever, and (b) since sonar operations typically occur near high density shipping environments, the presence of multiple targets is a rule rather than an exception. In addition, conventional optimum processor design based on a single target assumption suffers considerably when operating in a multitarget environment.

2. Multisensor Arrays. We assume that each sensor array consists of multiple sensing elements (hydrophone) whose received target waveforms are available for processing. We assume that location of each sensor array is known w.r.t. a well defined point of reference.
3. Optimum Estimation of Localization Parameters. We assume that targets are stationary and we investigate the optimum processor which yields the best estimate of each target's range and bearing from a known reference point. We explore in some detail the differences between a one-step (direct) localization parameter estimation approach and a two-step (indirect) time delay followed by localization

parameter approach. We also investigate various sub-optimum approaches and evaluate their relative performances compared to the optimum processor.

4. Optimum Variable Localization Parameter Estimation and Tracking. Here we assume that each target is moving with a well defined trajectory and we seek an optimum localization parameter estimation and tracking algorithm operating in a multisensor, multitarget environment.
5. Weak Signal in Noise Environment. We assume that improved sensor technology increases sensor sensitivity, resulting in an improved capability to respond to a target which has a weak signal level. Very often targets with very weak signal levels are the targets of interest. Since signal level attenuates inversely proportional to the square of range, long range targets are, therefore, usually weak signal level targets.

1.1 BACKGROUND

The reasons for using sensor arrays to localize and track targets of interest are twofold. First, it is to gain spatial diversity, whereby target signals are received simultaneously at different points in space; their spatial separations contain informa-

tion on target location parameters. Second, it is to improve the signal-to-noise ratio (SNR) via spatial coherent integration of sensor outputs. This process is known as array processing or beam-forming. Subsequent to the array processing, the SNRs are further enhanced by time domain processing for the purpose of detection, classification, parameter estimations, and tracking.

The combined array and temporal signal enhancement process is known as space-time processing. It can be pointed out here that a fundamental factor which limits the space-time processing gain is given by the triplet BLT, where B is the signal bandwidth, L is the array effective length, and T is the duration of time domain integration. Note that the overall processing gain directly limits the performance bound on detection, classification, parameter estimation, and tracking.

Implicit in any range and bearing estimation is the estimation of time difference of arrival (TDOA), or simply time delays between sensor pairs. These time delays contain all the available information about the target parameters of interest. Thus the time delay is the basic unit of information from which all other parameters of interest are extracted.

The measurement of time delay is mechanized through a Generalized Cross Correlation (GCC) function. The GCC is derived as a Maximum Likelihood Estimator (MLE) operating between any two sensor

arrays. Detailed discussion on the subject of the GCC can be found in Knapp and Carter,¹ Carter,² Hahn and Tretter,³ and Hassab and Boucher.⁴

In the above literature, the GCC is optimized under a single target assumption (or more specifically, a single coherent noise source). In the presence of multiple targets, or multipath environment, there are multiple correlation peaks. The existence of multiple correlation peaks causes performance degradation to the existing measurement system. The extent of this degradation is a function of signal spectral characteristics, SNR, signal-to-interference ratio (SIR), and the relative time delay separation.

In a multisensor, multitarget environment the primary cause of performance degradation of the existing system is due to the mismatch between the signal processor design and the environment in which the signal processor must operate. Therefore, a logical approach to minimize the loss of performance is to examine the optimum structure of the signal processor under a multisensor, multitarget environment. Knowing the form of the optimum processor, one can then explore various options for a practical system realization.

1.2 TECHNICAL OBJECTIVES

The primary objectives of this study are to (1) derive the optimum time delay estimator under a multisensor, multitarget environment, (2) evaluate the appropriate performance bound, (3) investigate suboptimal processor realizations and methods of improved multitarget parameter resolution, (4) extend the optimum multisensor, multitarget time delay processor to include variable time delay estimation, and (5) examine the problem of optimum variable localization parameter estimation and tracking.

1.3 PREVIOUS WORK

Optimum signal processor design under a stationary multisensor, multitarget environment has been studied by a number of researchers, i.e., the work by Scheweppe⁵ on sensor array data processing for multiple signal source, Schultheiss⁶ on passive sonar detection in the presence of interference, and Anderson and Rudnick⁷ on rejection of coherent signal arrival. In addition, there are the works by Capon,⁸ Steinberg,⁹ Cox,¹⁰ McGarty,¹¹ Rockmore and Bershad,¹² and Owsley and Swope¹³. With the possible exception of the work by Scheweppe and Owsley-Swope, the primary efforts of these studies were on determining the effect of interference on the existing (single target) processor. Using a Least

Mean Square approach, Scheweppe derived a decoupled beamformer. However, his formulation ignored the effect of dependence of the covariance matrix on the unknown parameter. On the other hand, Owsley and Swope derived a single frequency multichannel focused beamformer using a Weighted Least Square approach. However, Owsley and Swope's formulation did not include the bias correction term.

Optimum signal processor design under a non-stationary multi-sensor, multitarget environment has not been seen in the open literature. However, a few papers have been published in this area for a single target case. For example, Knapp and Carter¹⁴ studied the optimum GCC in the presence of source motion. Schultheiss and Weinstein¹⁵ calculated the lower bounds on the localization error. Chan, Riley and Plant¹⁶ investigated estimation of non-stationary delay by modeling the time delay as a finite impulse response (FIR) process. Finally, Friedlander¹⁷ studied the joint time delay and signal spectrum estimation using an Auto-Regressive Moving Average (ARMA) model.

The study of passive estimation and tracking of variable target parameters has received considerable interest in the literature. Most of the early studies have been concentrated on single target and single sensor array. However, the extension to multi-target, multisensor environments has received increasingly more attention. The complexity of this problem increases rapidly as the

number of targets and sensors increases. There are two notably different approaches in attacking this problem. The first approach starts from the target dynamic tracking filter (or data processor) and attempts to model the measurement processes. One approach which has received considerable attention recently is the Joint Probability Data Association Filter (JPDAF) discussed by Bar-Shalom,¹⁸ Bar-Shalom and Tze,¹⁹ and Fortmann, Bar-Shalom, and Scheffe.²⁰ Here the measurements were assumed to have a probabilistic model. An underlying assumption for this approach is that the signal process which produces the measurements cannot be modified to account for the multitarget problem. Therefore, one must rely on modeling the measurement process. In fact, using a linear superposition assumption, Ng and Bar-Shalom presented a model of unresolved measurement for multitarget tracking.^{21,22} However, the inability to change the signal process is a major limitation in obtaining an overall satisfactory solution. This is true because an optimum solution requires the implementation of an optimum signal processor.

The second approach, on the other hand, starts the investigation from the signal processor. Here one finds that the signal processing gain increases in proportion to time. However, by increasing the processing time one can no longer assume a Stationary Parameter Long Observation Time (SPLOT) process, which is the basic assumption used in many existing signal processor

designs. Typically, one finds that under a moving target assumption, a signal processor must estimate both the static and dynamic parameters. Failure to compensate for the parameter dynamic will result in a substantial loss in coherent integration. Consequently, it negates the very purpose of long integration time. Studies in these areas are notably pursued by Carter and Abraham,²³ Schultheiss and Weinstein,¹⁵ and Moura and Baggeroer.²⁴

1.4 TECHNICAL APPROACH AND ORGANIZATION

This study provides a fundamental examination of the optimum signal processor design for time delay estimation under the assumption of a multisensor, multitarget environment. Using an MLE procedure, an optimum multisensor, multitarget time delay estimator is derived. The resulting signal processor is reduced to its simplest form for system realization. In addition, this study derives the appropriate performance bound for the resulting estimator. Comparisons between optimum and suboptimum realizations are also discussed. The optimum multisensor, multitarget time delay estimator is then refined to include the moving target environment. Finally, the variable time delay estimator is applied to the problem of variable localization parameter estimation and tracking.

The organization of this report is as follows: Chapter 2 discusses and formulates the multisensor, multitarget time delay estimation problem. Chapter 3 derives the optimum time delay estimator and an appropriate performance bound. In addition, the extension of time delay estimation to localization parameter estimation and power spectral estimation is considered. Chapter 4 provides some discussion on suboptimum processor realization. Chapter 5 discusses alternate approaches for improved multitarget parameter resolution. Chapter 6 extends the optimum time delay processor to include variable time delays. Chapter 7 examines the problem of optimum variable localization parameter estimation and tracking. Finally, Chapter 8 presents the summary, conclusions, and recommendations of the study.

1.5 STATEMENTS OF CONTRIBUTION AND SUMMARY

Under the assumption of a SPLOT process, the optimum multisensor, multitarget time delay processor was derived from a Maximum Likelihood (ML) viewpoint. The resulting processor was obtained by reducing the vector likelihood equation via straightforward, but somewhat tedious, manipulations to the simplest form. The optimum multisensor, multitarget processor provided the basis for the

subsequent detailed studies on time delay vector estimation, localization parameter estimation, power spectral estimation, suboptimum processor realization, and post GCC multitarget parameter estimation.

However, under a target or source motion environment, the SPLIT assumption is no longer valid. Thus the optimum processors derived for the stationary parameter case need to be refined to account for the target motion. The approach we have taken was to segment the observation interval into smaller subintervals. It was shown that if the signal time bandwidth product satisfies a certain criterion, one can again represent a time-compressed (or expanded) waveform in terms of Fourier coefficients. Consequently, under the approach just described, a variable time delay processor can be derived from an ML viewpoint. The variable time delay processor was then used to estimate variable localization parameters and target motion parameters. We also discussed a sequential fixed interval time delay tracking processor which was proposed to be used in target state tracking. Major findings of this study are summarized below.

1. The optimum multisensor, multitarget time delay estimator is a highly coupled, multi-channel signal processor. The estimator's performance in terms of the Cramer-Rao Lower

Bound (CRLB) was evaluated for the following cases: one target and two sensors, two targets and two sensors, and one target and M sensors. For the one-target, two-sensor case, the optimum multisensor, multitarget processor reduces to the GCC studied by Knapp and Carter.¹ For the two-sensor, two-target case, the resulting processor was studied in detail. A closed-form analytical expression for the two-dimensional matrix CRLB was obtained. To the best of our knowledge, this result is original and did not appear in the open literature. The result of the study shows that the optimum processor provides a significant improvement over a conventional GCC processor. For the one-target, M -sensor case, the matrix CRLB for the time delay vector estimate was obtained. It is also believed that this result is original and does not appear elsewhere.

The results of this study indicate that for an M sensor array, the $M - 1$ inter-sensor time delays can be obtained from $M - 1$ correlations. This is a significant reduction from Hahn's approach,²⁵ where a total of $M(M - 1)^{\frac{1}{2}}$ correlations are required. Additionally, the results show that the variance of the time delay estimate between any two sensors decreases with M , the total number of sensors.

2. The localization parameter estimation was examined in detail using a one-target, three-sensor array as an example from two perspectives: (a) a one-step focused beamformer approach where a direct range and bearing estimate is sought, and (b) a two-step time delay to range and bearing approach where time delay estimates are first sought and range and bearing estimates are obtained via a geometric mapping. The study indicates that both approaches yield an identical performance bound. However, for practical implementation considerations, the two-step approach is generally preferred because of the symmetrical property of the GCC function in the time delay variable. Furthermore, the localization performance based on the optimum (ML) time delay processor was compared to the conventional approach, where the latter approach used two GCCs in parallel, one for each time delay. The result of this study shows that the optimum processor yields a one-sigma localization error ellipse, which is approximately one-half smaller than the conventional approach. This improvement comes directly from a better bearing estimation. The range variance is identical between the optimum and the conventional approach.

3. A major assumption used in the derivation of the optimum multisensor, multitarget time delay processor was the known target and noise spectra. To relax this constraint, a joint time delay and spectral estimator was derived. The result of this study shows that the time delay estimate and the spectral estimate are uncorrelated. This implies that for the unknown target spectrum case, a joint time delay and spectral estimator can be implemented. The spectral estimation process does not degrade the performance of the time delay estimate. Furthermore, it was found that while the variance of the time delay estimate decreases as an inverse function of the observation time, the variance of the spectral estimate decreases as an inverse square function of the observation time.
4. The optimum multisensor, multitarget time delay processor is an order of magnitude more complex than the conventional GCC processor. Therefore, for a practical implementation, a suboptimum realization should be considered. One suboptimum procedure is to assume a low target signal-to-background noise environment. It was found that the resulting processor is significantly simplified. From the multitarget viewpoint, the conventional GCC processor can be considered as a suboptimum processor. The performance of the GCC processor is compared to the optimum processor as a function of time delay separation.

5. Because of its simplicity, the conventional GCC processor is implemented in many existing sonar systems. On the other hand, the application of the optimum multisensor, multitarget processor requires a major modification of the conventional GCC approach. Therefore, an alternate approach is to provide additional multitarget processing at the GCC output. For this purpose, a post GCC multitarget estimator (or more appropriately the matched estimator) was investigated. In essence, the matched estimator determines the best estimate of the unknown parameter vector from a reference function which matches the observed noisy GCC output under a Least Mean Square (LMS) criterion. The matched estimator was simulated. The simulation results were compared to the theoretical predictions as well as to the optimum processor. The results of this study indicate that the matched estimator provides comparable performance with the optimum processor.
6. The optimum multisensor, multitarget processor which we have derived, studied, and discussed thus far was based on the assumption of a SPLOT process. This assumption is difficult to satisfy for a more general moving target environment. Therefore, we further refined our study to account for the effects of target motion.

The approach we have taken was to model the time delay motion by a finite order polynomial in time and partition the observation interval into N equal subintervals. It was shown that in order for the time-compressed waveform to be Fourier-representable, N must satisfy a certain constraint. When this assumption is valid, one can again express the multisensor, multitarget, multi-interval observations in terms of a multidimensional Fourier coefficient vector. The result of using an MLE approach yielded the multisensor, multitarget variable time delay processor. This processor provided an estimate of the time delay and its higher order derivatives at any time within the observation interval. It was shown that for time delay estimate, the minimum variance always occurs at the mid-point of the observation interval.

7. The time delay processors we have discussed thus far are batch processor; i.e., one must wait until the end of a T -second observation before one starts any computations. In many applications, this T -second solution delay is not acceptable. Therefore, we have investigated and proposed a sequential fixed-interval time delay processor. This processor obtains its current estimate by utilizing the most current subinterval observation and the prior estimates. We obtained an expression for the covariance calculation.

8. We next addressed the problem of variable localization parameter estimation and tracking. Our approach was similar to the stationary parameter case. We first estimated the time delay trajectory using the variable time delay processor. Localization parameters were then obtained via a geometric mapping from the time delay estimate. For target state estimation where we are interested in both the target position and velocity components, the mapping function utilized both time delay and time delay rate estimates.

CHAPTER 2

PROBLEM FORMULATION

Man cannot inherit the past; he has to recreate it.
-- A. KOESTLER, The Act of Creation

2.1 INTRODUCTION

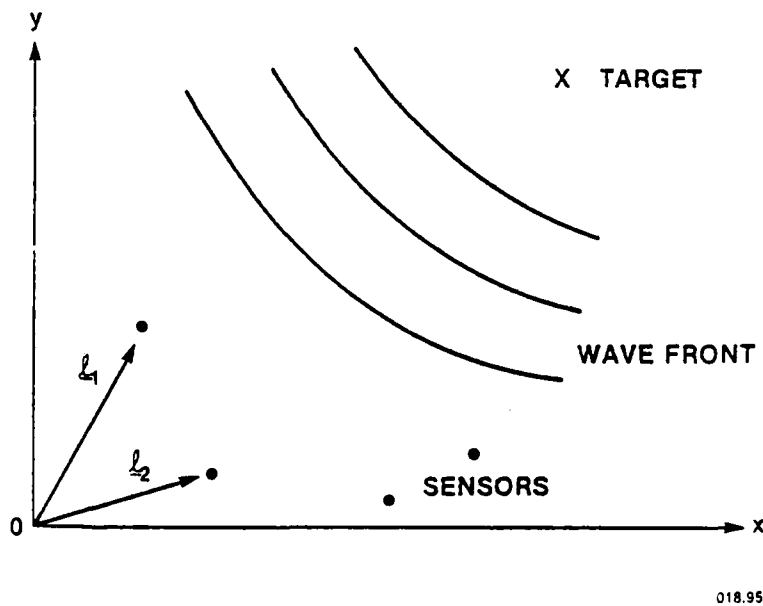
In this chapter we discuss the mathematical description of the sensor observations and formulate the general multisensor, multi-target time delay estimation problem. The optimum signal processor is sought via an MLE procedure. In general, we assume the target-sensor environment consists of M sensors and J targets (or J arrival paths). Target waveforms are assumed mutually uncorrelated. As an introduction to the general multitarget, multisensor problem formulation, we first consider the basic description of observables for a single target case.

2.2 DESCRIPTION OF OBSERVABLES

Let M sensor arrays be distributed arbitrarily in space. These M sensor arrays then produce M continuous waveforms which represent the M spatial samples of a random field generated by the target signal in additive ambient noise. Let the M waveforms be observed for a duration of T seconds and let the received waveforms be written as:

$$y(t, \underline{\ell}_i) = a_i s_i(t) + n_i(t); \quad i = 1, 2, \dots, M \quad t \in [0, T] \quad (2.2-1)$$

where a_i , $s_i(t)$, and $n_i(t)$ are the signal attenuation factor, signal waveform, and the noise waveform, respectively, for the i th sensor. We note that the observed waveform $y(t, \underline{\ell}_i)$ is a random function of space and time, and $\underline{\ell}_i$ is the location vector of the i th sensor with respect to a known reference point. See Figure 2-1.



018.950

Figure 2-1. Description of Passive Sensor Observation

To simplify the analysis, the following assumptions have been made:

1. Pure Time Delay Channel - The signal waveforms received at each sensor are identical except for a pure time delay. Thus, the signal waveform (for the single target case) of the i th sensor can be written as $s_i(t) = s(t + D_i)$, where D_i is the propagation delay from the signal source to the i th sensor. Therefore, Equation (2.2-1) can be rewritten as:

$$y(t, \underline{\ell}_i) = a_i s(t + D_i) + n_i(t); \quad i = 1, 2, \dots, M \quad (2.2-2)$$

$t \in [0, T]$.

From Figure 2-2, we see that the propagation time delay is given by the relation

$$D_i = \frac{|\underline{r} - \underline{\ell}_i|}{c} \quad (2.2-3)$$

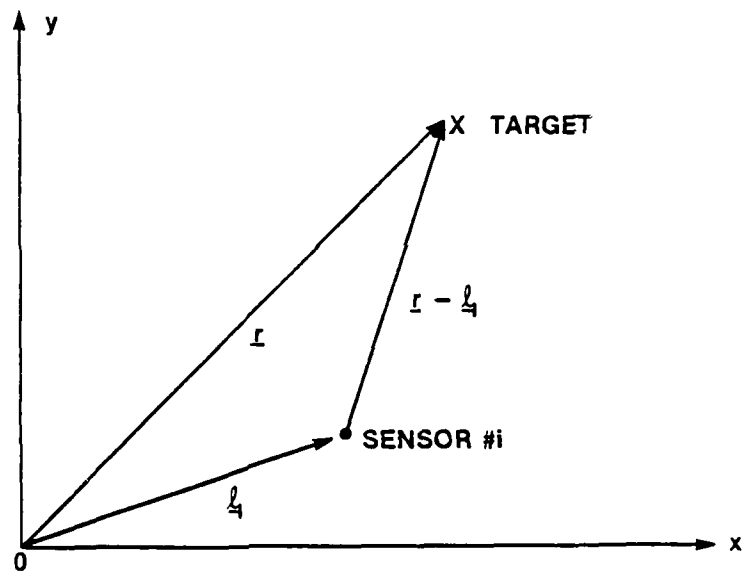
where

\underline{r} = position vector of the signal source

$\underline{\ell}_i$ = location vector of the i th sensor

c = propagation speed of the medium.

2. Noise at each sensor is assumed additive with known spatial and temporal correlation function.



018.954

Figure 2-2. Target-to-Sensor Geometry

3. The observation time T is much longer than the travel time of the wavefront across the sensor array.
4. Both the signal process and the noise process are mutually uncorrelated, zero mean, Gaussian, stationary in time, homogeneous in space (Yaglom²⁶), and have a known band-limited power spectrum.

We note that the set of observations $y(t, \underline{l}_i); i = 1, 2, \dots, M; t \in [0, T]$ contains a complete description of the observables. However, it has infinite dimensions and is analytically intractable. Therefore, we wish to represent the time-limited observation of the waveform by a finite set of discrete random variables. Because of

the time delays in the signal waveform, a convenient approach is to represent the observation in terms of a Fourier series expansion as discussed by MacDonald and Schultheiss,²⁷ Knapp and Carter,¹ and Rockmore.²⁸ The resulting coefficients are almost uncorrelated for a large bandwidth time product as demonstrated by Hodgkiss and Nolte.²⁹ Therefore, Equation (2.2-2) can be represented by a Fourier coefficient vector as:

$$\underline{\alpha}_k = \beta_k \underline{v}_k + \underline{n}_k ; \quad k = \pm 1, \pm 2, \dots \quad (2.2-4)$$

where

$$\underline{\alpha}_k = (\alpha_{1k} \alpha_{2k} \dots \alpha_{Mk})^T \quad (2.2-5a)$$

$$\underline{v}_k = \left(a_1 e^{j\omega_k D_1} a_2 e^{j\omega_k D_2} \dots a_M e^{j\omega_k D_M} \right)^T \quad (2.2-5b)$$

$$\underline{n}_k = (n_{1k} n_{2k} \dots n_{Mk})^T \quad (2.2-5c)$$

are the vectors of observation, signal steering, and additive noise, respectively, for all sensor outputs at frequency $\omega_k = (2\pi k)\frac{1}{T}$. Furthermore, the variables α_{ik} , β_k and n_{ik} are defined as follows:

$$\alpha_{ik} = \frac{1}{T} \int_0^T y(t, \underline{l}_i) e^{-j\omega_k t} dt \quad (2.2-6a)$$

$$B_k = \frac{1}{T} \int_0^T s(t) e^{-j\omega_k t} dt \quad (2.2-6b)$$

$$n_{ik} = \frac{1}{T} \int_0^T n_i(t) e^{-j\omega_k t} dt . \quad (2.2-6c)$$

Note that for real signal and noise waveforms, the Fourier coefficients are conjugate symmetric; i.e., $\alpha_{j,-k} = \alpha_{ik}^*$. Thus, for a band-limited process one only needs to consider frequency components $k = 1, 2, \dots, B$, where B is the highest cut-off frequency of either the signal or the noise spectrum. For a low pass power spectrum, B can be identified as the one-sided bandwidth.

Since both the signal and noise are zero mean Gaussian processes, it is easily established that $\underline{\alpha}_k$ is a zero mean Gaussian random vector with covariance matrix:

$$\begin{aligned} R_k &= E(\underline{\alpha}_k \underline{\alpha}_k^*) \\ &= S_k V_k V_k^* + N_k Q_k \end{aligned} \quad (2.2-7a)$$

where $\underline{\alpha}_k^*$ is the complex conjugate transpose of $\underline{\alpha}_k$; S_k and N_k are the discrete signal and noise power spectral density, respectively, at frequency ω_k ; and Q_k is the normalized spatial covariance matrix of the noise vector such that

$$\text{tr}(Q_k) = M \quad (2.2-7b)$$

where $\text{tr}(\cdot)$ defines the trace of a matrix.

Now writing

$$\underline{\alpha} = (\underline{\alpha}_1^T \underline{\alpha}_2^T \dots \underline{\alpha}_B^T)^T$$

as an MB dimensional complex column observation vector, we obtain the first and the second order moments of $\underline{\alpha}$ as:

$$E(\underline{\alpha}) = \underline{0} \quad (2.2-8a)$$

$$E(\underline{\alpha} \underline{\alpha}^*) = \text{diag}\{R_k\} \quad (2.2-8b)$$

which is a block diagonal since for a large bandwidth-time product,

$$E(\underline{\alpha}_k \underline{\alpha}_l^*) \approx 0 \quad \text{for } k \neq l .$$

Now let

$$\underline{D} = (D_1 \ D_2 \ \dots \ D_M)^T$$

be the propagation delay vector, then the probability density function (pdf) of $\underline{\alpha}_k$ conditioned on \underline{D} is complex Gaussian (Appendix A) given by

$$p(\underline{\alpha}_k | \underline{D}) = \pi^{-M} |R_k|^{-1} \exp\{-\underline{\alpha}_k^* R_k^{-1} \underline{\alpha}_k\} \quad (2.2-9)$$

and since $\underline{\alpha}_k$ and $\underline{\alpha}_l$ are uncorrelated for $k \neq l$, they are also independent. Hence, one can write

$$p(\underline{\alpha} | \underline{D}) = p(\underline{\alpha}_1, \underline{\alpha}_2, \dots, \underline{\alpha}_B | \underline{D})$$

$$= \prod_{k=1}^B p(\underline{\alpha}_k | \underline{D})$$

$$= \pi^{-MB} \prod_{k=1}^B |R_k|^{-1} \exp\{-\underline{\alpha}_k^* R_k^{-1} \underline{\alpha}_k\} \quad (2.2-10)$$

as the pdf of the complete observation vector $\underline{\alpha}$ conditioned on the propagation time delay vector \underline{D} . Thus Equation (2.2-10) provides a complete statistical description of the observation conditioned on the unknown time delay vector.

2.3 STATEMENT OF THE PROBLEM

In this section we formulate the general multisensor, multi-target time delay estimation problem in terms of the observation vector described in the previous section. We consider the problem of optimum time delay estimation from M sensor arrays in the presence of J possible targets. The final objective of sensor array time delay estimation is to provide optimum estimates of target localization parameters (i.e., range and bearing). We assume that interarray separation is large compared to the size of each sensor array. Such an arrangement is normally found in large aperture surveillance systems. See, for example, the large seismic array described by Capon.³⁰ A recent study by Carter² has shown that for passive localization of an acoustic source, the variance of the bearing error is inversely proportional to the square of the base length while the variance of the range error is proportional to the fourth-power of the ratio of the true range to the base length. Thus, a long base length is desirable in reducing the variance of the estimates.

Let the M sensor array outputs from J acoustic sources be written as:

$$y(t, \underline{\theta}_i) = \sum_{j=1}^J a_{ij} s_j(t + \tau_{ij}) + n_i(t); \quad t \in [0, T] \quad (2.3-1)$$

where $i = 1, 2, \dots, M$; a_{ij} is the signal attenuation factor for the j th target to the i th sensor; D_{ij} is the propagation time delay from target j to sensor i ; and $s_j(t)$ and $n_i(t)$ are the band-limited signal and noise processes with the usual assumptions of zero mean, Gaussian, time stationary, and spatially homogeneous. Fourier expansion of Equation (2.3-1) yields the finite dimensional frequency domain representation as:

$$\underline{\alpha}_k = W_k \underline{\beta}_k + \underline{n}_k ; \quad k = 1, 2, \dots, B \quad (2.3-2a)$$

where

$$\underline{\alpha}_k = (\alpha_{1k} \alpha_{2k} \dots \alpha_{Mk})^T \quad (2.3-2b)$$

$$\underline{\beta}_k = (\beta_{k1} \beta_{k2} \dots \beta_{kJ})^T \quad (2.3-2c)$$

$$\underline{n}_k = (n_{1k} n_{2k} \dots n_{Mk})^T \quad (2.3-2d)$$

and

$$W_k = \left(a_{ij} e^{j\omega_k D_{ij}} \right); \quad \begin{matrix} i = 1, 2, \dots, M \\ j = 1, 2, \dots, J \end{matrix} \quad (2.3-2e)$$

is a $M \times J$ complex "propagation delay" matrix, where M is the number of sensors, J is the number of targets, and $\omega_k = (2\pi k)\frac{1}{T}$ is the discrete frequency. Similar to the development in the last section, the observation vector $\underline{\alpha}_k$ is Gaussian with the following statistics:

$$E(\underline{\alpha}_k) = \underline{0} \quad (2.3-3a)$$

$$E(\underline{\alpha}_k \underline{\alpha}_k^*) = \begin{cases} 0; & \text{if } k \neq \ell \\ R_k; & \text{if } k = \ell \end{cases} \quad (2.3-3b)$$

where

$$R_k \triangleq W_k S_k W_k^* + N_k Q_k \quad (2.3-3c)$$

and

$$S_k = E(\underline{\beta}_k \underline{\beta}_k^*) . \quad (2.3-3d)$$

For uncorrelated sources, we have

$$S_k = \text{diag}\{S_{k1}, S_{k2}, \dots, S_{kJ}\} \quad (2.3-3e)$$

as a $J \times J$ diagonal matrix with element S_{kj} as the signal power at frequency ω_k of target j . Thus, the pdf of $\underline{\alpha}_k$ conditioned on the time delay matrix defined by

$$\mathbf{D} = \{D_{ij}\} ; \quad \begin{aligned} i &= 1, 2, \dots, M \\ j &= 1, 2, \dots, J \end{aligned} \quad (2.3-3f)$$

is

$$p(\underline{\alpha}_k | D) = \pi^{-M} |R_k|^{-1} \exp\{-\underline{\alpha}_k^* R_k^{-1} \underline{\alpha}_k\}. \quad (2.3-4)$$

Finally, writing

$$\underline{\alpha} = (\underline{\alpha}_1^T \ \underline{\alpha}_2^T \ \dots \ \underline{\alpha}_B^T)^T, \quad (2.3-5a)$$

then the pdf of $\underline{\alpha}$, the complete observation vector, conditioned on D , the multisensor, multitarget time delay matrix, can be written as

$$\begin{aligned} p(\underline{\alpha} | D) &= \prod_{k=1}^B p(\underline{\alpha}_k | D) \\ &= \pi^{-MB} \prod_{k=1}^B |R_k|^{-1} \exp\{-\underline{\alpha}_k^* R_k^{-1} \underline{\alpha}_k\}. \end{aligned} \quad (2.3-5b)$$

Equation (2.3-5b) constitutes the basis for the derivation of the multisensor, multitarget optimum time delay processor. An MLE is obtained by maximizing the conditional pdf with respect to each element of the propagation time delay matrix. Thus, symbolically one can write

$$\hat{D}_{ML} = \underset{D}{\operatorname{Max}} \operatorname{Arg} p(\underline{\alpha} | D). \quad (2.3-6)$$

CHAPTER 3

OPTIMUM MULTITARGET PARAMETER ESTIMATION

It is demonstrable, that things cannot be otherwise than as they are, as all things have been created for some end, they must necessarily have been created for the best end. -- VOLTAIRE

3.1 INTRODUCTION

In principle the optimum estimate of the time delay matrix D is obtained by solving Equation (2.3-6) numerically. In general, a direct implementation of Equation (2.3-6) results in a very complex processor. However, without loss of performance, Equation (2.3-6) can be reduced to its simplest form by mathematical manipulations. The resulting processor is usually realizable.

In this chapter we investigate the fine structure of the optimum multitarget time delay signal processor. Since time delays are modeled as unknown constants, we seek an optimum estimator via an MLE approach. We provide a performance bound for the resulting estimator. We study in detail the two-sensor, two-target case. For the three-sensor, one-target case we establish the relationship between optimum localization parameter estimation and optimum time delay estimation. Finally, we investigate the structure of the optimum power spectral estimator when the target signal power spectrum is not known a priori.

3.2 THE LIKELIHOOD EQUATION

It was shown in Chapter 2, Equation (2.3-5b), that the pdf of the sensor observation vector $\underline{\alpha}$ conditioned on the time delay matrix D is given by

$$p(\underline{\alpha}|D) = \prod_{k=1}^B p(\underline{\alpha}_k|D) \quad (3.2-1a)$$

where

$$p(\underline{\alpha}_k|D) = \pi^{-M} |R_k|^{-1} \exp\{-\underline{\alpha}_k^* R_k^{-1} \underline{\alpha}_k\}. \quad (3.2-1b)$$

The ij element of the time delay matrix D is given by (see Equation (2.3-3f))

$$D_{ij} = \frac{|\underline{r}_j - \underline{\ell}_i|}{c}; \quad \begin{matrix} i = 1, 2, \dots, M \\ j = 1, 2, \dots, J \end{matrix} \quad (3.2-2)$$

where \underline{r}_j and $\underline{\ell}_i$ denote the vector locations of target j and sensor i, respectively. The log-likelihood function of Equation (3.2-1a) is defined by

$$\begin{aligned} \Lambda(D) &= \sum_{k=1}^B \log p(\underline{\alpha}_k|D) \\ &= -MB \log(\pi) - \sum_{k=1}^B \Lambda_k(D) \end{aligned} \quad (3.2-3a)$$

where

$$\Lambda_k(D) = \log|R_k| + \underline{\alpha}_k^* R_k^{-1} \underline{\alpha}_k \quad (3.2-3b)$$

and R_k is the covariance matrix of the zero mean complex Gaussian vector $\underline{\alpha}_k$ given by (see Equation (2.3-3c))

$$R_k = W_k S_k W_k^* + N_k Q_k \quad (3.2-3c)$$

where for the uncorrelated source case,

$$S_k = \text{diag}\{S_{k1}, S_{k2}, \dots, S_{kJ}\} \quad (3.2-3d)$$

is a $J \times J$ diagonal signal power density matrix whose j th diagonal entry denotes the discrete signal power density of target j at frequency ω_k . N_k is the discrete noise power density, and Q_k is the normalized covariance matrix. Finally, the ij element of the $M \times J$ "propagation delay matrix", W_k , is defined by

$$W_k = \begin{pmatrix} e^{j\omega_k D_{ij}} \\ a_{ij} \end{pmatrix}; \quad i = 1, 2, \dots, M; \quad j = 1, 2, \dots, J \quad (3.2-3e)$$

where a_{ij} denotes the signal attenuation factor from target j to sensor i . Now writing

$$W_k = (\tilde{v}_{k1} \tilde{v}_{k2} \dots \tilde{v}_{kJ}) \quad (3.2-4a)$$

where

$$\tilde{v}_{kj} = \left(a_{1j} e^{j\omega_k D_{1j}} \ a_{2j} e^{j\omega_k D_{2j}} \ \dots \ a_{Mj} e^{j\omega_k D_{Mj}} \right)^T \quad (3.2-4b)$$

is the attenuated signal steering vector of target j at frequency ω_k . Using the fact that S_k is a diagonal matrix for uncorrelated sources, we have the obvious identity:

$$\begin{aligned} W_k \ S_k \ W_k^* &= \sum_{j=1}^J S_{kj} \ \tilde{v}_{kj} \ \tilde{v}_{kj}^* \\ &= \sum_{j=1}^J S_{kj} \ p_{kj} \end{aligned} \quad (3.2-4c)$$

where p_{kj} is defined by

$$\begin{aligned} p_{kj} &\stackrel{\Delta}{=} \frac{\tilde{v}_{kj}}{\tilde{v}_{kj}^*} \\ &= \frac{v_{kj}}{v_{kj}^*} \end{aligned}$$

Note that we have chosen to let

$$\tilde{v}_{kj} = e^{j\omega_k D_{1j}} v_{kj} \quad (3.2-4d)$$

or equivalently (to reference all time delays to the first sensor), one can write

$$v_{kj} = \left(a_{1j} \ a_{2j} e^{j\omega_k \Delta_{1j}} \ \dots \ a_{Mj} e^{j\omega_k \Delta_{M-1,j}} \right)^T \quad (3.2-4e)$$

where Δ_{ij} is given by the relation

$$\Delta_{ij} = D_{i+1,j} - D_{1j}; \quad i = 1, 2, \dots, M-1. \quad (3.2-4f)$$

Now P_{kj} is an $M \times M$ Hermitian matrix of rank one and is a function of the attenuation vector \underline{a}_j and the time delay vector $\underline{\Delta}_j$. The vectors \underline{a}_j and $\underline{\Delta}_j$ are given by

$$\underline{a}_j = (a_{1j} \ a_{2j} \ \dots \ a_{Mj})^T \quad (3.2-4g)$$

and

$$\underline{\Delta}_j = (\Delta_{1j} \ \Delta_{2j} \ \dots \ \Delta_{M-1,j})^T. \quad (3.2-4h)$$

Note that given M sensors, there are $M-1$ independent time delay pairs from a possible total of $M(M-1)\frac{1}{2}$. The selection of this set is not unique. However, for time delay estimation, it is reasonable to assume a set with minimum total delay. This set (for a line array) is given by the inter-sensor time delay vector:

$$\underline{\tau}_j = (\tau_{1j} \ \tau_{2j} \ \dots \ \tau_{M-1,j})^T; \quad j=1, 2, \dots, J \quad (3.2-4i)$$

where $\tau_{ij} = D_{i+1,j} - D_{ij}$.

Note that the Δ_{ij} 's can be expressed in terms of the τ_{ij} 's. For example:

$$\Delta_{ij} = D_{i+1,j} - D_{1j}$$

$$= \sum_{n=1}^i D_{n+1,j} - D_{nj}$$

$$= \sum_{n=1}^i \tau_{nj}$$

$$= \underline{U}_i^T \underline{\tau}_j \quad (3.2-4j)$$

where \underline{U}_i is a column vector whose first i entries are one and the remainder are zero.

Furthermore, by writing the mn element of the matrix P_{kj} as P_{kj}^{mn} , and from Equation (3.2-4e), we can identify the relation

$$P_{kj}^{mn} = a_{mj} a_{nj} e^{j\omega_k (\Delta_{m-1,j} - \Delta_{n-1,j})} ; \quad m = 1, 2, \dots, M \\ n = 1, 2, \dots, M . \quad (3.2-5a)$$

Now utilizing the relation in Equation (3.2-4j), we obtain

$$P_{kj}^{mn} = a_{mj} a_{nj} e^{j\omega_k (\underline{U}_{m-1} - \underline{U}_{n-1})^T \underline{\tau}_j} . \quad (3.2-5b)$$

Thus we have shown that the observation covariance matrix can be expressed as a function of inter-sensor time delays instead of the actual propagation delays. Therefore, the direct observable quantities are time delays instead of the propagation delays.

Using Equation (3.2-4c) in (3.2-3c), one obtains an alternate expression for the observation covariance matrix:

$$R_k = \sum_{j=1}^J S_{kj} P_{kj} + N_k Q_k . \quad (3.2-6)$$

Equation (3.2-6) can also be summed in the following way:

$$\begin{aligned} R_k &= S_{k1} P_{k1} + \tilde{N}_{k1} \tilde{Q}_{k1} \\ &= S_{k2} P_{k2} + \tilde{N}_{k2} \tilde{Q}_{k2} \\ &\quad \cdot \quad \cdot \quad \cdot \quad \cdot \\ &\quad \cdot \quad \cdot \quad \cdot \quad \cdot \\ &\quad \cdot \quad \cdot \quad \cdot \quad \cdot \\ &= S_{kJ} P_{kJ} + \tilde{N}_{kJ} \tilde{Q}_{kJ} \end{aligned} \quad (3.2-7a)$$

where

$$\tilde{N}_{kj} = \sum_{\substack{i=1 \\ i \neq j}}^J S_{ki} + N_k ; \quad j = 1, 2, \dots, J \quad (3.2-7b)$$

and

$$\tilde{Q}_{kj} = \left(\sum_{\substack{i=1 \\ i \neq j}}^J S_{ki} P_{ki} + N_k Q_k \right) / \tilde{N}_{kj} . \quad (3.2-7c)$$

Note that \tilde{Q}_{kj} can be regarded as an equivalent noise process and is independent of the parameter τ_j . For simplicity we shall assume the propagation attenuation coefficients are known and, for convenience, assume they are equal to unity.

Finally, writing the incremental (intersensor) time delay vector for all targets as

$$\underline{\theta} = (\underline{\tau}_1^T \underline{\tau}_2^T \dots \underline{\tau}_J^T)^T , \quad (3.2-8)$$

a p-parameter column vector where $p = J(M-1)$, the vector log-likelihood function (Equations (3.2-3a) and (3.2-3b)) becomes

$$\Lambda(\underline{\theta}) = -MB \log(\pi) - \sum_{k=1}^B \Lambda_k(\underline{\theta}) \quad (3.2-9)$$

where

$$\Lambda_k(\underline{\theta}) = \log |R_k| + \underline{\alpha}_k^* R_k^{-1} \underline{\alpha}_k . \quad (3.2-10)$$

The MLE of $\underline{\theta}$ is one that maximizes the likelihood function $\Lambda(\underline{\theta})$. A necessary condition for the location of the maximum is given by the vector likelihood equation

$$\nabla \Lambda(\underline{\theta}) = - \sum_{k=1}^B \nabla \Lambda_k(\underline{\theta}) = \underline{0} \quad (3.2-11)$$

where ∇ is the gradient operator given by the column vector

$$\nabla = \left(\frac{\partial}{\partial \theta_1} \frac{\partial}{\partial \theta_2} \cdots \frac{\partial}{\partial \theta_p} \right)^T. \quad (3.2-12)$$

3.3 MULTIPLE PARAMETER ESTIMATION

It was shown in the previous section that the optimal estimate of the time delay vector is hinged on solving the vector likelihood equation. For the MLE, we have

$$\underline{f}(\underline{\theta}) \triangleq \nabla \Lambda(\underline{\theta}) = - \sum_{k=1}^B \nabla \Lambda_k(\underline{\theta}) = \underline{0} \quad (3.3-1)$$

where $\underline{f}(\underline{\theta})$ is a vector function. The likelihood function $\Lambda_k(\underline{\theta})$ is defined as in Equation (3.2-10).

In this section we examine the solution of the likelihood equation in general and in Section 3.5 we explore in detail the structure of the optimum multitarget, multisensor processor.

Let θ_j denote the jth element of the time delay vector $\underline{\theta}$, then Equation (3.3-1) can be written as

$$\frac{\partial}{\partial \theta_j} \Lambda(\underline{\theta}) = - \sum_{k=1}^B \frac{\partial}{\partial \theta_j} \Lambda_k(\underline{\theta}) = 0 ; \quad j = 1, 2, \dots, p . \quad (3.3-2)$$

From Equation (3.2-10) we obtain

$$\begin{aligned} \frac{\partial}{\partial \theta_j} \Lambda_k(\underline{\theta}) &= |R_k|^{-1} \frac{\partial}{\partial \theta_j} |R_k| + \underline{\alpha}_k^* \frac{\partial R_k^{-1}}{\partial \theta_j} \underline{\alpha}_k \\ &= \text{tr} \left(R_k^{-1} \frac{\partial R_k}{\partial \theta_j} \right) + \underline{\alpha}_k^* \frac{\partial R_k^{-1}}{\partial \theta_j} \underline{\alpha}_k \end{aligned} \quad (3.3-3)$$

where $\text{tr}()$ denotes the trace of a matrix. Note that the evaluation of the first term is a straightforward application of the chain rule. The exact procedure can be found in Rockmore.²⁸ The derivative of Equation (3.3-3) w.r.t. θ_i is

$$\frac{\partial^2 \Lambda_k}{\partial \theta_i \partial \theta_j} (\underline{\theta}) = \text{tr} \left(\frac{\partial R_k^{-1}}{\partial \theta_i} \frac{\partial R_k}{\partial \theta_j} + R_k^{-1} \frac{\partial^2 R_k}{\partial \theta_i \partial \theta_j} \right) + \underline{\alpha}_k^* \frac{\partial^2 R_k^{-1}}{\partial \theta_i \partial \theta_j} \underline{\alpha}_k . \quad (3.3-4)$$

Using the linear property of the trace operator and the relation

$$\frac{\partial R_k^{-1}}{\partial \theta_i} = -R_k^{-1} \frac{\partial R_k}{\partial \theta_i} R_k^{-1} ,$$

Equation (3.3-4) becomes

$$\frac{\partial^2 \Lambda_k(\underline{\theta})}{\partial \theta_i \partial \theta_j} = -\text{tr} \left(R_k^{-1} \frac{\partial R_k}{\partial \theta_i} R_k^{-1} \frac{\partial R_k}{\partial \theta_j} \right) + \text{tr} \left(R_k^{-1} \frac{\partial^2 R_k}{\partial \theta_i \partial \theta_j} \right) + \underline{\alpha}_k^* \frac{\partial^2 R_k^{-1}}{\partial \theta_i \partial \theta_j} \underline{\alpha}_k. \quad (3.3-5)$$

Equation (3.3-5) is important in evaluating the performance bound of an estimator. Substituting Equation (3.3-3) in Equation (3.3-1), one obtains the set of necessary conditions for the ML estimate:

$$f_i(\underline{\theta}) = - \sum_{k=1}^B \left[\text{tr} \left(R_k^{-1} \frac{\partial R_k}{\partial \theta_i} \right) + \underline{\alpha}_k^* \frac{\partial R_k^{-1}}{\partial \theta_i} \underline{\alpha}_k \right] = 0; i = 1, 2, \dots, p. \quad (3.3-6)$$

Equation (3.3-6) is usually non-linear. The structure of the optimum processor can be found by reducing the required mathematical operations to simplest form. In principle, Equation (3.3-6) can be solved by searching the p-parameter space for a simultaneous null. A more efficient algorithm, however, is implementing a closed-loop null tracker. Further discussion on this important subject is beyond the scope of this study.

We remark that Equation (3.3-6) is the necessary condition for the existence of a maximum. For sufficiency it requires not only

the condition given in Equation (3.3-6) but also the following (Bryson and Ho³¹):

$$\frac{\partial}{\partial \underline{\theta}} f(\underline{\theta}) = \frac{\partial^2 \Lambda(\underline{\theta})}{\partial \underline{\theta}^2} < 0 . \quad (3.3-7)$$

By this we mean the square matrix $\partial^2 \Lambda(\underline{\theta}) / \partial \underline{\theta}^2$ must be negative definite.

3.4 ESTIMATOR PERFORMANCE EVALUATION

In this section we derive the multi-parameter CRLB and show that the resulting estimate obtained from solving Equation (3.3-6) satisfies the bound for a large observation time. Therefore, the resulting estimate is efficient.

The CRLB for an unbiased estimate of the i th parameter is given by Van Trees:³²

$$\text{VAR}(\hat{\theta}_i)_{ML} \geq (J^{-1})_{ii} \quad (3.4-1)$$

where $()_{ii}$ denotes the i th diagonal element of a matrix and J is the Fisher Information Matrix whose ij element is defined by

$$J_{ij} \stackrel{\Delta}{=} -E \left(\frac{\partial^2 \Lambda(\underline{\theta})}{\partial \theta_i \partial \theta_j} \right) ; \quad i = 1, 2, \dots, p \quad j = 1, 2, \dots, p \quad (3.4-2)$$

where $\Lambda(\underline{\theta})$ is the log-likelihood function. Using Equations (3.3-2) and (3.3-5) in (3.4-2), we immediately obtain

$$J_{ij} \stackrel{\Delta}{=} - \sum_{k=1}^B \left[\text{tr} \left(R_k^{-1} \frac{\partial R_k}{\partial \theta_i} R_k^{-1} \frac{\partial R_k}{\partial \theta_j} \right) - \text{tr} \left(R_k^{-1} \frac{\partial^2 R_k}{\partial \theta_i \partial \theta_j} + \frac{\partial^2 R_k^{-1}}{\partial \theta_i \partial \theta_j} R_k \right) \right] \Bigg|_{\underline{\theta} = \underline{\theta}_0} \quad (3.4-3)$$

where $\underline{\theta}_0$ denotes the true parameter value. Equation (3.4-3) can be simplified as follows: Taking the derivative of the identity $R_k^{-1} R_k = I$ first w.r.t. θ_j and then w.r.t. θ_i , one obtains the relation

$$\left(R_k^{-1} \frac{\partial^2 R_k}{\partial \theta_i \partial \theta_j} + \frac{\partial^2 R_k^{-1}}{\partial \theta_i \partial \theta_j} R_k \right) = - \left(\frac{\partial R_k^{-1}}{\partial \theta_j} \frac{\partial R_k}{\partial \theta_i} + \frac{\partial R_k^{-1}}{\partial \theta_i} \frac{\partial R_k}{\partial \theta_j} \right). \quad (3.4-4)$$

Substituting Equation (3.4-4) in Equation (3.4-3), the latter can be simplified to

$$J_{ij} = \sum_{k=1}^B \text{tr} \left(R_k^{-1} \frac{\partial R_k}{\partial \theta_j} R_k^{-1} \frac{\partial R_k}{\partial \theta_i} \right) \Bigg|_{\underline{\theta} = \underline{\theta}_0} \quad (3.4-5a)$$

$$= \sum_{k=1}^B \text{tr} \left(- \frac{\partial R_k^{-1}}{\partial \theta_j} \frac{\partial R_k}{\partial \theta_i} \right) \Bigg|_{\underline{\theta} = \underline{\theta}_0} \quad (3.4-5b)$$

Note that because $\text{tr}(AB) = \text{tr}(BA)$, we have $J_{ij} = J_{ji}$. Equation (3.4-5b) agrees with the expression obtained by Bangs.³³ However, the derivation presented here is somewhat simpler and more direct.

Next we proceed to show that the MLE, $\hat{\underline{\theta}}_{ML}$, of $\underline{\theta}$ obtained by simultaneously solving the set of equations in Equation (3.3-6) is unbiased and achieves the CRLB.

$$\text{Let } \underline{f}(\underline{\theta}) = (f_1(\underline{\theta}) \ f_2(\underline{\theta}) \dots \ f_p(\underline{\theta}))^T$$

and write the Taylor series expansion of $\underline{f}(\underline{\theta})$ about the true parameter value $\underline{\theta}_0$ as follows:

$$\underline{f}(\underline{\theta}) = \underline{f}(\underline{\theta}_0) + \left. \frac{\partial \underline{f}(\underline{\theta})}{\partial \underline{\theta}} \right|_{\underline{\theta} = \underline{\theta}_0} (\underline{\theta} - \underline{\theta}_0)_0 + \dots . \quad (3.4-6)$$

Since $\underline{f}(\hat{\underline{\theta}}_{ML}) = 0$ by definition, we have after neglecting higher order terms (small random error assumption):

$$-\underline{f}(\underline{\theta}_0) = \left. \frac{\partial \underline{f}(\underline{\theta}_0)}{\partial \underline{\theta}} \right|_{\underline{\theta} = \underline{\theta}_0} (\hat{\underline{\theta}}_{ML} - \underline{\theta}_0) . \quad (3.4-7)$$

Now assume the law of large number applies so that (for a sufficiently long observation time) one can replace the derivative by its expected value. Taking the expected value on both sides of Equation (3.4-7), one obtains

$$E(\hat{\underline{\theta}}_{ML}) = \underline{\theta}_0 - \left\{ E\left[\frac{\partial \underline{f}(\underline{\theta}_0)}{\partial \underline{\theta}} \right] \right\}^{-1} E[\underline{f}(\underline{\theta}_0)] . \quad (3.4-8)$$

But from Equation (3.3-6)

$$\begin{aligned}
 E[f_i(\underline{\theta}_0)] &= - \sum_{k=1}^B \left[\text{tr} \left(R_k^{-1} \frac{\partial R_k}{\partial \theta_i} \right) + \text{tr} \left(\frac{\partial R_k^{-1}}{\partial \theta_i} R_k \right) \right] \Bigg|_{\underline{\theta} = \underline{\theta}_0} \\
 &= - \sum_{k=1}^B \left[\text{tr} \left(R_k^{-1} \frac{\partial R_k}{\partial \theta_i} + \frac{\partial R_k^{-1}}{\partial \theta_i} R_k \right) \right] \Bigg|_{\underline{\theta} = \underline{\theta}_0}
 \end{aligned}
 \tag{3.4-9}$$

Therefore, $E(\hat{\underline{\theta}}_{ML}) = \underline{\theta}_0$, and $\hat{\underline{\theta}}_{ML}$ is an unbiased estimator. Post multiplying Equation (3.4-7) by its conjugate transpose and taking the expectation yields

$$\begin{aligned}
 E[\underline{f}(\underline{\theta}_0) \underline{f}^*(\underline{\theta}_0)] &= E \left[\frac{\partial \underline{f}(\underline{\theta}_0)}{\partial \underline{\theta}} \right] E \left[(\hat{\underline{\theta}}_{ML} - \underline{\theta}_0) (\hat{\underline{\theta}}_{ML} - \underline{\theta}_0)^T \right] \\
 &\quad E \left[\frac{\partial \underline{f}(\underline{\theta}_0)^*}{\partial \underline{\theta}} \right] .
 \end{aligned}
 \tag{3.4-10}$$

Now recall that $\underline{f}(\underline{\theta}) = \nabla \Lambda(\underline{\theta})$, so one can write

$$E \left[\frac{\partial \underline{f}(\underline{\theta}_0)}{\partial \underline{\theta}} \right] = E \left[\frac{\partial^2 \Lambda(\underline{\theta})}{\partial \underline{\theta}^2} \right] \Bigg|_{\underline{\theta} = \underline{\theta}_0}$$

$$\begin{aligned}
 & \left[\begin{array}{cccc} \frac{\partial^2 \Lambda(\underline{\theta})}{\partial \theta_1^2} & \frac{\partial^2 \Lambda(\underline{\theta})}{\partial \theta_1 \partial \theta_2} & \dots & \frac{\partial^2 \Lambda(\underline{\theta})}{\partial \theta_1 \partial \theta_p} \\ \frac{\partial^2 \Lambda(\underline{\theta})}{\partial \theta_2 \partial \theta_1} & \frac{\partial^2 \Lambda(\underline{\theta})}{\partial \theta_2^2} & \dots & \frac{\partial^2 \Lambda(\underline{\theta})}{\partial \theta_2 \partial \theta_p} \\ \vdots & \vdots & \ddots & \vdots \\ \frac{\partial^2 \Lambda(\underline{\theta})}{\partial \theta_p \partial \theta_1} & \frac{\partial^2 \Lambda(\underline{\theta})}{\partial \theta_p \partial \theta_2} & \dots & \frac{\partial^2 \Lambda(\underline{\theta})}{\partial \theta_p^2} \end{array} \right]_{\underline{\theta} = \underline{\theta}_0} = -J \\
 & = -J .
 \end{aligned} \tag{3.4-11}$$

Furthermore, we have the relation

$$E[\underline{f}(\underline{\theta}_0) \underline{f}^*(\underline{\theta}_0)] = E[\nabla \Lambda(\underline{\theta}) \nabla^T \Lambda(\underline{\theta})]_{\underline{\theta} = \underline{\theta}_0} = J . \tag{3.4-12}$$

Therefore, substituting Equations (3.4-11) and (3.4-12) in (3.4-10) yields

$$\begin{aligned}
 E[(\hat{\underline{\theta}}_{ML} - \underline{\theta}_0)(\hat{\underline{\theta}}_{ML} - \underline{\theta}_0)^T] &= J^{-1} E[\underline{f}(\underline{\theta}_0) \underline{f}^*(\underline{\theta}_0)] J^{-1} \\
 &= J^{-1}
 \end{aligned} \tag{3.4-13a}$$

$$\text{or } \text{VAR}(\hat{\theta}_i)_{ML} = (J^{-1})_{ii} . \tag{3.4-13b}$$

Thus we have shown that the multi-parameter MLE is an efficient, unbiased estimator for large observation time.

3.5 MULTISENSOR, MULTITARGET PARAMETER ESTIMATION

In this section we investigate the detailed structure of the optimum signal processor for multiple parameter estimation. For the purpose of target localization, the parameter set of interest is time delays, range, and bearing. There are two possible approaches in estimating the localization parameters. The first is via a geometric transformation from measured time delays; the second is via a direct range and bearing signal processor. From the results of this study, we will clarify the relative merits between these two approaches. In Section 3.5.1, we derive the optimum multisensor, multitarget time delay processor. In Section 3.5.2 we discuss the various methodologies of obtaining range and bearing. Finally, in Section 3.5.3 we briefly discuss the problem of optimum time delay estimation with unknown target power spectra.

3.5.1 Time Delay Estimation

It was shown in Section 3.3 that the MLE of the time delay parameter vector $\underline{\theta}$ required the simultaneous solution of the vector likelihood equation:

$$\frac{\partial \Lambda(\underline{\theta})}{\partial \theta_j} = - \sum_{k=1}^3 \frac{\partial \Lambda_k(\underline{\theta})}{\partial \theta_j} = 0; \quad j = 1, 2, \dots, J(M-1) \quad (3.5.1-1a)$$

where

$$\frac{\partial \Lambda_k(\underline{\theta})}{\partial \theta_j} = \text{tr} \left(R_k^{-1} \frac{\partial R_k}{\partial \theta_j} \right) + \underline{\alpha}_k^* \frac{\partial R_k^{-1}}{\partial \theta_j} \underline{\alpha}_k . \quad (3.5.1-1b)$$

We will explore the detailed structure of the optimum signal processor by simplifying Equation (3.5.1-1a). Recall from Equation (3.2-6) that

$$R_k = S_{kj} P_{kj} + \tilde{N}_{kj} \tilde{Q}_{kj} \quad (3.5.1-2a)$$

where

$$\tilde{Q}_{kj} = \left(\sum_{\substack{i=1 \\ i \neq j}}^J S_{ki} P_{ki} + N_k Q_k \right) / \tilde{N}_{kj} \quad (3.5.1-2b)$$

and

$$\tilde{N}_{kj} = \sum_{\substack{i=1 \\ i \neq j}}^J S_{ki} + N_k . \quad (3.5.1-2c)$$

For notational simplicity we shall assume in Equation (3.5.1-1a) that there are J targets but with two sensors. The θ_j 's in this case correspond to the time delay for each target. In the case of more than two sensors, θ_j must be replaced by each element of the inter-sensor time delay vector $(\tau_{ij}, \tau_{2j}, \dots, \tau_{M-1,j})$ of target j , where τ_{ij} denotes the time delay between sensors $i+1$ and i of target j .

Applying the well-known matrix inversion Lemma

$(H^T R^{-1} H + M^{-1})^{-1} = M - M H^T (H M H^T + R)^{-1} H M$ to R_k^{-1} , we obtain

$$\begin{aligned} R_k^{-1} &= (S_{kj} P_{kj} + \tilde{N}_{kj} \tilde{Q}_{kj})^{-1} \\ &= \frac{\tilde{Q}_{kj}^{-1}}{\tilde{N}_{kj}} - \frac{S_{kj}/\tilde{N}_{kj}^2}{1 + G_{kj} S_{kj}/\tilde{N}_{kj}} \tilde{Q}_{kj}^{-1} P_{kj} \tilde{Q}_{kj}^{-1} \end{aligned} \quad (3.5.1-3)$$

where $G_{kj} = \underline{v}_k^* \tilde{Q}_{kj}^{-1} \underline{v}_k$ is defined as the effective array gain for target j. The derivative of R_k^{-1} w.r.t. θ_j can be written as

$$\frac{\partial R_k^{-1}}{\partial \theta_j} = -|\tilde{h}_{kj}|^2 \tilde{Q}_{kj}^{-1} \left(\frac{\partial P_{kj}}{\partial \theta_j} - \tilde{a}_{kj} \frac{\partial G_{kj}}{\partial \theta_j} P_{kj} \right) \tilde{Q}_{kj}^{-1} \quad (3.5.1-4a)$$

where we have defined

$$|\tilde{h}_{kj}|^2 = \frac{S_{kj}/\tilde{N}_{kj}^2}{1 + G_{kj} S_{kj}/\tilde{N}_{kj}} \quad (3.5.1-4b)$$

$$\tilde{a}_{kj} = \tilde{N}_{kj} |\tilde{h}_{kj}|^2. \quad (3.5.1-4c)$$

Using Equations (3.5.1-3) and (3.5.1-4a), the first term in Equation (3.5.1-1b) can be written as follows:

$$\begin{aligned} \text{tr} \left(R_k^{-1} \frac{\partial R_k}{\partial \theta_j} \right) &= \frac{S_{kj}}{\tilde{N}_{kj}} \text{tr} \left(\tilde{Q}_{kj}^{-1} \frac{\partial P_{kj}}{\partial \theta_j} \right) \\ &\quad - S_{kj} |\tilde{h}_{kj}|^2 \text{tr} \left(\tilde{Q}_{kj}^{-1} P_{kj} \tilde{Q}_{kj}^{-1} \frac{\partial P_{kj}}{\partial \theta_j} \right). \end{aligned} \quad (3.5.1-5a)$$

But this can be further simplified using the following relations:

$$\begin{aligned}
 \text{tr} \left(\tilde{Q}_{kj}^{-1} \frac{\partial P_{kj}}{\partial \theta_j} \right) &= \text{tr} \left[\tilde{Q}_{kj}^{-1} \left(\frac{\partial v_{kj}}{\partial \theta_j} v_{kj}^* + v_{kj} \frac{\partial v_{kj}^*}{\partial \theta_j} \right) \right] \\
 &= v_{kj}^* \tilde{Q}_{kj}^{-1} \frac{\partial v_{kj}}{\partial \theta_j} + \frac{\partial v_{kj}^*}{\partial \theta_j} \tilde{Q}_{kj}^{-1} v_{kj} \\
 &= \frac{\partial G_{kj}}{\partial \theta_j} \tag{3.5.1-5b}
 \end{aligned}$$

and

$$\begin{aligned}
 \text{tr} \left(\tilde{Q}_{kj}^{-1} P_{kj} \tilde{Q}_{kj}^{-1} \frac{\partial P_{kj}}{\partial \theta_j} \right) &= \text{tr} \left[\tilde{Q}_{kj}^{-1} v_{kj} v_{kj}^* \tilde{Q}_{kj}^{-1} \left(\frac{\partial v_{kj}}{\partial \theta_j} v_{kj}^* \right. \right. \\
 &\quad \left. \left. + v_{kj} \frac{\partial v_{kj}^*}{\partial \theta_j} \right) \right] \\
 &= G_{kj} \frac{\partial G_{kj}}{\partial \theta_j} . \tag{3.5.1-5c}
 \end{aligned}$$

Thus Equation (3.5.1-5a) reduces to

$$\begin{aligned}
 \text{tr} \left(R_k^{-1} \frac{\partial R_k}{\partial \theta_j} \right) &= \frac{s_{kj}}{N_{kj}} \frac{\partial G_{kj}}{\partial \theta_j} - s_{kj} |\tilde{h}_{kj}|^2 G_{kj} \frac{\partial G_{kj}}{\partial \theta_j} \\
 &= \tilde{a}_{kj} \frac{\partial G_{kj}}{\partial \theta_j} . \tag{3.5.1-6}
 \end{aligned}$$

Using Equations (3.5.1-1b), (3.5.1-4a) and (3.5.1-5c) in (3.5.1-1a), the likelihood equation becomes

$$\begin{aligned} \frac{\partial \Lambda(\theta)}{\partial \theta_j} = \sum_{k=1}^B |\tilde{h}_{kj}|^2 &\nabla \tilde{Q}_{kj}^{-1} \left(\frac{\partial p_{kj}}{\partial \theta_j} - \tilde{a}_{kj} \frac{\partial G_{kj}}{\partial \theta_j} p_{kj} \right) \tilde{Q}_{kj}^{-1} \nabla \\ &- \tilde{a}_{kj} \frac{\partial G_{kj}}{\partial \theta_j} \quad j = 1, 1 \dots J \\ &= 0. \end{aligned} \quad (3.5.1-7)$$

Equation (3.5.1-7) reduces to that obtained by Bangs^{33,34} for the single target case. It should be pointed out that our development up to here in many ways parallels Bang's work. However, there are also major differences. We are interested in a multitarget environment while Bangs' work dealt exclusively with single target. We are interested in joint time delay vector estimation while Bangs' work is primarily concerned with range and bearing estimation. Thus, our work in this section can be considered as an extension of Bangs' original work to include the multitarget, multisensor environment.

For time delay estimation, the likelihood equation (Equation (3.5.1-7)) can be further simplified as follows.

Recall from Equations (3.2-4e and (3.2-4j) that the steering vector for target j is

$$v_{kj} = \left(1 e^{j\omega_k U_1^T \tau_j} e^{j\omega_k U_2^T \tau_j} \dots e^{j\omega_k U_{M-1}^T \tau_j} \right)^T \quad (3.5.1-8a)$$

where the attenuation coefficients a_{ij} were assumed known and for convenience they were assumed to have unity.

Therefore, the mn element of P_{kj} is

$$P_{kj}^{mn} = e^{j\omega_k (U_{m-1} - U_{n-1})^T \tau_j}, \quad (3.5.1-8b)$$

but

$$\begin{aligned} \frac{\partial P_{kj}^{mn}}{\partial \tau_{ij}} &= j\omega_k (U_{m-1} - U_{n-1})^T \frac{\partial \tau_j}{\partial \tau_{ij}} \left[e^{j\omega_k (U_{m-1} - U_{n-1})^T \tau_j} \right] \\ &= j\omega_k \Phi_i^{mn} P_{kj}^{mn} \end{aligned} \quad (3.5.1-8c)$$

where $\Phi^{mn} = (U_{m-1} - U_{n-1})^T \tau_j$ and Φ_i^{mn} is defined as the mn element of the matrix Φ_i given by

$$\Phi_i^{mn} = \frac{\partial \Phi^{mn}}{\partial \tau_{ij}}$$

$$= (U_{m-1} - U_{n-1})^T \frac{\partial \tau_j}{\partial \tau_{ij}} ; \quad \begin{array}{l} i = 1, 2, \dots, M-1 \\ m = 1, 2, \dots, M \\ n = 1, 2, \dots, M \end{array}$$

$$= \begin{cases} 1 & ; \text{ if } n \leq i \leq m-1 \\ -1 & ; \text{ if } m \leq i \leq n-1 \\ 0 & ; \text{ otherwise} \end{cases} . \quad (3.5.1-8d)$$

Note that for a system of M sensors, Φ_i is an $M \times M$ matrix.

For example, let $M = 3$, then

$$\Phi_1 = \begin{bmatrix} 0 & -1 & -1 \\ 1 & 0 & 0 \\ 1 & 0 & 0 \end{bmatrix} ; \quad \Phi_2 = \begin{bmatrix} 0 & 0 & -1 \\ 0 & 0 & -1 \\ 1 & 1 & 0 \end{bmatrix} .$$

Define 1_M as an $M \times M$ square matrix of ones, and V_{kj} as a diagonal "steering matrix", whose diagonal elements correspond to the elements of the steering vector v_{kj} ; i.e.,

$$V_{kj} = \text{diag} \left\{ i, e^{j\omega_k U_1^T \tau_j}, e^{j\omega_k U_2^T \tau_j}, \dots, e^{j\omega_k U_{M-1}^T \tau_j} \right\}. \quad (3.5.1-9)$$

Then the following relations can be easily established:

$$P_{kj} = V_{kj} 1_M V_{kj}^* \quad (3.5.1-10a)$$

and

$$\frac{\partial P_{kj}}{\partial \tau_{ij}} = j\omega_k V_{kj} \Phi_i V_{kj}^*. \quad (3.5.1-10b)$$

Furthermore, using Equation (3.5.1-10b), Equation (3.5.1-5b) can be written as

$$\frac{\partial G_{kj}}{\partial \tau_{ij}} = j\omega_k \operatorname{tr}(\tilde{Q}_{kj}^{-1} v_{kj} \Phi_i v_{kj}^*) . \quad (3.5.1-10c)$$

Finally, using Equations (3.5.1-10a), (3.5.1-10b), (3.5.1-10c) and replacing e_j by τ_{ij} , the likelihood equation (Equation (3.5.1-7)) can be simplified to

$$\begin{aligned} \frac{\partial \Lambda(\underline{\tau})}{\partial \tau_{ij}} &= \sum_{k=1}^B j\omega_k \left[|\tilde{h}_{kj}|^2 \underline{\alpha}_k^* \tilde{Q}_{kj}^{-1} v_{kj} (\Phi_i - \tilde{b}_i^{kj} \mathbf{1}_M) v_{kj}^* \tilde{Q}_{kj}^{-1} \underline{\alpha}_k - \tilde{b}_i^{kj} \right] \\ &= 0 \end{aligned} \quad (3.5.1-11a)$$

where

$$\tilde{b}_i^{kj} = \tilde{a}_{kj} \operatorname{tr}(\tilde{Q}_{kj}^{-1} v_{kj} \Phi_i v_{kj}^*) \quad (3.5.1-11b)$$

is the bias correction term and for $i = 1, 2, \dots, M-1$ and $j = 1, 2, \dots, J$ where M is the number of sensors and J is the number of targets. Note that the $J(M - 1)$ equations are coupled and must be solved jointly for the stationary point. For long observation time such that the frequency samples are dense over the frequency bands of the signal and the noise, the summation in Equation (3.5.1-11a) can be replaced by integration as follows:

$$\begin{aligned}
 Z_{ij}(\underline{\tau}) &= \frac{\partial \Lambda(\underline{\tau})}{\partial \tau_{ij}} \\
 &= \frac{T}{2\pi} \int_0^\infty j\omega \left\{ |\tilde{h}_j(\omega)|^2 \underline{\alpha}^*(\omega) \tilde{Q}_j^{-1}(\omega) v_j(\omega) [\Phi_i - b_i^j(\omega) 1_M] \right. \\
 &\quad \left. v_j^*(\omega) \tilde{Q}_j^{-1}(\omega) \underline{\alpha}(\omega)/T - \tilde{b}_i^j(\omega) \right\} d\omega ; \\
 i &= 1, 2, \dots, M-1 \\
 j &= 1, 2, \dots, J.
 \end{aligned}
 \tag{3.5.1-12a}$$

Note that in obtaining Equation (3.5.1-12a) the relations $T\alpha_k = \alpha(\omega)$ and $|\tilde{h}_k|^2 = T|\tilde{h}(\omega)|^2$ have been used.

It is recalled that for the j th target

$$|\tilde{h}_j(\omega)|^2 = \frac{S_j(\omega)/\tilde{N}_j^2(\omega)}{1 + G_j(\omega) S_j(\omega)/\tilde{N}_j(\omega)}
 \tag{3.5.1-12b}$$

$$\tilde{a}_j(\omega) = \tilde{N}_j(\omega) |\tilde{h}_j(\omega)|^2
 \tag{3.5.1-12c}$$

$$\tilde{b}_i^j(\omega) = \tilde{a}_j(\omega) \operatorname{tr} [\tilde{Q}_j^{-1}(\omega) v_j(\omega) \Phi_i(\omega) v_j^*(\omega)]
 \tag{3.5.1-12d}$$

$$\tilde{Q}_j^{-1}(\omega) = \tilde{N}_j(\omega) \left[\sum_{\substack{i=1 \\ i \neq j}}^J S_i(\omega) P_i(\omega) + N(\omega) Q(\omega) \right]^{-1}
 \tag{3.5.1-12e}$$

$$\tilde{N}_j(\omega) = \sum_{\substack{i=1 \\ i \neq j}}^J S_i(\omega) + N(\omega) \quad (3.5.1-12f)$$

$$P_j(\omega) = V_j(\omega) I_M V_j^*(\omega) \quad (3.5.1-12g)$$

and

$$G_j(\omega) = V_j^*(\omega) \tilde{Q}_j^{-1}(\omega) V_j(\omega) . \quad (3.5.1-12h)$$

The optimum multitarget, multisensor time delay signal processor is shown in Figure 3-1. There is a total of $J(M - 1)$ processing channels for the case of M sensors and J targets. For simplicity we show a single processing channel. Note that the processing channels are tightly coupled. The signal conditioning filters depend on the time delay parameters from other processing channels as well. This is an order of magnitude more complex compared to a single target case. A number of suboptimal realizations can be found as discussed in Section 4. Finally, we remark that for convenience, we show the optimum processor (Figure 3-1) in the continuous frequency domain. For practical considerations, the discrete counterpart, Equation (3.5.1-11a), is normally used since the correlation process can be mechanized easily via the Fast Fourier Transform (FFT) algorithm.

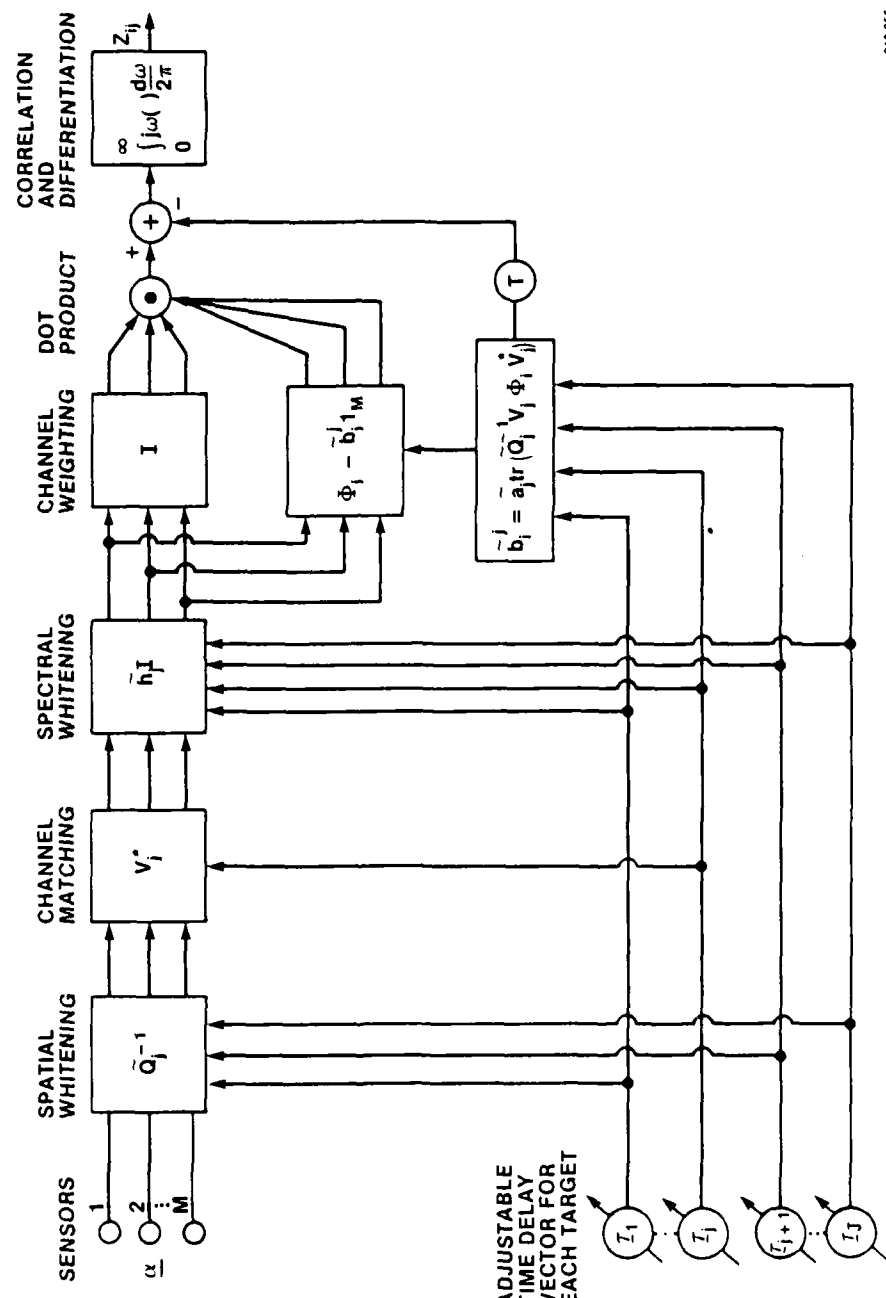


Figure 3-1. A Multisensor, Multitarget Time Delay Processing Channel

Using Equations (3.5.1-12b-f), we shall study the specific structure of the optimum time delay processor for a number of simple but important cases.

3.5.1.1 Case 1: One Target and Two Sensors ($J = 1, M = 2$).

For convenience we assume $Q(\omega) = I$; i.e., the noise processes are equal in power and uncorrelated between sensors. Noise processes being uncorrelated between sensors is a reasonable assumption since in practice sensors are separated at least at a half wavelength spacing.

The steering vector is $\underline{v} = (1 \ e^{j\omega\tau})^T$. The following relations can be verified easily:

$$\tilde{Q}^{-1}(\omega) = Q^{-1}(\omega) = I \quad (3.5.1-13a)$$

$$G(\omega) = \underline{v}^* Q^{-1} \underline{v} = 2 \quad (3.5.1-13b)$$

$$b(\omega) = \text{tr}(Q^{-1} V \Phi_1 V^*) = 0 \quad (3.5.1-13c)$$

$$|\tilde{h}(\omega)|^2 = \frac{S(\omega)/N^2(\omega)}{1 + 2 S(\omega)/N(\omega)} \quad (3.5.1-13d)$$

and

$$\Phi_1 = \begin{bmatrix} 0 & -1 \\ 1 & 0 \end{bmatrix}; V = \begin{bmatrix} 1 & 0 \\ 0 & e^{j\omega\tau} \end{bmatrix}. \quad (3.5.1-13e)$$

Thus from Equation (3.5.1-12a), the likelihood equation is

$$Z(\tau) = \frac{1}{2\pi} \int_0^\infty j\omega |\tilde{h}|^2 \underline{\alpha}^* V \Phi_1 V^* \underline{\alpha} d\omega = 0. \quad (3.5.1-14a)$$

This simple time delay processor is diagrammed in Figure 3-2. This processor is identical to the one studied by Carter³⁵ and can be shown as follows. From Equation (3.5.1-14a), we have

$$\begin{aligned} Z(\tau) &= \frac{1}{2\pi} \int_0^\infty j\omega |\tilde{h}|^2 \underline{\alpha}^* \begin{bmatrix} 1 & 0 \\ 0 & e^{j\omega\tau} \end{bmatrix} \begin{bmatrix} 0 & -1 \\ 1 & 0 \end{bmatrix} \begin{bmatrix} 1 & 0 \\ 0 & e^{-j\omega\tau} \end{bmatrix} \underline{\alpha} d\omega \\ &= \frac{T}{2\pi} \int_{-\infty}^\infty j\omega |\tilde{h}|^2 \frac{\alpha_1(\omega) \alpha_2^*(\omega)}{T} e^{j\omega\tau} d\omega \\ &= \frac{T}{2\pi} \int_{-\infty}^\infty j\omega |\tilde{h}|^2 G_{12}(\omega) e^{j\omega\tau} d\omega \\ &= T \frac{\partial}{\partial \tau} \int_{-\infty}^\infty |\tilde{h}|^2 G_{12}(\omega) e^{j\omega\tau} \frac{d\omega}{2\pi} \\ &= T \frac{\partial}{\partial \tau} R_{12}(\tau) \end{aligned} \quad (3.5.1-14b)$$

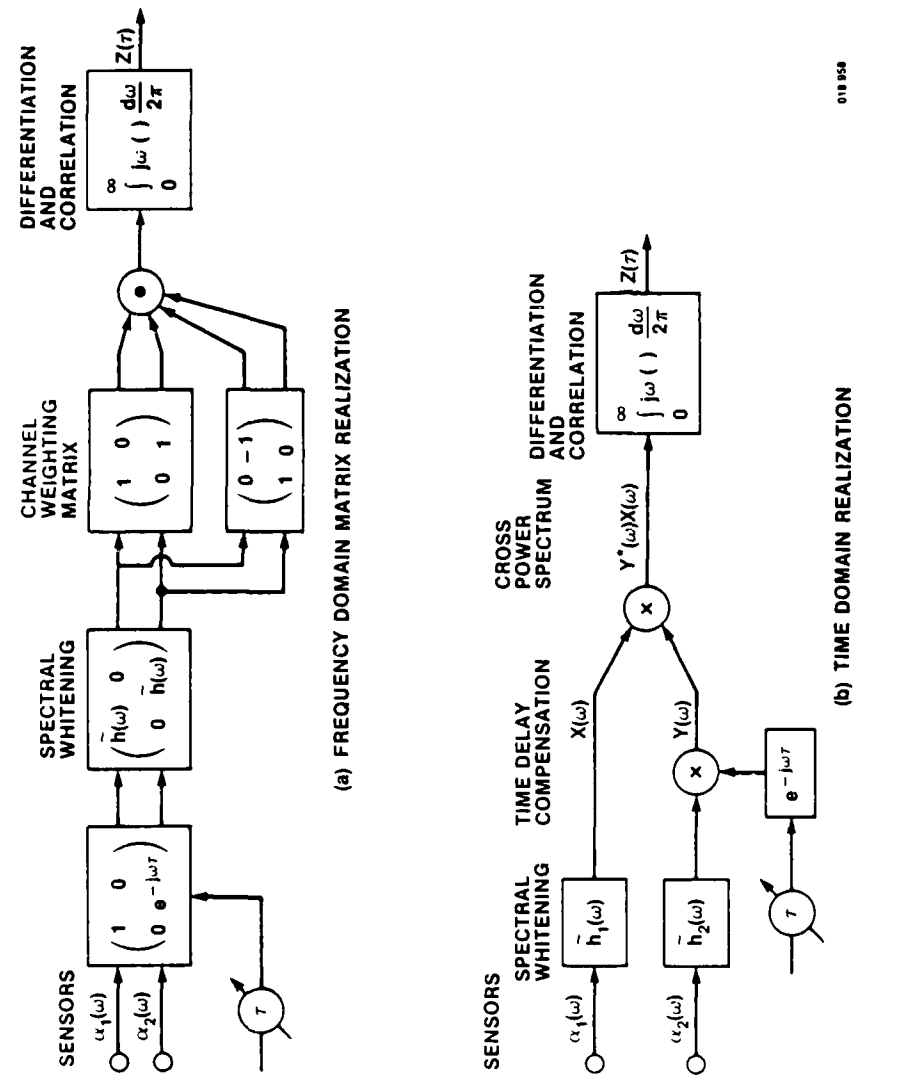


Figure 3-2. Optimum Two-Sensor, One-Target Time Delay Processor

where G_{12} is the estimated cross power spectrum between channels $\alpha_1(\omega)$ and $\alpha_2(\omega)$, and $R_{12}(\tau)$ is the GCC function studied by Knapp and Carter.¹ A block diagram of this processor is shown in Figure 3-2(b). Note that the null of $Z(\tau)$ corresponds to the peak of $R_{12}(\tau)$. Furthermore, the discrete form of Equation (3.5.1-14b) is

$$Z(\tau) = \sum_{k=-B}^B j\omega_k |h_k|^2 \alpha_{1k} \alpha_{2k}^* e^{j\omega_k \tau} \quad (3.5.1-14c)$$

$$= \frac{\partial}{\partial \tau} \sum_{k=-B}^B |h_k|^2 \alpha_{1k} \alpha_{2k}^* e^{j\omega_k \tau}. \quad (3.5.1-14d)$$

From Equation (3.5.1-14b), we note that the GCC function is directly proportional to the likelihood function. The optimum estimate is determined by locating the peak of the GCC function or, equivalently, the null of its derivative. We have shown in Section 3.4 that the MLE is efficient for a long observation time. We have also obtained a general closed form expression for the CRLB. The CRLB for this case can be determined easily. From Equations (3.4-1) and (3.4-5) we have

$$\text{VAR}(\hat{\tau}) \geq \left[\sum_{k=1}^B \text{tr} \left(- \frac{\partial R_k^{-1}}{\partial \tau} \frac{\partial R_k}{\partial \tau} \right) \right]^{-1}. \quad (3.5.1-15a)$$

Now combining Equations (3.5.1-4a) and (3.5.1-10b), we obtain

$$\frac{\partial R_k}{\partial \tau} = S_k \frac{\partial P_k}{\partial \tau} = j\omega_k S_k v_k \phi_1 v_k^* \quad (3.5.1-15b)$$

$$\frac{\partial R_k^{-1}}{\partial \tau} = -j\omega_k |\tilde{h}_k|^2 v_k \phi_1 v_k^*. \quad (3.5.1-15c)$$

Thus

$$\text{tr} \left(-\frac{\partial R_k^{-1}}{\partial \tau} \frac{\partial R_k}{\partial \tau} \right) = -\omega_k^2 |\tilde{h}_k|^2 S_k \text{tr}(v_k \phi_1^2 v_k^*) \quad (3.5.1-15d)$$

$$= 2\omega_k^2 |\tilde{h}_k|^2 S_k$$

and the CRLB is

$$\text{VAR}(\hat{\tau}) \geq \left(2 \sum_{k=1}^B \omega_k^2 \frac{S_k^2/N_k^2}{1 + 2 S_k/N_k} \right)^{-1} \quad (3.5.1-16a)$$

$$\geq 2\pi \left(2T \int_0^\infty \frac{c(\omega)}{1 - c(\omega)} \omega^2 d\omega \right)^{-1} \quad (3.5.1-16b)$$

which is identical to the expression derived by Carter.² Note that T is the observation time and

$$c(\omega) = \left(\frac{S(\omega)}{S(\omega) + N(\omega)} \right)^2 \quad (3.5.1-16c)$$

is known as the magnitude square coherence (MSC) function for the case of two equal-noise power channels.

3.5.1.2 Case 2: Two Targets and Two Sensors ($J = 2, M = 2$).

Again assuming $Q_k = I$ for simplicity. The parameter vector consists of two elements; i.e., $\underline{\theta} = (\tau_1, \tau_2)^T$, the time delays to target number one and target number two. The optimum estimates can be obtained by solving simultaneously the two likelihood equations:

$$\begin{aligned} \frac{\partial \Lambda(\tau_1, \tau_2)}{\partial \tau_1} &= \int_0^\infty j\omega \{ |\tilde{h}_1|^2 \underline{\alpha}^* \tilde{Q}_1^{-1} v_1 [\Phi_1 - \tilde{b}_1 1_M] v_1^* \tilde{Q}_1^{-1} \underline{\alpha} - T \tilde{b}_1 \} \frac{d\omega}{2\pi} \\ &= 0 \end{aligned} \quad (3.5.1-17a)$$

$$\begin{aligned} \frac{\partial \Lambda(\tau_1, \tau_2)}{\partial \tau_2} &= \int_0^\infty j\omega \{ |\tilde{h}_2|^2 \underline{\alpha}^* \tilde{Q}_2^{-1} v_2 [\Phi_1 - \tilde{b}_2 1_M] v_2^* \tilde{Q}_2^{-1} \underline{\alpha} - T \tilde{b}_2 \} \frac{d\omega}{2\pi} \\ &= 0 \end{aligned} \quad (3.5.1-17b)$$

where for notational simplicity, we have suppressed the frequency dependency. The two likelihood equations can be further simplified using the following relations:

$$|\tilde{h}_1|^2 = \frac{s_1/(s_2 + N)^2}{1 + G_1 s_1/(s_2 + N)} \quad (3.5.1-17c)$$

$$\tilde{a}_1 = \frac{s_1/(s_2 + N)}{1 + G_1 s_1/(s_2 + N)} \quad (3.5.1-17d)$$

$$\begin{aligned} \tilde{b}_1 &= \tilde{a}_1 \operatorname{tr} \left(\tilde{\Phi}_1^{-1} \frac{\partial p_1}{\partial \tau_1} \right) \\ &= -\tilde{a}_1 \tilde{c}_2 \operatorname{tr} [(\underline{v}_2^* \underline{v}_1)^* \mathbf{1}_M (\underline{v}_2^* \underline{v}_1) \Phi_1] \end{aligned} \quad (3.5.1-17e)$$

$$\tilde{c}_2 = \frac{(1 + s_2/N) s_2/N}{1 + 2 s_2/N} \quad (3.5.1-17f)$$

$$G_1 = 2(1 + s_2/N) - \tilde{c}_2 |\underline{v}_1^* \underline{v}_2|^2 \quad (3.5.1-17g)$$

and

$$\Phi_1 = \begin{bmatrix} 0 & -1 \\ 1 & 0 \end{bmatrix}. \quad (3.5.1-17h)$$

By exchanging indices between 1 and 2, we obtain a similar set of equations for the second processor channel. Therefore, a simpler form of the likelihood equation is:

$$\begin{aligned} \frac{\partial \Lambda(\tau_1, \tau_2)}{\partial \tau_1} &= \frac{T}{2\pi} \int_0^\infty j\omega e^{j\omega\tau_1} d\omega \left[|\tilde{h}_1|^2 \tilde{G}_{x_1 x_2}(\omega) \right. \\ &\quad \left. + \tilde{a}_1 \tilde{c}_2 (1 + \frac{1}{T} |\tilde{h}_1 v_1^* \tilde{Q}_1^{-1} \underline{a}|^2) e^{-j\omega\tau_2} \right] \\ &= 0 \end{aligned} \quad (3.5.1-18a)$$

$$\begin{aligned} \frac{\partial \Lambda(\tau_1, \tau_2)}{\partial \tau_2} &= \frac{T}{2\pi} \int_0^\infty j\omega e^{j\omega\tau_2} d\omega \left[|\tilde{h}_2|^2 \tilde{G}_{y_1 y_2}(\omega) \right. \\ &\quad \left. + \bar{a}_2 c_1 (1 + \frac{1}{T} |\tilde{h}_2 v_2^* \tilde{Q}_2^{-1} \underline{a}|^2) e^{-j\omega\tau_1} \right] \\ &= 0 \end{aligned} \quad (3.5.1-18b)$$

where

$$\underline{x} = \tilde{Q}_1^{-1} \underline{a}$$

$$\underline{y} = \tilde{Q}_2^{-1} \underline{a}$$

and

$$\tilde{G}_{x_1 x_2}(\omega) = \frac{x_1(\omega) x_2^*(\omega)}{T}$$

$$\tilde{G}_{y_1 y_2}(\omega) = \frac{y_1(\omega) y_2^*(\omega)}{T}$$

are the cross power spectra, respectively, for \underline{x} and \underline{y} .

Substituting Equations (3.5.1-17g and f) in Equation (3.5.1-17c) yields the optimum two-target, two-sensor spectral shaping filters:

$$|\tilde{h}_1|^2 = \frac{s_1/(s_2+N)^2}{1 + \left(2 - \frac{s_2/N}{1 + 2 s_2/N} |\underline{v}_1^* \underline{v}_2|^2 \right) s_1/N} \quad (3.5.1-18c)$$

and similarly,

$$|\tilde{h}_2|^2 = \frac{s_2/(s_1+N)^2}{1 + \left(2 - \frac{s_1/N}{1 + 2 s_1/N} |\underline{v}_2^* \underline{v}_1|^2 \right) s_2/N} . \quad (3.5.1-18d)$$

Note that the filters $|\tilde{h}_1|^2$ and $|\tilde{h}_2|^2$ are a function of the steering vectors, and that the target of interest is treated as part of the signal process and remaining targets are treated as part of the noise process.

A block diagram of this dual channel processor is shown in Figure 3-3. It is seen that the dual processor is tightly coupled. In Chapters 4 and 5 we discuss a number of suboptimum procedures for simplifying the complex structure of this processor in light of improved multitarget time delay resolution.

Using Equations (3.4-1) and (3.4-5), the CRLB of the time delay estimates for the two-target, two-sensor case can be found as follows:

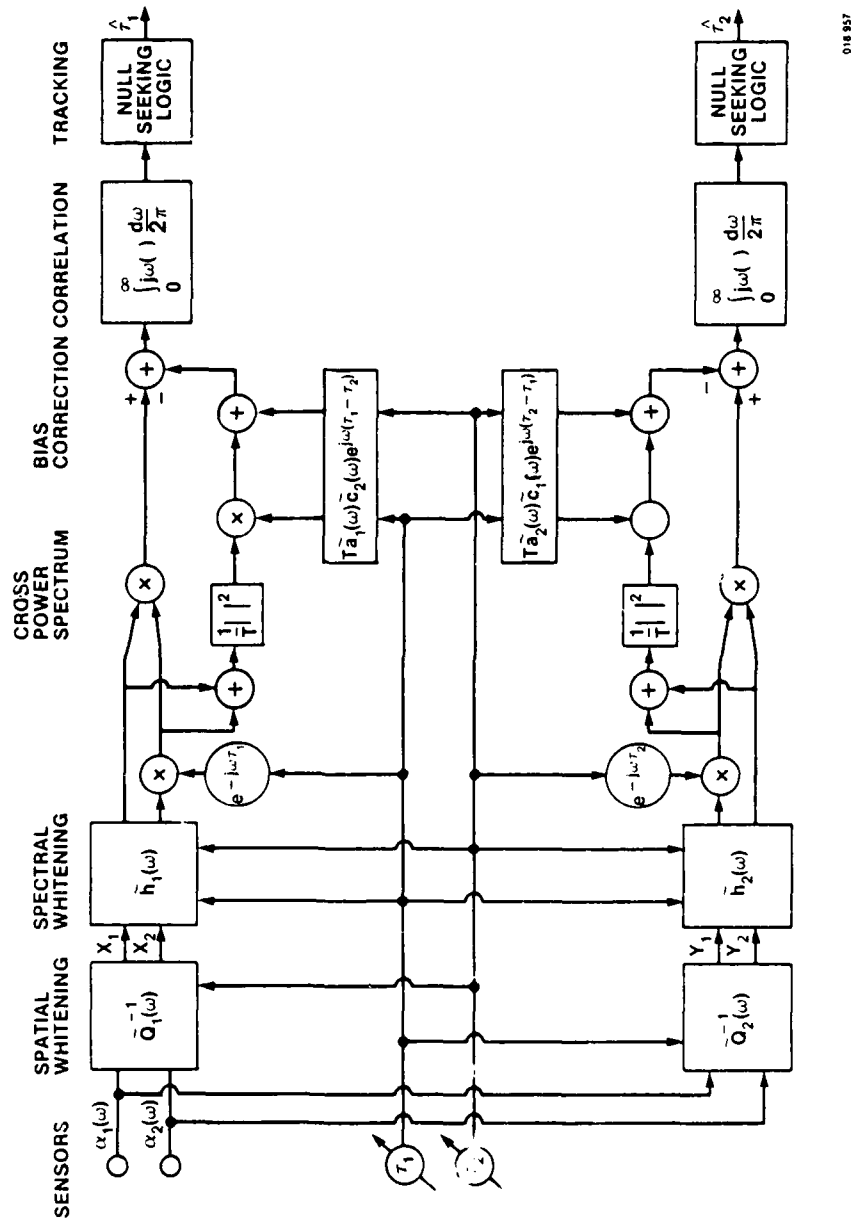


Figure 3-3. Optimum Two-Sensor, Two-Target Time Delay Processor

018 557

$$\text{VAR}(\hat{\tau}_i) \geq \frac{1}{(1 - M_{12}^2)} \frac{1}{J_{ii}} ; \quad i = 1, 2 \quad (3.5.1-19a)$$

where M_{12} is the coefficient of mutual dependence given by

$$M_{12} = \frac{J_{12}}{(J_{11} J_{22})^{1/2}} \quad (3.5.1-19b)$$

and the quantities J_{ij} are defined by (Equation (3.4-5))

$$J_{ij} = \sum_{k=1}^B \left[\text{tr} \left(- \frac{\partial R_k^{-1}}{\partial \tau_i} \frac{\partial R_k}{\partial \tau_j} \right) \right] . \quad (3.5.1-19c)$$

From the relations

$$R_k = S_{k1} P_{k1} + S_{k2} P_{k2} + N_k I \quad (3.5.1-19d)$$

and

$$- \frac{\partial R_k^{-1}}{\partial \tau_i} = |\tilde{h}_{ki}|^2 \tilde{Q}_{ki}^{-1} \left(\frac{\partial P_{ki}}{\partial \tau_i} - \tilde{\alpha}_{ki} \frac{\partial G_{ki}}{\partial \tau_i} P_{ki} \right) \tilde{Q}_{ki}^{-1} ; \quad i = 1, 2 \quad (3.5.1-19e)$$

one obtains after some straightforward but tedious algebraic manipulations: (See Appendix B)

$$J_{11} = \frac{\pi}{\pi} \int_0^\infty \omega^2 \left[\frac{(S_1/N)^2}{1 + G_1 S_1 / (S_2 + N)} \right] \left[\frac{1 + S_2/N}{1 + 2 S_2/N} \right]^2 \gamma_1 d\omega \quad (3.5.1-20a)$$

$$J_{12} = \frac{T}{\pi} \int_0^\infty \omega^2 \left[\frac{S_1 S_2 / N^2}{1 + G_1 S_1 / (S_2 + N)} \right] \left[\frac{1}{1 + 2 S_2 / N} \right] \gamma_{12} d\omega \quad (3.5.1-20b)$$

$$J_{22} = \frac{T}{\pi} \int_0^\infty \omega^2 \left[\frac{(S_2 / N)^2}{1 + G_2 S_2 / (S_1 + N)} \right] \left[\frac{1 + S_1 / N}{1 + 2 S_1 / N} \right]^2 \gamma_2 d\omega. \quad (3.5.1-20c)$$

Therefore, using Equation (3.5.1-19) the CRLB of the optimum two-sensor two-target time delay estimates is given by

$$\text{VAR}(\hat{\tau}_1) \geq \frac{2\pi}{(1 - M_{12}^2)} \left\{ 2T \int_0^\infty \omega^2 \left[\frac{(S_1 / N)^2}{1 + G_1 S_1 / (S_2 + N)} \right] \left[\frac{1 + S_2 / N}{1 + 2 S_2 / N} \right]^2 \gamma_1 d\omega \right\}^{-1} \quad (3.5.1-21a)$$

$$\text{VAR}(\hat{\tau}_2) \geq \frac{2\pi}{(1 - M_{12}^2)} \left\{ 2T \int_0^\infty \omega^2 \left[\frac{(S_2 / N)^2}{1 + G_2 S_2 / (S_1 + N)} \right] \left[\frac{1 + S_1 / N}{1 + 2 S_1 / N} \right]^2 \gamma_2 d\omega \right\}^{-1} \quad (3.5.1-21b)$$

where

$$G_1 = (1 + S_2/N) \left[2 - \left(\frac{S_2/N}{1 + 2 S_2/N} \right) |\underline{v}_1^* \underline{v}_2|^2 \right] \quad (3.5.1-22a)$$

$$G_2 = (1 + S_1/N) \left[2 - \left(\frac{S_1/N}{1 + 2 S_1/N} \right) |\underline{v}_2^* \underline{v}_1|^2 \right] \quad (3.5.1-22b)$$

and the quantities γ_1 , γ_{12} and γ_2 are given by (Appendix B):

$$\gamma_1 = 1 - \left(\frac{S_2/N}{1 + S_2/N} \right)^2 \sum_{n=0}^3 A_n \cos^n \omega \Delta_{12} \quad (3.5.1-23a)$$

$$\gamma_{12} = \cos \omega \Delta_{12} - 2 \left\{ \frac{S_1 S_2/N^2}{[1 + G_1 S_1/(S_2 + N)] (1 + 2 S_2/N)} \right\} \sin^2 \omega \Delta_{12} \quad (3.5.1-23b)$$

and

$$\gamma_2 = 1 - \left(\frac{S_1/N}{1 + S_1/N} \right)^2 \sum_{n=0}^3 B_n \cos^n \omega \Delta_{12} \quad (3.5.1-23c)$$

where $\Delta_{12} = \tau_1 - \tau_2$ is the time delay separation between targets 1 and 2. A_n , B_n are defined by the following:

$$A_0 = 4 \left[\frac{S_1/N}{1 + G_1 S_1/(S_2 + N)} \right] \left[\frac{1 + S_2/N}{1 + 2 S_2/N} \right] - 1 \quad (3.5.1-24a)$$

$$A_1 = -4 \left[\frac{S_1/N}{1 + G_1 S_1/(S_2 + N)} \right] \left[\frac{S_2/N}{1 + 2 S_2/N} \right] \quad (3.5.1-24b)$$

$$A_2 = 1 - A_0 \quad (3.5.1-24c)$$

$$A_3 = -A_1 \quad (3.5.1-24d)$$

$$B_0 = 4 \left[\frac{S_2/N}{1 + G_2 S_2/(S_1 + N)} \right] \left[\frac{1 + S_1/N}{1 + 2 S_1/N} \right] - 1 \quad (3.5.1-24e)$$

$$B_1 = -4 \left[\frac{S_1/N}{1 + G_2 S_2/(S_1 + N)} \right] \left[\frac{S_2/N}{1 + 2 S_1/N} \right] \quad (3.5.1-24f)$$

$$B_2 = 1 - B_0 \quad (3.5.1-24g)$$

$$B_3 = -B_1 . \quad (3.5.1-24h)$$

Note that if both targets have identical power spectra ($S_1 = S_2$) and identical time delays ($\tau_1 = \tau_2$) then it can be shown that

$$\gamma_1 = \frac{1 + 2 (S_2/N)}{(1 + S_2/N)^2} \quad (3.5.1-25a)$$

$$\gamma_2 = \frac{1 + 2 S_1/N}{(1 + S_1/N)^2} \quad (3.5.1-25b)$$

$$\gamma_{12} = 1 . \quad (3.5.1-25c)$$

Therefore, using Equations (3.5.1-25a-c) in (3.5.1-20a-c), we obtain $J_{11} = J_{22} = J_{12}$. Hence, $M_{12}^2 = J_{12}^2/(J_{11}J_{22}) = 1$. Thus, the time delay variance is infinite indicating the inherent inappropriateness of a two-target formulation to a one-target problem.

Another observation is that letting the interference power be zero (i.e., $S_2 = 0$), Equation (3.5.1-20a) reduces to Equation (3.5.1-16a), the time delay CRLB for the single target case. Note that because of the following inequality:

$$\int_0^\infty \omega^2 \left[\frac{(S_1/N)^2}{I + G_1 S_1/(S_2+N)} \right] \left[\frac{1 + S_2/N}{I + 2 S_2/N} \right]^2 \gamma_1 d\omega \\ \leq \frac{1}{(1 - M_{12}^2)} \int_0^\infty \omega^2 \frac{(S_1/N)^2}{I + 2 S_1/N} d\omega , \quad (3.5.1-26)$$

we conclude that the time delay CRLB of the two-target case (Equation (3.5.1-21a)) is always larger than the time delay CRLB of a single target case (Equation (3.5.1-16)). For convenience, let $S = S_1$ be the target power spectrum and $I = S_2$ be the interference power spectrum, then one can define a degradation ratio of a two-target CRBL over a single target CRLB as

$$\begin{aligned}
 R_d &= \sqrt{\frac{\text{two-target CRLB}}{\text{one-target CRLB}}} \\
 &= \frac{1}{(1 - M_{12}^2)^{\frac{1}{2}}} \left[\frac{\int_0^\infty \omega^2 \frac{(S/N)^2}{I + 2 S/N} d\omega}{\int_0^\infty \omega^2 \left[\frac{(S/N)^2}{I + G_1 S/(I + N)} \right] \left[\frac{1 + I/N}{I + 2 I/N} \right]^2 \gamma_1 d\omega} \right]^{\frac{1}{2}}
 \end{aligned} \tag{3.5.1-27}$$

Note that $R_d \geq 1$ and that R_d is a function of SNR, interference-to-noise ratio (INR), and relative time delay separation.

For the purpose of illustrating the two-sensor, two-target CRLB performance behavior, we assume a one-sided power spectrum of 100 Hz bandwidth centered at 50 Hz. Furthermore, we assume that signal, interference, and noise processes have identical bandwidths.

Figures 3-4 and 3-5 present the multitar get shaping function γ_1 , and γ_{12} , respectively, as a function of frequency for a number of interference-to-signal ratios (ISRs). Two effects can be seen: (1) the function $\gamma_1(\omega)$ reduces the low frequency band contribution to the CRLB while the function $\gamma_{12}(\omega)$ reduces the high frequency band contribution to the coefficient of mutual dependence; (2) as ISR decreases, both $\gamma_1(\omega)$ and $\gamma_{12}(\omega)$ approach unity. Figure 3-6 presents the two-sensor, two-target degradation ratio (Equation (3.5.1-27)) as a function of time delay separation for a number of ISR values. Note that identical signal, interference, and noise power spectra of 100 Hz bandwidth are used. As shown in Figure 3-6, the degradation ratio is oscillatory as a function of time delay separation, which is

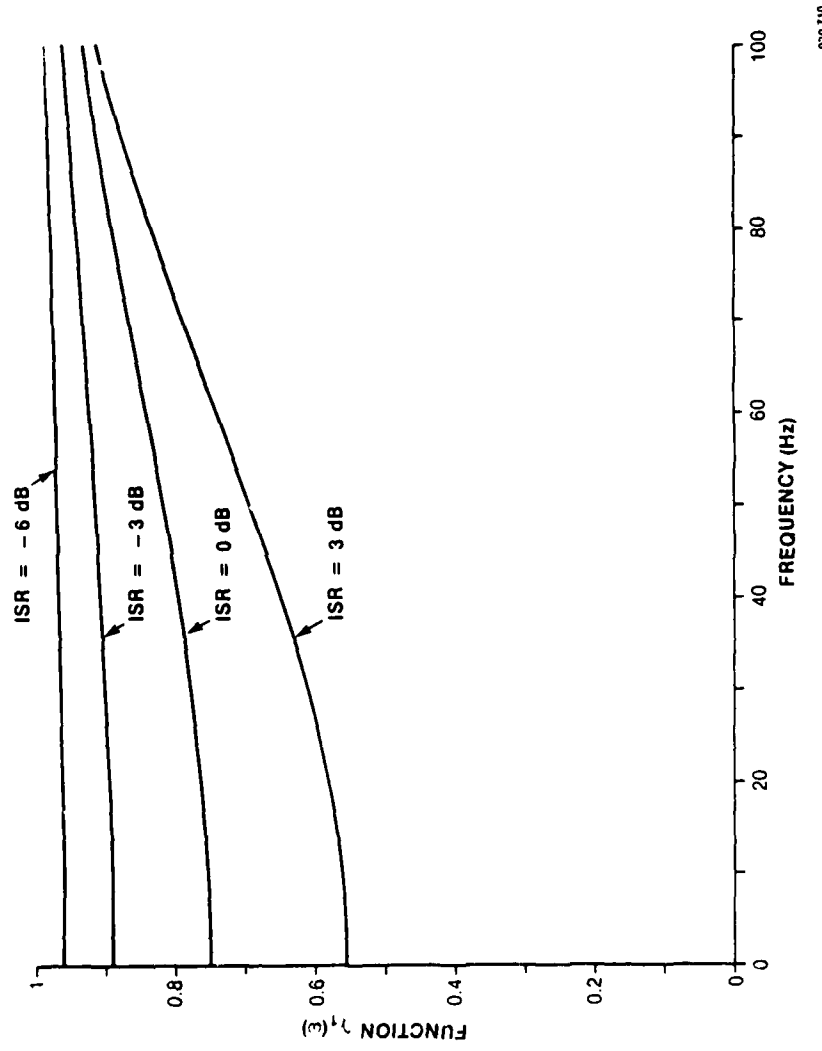


Figure 3-4. Frequency Response of the Function $\gamma_1(\omega)$ at Different Interference-to-Signal Ratios ($\text{SNR} = 0 \text{ dB}$)

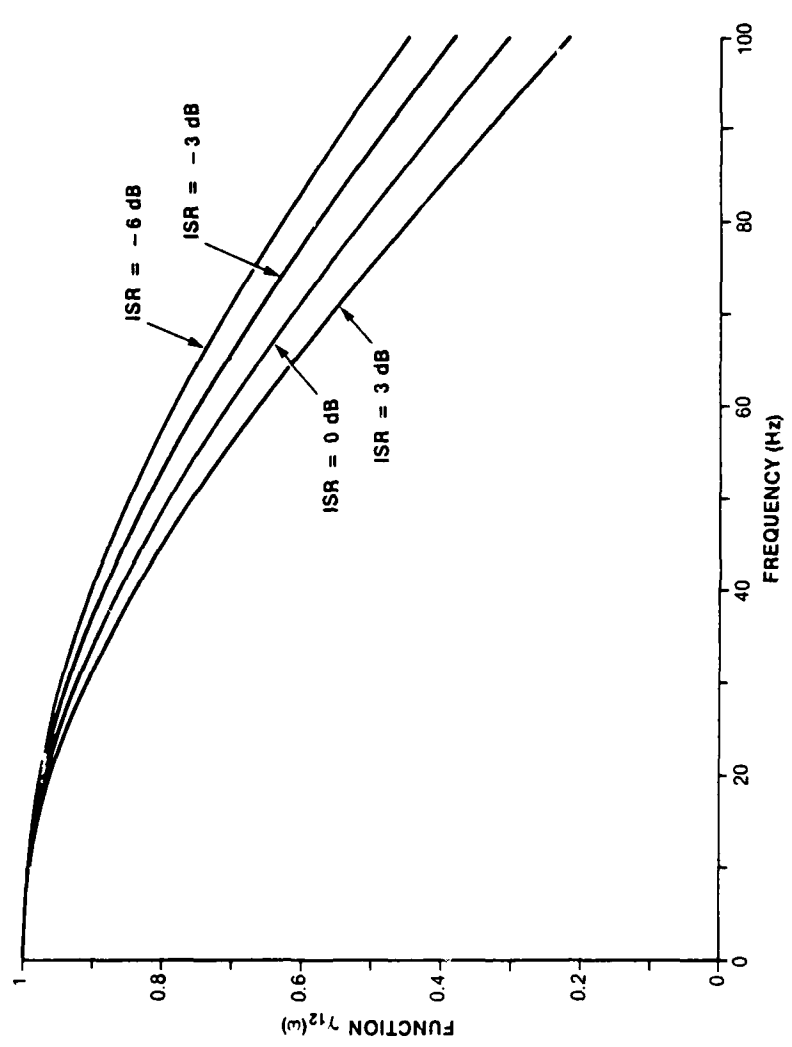


Figure 3-5. Frequency Response of the Function $\gamma_{12}(\omega)$ at Different Interference-to-Signal Ratios (SNR = 0 dB)
020711

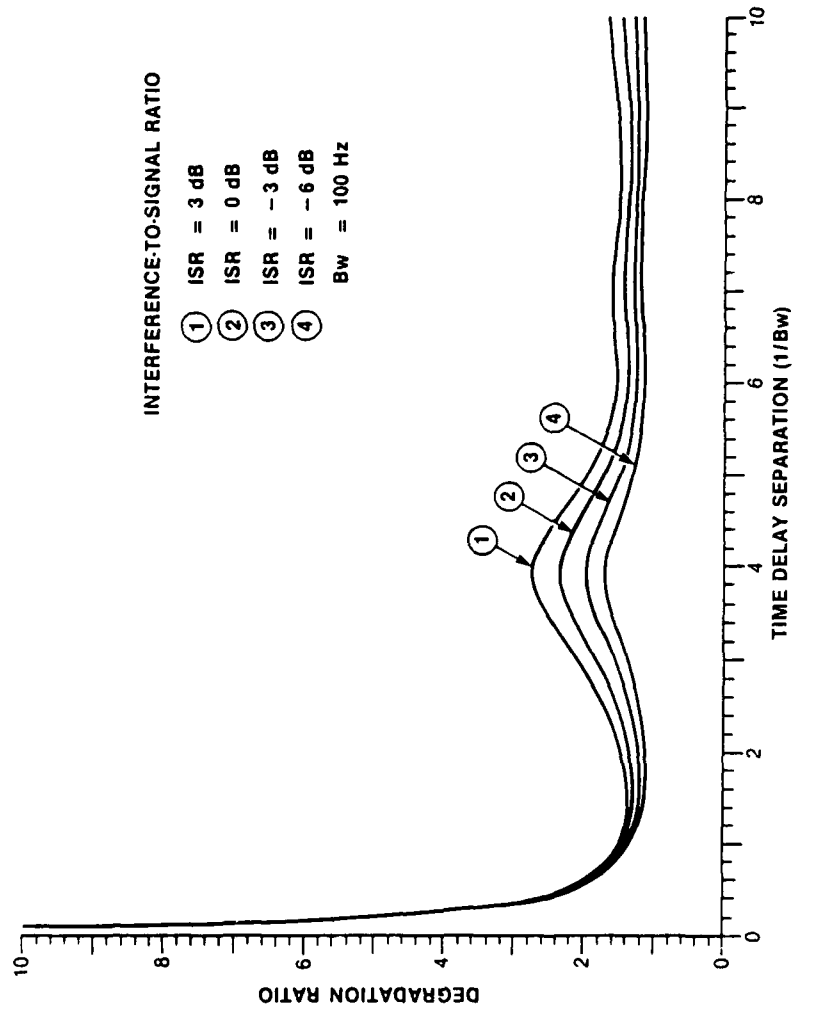


Figure 3-6. Two-Sensor, Two-Target Cramer-Rao Lower Bound Degradation Ratio Versus Time Delay Separation (SNR = 0 dB)

plotted in terms of the noise inverse bandwidth. The oscillatory behavior decreases as separation increases. Two major peaks are observed. The first occurs when time delay separation approaches zero and the other occurs at 4 times the inverse bandwidth. Note that the first peak goes to infinity at zero while the second decreases as ISR decreases. Thus, targets with identical spectrum and spatial location yield the worst estimate since they are not separable in frequency and(or) space. In order to see the effect of different signal and interference spectra on the resulting estimate, we fix the ISR but vary the interference spectrum. We choose a noise bandwidth of 5000 Hz ($B = 5000$). The results are presented in Figures 3-7 and 3-8. Two observations can be made: (1) degradation ratio is no longer infinite at zero time delay separation with non-identical signal and interference spectra, and (2) comparison between Figures 3-6 and 3-7 shows that the degradation ratio as a function of time delay separation is bandwidth independent.

3.5.1.3 Case 3: One Target and M Sensors ($J = 1, M = M$). For M sensors and with $Q_k = I$, the parameter set consists of $M-1$ independent time delays. For convenience we select the intersensor time delay as the minimum time delay set. If we denote this parameter set by $\underline{\theta} = (\tau_1, \tau_2, \dots, \tau_{M-1})^T$, then the optimum estimate of this time delay set is given by the $M-1$ likelihood equation:

$$\frac{\partial \Lambda}{\partial \tau_i} = \int_0^\infty j\omega \left[|\tilde{h}_i|^2 \underline{\alpha}^* \tilde{Q}_i^{-1} v_i (\Phi_i - \tilde{b}_i 1_M) v_i^* Q_i^{-1} \underline{\alpha} - T \tilde{b}_i \right] \frac{d\omega}{2\pi} = 0 \quad (3.5.1-28)$$

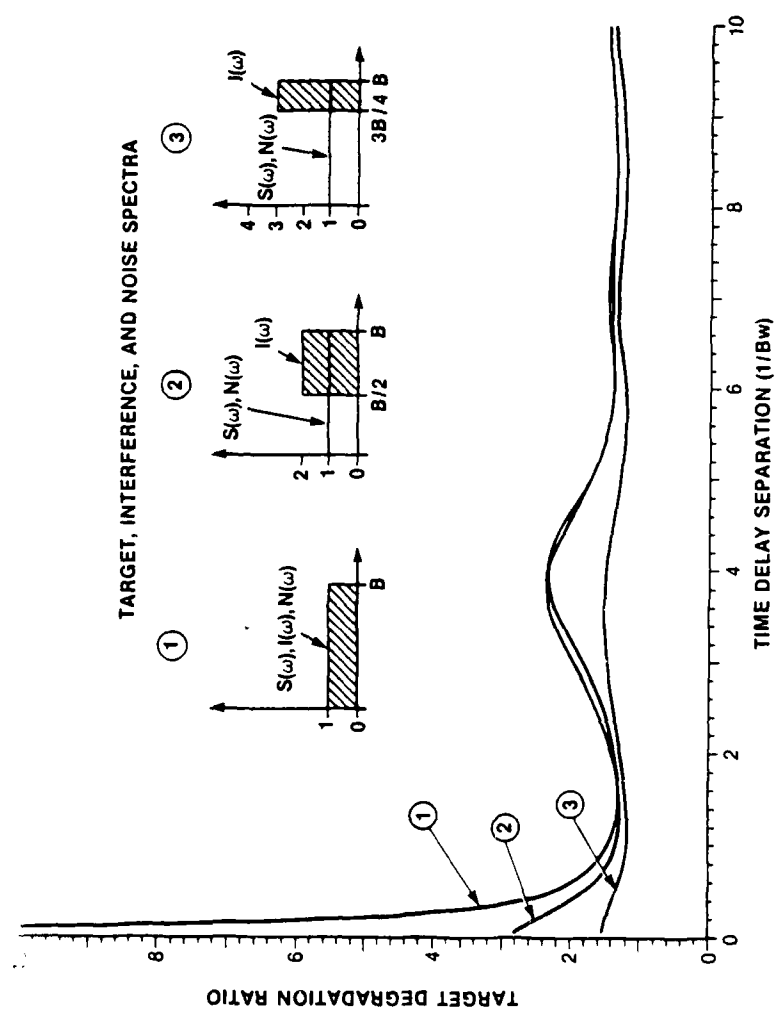


Figure 3-7. Two-Sensor, Two-Target CRLB Degradation Ratio Versus Time Delay Separation and Interference Spectrum (SNR = 0 dB, INR = 0 dB)

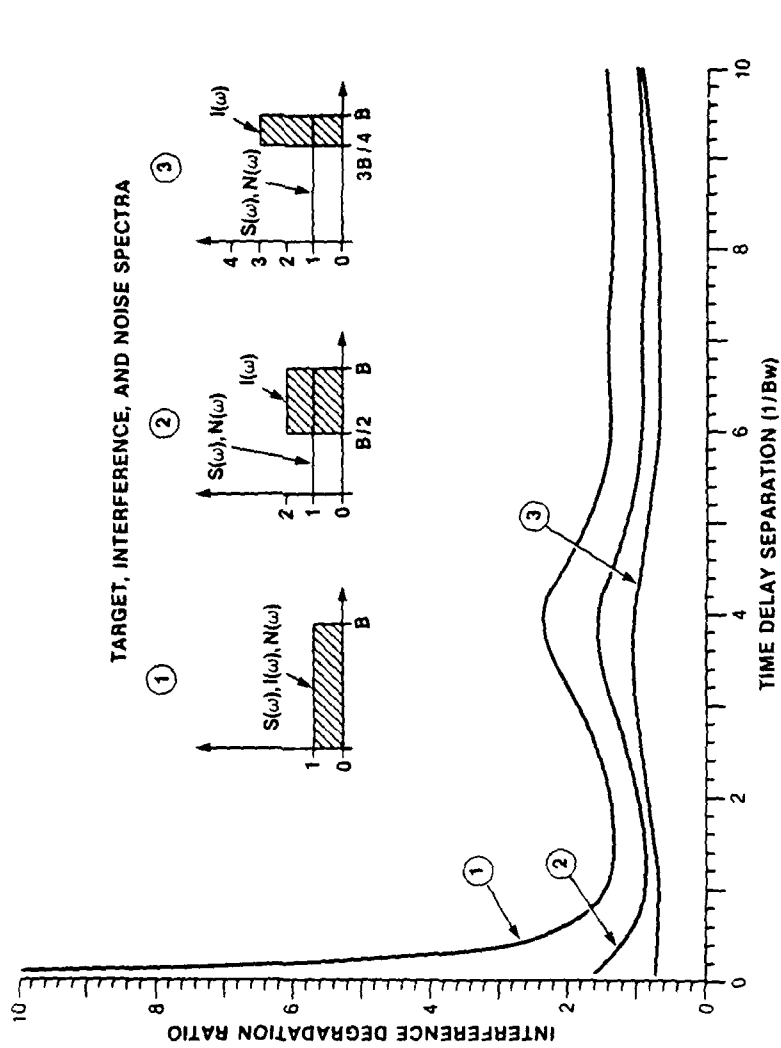


Figure 3-8. Two-Sensor, Two-Target CRLB Degradation Ratio Versus Time Delay Separation and Interference Spectrum ($\text{SNR} = 0 \text{ dB}$, $\text{INR} = 0 \text{ dB}$)

for $i = 1, 2, \dots, M-1$.

It was derived in Appendix C that the CRLB of time delay estimate for every inter-sensor time delay is identical and is given by

$$\text{VAR}(\hat{\tau}_i) \geq \left[M \sum_{k=1}^B \omega_k^2 \frac{s_k^2/n_k^2}{1 + M s_k^2/n_k^2} \right]^{-1}; \quad i = 1, 2, \dots, M-1 \quad (3.5.1-29a)$$

or in continuous form

$$\text{VAR}(\hat{\tau}_i) \geq 2\pi \left[MT \int_0^\infty \frac{s^2(\omega)/n^2(\omega)}{1 + M s(\omega)/n(\omega)} \omega^2 d\omega \right]^{-1} \quad (3.5.1-29b)$$

Thus, the CRLB of any two adjacent sensors improves with increased M , the total number of sensors. Furthermore, Appendix C shows that the time delay estimate between any two sensors also has the same CRLB. In addition, the covariance of any two time delay estimates is

$$\text{COV}(\hat{\tau}_i, \hat{\tau}_j) = \begin{cases} -\frac{1}{2} \text{VAR}(\hat{\tau}_i) & ; \quad \text{if } |i-j| = 1 \\ 0 & ; \quad \text{if } |i-j| > 1 \end{cases} \quad (3.5.1-30a)$$

In other words, the correlation coefficient is

AD-R129 805

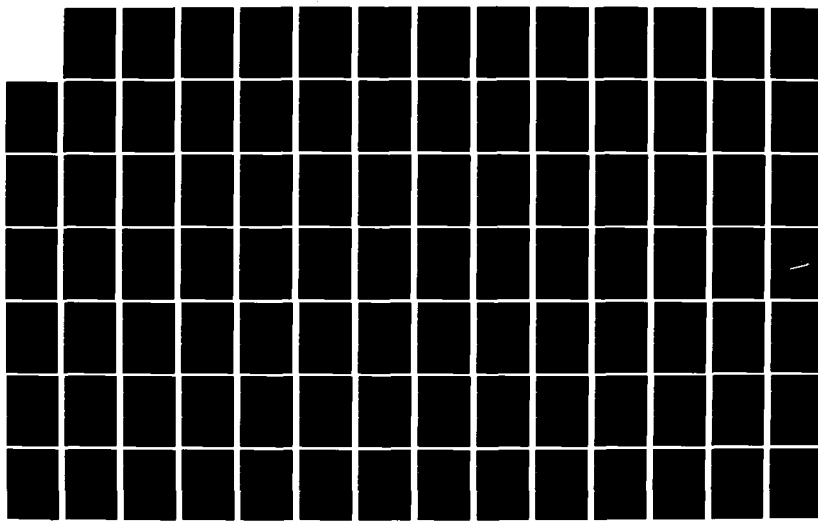
OPTIMUM MULTISENSOR MULTITARGET LOCALIZATION AND
TRACKING(U) NAVAL UNDERWATER SYSTEMS CENTER NEW LONDON
CT NEW LONDON LAB L C NG 07 JUN 83 NUSC-TR-6931

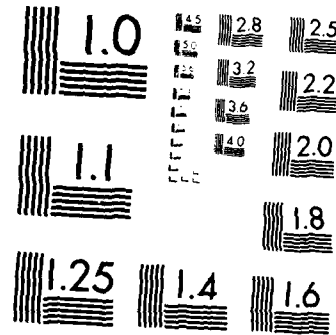
2/4

UNCLASSIFIED

F/G 12/1

NL





MICROCOPY RESOLUTION TEST CHART
NATIONAL BUREAU OF STANDARDS 1963-A

$$\rho_{ij} = \frac{\text{COV}(\hat{\tau}_i, \hat{\tau}_j)}{[\text{VAR}(\hat{\tau}_i) \text{VAR}(\hat{\tau}_j)]^{1/2}}$$

$$= \begin{cases} -\frac{1}{2} & ; \text{ if } |i - j| = 1 \\ 0 & ; \text{ if } |i - j| > 1 \end{cases} \quad (3.5.1-30b)$$

Thus far, we have studied only the optimal time delay processing of a multisensor array system. The objective of a passive sonar system, however, is to localize an acoustic source of interest (i.e., obtaining its range and bearing). For passive localization, a minimum of three sensors (assuming omni-directional response) is needed. However, for a far field assumption, two sensors can yield good bearing information. In the following section, we study in some detail the optimum processor structure for range and bearing estimations from a three-sensor array.

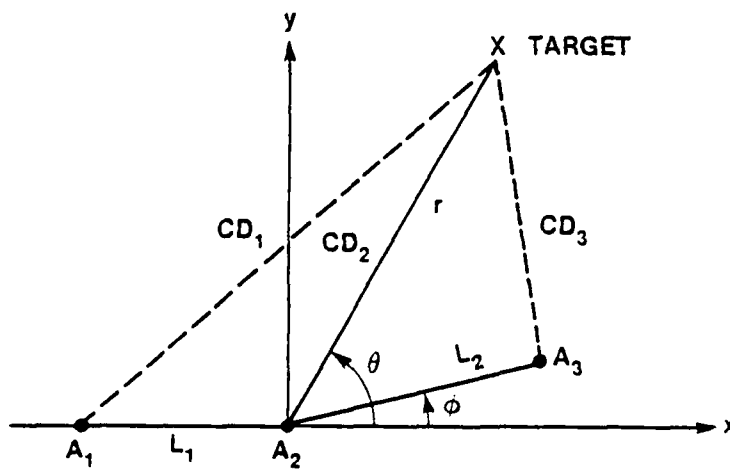
3.5.2 Localization Parameter Estimation

In this section we examine in detail the optimum processor structure for estimating localization parameters (i.e., range and bearing). We compare the performance of the optimum processor to the conventional approach, where range and bearing are obtained from the measurement of two time delay pairs. We discuss briefly the optimality of the direct range and bearing estimation approach and of the indirect time delay estimation approach.

Consider a general three-sensor array geometry shown in Figure 3-9. We are interested in obtaining an optimum estimation of range and bearing using outputs from a three-sensor array. From Appendix D, we note that the range and bearing information is contained in the two incremental time delays. Let τ_1 denote the time delay between sensor 1 and 2, and let τ_2 denote the time delay between sensors 2 and 3. Then one can write

$$\tau_1 = D_2 - D_1 = \frac{r - \sqrt{r^2 + L_1^2 - 2rL_1 \cos(\pi - \theta)}}{c} \quad (3.5.2-1)$$

$$\tau_2 = D_3 - D_2 = \frac{\sqrt{r^2 + L_2^2 - 2rL_2 \cos(\theta - \phi)} - r}{c} \quad (3.5.2-2)$$



018 952

Figure 3-9. A Three-Sensor Array System

where D_i ; $i = 1, 2$, and 3 are the propagation delays. The steering matrix is

$$V_k = \text{diag} \left\{ e^{-j\omega_k \tau_1} \quad 1 \quad e^{j\omega_k \tau_2} \right\}. \quad (3.5.2-3)$$

Therefore, Equations (3.5.1-10a) and (3.5.1-10b) become

$$P_k = V_k I_M V_k^* \quad (3.5.2-4a)$$

$$\frac{\partial P_k}{\partial \theta_i} = j\omega_k V_k \frac{\partial \Phi}{\partial \theta_i} V_k^* \quad (3.5.2-4b)$$

where θ_i is any time-delay related parameter of interest, and the matrix Φ is given by (see Equation 3.5.1-8d)

$$\Phi = \begin{bmatrix} 0 & -\tau_1 & -(\tau_1 + \tau_2) \\ \tau_1 & 0 & -\tau_2 \\ (\tau_1 + \tau_2) & \tau_2 & 0 \end{bmatrix}. \quad (3.5.2-4c)$$

The likelihood equations for range and bearing can be obtained from Equation (3.5.1-11a) as

$$\frac{\partial \Lambda(r, \theta)}{\partial r} = \sum_{k=1}^B j\omega_k \left[|\tilde{h}_k|^2 \tilde{a}_k^* \tilde{Q}_k^{-1} v_k \left(\frac{\partial \Phi}{\partial r} - \tilde{b}_r I_M \right) v_k^* \tilde{Q}_k^{-1} \tilde{a}_k - \tilde{b}_r \right] \\ = 0 \quad (3.5.2-5a)$$

and

$$\frac{\partial \Lambda(r, \theta)}{\partial \theta} = \sum_{k=1}^B j\omega_k \left[|\tilde{h}_k|^2 \tilde{a}_k^* \tilde{Q}_k^{-1} v_k \left(\frac{\partial \Phi}{\partial \theta} - \tilde{b}_\theta I_M \right) v_k^* \tilde{Q}_k^{-1} \tilde{a}_k - \tilde{b}_\theta \right] \\ = 0 \quad (3.5.2-5b)$$

where from Equation (3.5.1-11b) we have

$$\tilde{b}_r = \tilde{a}_k \operatorname{tr} \left(\tilde{Q}_k^{-1} v_k \frac{\partial \Phi}{\partial r} v_k^* \right) \quad (3.5.2-5c)$$

$$\tilde{b}_\theta = \tilde{a}_k \operatorname{tr} \left(\tilde{Q}_k^{-1} v_k \frac{\partial \Phi}{\partial \theta} v_k^* \right). \quad (3.5.2-5d)$$

For a single target in uncorrelated noise, it is easily verified that the biases are zero, i.e., $b_r = b_\theta = 0$. Furthermore, for convenience we write $|\tilde{h}_k| = |h_k|$ and $\tilde{Q}_k^{-1} = I$, i.e., assuming spectrally identical but spatially uncorrelated noise power spectrum for each sensor.

Therefore, the range and bearing likelihood equations reduce to

$$\frac{\partial \Lambda(r, \theta)}{\partial r} = \sum_{k=1}^B j\omega_k |h_k|^2 \tilde{a}_k^* v_k \frac{\partial \Phi}{\partial r} v_k^* \tilde{a}_k = 0 \quad (3.5.2-6a)$$

$$\frac{\partial \Lambda(r, \theta)}{\partial \theta} = \sum_{k=1}^8 j\omega_k |h_k|^2 \alpha_k^* v_k \frac{\partial \Phi}{\partial \theta} v_k^* \alpha_k = 0. \quad (3.5.2-6b)$$

where from Equation (3.5.1-4b) one obtains

$$|h_k|^2 = \frac{S_k/N_k^2}{1 + 3 S_k/N_k}. \quad (3.5.2-6c)$$

Using the definitions of v_k , Φ and the resulting derivatives $\partial \Phi / \partial r$ and $\partial \Phi / \partial \theta$, the likelihood equations can be manipulated to yield (Appendix F)

$$\frac{\partial \Lambda(r, \theta)}{\partial r} = \frac{T}{2\pi} \frac{\partial}{\partial r} \int_{-\infty}^{\infty} |h(\omega)|^2 G(\omega; \tau_1, \tau_2) d\omega = 0 \quad (3.5.2-7a)$$

$$\frac{\partial \Lambda(r, \theta)}{\partial \theta} = \frac{T}{2\pi} \frac{\partial}{\partial \theta} \int_{-\infty}^{\infty} |h(\omega)|^2 G(\omega; \tau_1, \tau_2) d\omega = 0 \quad (3.5.2-7b)$$

where

$$G(\omega; \tau_1, \tau_2) = G_{21}(\omega)e^{j\omega\tau_1} + G_{32}(\omega)e^{j\omega\tau_2} + G_{31}(\omega)e^{j\omega(\tau_1+\tau_2)} \quad (3.5.2-7c)$$

and $G_{ij}(\omega) = T\alpha_i\alpha_j^*$ is the estimated cross-power spectrum between sensor i and j. Now we define the joint parameter ambiguity function by

$$R(\tau_1, \tau_2) = \int_{-\infty}^{\infty} |h(\omega)|^2 G(\omega; \tau_1, \tau_2) \frac{d\omega}{2\pi}$$

$$\begin{aligned}
 &= \int_{-\infty}^{\infty} |h(\omega)|^2 \left[G_{21}(\omega) e^{j\omega\tau_1} + G_{32}(\omega) e^{j\omega\tau_2} \right. \\
 &\quad \left. + G_{31}(\omega) e^{j\omega(\tau_1+\tau_2)} \right] \frac{d\omega}{2\pi} \\
 &= R_{21}(\tau_1) + R_{32}(\tau_2) + R_{31}(\tau_1 + \tau_2) . \tag{3.5.2-8}
 \end{aligned}$$

Therefore, the optimum (ML) estimate of range and bearing is obtained by seeking the simultaneous nulls of the likelihood equations:

$$\frac{\partial \Lambda(r, \theta)}{\partial r} = T \frac{\partial}{\partial r} R(\tau_1, \tau_2) = 0 \tag{3.5.2-9a}$$

$$\frac{\partial \Lambda(r, \theta)}{\partial \theta} = T \frac{\partial}{\partial \theta} R(\tau_1, \tau_2) = 0 . \tag{3.5.2-9b}$$

Now relate the time delays to range and bearing by

$$\begin{bmatrix} r \\ \theta \end{bmatrix} = \begin{bmatrix} f_1(\tau_1, \tau_2) \\ f_2(\tau_1, \tau_2) \end{bmatrix} = \underline{f}(\tau_1, \tau_2) \tag{3.2.5-9c}$$

and its inverse by

$$\begin{bmatrix} \tau_1 \\ \tau_2 \end{bmatrix} = \underline{f}^{-1}(r, \theta) . \tag{3.5.2-9d}$$

Then the joint estimation of range and bearing can be realized by an open loop processor described in Figure 3-10. In the literature, this is known as a focused beamformer because the optimum estimate of range and bearing is obtained when the beam is focused on the target.

Note that the optimum estimate of range and bearing (r^* , θ^*) must correspond to the time delay pair (τ_1^*, τ_2^*) which defines the peak of the joint time delay ambiguity function $R(\tau_1, \tau_2)$. Therefore, an equivalent theoretical approach is to first seek the optimum time delay pair (τ_1^*, τ_2^*) and then transform it to the corresponding range and bearing. For practical applications, however, it is sometimes more convenient and simpler to search and track in the time delay parameter than the range and bearing parameters since the ambiguity function is symmetrical and uni-modal (for high SNR) in the time delay variables. More importantly, for a low SNR environment where a T-second observation MLE processor fails to be efficient, the symmetric property of the time delay ambiguity function allows a simple tracking filter design which could provide optimum estimates by increasing the effective coherent integration time. Unfortunately, the resulting non-linear transformation from time delays to range and bearing for the practical approach renders the otherwise Gaussian noise process to be non-Gaussian.

Note the focused beamformer implementation shown in Figure 3-10 requires a two-dimensional (2-D) peak detector. However, a time delay approach using only two 1-D null detectors can be realized

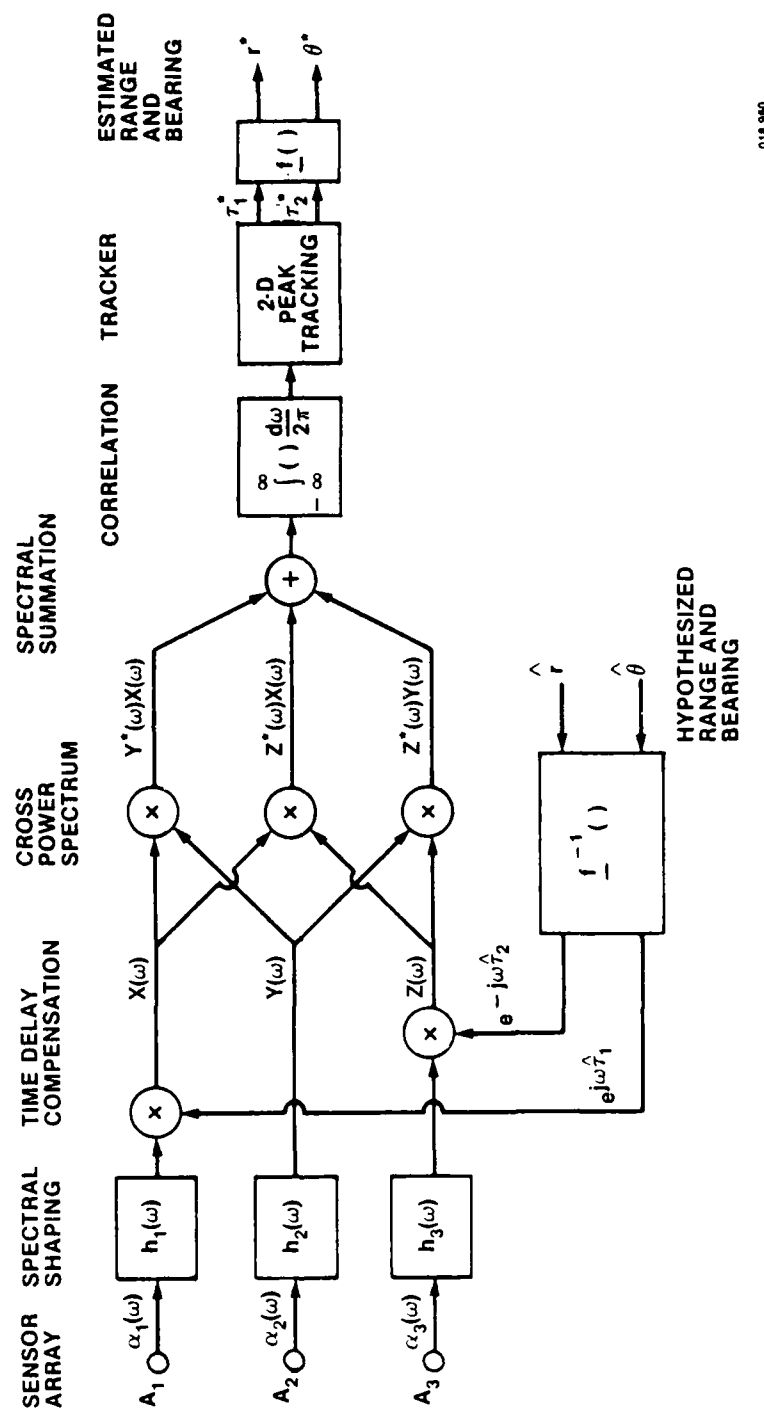


Figure 3-10. Optimum Range and Bearing Estimation from Three-Sensor Arrays (Focused Beamformer)

018960

without any loss of performance. This can be seen as follows. Rewriting Equations (3.5.2-9a and b) in terms of the time delay variables and using the chain rule of differentiation yields

$$\frac{\partial \Lambda(r, \theta)}{\partial r} = T \left[\frac{\partial R(\tau_1, \tau_2)}{\partial \tau_1} \frac{\partial \tau_1}{\partial r} + \frac{\partial R(\tau_1, \tau_2)}{\partial \tau_2} \frac{\partial \tau_2}{\partial r} \right] = 0 \quad (3.5.2-10a)$$

$$\frac{\partial \Lambda(r, \theta)}{\partial \theta} = T \left[\frac{\partial R(\tau_1, \tau_2)}{\partial \tau_1} \frac{\partial \tau_1}{\partial \theta} + \frac{\partial R(\tau_1, \tau_2)}{\partial \tau_2} \frac{\partial \tau_2}{\partial \theta} \right] = 0 .$$

(3.5.2-10b)

Using the simple relations

$$\tau_1 = -\frac{L_1}{c} \cos \theta - \frac{L_1^2 \sin^2 \theta}{2rc} \text{ and}$$

$$\tau_2 = -\frac{L_2}{c} \cos \theta + \frac{L_2^2 \sin^2 \theta}{2rc}$$

as shown in Equations (D-2a) and (D-2b), respectively in Appendix D, we observe that the derivatives of τ_1 and τ_2 w.r.t. range are zero only for infinite range and the derivatives w.r.t. bearing are zero only at the endfire direction. Therefore, for all other situations, the necessary and sufficient conditions for Equations (3.5.2-10a) and (3.5.2-10b) to be true are

$$\frac{\partial R(\tau_1, \tau_2)}{\partial \tau_1} = 0 \quad (3.5.2-10c)$$

$$\frac{\partial R(\tau_1, \tau_2)}{\partial \tau_2} = 0 . \quad (3.5.2-10d)$$

Thus, using Equation (3.5.2-8) in (3.5.2-10a-d) yields

$$\begin{aligned} \frac{\partial R(\tau_1, \tau_2)}{\partial \tau_1} &= T \frac{\partial}{\partial \tau_1} [R_{21}(\tau_1) + R_{31}(\tau_1 + \tau_2)] \\ &= \frac{T}{2\pi} \frac{\partial}{\partial \tau_1} \int_{-\infty}^{\infty} |h(\omega)|^2 \\ &\quad [G_{21}(\omega)e^{j\omega\tau_1} + G_{31}(\omega)e^{j\omega(\tau_1+\tau_2)}] d\omega \end{aligned} \quad (3.5.2-10e)$$

and

$$\begin{aligned} \frac{\partial R(\tau_1, \tau_2)}{\partial \tau_2} &= T \frac{\partial}{\partial \tau_2} [R_{32}(\tau_2) + R_{31}(\tau_1 + \tau_2)] \\ &= \frac{T}{2\pi} \frac{\partial}{\partial \tau_2} \int_{-\infty}^{\infty} |h(\omega)|^2 \\ &\quad [G_{32}(\omega)e^{j\omega\tau_2} + G_{31}(\omega)e^{j\omega(\tau_1+\tau_2)}] d\omega \end{aligned} \quad (3.5.2-10f)$$

where we have used the fact that

$$\frac{\partial R_{32}(\tau_2)}{\partial \tau_1} = \frac{\partial R_{21}(\tau_1)}{\partial \tau_2} = 0. \quad (3.5.2-10g)$$

An optimum three-sensor array processor using two correlators is shown in Figure 3-11.

We next calculate the CRLB for the optimum three-sensor array processor. First we calculate the CRLB for the optimum time delay estimate and compare it to the conventional approach. Then the CRLB for the localization parameters is obtained by relating it to the time delay estimate.

From Appendix C, we obtain the elements of the Fisher Information matrix for optimum one-target three-sensor time delay estimation as:

$$J_{ij} = -\text{tr} \left(\frac{\partial \Phi}{\partial \tau_i} \frac{\partial \Phi}{\partial \tau_j} \right) \sum_{k=1}^B \omega_k^2 \left(\frac{s_k^2/n_k^2}{1 + 3 s_k^2/n_k^2} \right). \quad (3.5.2-11)$$

From Equation (3.5.2-4c) we find

$$\frac{\partial \Phi}{\partial \tau_1} = \begin{bmatrix} 0 & -1 & -1 \\ 1 & 0 & 0 \\ 1 & 0 & 0 \end{bmatrix}; \quad \frac{\partial \Phi}{\partial \tau_2} = \begin{bmatrix} 0 & 0 & -1 \\ 0 & 0 & -1 \\ 1 & 1 & 0 \end{bmatrix} \quad (3.5.2-12a)$$

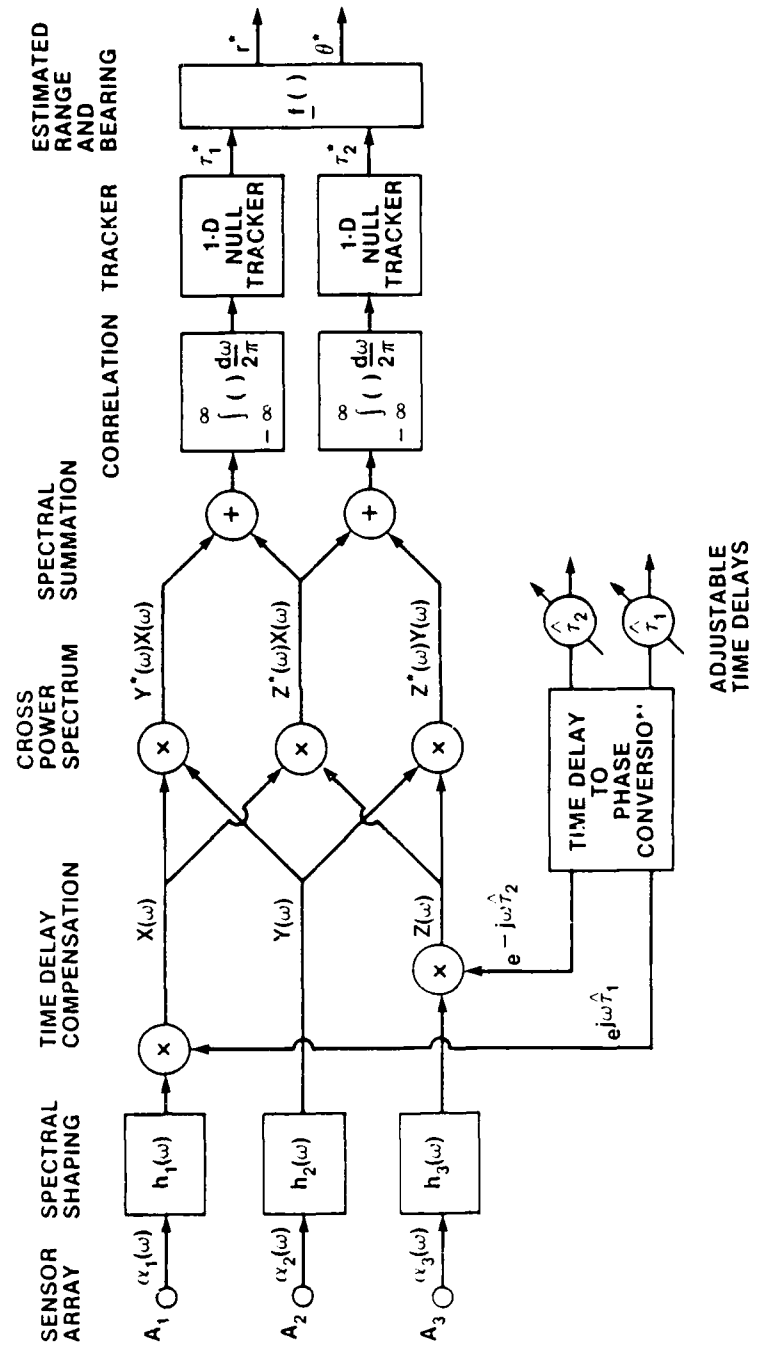


Figure 3-11. Optimum Range and Bearing Estimation from Three-Sensor Arrays Using Two Correlators

018959

and therefore

$$\text{tr} \left(\frac{\partial \Phi}{\partial \tau_1} \frac{\partial \Phi}{\partial \tau_1} \right) = -4 \quad (3.5.2-12b)$$

$$\text{tr} \left(\frac{\partial \Phi}{\partial \tau_1} \frac{\partial \Phi}{\partial \tau_2} \right) = -2 \quad (3.5.2-12c)$$

and

$$\text{tr} \left(\frac{\partial \Phi}{\partial \tau_2} \frac{\partial \Phi}{\partial \tau_2} \right) = -4 . \quad (3.5.2-12d)$$

From Appendix B, the CRLB for a two-parameter joint estimation is:

$$\text{VAR}(\hat{\tau}_1) \geq \frac{1}{(1 - M_{12}^2)} \frac{1}{J_{11}} \quad (3.5.2-13a)$$

$$\text{VAR}(\hat{\tau}_2) \geq \frac{1}{(1 - M_{12}^2)} \frac{1}{J_{22}} \quad (3.5.2-13b)$$

where M_{12} , the coefficient of mutual dependence, is given by

$$M_{12} = \frac{J_{12}}{(J_{11} J_{22})^{1/2}} . \quad (3.5.2-13c)$$

Now using Equations (3.5.2-11) and (3.5.2-12a-d) or Equation (3.5.1-29a), we obtain

$$\text{VAR}(\hat{\tau}_1) = \text{VAR}(\hat{\tau}_2) \geq \left[3 \sum_{k=1}^B \omega_k^2 \left(\frac{s_k^2/n_k^2}{1 + 3 s_k^2 n_k} \right) \right]^{-1} . \quad (3.5.2-14)$$

Note that for the general case of M sensors it was shown in Appendix C that the CRLB of the incremental time delay estimates is given by

$$\text{VAR}(\hat{\tau}_i) \geq \left[M \sum_{k=1}^B \omega_k^2 \left(\frac{s_k^2/n_k^2}{1 + M s_k/n_k} \right) \right]^{-1}; \quad i = 1, 2, \dots, M-1. \quad (3.5.2-15)$$

Thus, the time delay estimate improves with the increased number of spatial sensor observations.

We now discuss the conventional approach to estimating range and bearing. A conventional three-sensor array signal processor is shown in Figure 3-12. In the conventional approach, only two cross-power spectra are processed. For this case, the CRLB of the time delay estimate is given by (see Equation (3.5.1-16a))

$$\text{VAR}_c(\hat{\tau}_1) = \text{VAR}_c(\tau_2) \geq \left[2 \sum_{k=1}^B \omega_k^2 \left(\frac{s_k^2/n_k^2}{1 + 2 s_k/n_k} \right) \right]^{-1}. \quad (3.5.2-16a)$$

Therefore, the time delay variance ratio of the optimum to the conventional is

$$\frac{\text{VAR}(\hat{\tau}_1)}{\text{VAR}_c(\hat{\tau}_1)} = \frac{2}{3} \frac{\sum_{k=1}^B \omega_k^2 \left(\frac{s_k^2/n_k^2}{1 + 2 s_k/n_k} \right)}{\sum_{k=1}^B \omega_k^2 \left(\frac{s_k^2/n_k^2}{1 + 3 s_k/n_k} \right)} \quad (3.5.2-16b)$$

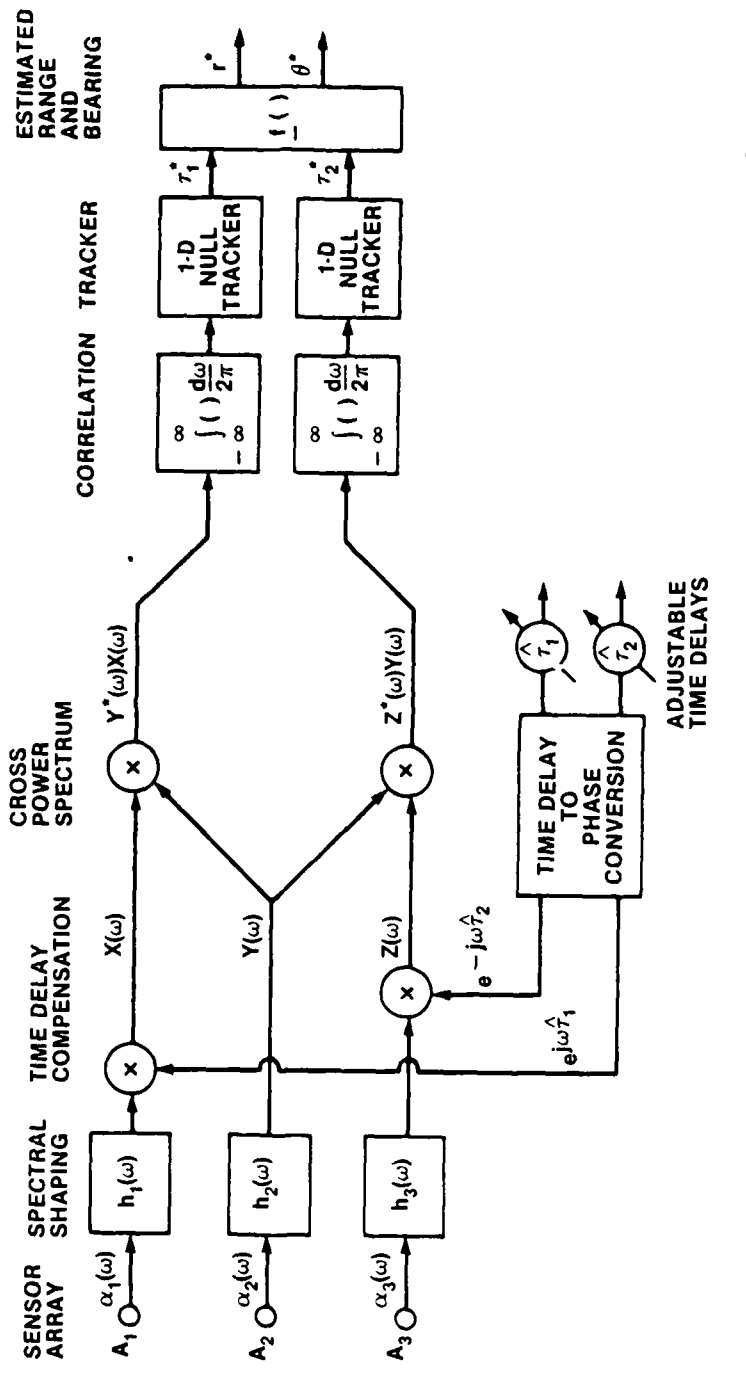


Figure 3-12. Conventional Range and Bearing Estimation from Three-Sensor Arrays Using Two Correlators

010 955

and for a flat signal and noise power spectra, Equation (3.5.2-16b) is simplified to

$$\frac{\text{VAR}(\hat{\tau}_1)}{\text{VAR}_c(\hat{\tau}_1)} = \left(\frac{2}{3}\right) \left(\frac{1 + 3 \text{ S/N}}{1 + 2 \text{ S/N}}\right). \quad (3.5.2-16c)$$

Thus, at low SNR, the CRLB of the optimum processor is improved by a factor of $\frac{2}{3}$ (1.8 dB) with respect to the conventional approach.

Because the two time delays are correlated due to common noise channels, a more meaningful approach is to compare the one sigma error ellipse area between the optimum and the conventional. From Appendices C and E, we obtain the two time delay covariance matrices as

$$P_o = \begin{bmatrix} 1 & -\frac{1}{2} \\ -\frac{1}{2} & 1 \end{bmatrix} \quad \text{VAR}(\hat{\tau}_1) \quad (3.5.2-16d)$$

$$P_c = \begin{bmatrix} 1 & \frac{-S/N}{1 + 2 S/N} \\ \frac{-S/N}{1 + 2 S/N} & 1 \end{bmatrix} \quad \text{VAR}_c(\hat{\tau}_1) \quad (3.5.2-16e)$$

where P_o and P_c denote, respectively, the optimum and conventional covariance matrices. Therefore, the ratio of their area is

$$\frac{A_o}{A_c} = \frac{\pi |P_o|^{\frac{1}{2}}}{\pi |P_c|^{\frac{1}{2}}}$$

$$= \sqrt{\frac{3}{4} \frac{(1 + 2 S/N)^2}{(1 + 3 S/N)(1 + S/N)}} \cdot \frac{VAR(\hat{r}_1)}{VAR_c(\hat{r}_1)} . \quad (3.5.2-16f)$$

Using Equations (3.5.2-16d-e) in Equation (3.5.2-16f) yields the desired result:

$$\frac{A_0}{A_c} = \sqrt{\frac{1}{3} \frac{1 + 3 S/N}{1 + S/N}} . \quad (3.5.2-16g)$$

Thus Equation (3.5.2-16g) states that in a low SNR environment ($\frac{S}{N} \ll 1$), the error ellipse of the optimum approach has an area equal approximately to one half the conventional approach. This represents a substantial loss in performance by the conventional approach. On the other hand, in a high SNR environment ($\frac{S}{N} \gg 1$) the conventional processor approaches the optimum.

The CRLB on the localization parameters for the focused beam-former can be obtained as follows. Defining the Fisher Information matrix by

$$F = \begin{bmatrix} F_{rr} & F_{r\theta} \\ F_{\theta r} & F_{\theta\theta} \end{bmatrix} ,$$

then the CRLB for the range and bearing estimates is:

$$VAR(\hat{r}) = \frac{1}{(1 - M_{12}^2)} \frac{1}{F_{rr}} \quad (3.5.2-17a)$$

$$\text{VAR}(\hat{\theta}) = \frac{1}{(1 - M_{12}^2)} \frac{1}{F_{\theta\theta}} \quad (3.5.2-17b)$$

where

$$M_{12} = \frac{F_{r\theta}}{(F_{rr} F_{\theta\theta})^{1/2}}. \quad (3.5.2-17c)$$

Again from Appendix C, we find:

$$F_{rr} = -\text{tr} \left(\frac{\partial \Phi}{\partial r} \frac{\partial \Phi}{\partial r} \right) \sum_{k=1}^B \omega_k^2 \left(\frac{S_k^2/N_k^2}{1 + 3 S_k/N_k} \right) \quad (3.5.2-18a)$$

$$F_{r\theta} = -\text{tr} \left(\frac{\partial \Phi}{\partial r} \frac{\partial \Phi}{\partial \theta} \right) \sum_{k=1}^B \omega_k^2 \left(\frac{S_k^2/N_k^2}{1 + 3 S_k/N_k} \right) \quad (3.5.2-18b)$$

and

$$F_{\theta\theta} = -\text{tr} \left(\frac{\partial \Phi}{\partial \theta} \frac{\partial \Phi}{\partial \theta} \right) \sum_{k=1}^B \omega_k^2 \left(\frac{S_k^2/N_k^2}{1 + 3 S_k/N_k} \right). \quad (3.5.2-18c)$$

Now

$$\begin{aligned} \text{tr} \left(\frac{\partial \Phi}{\partial r} \frac{\partial \Phi}{\partial \theta} \right) &= \text{tr} \left[\left(\sum_{i=1}^2 \frac{\partial \Phi}{\partial \tau_i} \frac{\partial \tau_i}{\partial r} \right) \left(\sum_{j=1}^2 \frac{\partial \Phi}{\partial \tau_j} \frac{\partial \tau_j}{\partial \theta} \right) \right] \\ &= \sum_{i=1}^2 \sum_{j=1}^2 \left(\frac{\partial \tau_i}{\partial r} \frac{\partial \tau_j}{\partial \theta} \right) \text{tr} \left(\frac{\partial \Phi}{\partial \tau_i} \frac{\partial \Phi}{\partial \tau_j} \right) \quad (3.5.2-19a) \end{aligned}$$

and using Equations (3.5.2-12a-d), we obtain

$$\text{tr} \left(\frac{\partial \Phi}{\partial r} \frac{\partial \Phi}{\partial \theta} \right) = -4 \left(\frac{\partial \tau_1}{\partial r} \frac{\partial \tau_1}{\partial \theta} + \frac{\partial \tau_1}{\partial r} \frac{\partial \tau_2}{\partial \theta} + \frac{\partial \tau_2}{\partial r} \frac{\partial \tau_2}{\partial \theta} + \frac{\partial \tau_2}{\partial r} \frac{\partial \tau_1}{\partial \theta} \right) \quad (3.5.2-19b)$$

and similarly

$$\text{tr} \left(\frac{\partial \Phi}{\partial r} \frac{\partial \Phi}{\partial r} \right) = -4 \left[\left(\frac{\partial \tau_1}{\partial r} \right)^2 + \frac{\partial \tau_1}{\partial r} \frac{\partial \tau_2}{\partial r} + \left(\frac{\partial \tau_2}{\partial r} \right)^2 \right] \quad (3.5.2-19c)$$

$$\text{tr} \left(\frac{\partial \Phi}{\partial \theta} \frac{\partial \Phi}{\partial \theta} \right) = -4 \left[\left(\frac{\partial \tau_1}{\partial \theta} \right)^2 + \frac{\partial \tau_1}{\partial \theta} \frac{\partial \tau_2}{\partial \theta} + \left(\frac{\partial \tau_2}{\partial \theta} \right)^2 \right]. \quad (3.5.2-19d)$$

Using Equations (3.5.2-1) and (3.5.2-2) and evaluating the derivatives at the true range and bearing (R, B), we obtain the following:

$$\left. \frac{\partial \tau_1}{\partial r} \right|_{R, B} = \frac{1}{2c} \left(\frac{L_1 \sin B}{R} \right)^2 \quad (3.5.2-20a)$$

$$\left. \frac{\partial \tau_2}{\partial r} \right|_{R, B} = -\frac{1}{2} \left(\frac{L_2 \sin(B - \phi)}{R} \right)^2 \quad (3.5.2-20b)$$

$$\left. \frac{\partial \tau_1}{\partial \theta} \right|_{R, B} = \frac{L_1}{c} \sin B - \frac{L_1^2}{c} \left(\frac{\sin 2B}{R} \right) \quad (3.5.2-20c)$$

and

$$\left. \frac{\partial \tau_2}{\partial \theta} \right|_{R, B} = \frac{L_2}{c} \sin(B - \phi) + \frac{L_2^2}{2c} \left(\frac{\sin 2(B - \phi)}{R} \right). \quad (3.5.2-20d)$$

For simplicity we assume a special case where the sensor arrays are co-linear with equal separation ($L = L_1 = L_2$) and the target is at broadside. Thus, substituting Equations (3.5.2-20a-d) in Equations (3.5.2-9b-d) yields:

$$\text{tr} \left(\frac{\partial \Phi}{\partial r} \frac{\partial \Phi}{\partial \theta} \right) \Big|_{R, B} = 0 \quad (3.5.2-21a)$$

$$\text{tr} \left(\frac{\partial \Phi}{\partial r} \frac{\partial \Phi}{\partial r} \right) \Big|_{R, B} = \frac{-1}{c^2} \left(\frac{L}{R} \right)^4 \quad (3.5.2-21b)$$

and

$$\text{tr} \left(\frac{\partial \Phi}{\partial \theta} \frac{\partial \Phi}{\partial \theta} \right) \Big|_{R, B} = -12 \left(\frac{L}{c} \right)^2. \quad (3.5.2-21c)$$

Therefore, the CRLB of range and bearing evaluated at the true range and bearing is given by:

$$\text{VAR}(\hat{r}) \geq \frac{1}{(1 - M_{12}^2)} \left\{ -\text{tr} \left[\left(\frac{\partial \Phi}{\partial r} \right)^2 \right] \sum_{k=1}^B \omega_k^2 \left(\frac{s_k^2/n_k^2}{1 + 3 s_k^2/n_k} \right) \right\}^{-1} \quad (3.5.2-22a)$$

$$\text{VAR}(\hat{\theta}) \geq \frac{1}{(1 - M_{12}^2)} \left\{ -\text{tr} \left[\left(\frac{\partial \Phi}{\partial \theta} \right)^2 \right] \sum_{k=1}^B \omega_k^2 \left(\frac{s_k^2/N_k^2}{I + 3 s_k^2/N_k} \right) \right\}^{-1} \quad (3.5.2-22b)$$

And because of Equation (3.5.2-21a), range and bearing estimates are uncorrelated. Using Equation (3.5.2-14) these can be expressed in terms of the variance of the time delay estimate as follows:

$$\text{VAR}(\hat{r}) \geq \frac{3 \text{VAR}(\hat{\tau}_1)}{-\text{tr} \left(\frac{\partial \Phi}{\partial r} \right)^2} \quad (3.5.2-23a)$$

$$\text{VAR}(\hat{\theta}) \geq \frac{3 \text{VAR}(\hat{\tau}_1)}{-\text{tr} \left(\frac{\partial \Phi}{\partial \theta} \right)^2}. \quad (3.5.2-23b)$$

For the special case of a co-linear array and a broadside target, we find

$$\text{VAR}(\hat{r}) \geq 3c^2 \left(\frac{R}{L} \right)^4 \text{VAR}(\hat{\tau}_1) \quad (3.5.2-24a)$$

$$\text{VAR}(\hat{\theta}) \geq \frac{1}{4} \left(\frac{c}{L} \right)^2 \text{VAR}(\hat{\tau}_1). \quad (3.5.2-24b)$$

Taking the ratio of Equation (3.5.2-24a) to Equation (3.5.2-24b) yields

$$\text{VAR}(\hat{r}) \geq 12 \frac{R^4}{L^2} \text{VAR}(\hat{\theta}), \quad (3.5.2-24c)$$

which relates the range variance to the bearing variance. Thus, we obtain the well known results that the variance of the range estimate is proportional to the fourth power ratio of the true range to base line length, and the variance of the bearing estimate is inversely proportional to the square of the base length.

Note that the range and bearing variances of the focused beamformer approach (Equations (3.5.2-24a-b)) agree with Equations (G-15) and (G-16) of Appendix G, which were obtained via a geometric mapping from time delay measurements. Therefore, the one-step focused beamformer approach and the two-step time delay approach yield identical statistical performance.

Let S_0 and S_c denote the area of the range/bearing one-sigma localization error ellipse for the optimum and the conventional approach, respectively. Then from Equations (3.5.2-24a) and (3.5.2-24b) one obtains

$$\begin{aligned} S_0 &= \pi \sqrt{\text{VAR}(\hat{r}) \text{VAR}(\hat{\theta})} \\ &= \frac{\sqrt{3}}{2} \left(\frac{\pi R_c^2}{L^3} \right) \text{VAR}(\hat{\tau}_1). \end{aligned} \quad (3.5.2-25a)$$

On the other hand, for the conventional approach, it can be shown (Appendix G) that

$$S_c = \left(\frac{\pi R^2 c^2}{L^3} \right) \sqrt{\frac{(1 + 3 S/N)(1 + S/N)}{(1 + 2 S/N)}} \text{ VAR}_c(\hat{\tau}_1). \quad (3.5.2-25b)$$

Therefore, using the relation given in Equation (3.2.5-16d), the ratio of the error ellipse area is

$$\frac{S_0}{S_c} = \sqrt{\frac{1}{3} \left(\frac{1 + 3 S/N}{1 + S/N} \right)} \quad (3.5.2-25c)$$

which has the same ratio as in time delay estimation (see Equation 3.5.2-16g). Thus Equation (3.5.2-25c) implies that the optimum processor yields a one-sigma localization error ellipse which is approximately one half ($1/\sqrt{3}$) that of the conventional approach in a low SNR environment. This improvement comes directly from a better bearing estimation using the optimum approach.* Note, it can be shown that the ranging performance is identical between the conventional and the optimum approach. (See Appendix G.)

*It was pointed out by Dr. J. Iannielo of the Naval Underwater Systems Center that optimum range and bearing estimation can also be achieved using the conventional approach. However, one must provide separate and different spectral shaping filters for range and bearing estimation.

3.5.3 Power Spectral Estimation

Our discussion thus far assumes that all target power spectra are known. This is one of the strongest assumptions we have made in studying the optimum signal processor. The resulting processors contain spectral shaping filters which are functions of the known target power spectra. In an actual implementation, the power spectra must be either known a priori or estimated. In this section we briefly examine the methodology of spectral estimation in a multisensor, multi-target environment and the relations between power spectral estimation and time delay estimation.

Thus, we seek the estimate \hat{S}_{kj} , the signal power spectral level of target j at frequency k . Recall from Equation (3.2-6) that the spectral levels are contained in the observation covariance matrix R_k . Let \underline{S} be a column vector of all the unknown spectral levels. Thus, $\underline{S} = (S_{11} \ S_{21} \ \dots \ S_{B1}; \ S_{12} \ S_{22} \ \dots \ S_{B2}; \ \dots; \ S_{1J} \ S_{2J} \ \dots \ S_{BJ})^T$ is a JB dimension vector. Therefore, from Equation (3.2-9) the likelihood equation for \hat{S}_{kj} is

$$\frac{\partial \Lambda(\underline{S})}{\partial S_{kj}} = - \frac{\partial \Lambda_k(\underline{S})}{\partial S_{kj}} = 0; \quad j = 1, 2, \dots, J \quad k = 1, 2, \dots, B \quad (3.5.3-1)$$

Note that the likelihood equations are decoupled in frequency. This implies that each equation can be solved separately. Now from Equation (3.2-10) we obtain

$$\frac{\partial \Lambda_k(S)}{\partial S_{kj}} = \text{tr} \left(R_k^{-1} \frac{\partial R_k}{\partial S_{kj}} \right) + \alpha_k^* \frac{\partial R_k^{-1}}{\partial S_{kj}} \alpha_k \quad (3.5.3-2)$$

where R_k and R_k^{-1} are given by Equations (3.5.1-2a) and (3.5.1-3).

Hence, the derivative of R_k and R_k^{-1} w.r.t. S_{kj} is given by

$$\frac{\partial R_k}{\partial S_{kj}} = P_{kj} = V_{kj} V_{kj}^* \quad (3.5.3-3a)$$

$$\begin{aligned} \frac{\partial R_k^{-1}}{\partial S_{kj}} &= \frac{\partial}{\partial S_{kj}} (S_{kj} P_{kj} + \tilde{N}_{kj} \tilde{Q}_{kj})^{-1} \\ &= \frac{\partial}{\partial S_{kj}} \left(\frac{\tilde{Q}_{kj}^{-1}}{\tilde{N}_{kj}} - \frac{S_{kj}/\tilde{N}_{kj}^2}{1 + G_{kj} S_{kj}/\tilde{N}_{kj}} \tilde{Q}_{kj}^{-1} P_{kj} \tilde{Q}_{kj}^{-1} \right) \\ &= - \left[\frac{1/\tilde{N}_{kj}^2}{1 + G_{kj} S_{kj}/\tilde{N}_{kj}} - \frac{G_{kj} S_{kj}/\tilde{N}_{kj}^3}{(1 + G_{kj} S_{kj}/\tilde{N}_{kj})^2} \right] \tilde{Q}_{kj}^{-1} P_{kj} \tilde{Q}_{kj}^{-1} \\ &= - \frac{\tilde{Q}_{kj}^{-1} P_{kj} \tilde{Q}_{kj}^{-1}/\tilde{N}_{kj}^2}{(1 + G_{kj} S_{kj}/\tilde{N}_{kj})^2}. \end{aligned} \quad (3.5.3-3b)$$

Therefore, the first term in Equation (3.5.3-2) can be written as

$$\begin{aligned} \text{tr} \left(R_k^{-1} \frac{\partial R_k}{\partial S_{kj}} \right) &= \text{tr} \left(\frac{\tilde{Q}_{kj}^{-1} V_{kj} V_{kj}^*}{\tilde{N}_{kj}} \right. \\ &\quad \left. - \frac{S_{kj}/\tilde{N}_{kj}^2}{1 + G_{kj} S_{kj}/\tilde{N}_{kj}} \tilde{Q}_{kj}^{-1} V_{kj} V_{kj}^* \tilde{Q}_{kj}^{-1} \tilde{Q}_{kj}^{-1} V_{kj} V_{kj}^* \right) \end{aligned}$$

$$\begin{aligned}
 &= \frac{G_{kj}}{\tilde{N}_{kj}} - \frac{S_{kj}/\tilde{N}_{kj}^2}{1 + G_{kj} S_{kj}/\tilde{N}_{kj}} G_{kj}^2 \\
 &= \frac{G_{kj}/\tilde{N}_{kj}}{1 + G_{kj} S_{kj}/\tilde{N}_{kj}} .
 \end{aligned} \tag{3.5.3-4}$$

Substituting Equations (3.5.3-3b) and (3.5.3-4) into (3.5.3-2), one obtains

$$\frac{\partial A(S)}{\partial S_{kj}} = - \frac{G_{kj}/\tilde{N}_{kj}}{1 + G_{kj} S_{kj}/\tilde{N}_{kj}} + \frac{|V_{kj}^* \tilde{Q}_{kj}^{-1} \alpha_k|^2}{(1 + G_{kj} S_{kj}/\tilde{N}_{kj})^2 \tilde{N}_{kj}^2} = 0 . \tag{3.5.3-5}$$

Solving Equation (3.5.3-5) yields

$$\hat{S}_{kj} = \frac{|V_{kj}^* \tilde{Q}_{kj}^{-1} \alpha_k|^2}{G_{kj}^2} - \frac{\tilde{N}_{kj}}{G_{kj}} ; \quad k = 1, 2, \dots, B \\
 j = 1, 2, \dots, J . \tag{3.5.3-6}$$

Thus, in order to estimate the J target power spectra, a total of JB equations must be solved if the optimum steering vector V_{kj}^* is known. If it is not known, then the $J(M - 1)$ time delay equations must be solved simultaneously with the JB spectral equations. However, in practice the target spectrum can be modeled with a considerably smaller set of unknown parameters. Therefore, sampling the spectrum

at appropriate frequencies should provide sufficient information to estimate the unknown spectral parameters.

Note that Equation (3.5.3-6) is an unbiased spectral estimator. This can be shown easily as follows.

Taking the expected value of Equation (3.5.3-6) yields

$$\begin{aligned} E(\hat{S}_{kj}) &= \frac{1}{G_{kj}^2} E|\underline{v}_{kj}^* \tilde{\underline{Q}}_{kj}^{-1} \underline{\alpha}_k|^2 - \frac{\tilde{N}_{kj}}{G_{kj}} \\ &= \frac{1}{G_{kj}^2} \underline{v}_{kj}^* \tilde{\underline{Q}}_{kj}^{-1} E(\underline{\alpha}_k \underline{\alpha}_k^*) \tilde{\underline{Q}}_{kj}^{-1} \underline{v}_{kj} - \frac{\tilde{N}_{kj}}{G_{kj}} . \end{aligned} \quad (3.5.3-7)$$

But from Equations (2.3-3a) and (3.2-7a):

$$E(\underline{\alpha}_k \underline{\alpha}_k^*) = S_{kj} \underline{v}_{kj} \underline{v}_{kj}^* + \tilde{N}_{kj} \tilde{\underline{Q}}_{kj} . \quad (3.5.3-8)$$

Substituting Equation (3.5.3-8) into (3.5.3-7) yields

$$\begin{aligned} E(\hat{S}_{kj}) &= S_{kj} + \frac{N_{kj} \underline{v}_{kj}^* \tilde{\underline{Q}}_{kj}^{-1} \tilde{\underline{Q}}_{kj} \tilde{\underline{Q}}_{kj}^{-1} \underline{v}_{kj}}{G_{kj}^2} - \frac{\tilde{N}_{kj}}{G_{kj}} . \\ &= S_{kj} \end{aligned} \quad (3.5.3-9)$$

Next we briefly examine the optimum spectral estimator for the one-target and two-target cases.

3.5.3.1 Case 1: One Target, M Sensors (J=1, M=M). For a single target, we have $\hat{N}_{kj} = N_k$, $\tilde{Q}_{kj}^{-1} = Q_k$, and $\tilde{G}_{kj} = G_k = \underline{v}_k^* \underline{Q}_k^{-1} \underline{v}_k$. Equation (3.5.3-6) becomes

$$\hat{s}_k = \frac{|\underline{v}_k^* \underline{Q}_k^{-1} \underline{a}_k|^2}{G_k^2} - \frac{N_k}{G_k}. \quad (3.5.3-10)$$

Furthermore, by letting $Q_k = I$ (i.e., noises are uncorrelated from sensor to sensor), then Equation (3.5.3-10) can be simplified to

$$\hat{s}_k = \frac{|\underline{v}_k^* \underline{a}_k|^2}{M^2} - \frac{N_k}{M}. \quad (3.5.3-11)$$

Figure 3-13 shows the optimum one-target multisensor spectral estimator.

3.5.3.2 Case 2: Two Targets, M Sensors (J=2, M=M). For the two-target case, Equation (3.5.3-6) becomes

$$\hat{s}_{k1} = \frac{|\underline{v}_{k1}^* \tilde{Q}_{k1}^{-1} \underline{a}_k|^2}{G_{k1}^2} - \frac{\hat{s}_{k2} + N_k}{G_{k1}}. \quad (3.5.3-12a)$$

$$\hat{s}_{k2} = \frac{|\underline{v}_{k2}^* \tilde{Q}_{k2}^{-1} \underline{a}_k|^2}{G_{k2}^2} - \frac{\hat{s}_{k1} + N_k}{G_{k2}}. \quad (3.5.3-12b)$$

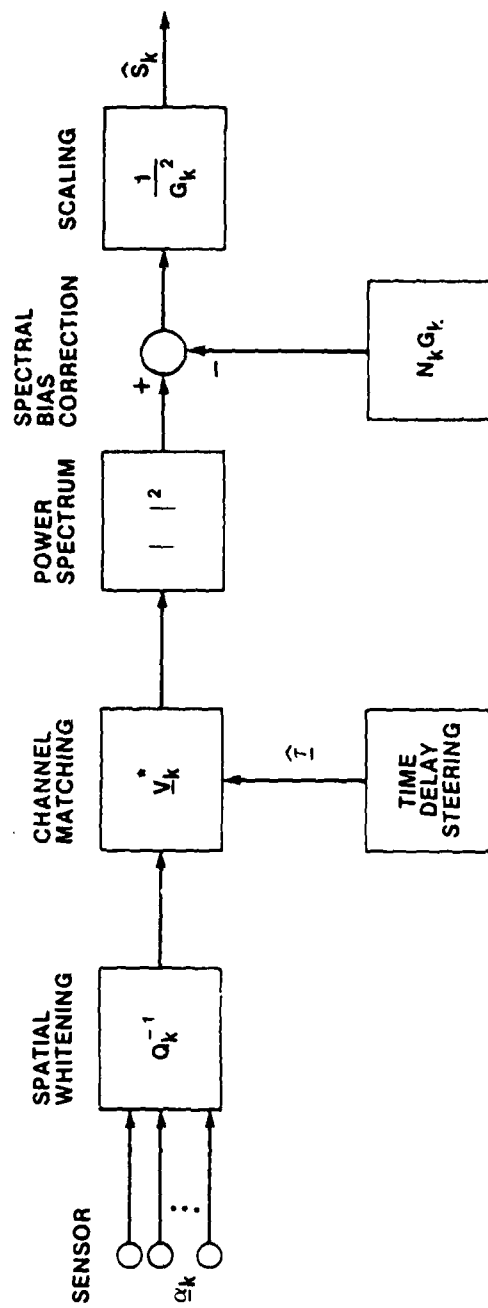


Figure 3-13. Optimum One-Target, Multisensor Spectral Estimator

Recall that

$$\begin{aligned}\tilde{Q}_{k1}^{-1} &= (\hat{S}_{k2} + N_k) (S_{k2} \underline{v}_{k2} \underline{v}_{k2}^* + N_k Q_k)^{-1} \\ &= (1 + \hat{S}_{k2}/N_k) \left[Q_k^{-1} - \frac{\hat{S}_{k2}/N_k}{1 + M \hat{S}_{k2}/N_k} Q_k^{-1} \underline{v}_{k2} \underline{v}_{k2}^* Q_k^{-1} \right].\end{aligned}\quad (3.5.3-13a)$$

Similarly,

$$\tilde{Q}_{k2}^{-1} = (1 + \hat{S}_{k1}/N_k) \left[Q_k^{-1} - \frac{\hat{S}_{k1}/N_k}{1 + M \hat{S}_{k1}/N_k} Q_k^{-1} \underline{v}_{k1} \underline{v}_{k1}^* Q_k^{-1} \right].\quad (3.5.3-13b)$$

Also

$$\begin{aligned}G_{k1} &= \underline{v}_{k1}^* \tilde{Q}_{k1}^{-1} \underline{v}_{k1} \\ &= (1 + \hat{S}_{k2}/N_k) \left[\underline{v}_{k1}^* Q_k^{-1} \underline{v}_{k1} - \frac{\hat{S}_{k2}/N_k}{1 + M \hat{S}_{k2}/N_k} (\underline{v}_{k1}^* Q_k^{-1} \underline{v}_{k1})^2 \right]\end{aligned}\quad (3.5.3-13c)$$

and

$$G_{k2} = (1 + \hat{S}_{k1}/N_k) \left[\underline{v}_{k2}^* Q_k^{-1} \underline{v}_{k2} - \frac{\hat{S}_{k1}/N_k}{1 + M \hat{S}_{k1}/N_k} (\underline{v}_{k2}^* Q_k^{-1} \underline{v}_{k2})^2 \right].\quad (3.5.3-13d)$$

For simplicity assume $Q_k = I$, then $\underline{v}_{k1}^* Q_k^{-1} \underline{v}_{k1} = \underline{v}_{k2}^* Q_k^{-1} \underline{v}_{k2} = M$. Now the following relations can be obtained:

$$G_{k1} = \frac{M (1 + \hat{s}_{k2}/N_k)}{1 + M \hat{s}_{k2}/N_k} \quad (3.5.3-14a)$$

$$G_{k2} = \frac{M (1 + \hat{s}_{k1}/N_k)}{1 + M \hat{s}_{k1}/N_k} \quad (3.5.3-14b)$$

$$|\underline{v}_{k1}^* \tilde{Q}_{k1}^{-1} \underline{a}_k|^2 = (1 + \hat{s}_{k2}/N_k)^2 \left| \underline{v}_{k1}^* \underline{a}_k - \frac{\hat{s}_{k2}/N_k}{1 + M \hat{s}_{k2}/N_k} \right. \\ \left. (\underline{v}_{k1}^* \underline{v}_{k2}) (\underline{v}_{k2}^* \underline{a}_k) \right|^2 \quad (3.5.3-14c)$$

$$|\underline{v}_{k2}^* \tilde{Q}_{k2}^{-1} \underline{a}_k|^2 = (1 + \hat{s}_{k1}/N_k)^2 \left| \underline{v}_{k2}^* \underline{a}_k - \frac{\hat{s}_{k1}/N_k}{1 + M \hat{s}_{k1}/N_k} \right. \\ \left. (\underline{v}_{k1}^* \underline{v}_{k2}) (\underline{v}_{k1}^* \underline{a}_k) \right|^2. \quad (3.5.3-14d)$$

Substituting the above into Equation (3.5.3-12a-b) and simplifying yields

$$\hat{S}_{k1} = A_{k2} \left[A_{k2} |v_{k1}^* \alpha_k - B_{k2} v_{k2}^* \alpha_k|^2 - N_k \right] \quad (3.5.3-15a)$$

$$\hat{S}_{k2} = A_{k1} \left[A_{k1} |v_{k2}^* \alpha_k - B_{k1} v_{k1}^* \alpha_k|^2 - N_k \right] \quad (3.5.3-15b)$$

where A_{ki} and B_{ki} are defined by

$$A_{ki} = \frac{1 + M \hat{S}_{ki} / N_k}{M}; \quad i = 1, 2 \quad (3.5.3-15c)$$

and

$$B_{ki} = \frac{\hat{S}_{ki} / N_k}{1 + M \hat{S}_{ki} / N_k} v_{k1}^* v_{k2}; \quad i = 1, 2. \quad (3.5.3-15d)$$

The optimum two-target M sensor spectral estimator is shown in Figure 3-14.

We have already shown that the optimum spectral estimator is an unbiased estimator. In the remainder of this section we briefly discuss the estimator performance bound. There are two cases of particular interest: (1) power spectral estimation with known time delay, and (2) joint time delay and spectral estimation.

3.5.3.3 Case 1: Power Spectral Estimation with Known Time Delay. Consider the two-target M sensor problem. The optimum power spectral estimator is given in Figure 3-14. The spectral CRLB can be derived as follows.

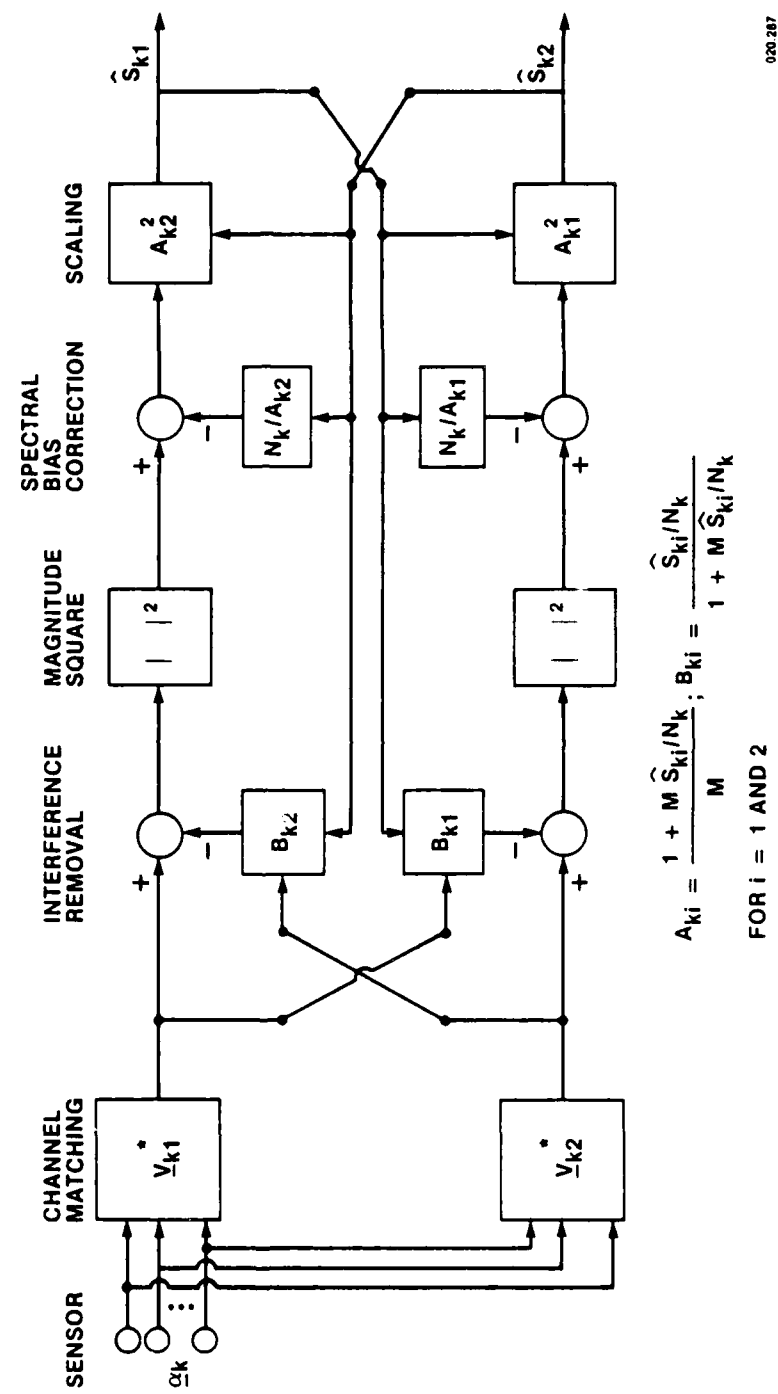


Figure 3-14. Optimum Two-Target Power Spectral Estimator

For each frequency ω_k , we have the relation

$$\text{VAR}(\hat{s}_{kj}) = [F^{-1}]_{jj}; \quad j = 1, 2 \quad (3.5.3-16)$$

where F is the 2×2 Fisher information matrix whose jl element is given by

$$\begin{aligned} F_{jl} &= -E \left[\frac{\partial^2 \Lambda(S)}{\partial s_{kj} \partial s_{kl}} \right] \\ &= \text{tr} \left(R_k^{-1} \frac{\partial R_k}{\partial s_{kj}} R_k^{-1} \frac{\partial R_k}{\partial s_{kl}} \right) \\ &= -\text{tr} \left(\frac{\partial R_k^{-1}}{\partial s_{kj}} \frac{\partial R_k}{\partial s_{kl}} \right) \end{aligned} \quad (3.5.3-17)$$

where Equations (3.5.3-2) and (3.4-4) have been used. Using Equations (3.5.3-3a) and (3.5.3-3b), Equation (3.5.3-17) reduces to

$$\begin{aligned} F_{jl} &= \text{tr} \left(\frac{\tilde{Q}_{kj}^{-1} v_{kj}^* v_{kj} \tilde{Q}_{kj}^{-1} / \tilde{N}_{kj}^2}{(1 + G_{kj} S_{kj} / \tilde{N}_{kj})^2} v_{kl} v_{kl}^* \right) \\ &= \frac{|v_{kl}^* \tilde{Q}_{kj}^{-1} v_{kj}^*|^2 / \tilde{N}_{kj}^2}{(1 + G_{kj} S_{kj} / \tilde{N}_{kj})} . \end{aligned} \quad (3.5.3-18a)$$

Note for $j = \&$, Equation (3.5.3-18a) further reduces to

$$F_{jj} = \left[\frac{G_{kj}/\tilde{N}_{kj}}{1 + G_{kj} S_{kj}/\tilde{N}_{kj}} \right]^2 . \quad (3.5.3-18b)$$

Thus, the spectral CRLB is

$$\begin{aligned} \text{VAR}(\hat{S}_{kj}) &= \frac{1}{(1 - M_{12}^2)} \frac{1}{F_{jj}} \\ &= \frac{1}{(1 - M_{12}^2)} \left(S_{kj} + \frac{\tilde{N}_{kj}}{G_{kj}} \right)^2 ; \quad j = 1, 2 \end{aligned} \quad (3.5.3-19a)$$

where

$$\begin{aligned} M_{12} &= \frac{F_{12}}{(F_{11} F_{22})^{1/2}} \\ &= \frac{|v_{k2}^* \tilde{Q}_{k1}^{-1} v_{k1}^*|^2}{(G_{k1} G_{k2})} \end{aligned} \quad (3.5.3-19b)$$

is the spectral coefficient of mutual dependence. Note that for a single target case, the spectral CRLB is

$$\begin{aligned}
 \text{VAR}(\hat{S}_k) &= - \left\{ E \left[\frac{\partial^2 \Lambda(S)}{\partial S_k^2} \right] \right\}^{-1} \\
 &= \left\{ \text{tr} \left(\frac{\partial R_k^{-1}}{\partial S_k} \frac{\partial R_k}{\partial S_k} \right) \right\}^{-1} \\
 &= \left[S_k + \frac{N_k}{G_k} \right]^2 \tag{3.5.3-20}
 \end{aligned}$$

where $G_k = V_k^* Q_k^{-1} V_k$ is known as the array gain.

3.5.3.4 Case 2: Joint Time Delay and Spectral Estimation. For simplicity, we assume a single target and two sensors. Therefore, the unknowns are τ , the time delay, and S_k , the spectral level at frequency ω_k . Note that because the spectral likelihood equation is independent for each frequency ω_k , we only need to consider the joint estimate between τ and S_k . Now let $\theta_1 = \tau$, and $\theta_2 = S_k$, then the joint time delay spectral CRLB evaluated at the true parameter values is

$$\text{VAR}(\hat{\theta}_i) \geq (F^{-1})_{ii}, \quad i = 1, 2 \tag{3.5.3-21a}$$

where the ij element of the Fisher information matrix is given by

$$F_{ij} = -E \left(\frac{\partial^2 \Lambda(S, \tau)}{\partial \theta_i \partial \theta_j} \right). \tag{3.5.3-21b}$$

Now

$$\begin{aligned}
 F_{11} &= -E \left(\frac{\partial^2 \Lambda(S, \tau)}{\partial \tau^2} \right) \\
 &= - \sum_{k=1}^B \text{tr} \left(\frac{\partial R_k^{-1}}{\partial \tau} \frac{\partial R_k}{\partial \tau} \right) \\
 &= 2 \sum_{k=1}^B \omega_k^2 |h_k|^2 S_k
 \end{aligned} \tag{3.5.3-21c}$$

where Equation (3.5.1-15c) has been used. Also
 $|h_k|^2 = (S_k/N_k^2)/(1 + 2 S_k/N_k)$.

From Equation (3.5.3-18b) we obtain

$$\begin{aligned}
 F_{22} &= -E \left(\frac{\partial^2 \Lambda(S, \tau)}{\partial S_k^2} \right) \\
 &= \left(\frac{G_k/N_k}{1 + G_k S_k/N_k} \right)^2.
 \end{aligned} \tag{3.5.3-21d}$$

Finally, the cross term is

$$\begin{aligned}
 F_{12} &= -E \left(\frac{\partial^2 \Lambda(S, \tau)}{\partial \tau \partial S_k} \right) \\
 &= -\text{tr} \left(\frac{\partial R_k^{-1}}{\partial \tau} \frac{\partial R_k}{\partial S_k} \right) \\
 &= j\omega_k |h_k|^2 \text{tr}(V_k \Phi_1 V_k^* V_k I_M V_k^*) \quad (3.5.3-21e)
 \end{aligned}$$

where relations in Equations (3.4-2) and (3.4-5b) have been used.

But from Equation (3.5.1-13e), we obtain

$$\begin{aligned}
 \text{tr}(V_k \Phi_1 V_k^* V_k I_M V_k^*) &= \text{tr} \left\{ \begin{bmatrix} 1 & 0 \\ 0 & e^{-j\omega\tau} \end{bmatrix} \begin{bmatrix} 0 & -1 \\ 1 & 0 \end{bmatrix} \begin{bmatrix} 1 & 0 \\ 0 & e^{-j\omega\tau} \end{bmatrix} \right. \\
 &\quad \left. \begin{bmatrix} 1 & 0 \\ 0 & e^{j\omega\tau} \end{bmatrix} \begin{bmatrix} 1 & 1 \\ 1 & 1 \end{bmatrix} \begin{bmatrix} 1 & 0 \\ 0 & e^{-j\omega\tau} \end{bmatrix} \right\} \\
 &= \text{tr} \begin{bmatrix} -1 & -e^{-j\omega\tau} \\ e^{j\omega\tau} & 1 \end{bmatrix} \\
 &= 0 . \quad (3.5.3-21f)
 \end{aligned}$$

Thus, $F_{12} = 0$, indicating that spectral estimates and time delay estimate are uncorrelated. Hence, using Equation (3.5.3-21a) the CRLB is given by

$$\text{VAR}(\hat{\tau}) = \left(2 \sum_{k=1}^B \omega_k^2 |h_k|^2 S_k \right)^{-1} \quad (3.5.3-22a)$$

and

$$\text{VAR}(\hat{S}_k) = \left(S_k + \frac{N_k}{G_k} \right)^2 \quad (3.5.3-22b)$$

which is identical to the time delay estimate with a known spectrum and to the spectral estimate with a known time delay, respectively. Thus, we conclude that joint time delay spectral estimation does not degrade the time delay estimates nor the spectral estimates.

It is interesting and revealing to show the explicit dependence of the time delay spectral performance on the observation time T . Let $S(\omega)$ and $N(\omega)$ be the true continuous signal and noise power spectra. Now recall from Equations (2-13d) and (3.5.1-13d) that $S_k = E(\beta_k \beta_k^*)$ and $|h_k|^2 = S_k / N_k^2 / (1 + 2 S_k / N_k)$, where β_k is the Fourier coefficient of the signal waveform from T seconds of observation. Also recall the relation that for sufficiently large T , we have $TS_k = S(\omega_k)$, $TN_k = N(\omega_k)$, and $|h_k|^2 = T|h(\omega_k)|^2$. Consequently, Equations (3.5.1-22a) and (3.5.1-22b) can be manipulated as follows to yield

$$\begin{aligned} \text{VAR}(\hat{\tau}) &= \left[\frac{T}{\pi} \sum_{k=1}^B \omega_k^2 |h(\omega_k)|^2 S(\omega_k) - \frac{2\pi}{T} \right]^{-1} \\ &= \frac{\pi}{T} \left[\int_0^B \omega^2 \left(\frac{S^2(\omega)/N^2(\omega)}{1 + 2 S(\omega)/N(\omega)} \right) d\omega \right]^{-1} \quad (3.5.3-23a) \end{aligned}$$

$$\begin{aligned} \text{VAR}(\hat{S}_k) &= \frac{1}{T^2} \left[(TS_k) + \frac{(TN_k)}{G_k} \right]^2 \\ &= \frac{1}{T^2} \left[S(\omega_k) + \frac{N(\omega_k)}{G(\omega_k)} \right]^2 \quad (3.5.3-23b) \end{aligned}$$

where $S(\omega_k)$ denotes $S(\omega)$ evaluated at frequency $\omega = (2\pi k)\frac{1}{T}$.

Thus, Equations (3.5.3-23a) and (3.5.3-23b) indicate that while the time delay variance is inversely proportional to T , the spectral variance is inversely proportional to the square of T . In other words, the spectral variance is more effectively reduced by increasing the observation time than the time delay variance.

CHAPTER 4
SUBOPTIMUM REALIZATION OF MULTISENSOR, MULTITARGET
TIME DELAY PROCESSOR

*One must learn by doing the thing: for though you think
you know it, you have no certainty until you
try.* -- SOPHOCLES

4.1 INTRODUCTION

In Chapter 3 we derived the optimum (MLE) multisensor, multi-target time delay estimator. The result yields a highly coupled multi-channel processor. For practical applications, it is desired to seek suboptimum realizations which can substantially simplify the required implementation. In this section we examine the suboptimum processor based on a weak signal in noise assumption. This is the case of considerable interest since in passive signal processing, a weak signal in noise represents the usual environment at which a signal processor must operate.

4.2 WEAK SIGNAL IN NOISE SUBOPTIMUM PROCESSOR REALIZATION

Assuming that

$$S(\omega)_j/N(\omega) \ll 1 \text{ for } j = 1, 2, \dots, J \quad (4.2-1a)$$

and using Equations (3.5.1-17c-g), Equation (3.5.1-12) becomes

$$|\tilde{h}_j(\omega)|^2 = \frac{S_j(\omega)/\tilde{N}_j^2(\omega)}{1 + G_j(\omega) S_j(\omega)/\tilde{N}_j(\omega)} \approx \frac{S_j(\omega)/N_j^2(\omega)}{1 + M S_j(\omega)/N(\omega)} \quad (4.2-1b)$$

$$\tilde{a}_j(\omega) = \tilde{N}_j(\omega) |\tilde{h}_j(\omega)|^2 \approx \frac{S_j(\omega)/\tilde{N}_j(\omega)}{1 + M S_j(\omega)/N(\omega)} \quad (4.2-1c)$$

$$\tilde{Q}_j^{-1}(\omega) = \tilde{N}_j(\omega) \left[\sum_{\substack{i=1 \\ i \neq j}}^J S_i(\omega) P_i(\omega) + N(\omega) Q(\omega) \right]^{-1} \quad (4.2-1d)$$

$$\approx Q^{-1}(\omega) \tilde{N}_j(\omega)/N(\omega) \quad (4.2-1e)$$

$$\tilde{N}_j(\omega) = \sum_{\substack{i=1 \\ i \neq j}}^J S_i(\omega) + N(\omega) \quad (4.2-1f)$$

$$P_j(\omega) = V_j(\omega) I_M V_j^*(\omega) \quad (4.2-1g)$$

$$\tilde{b}_i^j(\omega) \approx \left[\frac{S_j(\omega)/\tilde{N}_j(\omega)}{1 + M S_j(\omega)/N(\omega)} \right] \text{tr} \left[\tilde{Q}_j^{-1} V_j(\omega) \Phi_i V_j^*(\omega) \right] \quad (4.2-1h)$$

and the simplified likelihood Equation (3.5.1-12) of estimating time delay between sensors i and $i + 1$ due to target j becomes:

$$Z_{ij}(\underline{\tau}) = \frac{\partial \Lambda(\underline{\tau})}{\partial \tau_{ij}}$$

$$= \int_0^\infty \left\{ j\omega |h_j(\omega)|^2 \underline{\alpha}^*(\omega) Q^{-1}(\omega) v_j(\omega) [\Phi_i - \tilde{b}_i^j(\omega) I_M] \right. \\ \left. v_j^*(\omega) Q^{-1}(\omega) \underline{\alpha}(\omega) - T \tilde{b}_i^j(\omega) \right\} \frac{d\omega}{2\pi} \quad (4.2-2)$$

Note that Equation (4.2-2) results in a substantial simplification of Equation (3.5.1-12). For the two-target and two-sensor case studied in Section 3.5.1, the resulting two likelihood equations (3.5.1-17a) and (3.5.1-17b) become:

$$\frac{\partial \Lambda(\tau_1, \tau_2)}{\partial \tau_1} = \int_0^\infty j\omega \left\{ |h_1|^2 \underline{\alpha}^* Q^{-1} v_1 (\Phi_1 - b_1 I_M) \right. \\ \left. v_1^* Q^{-1} \underline{\alpha} - T b_1 \right\} \frac{d\omega}{2\pi} \\ = 0 \quad (4.2-3a)$$

$$\frac{\partial \Lambda(\tau_1, \tau_2)}{\partial \tau_2} = \int_0^\infty j\omega \left\{ |h_2|^2 \underline{\alpha}^* Q^{-1} v_2 (\Phi_2 - b_2 I_M) \right. \\ \left. v_2^* Q^{-1} \underline{\alpha} - T b_2 \right\} \frac{d\omega}{2\pi} \\ = 0 \quad (4.2-3b)$$

where

$$|h_1|^2 = \frac{s_1/(s_2 + N)^2}{1 + 2 s_1/N} \quad (4.2-3c)$$

$$|h_2|^2 = \frac{s_2/(s_1 + N)^2}{1 + 2 s_2/N} \quad (4.2-3d)$$

$$Q^{-1} = I \quad (4.2-3e)$$

$$\Phi_1 = \begin{bmatrix} 0 & -1 \\ 1 & 0 \end{bmatrix} \quad (4.2-3f)$$

$$b_1 = - \left(\frac{s_1/N}{1 + 2 s_1/N} \right) \left(\frac{s_2/N}{1 + 2 s_2/N} \right) \left[e^{j\omega(\tau_1 - \tau_2)} - e^{-j\omega(\tau_1 - \tau_2)} \right] \quad (4.2-3g)$$

$$b_2 = - \left(\frac{s_1/N}{1 + 2 s_1/N} \right) \left(\frac{s_2/N}{1 + 2 s_2/N} \right) \left[e^{j\omega(\tau_2 - \tau_1)} - e^{-j\omega(\tau_2 - \tau_1)} \right]. \quad (4.2-3h)$$

Using Equations (4.2-3c) through (4.2-3h), Equations (4.2-3a) and (4.2-3b) can be further simplified to

$$\begin{aligned} \frac{\partial \Lambda(\tau_1, \tau_2)}{\partial \tau_1} &= \frac{T}{2\pi} \int_{-\infty}^{\infty} j\omega \left\{ |h_1|^2 \tilde{G}_{x_1 x_2} + \frac{s_1 s_2 / N^2}{(1 + 2 s_1/N)(1 + 2 s_2/N)} \right. \\ &\quad \left. \left(1 + \frac{1}{T} |h_1|^2 Q^{-1} \alpha^2 \right) e^{-j\omega\tau_2} \right\} e^{j\omega\tau_1} d\omega \\ &= 0 \end{aligned} \quad (4.2-4a)$$

$$\begin{aligned}
 \frac{\partial \Lambda(\tau_1, \tau_2)}{\partial \tau_2} &= \frac{T}{2\pi} \int_{-\infty}^{\infty} j\omega \left\{ |h_2|^2 \hat{G}_{x_1 x_2} + \frac{s_1 s_2 / N^2}{(T + 2s_1/N)(T + 2s_2/N)} \right. \\
 &\quad \left. \left(1 + \frac{1}{T} |h_2 v_2^* Q^{-1} \underline{\alpha}|^2 \right) e^{-j\omega\tau_1} \right\} e^{j\omega\tau_2} d\omega \\
 &= 0
 \end{aligned} \tag{4.2-4b}$$

where $\underline{x} = (x_1 \ x_2)^T = Q^{-1} \underline{\alpha}$, $\hat{G}_{x_1 x_2}$ is the estimated cross power spectrum, and v_1, v_2 are the time delay steering vectors. A block diagram of this processor is shown in Figure 4-1. Note that given two sensors, a single channel GCC under a multiple target environment is known to be biased. The coupling shown in Figure 4-1 provides the required bias correction. Note that the bias correction term is a function of SNR and INR. When the power spectra are not known, the quantities SNR and INR must be substituted by their estimated values. Thus, the optimum power spectral estimator discussed in Section 3.5.3 is applicable. Finally, if the signal spectrum and interference spectrum are separable (i.e., no overlapped region), the two channels become uncoupled.

4.3 A SINGLE TARGET ASSUMPTION SUBOPTIMUM PROCESSOR

For completeness we now include a study on the suboptimum multi-target processor using a single target formulation. The resulting

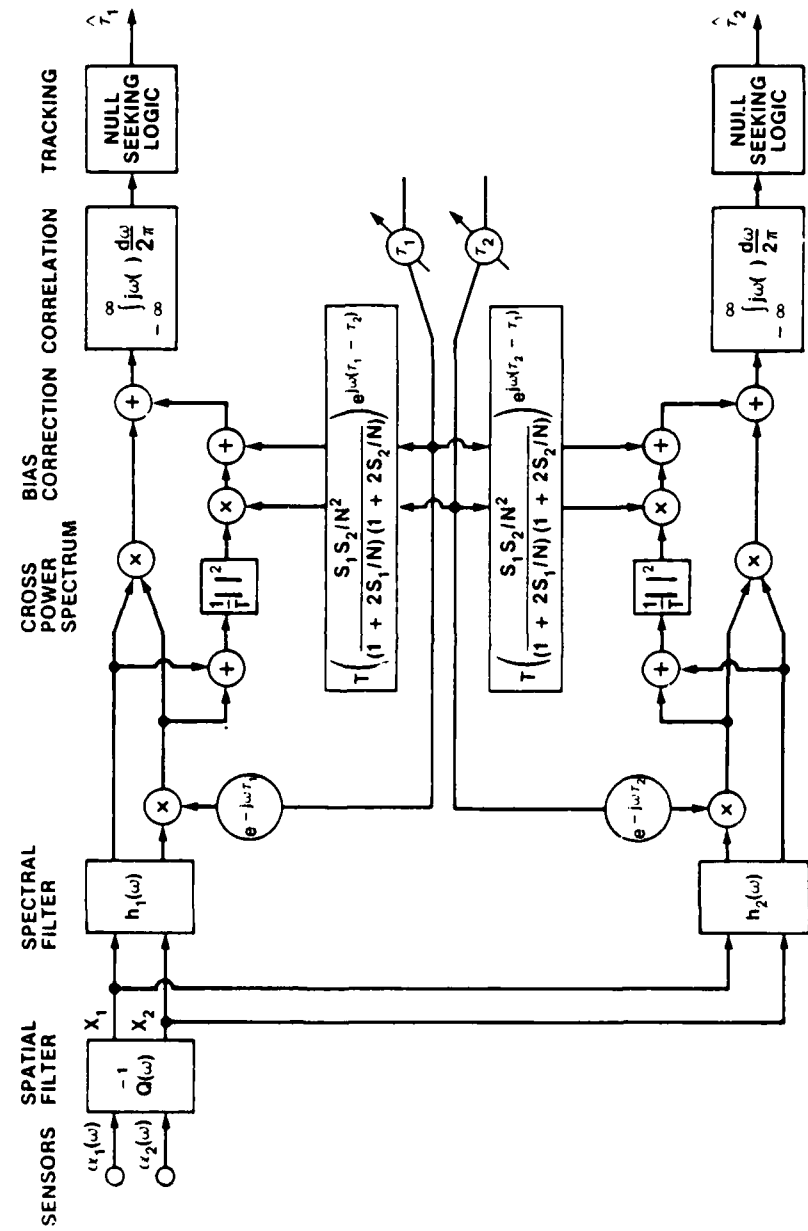


Figure 4-1. Suboptimum Two-Sensor, Two-Target Time Delay Processor

018 841

processor performance has been studied widely in the context of the localization variables (i.e., range and bearing^{7,10,11,12,34,36}). However, a direct study on the time delay variable has not been seen in the open literature.

A single target processor can be obtained from the multitarget processor by setting the interference power spectra to zero. For the two-sensor case, the resulting processor reduces to the GCC processor discussed in Section 3.5.1. The time delay is obtained from the GCC by locating the peak of the GCC function (assuming that SNR is sufficiently high so that a dominant peak can be detected). In the presence of interference the resulting estimates are known to be biased. In addition, they affect the time delay variance performance. Here we shall quantify the performance in more detail.

Consider a general two-sensor, J target problem. Let the true time delay to target j be τ_j for $j = 1, 2, \dots, J$. Then the frequency domain representation from T seconds of observation time can be written as

$$\alpha_{1k} = \underline{v}_{1k} \beta_k + n_{1k} \quad (4.3-1a)$$

$$\alpha_{2k} = \underline{v}_{2k} \beta_k + n_{2k}; \quad k = 1, 2, \dots, B \quad (4.3-1b)$$

where the complex vectors \underline{v}_{1k} , \underline{v}_{2k} and β_k are defined by

$$\underline{v}_{ik} = \left(e^{j\omega_k D_{i1}} e^{j\omega_k D_{i2}} \dots e^{j\omega_k D_{iJ}} \right) ; \quad i = 1, 2 \quad (4.3-2a)$$

and

$$\underline{\beta}_k = (\beta_{k1} \beta_{k2} \dots \beta_{kJ})^T \quad (4.3-2b)$$

where D_{ij} is the propagation time delay from target j to sensor i and β_{kj} is the Fourier component of the signal spectrum of target j . The peak of the GCC is obtained by locating the null of the function (see Equation 3.5.1-14c)

$$f(\tau) = \sum_{k=-B}^B j\omega_k |h_k|^2 \alpha_{1k} \alpha_{2k}^* e^{j\omega_k \tau} \quad (4.3-3a)$$

where $|h_k|^2$, the spectral shaping filter, is given by

$$|h_k|^2 = \frac{s_{k1}/N_k^2}{1 + 2 s_{k1}/N_k} . \quad (4.3-3b)$$

Note that without loss of generality we have let $j = 1$ be the target of interest and let the remaining $J - 1$ targets be interferences. An alternate selection of the frequency shaping filter is the multi-target spectral shaping filter (see Equation (3.5.1-4b)):

$$|\tilde{h}_k|^2 = \frac{s_{k1}/\tilde{N}_{k1}^2}{1 + G_{k1} s_{k1}/\tilde{N}_{k1}} \quad (4.3-4a)$$

where from Equations (3.5.1-2c) and (3.5.1-3)

$$\tilde{N}_{k1} = \sum_{j=2}^J S_{kj} + N \quad (4.3-4b)$$

and

$$\begin{aligned} G_{k1} &= v_{k1}^* \tilde{Q}_{k1}^{-1} v_{k1} \\ &= v_{k1}^* \left[\tilde{N}_{k1} \left(\sum_{j=2}^J S_{kj} P_{kj} + N_k Q_k \right)^{-1} \right] v_{k1} \\ &\approx \frac{\tilde{N}_{k1}}{N_k} v_{k1}^* Q_k^{-1} v_{k1} \\ &\approx 2 \frac{\tilde{N}_{k1}}{N_k} \end{aligned} \quad (4.3-4c)$$

for the two sensors with $Q_k = I$.

Therefore, a simpler form of Equation (4.3-4a) is

$$|\tilde{h}_k|^2 = \frac{S_{k1}/\tilde{N}_{k1}}{1 + 2 S_{k1}/N_k} . \quad (4.3-4d)$$

For example, for the two-target case, Equation (4.3-4d) reduces to

$$|\tilde{h}_k|^2 = \frac{S_{k1}/(S_{k2} + N_k)}{1 + 2 S_{k1}/N_k} . \quad (4.3-4e)$$

The basic derivation of the bias and variance is shown in Appendix H (Equations (H-8e) and (H-17b)). The expressions for the bias and the variance for the two-target case with identically flat signal, interference, and noise power spectra are given by Equations (H-12) and (H-21a) as

$$\delta_1 = \frac{1}{1 + S/I} (\tau_2 - \tau_1) \quad (4.3-5a)$$

and

$$\text{VAR}(\hat{\tau}_1) = \frac{2\pi}{T} \left[\frac{1 - (a_1^2 \rho(2\Delta_1) + a_2^2 \rho(2\Delta_2) + 2a_1 a_2 \rho(\Delta_1 + \Delta_2))}{2(a_1 \rho(\Delta_1) + a_2 \rho(\Delta_2))^2 R(0)} \right] \quad (4.3-5b)$$

where $\frac{S}{I}$ is the signal-to-interference ratio and

$$a_1 = \frac{S/N}{I + S/N + I/N} \quad (4.3-6a)$$

$$a_2 = \frac{I/N}{I + S/N + I/N} \quad (4.3-6b)$$

$$\Delta_1 = \hat{\tau}_1 - \tau_1 \quad (4.3-6c)$$

$$\Delta_2 = \hat{\tau}_1 - \tau_2 \quad (4.3-6d)$$

$$R(\tau) = \int_{\omega_1}^{\omega_2} \omega^2 \cos \omega \tau \, d\omega \quad (4.3-6e)$$

$$\rho(\tau) = R(\tau)/R(0) . \quad (4.3-6f)$$

Note that in the limit as $\Delta_1 \rightarrow 0$, $\Delta_2 \rightarrow \infty$, we have $\rho(\Delta_2) \rightarrow 0$, $\rho(\Delta_1) \rightarrow 1$ and the steady state variance is

$$\begin{aligned} \text{VAR}_{\infty}(\hat{\tau}_1) &= \lim_{\substack{\Delta_1 \rightarrow 0 \\ \Delta_2 \rightarrow \infty}} \text{VAR}(\hat{\tau}_1) \\ &= \frac{2\pi}{T} \left(\frac{1 - a_1^2}{2 a_1^2} \right) \frac{1}{R(0)} . \end{aligned} \quad (4.3-7)$$

Therefore, one can define a normalized variance as

$$\begin{aligned} \frac{\text{VAR}(\hat{\tau}_1)}{\text{VAR}_{\infty}(\hat{\tau}_1)} &= \left(\frac{a_1^2}{1 - a_1^2} \right) \\ &\quad \left[\frac{1 - (a_1^2 \rho(\Delta_1) + 2a_1 a_2 \rho(\Delta_1 + \Delta_2) + a_2^2 \rho(\Delta_2))}{2(a_1 \rho(\Delta_1) + a_2 \rho(\Delta_2))^2} \right]. \end{aligned} \quad (4.3-8)$$

Note that Equation (4.3-7) does not reduce to the single target case because of the presence of spectral interference. This is certainly true for the case of two omni-directional sensor arrays since interference power is not spatially attenuated as a function of time delay separation. However, for sensor arrays with large base length

separation, this condition is again satisfied since a small spatial separation could produce a large time delay separation and insignificant spatial attenuation.

4.4 GCC PERFORMANCE IN THE PRESENCE OF INTERFERENCE

Performance of the GCC in the presence of interference is compared to the optimum processor in the remainder of this section.

Figure 4-2 shows the interference of the expected value of the GCC due to signal only by the GCC from a second target with an identical spectrum shape but a 3 dB smaller signal power. It can be seen that (1) the two GCCs are merged to one (i.e., it fails to resolve the target from the interference), and (2) the peak of the combined GCC is biased. Figure 4-3 shows the same GCC in the form of a 3-D interference pattern as a function of target-interference time delay separation. (Note the combined GCC in Figure 4-2 corresponds to the curve with unity separation in Figure 4-3.) Since the MLE is asymptotically an unbiased estimator, the optimum processor has no bias for sufficient integration time. Therefore, it resolves the multitarget ambiguity. This is the primary advantage of the optimum multitarget processor. Figure 4-4 shows the bias characteristics of the GCC. Note that when the time delay separation is small, the bias is proportional to the separation, indicated by Equation (4.3-5a). Figure 4-5 presents the resulting GCC variance. The GCC variance about the estimated mean is

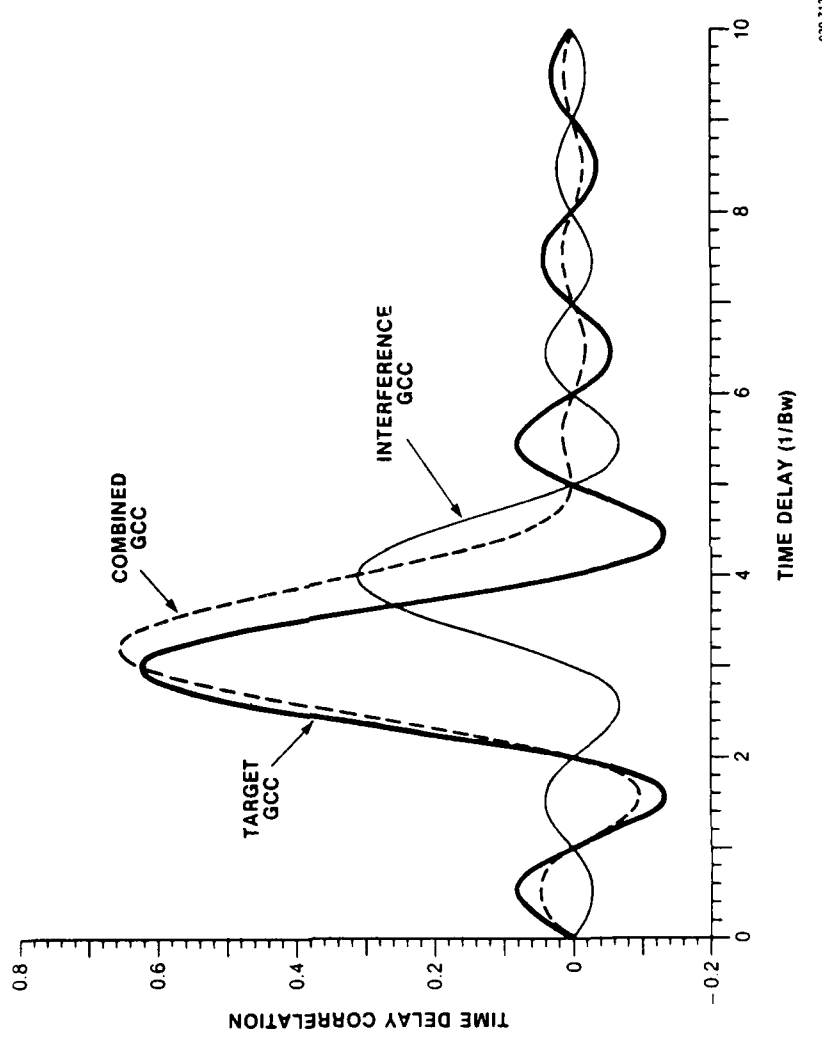


Figure 4-2. Multitarget Time Delay Interference (SNR = 20 dB, INR = 7 dB)

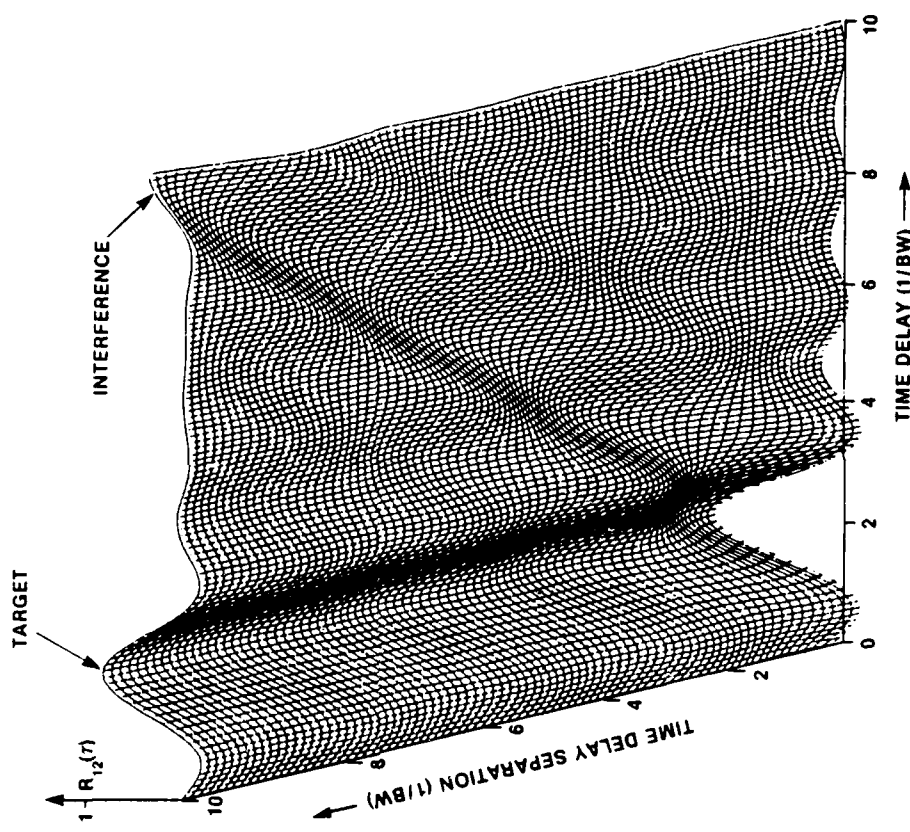


Figure 4-3. Multitarget Time Delay Interference as a Function of Time Delay Separation
 $(SNR = 10 \text{ dB}, INR = 7 \text{ dB})$

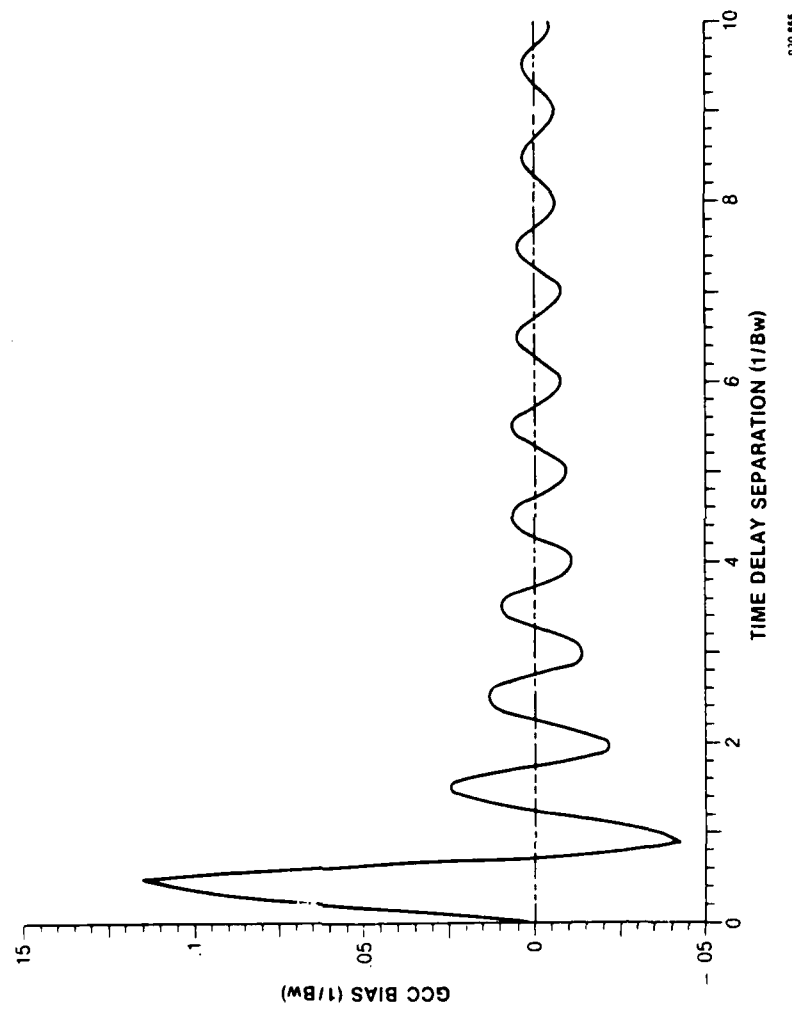


Figure 4-4. GCC Bias in the Presence of Interference (SNR = 10 dB, INR = 7 dB)

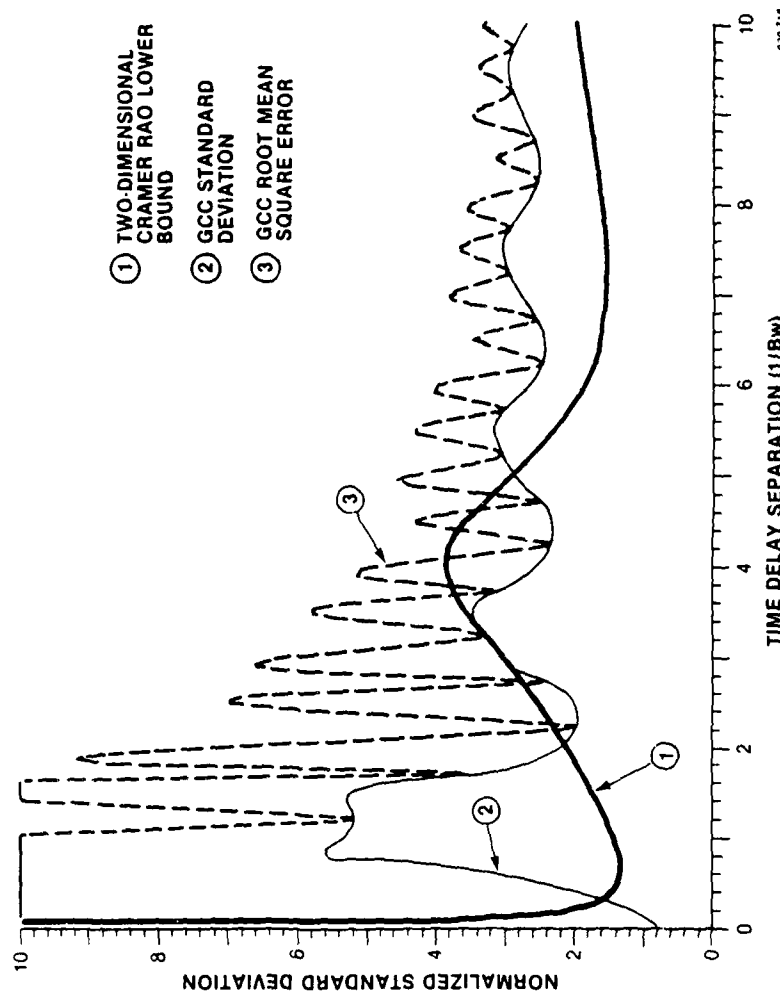


Figure 4-5. Normalized GCC Variance in the Presence of Interference (SNR = 10 dB, INR = 7 dB)

normalized by the corresponding variance with no interference (Equation (3.5.1-16b)). Also shown in Figure 4-5 is the CRLB of the optimum two-target processor. This optimum processor not only resolves the bias but also has a smaller steady state variance. Note that even with no time delay interference, the variance of the GCC does not approach the bound because of the presence of interference in the frequency domain. Also note that with no time delay separation between target and interference, the CRLB is singular, reflecting the inherent inappropriateness of a two-target formulation to a one-target estimation problem.

Also shown in Figure 4-5 is the total Root Mean Square (RMS) error of the conventional GCC processor in the presence of interference. Note that the CRLB of the optimum two-target processor results in a significantly reduced total RMS error. Finally, we remark that identical signal and interference power spectra are the worst conditions. For different signal and interference spectra, the optimum processor is well behaved even at zero time delay separation (see Figure 3-7).

CHAPTER 5

IMPROVED MULTITARGET PARAMETER RESOLUTION

Ideas must work through the brains and the arms of good and brave men, or they are no better than dreams. -- EMERSON

5.1 INTRODUCTION

In Chapter 3 we studied the optimum multitarget multisensor parameter estimator using the MLE procedure. In Chapter 4 we studied a number of suboptimum realizations. We pointed out that the GCC processor can be considered as a suboptimum processor in a multitarget environment. The use of GCC in a multitarget environment results in a poor multitarget parameter resolution; i.e., it yields a single biased estimate when separation between targets is small. The use of an Optimum Multitarget Processor (OMP) can provide a significant improvement in resolution (as shown in Figure 4-5). Unfortunately, the OMP also requires a major modification of many existing systems where GCC processors have already been implemented. Therefore in this chapter we investigate alternate procedures for improved multitarget parameter resolution.

The particular approach to be studied is the post GCC multitarget processor. In this approach, additional multitarget processing capability is provided at the GCC outputs. Thus with this

approach, the GCC processor needs no modification. In effect, the existing GCC processor can serve conveniently as a pre-processor of a multitarget estimator.

This chapter is organized as follows. Section 5.2 derives the post GCC multitarget processor. Section 5.3 presents the estimator performance bound. Section 5.4 discusses the simulation procedure and results. Specifically, we compare the performance of the conventional GCC processor, the post GCC multitarget processor, and the optimum multitarget processor.

5.2 POST GCC MULTITARGET PROCESSOR

From Equation (3.5.1-14b), the GCC output can be written as

$$R(\tau) = \sum_{k=-B}^B |h_k|^2 \alpha_{1k} \alpha_{2k}^* e^{j\omega_k \tau} \quad (5.2-1)$$

where $|h_k|$, α_{1k} and α_{2k}^* are defined as shown in Appendix H. Now Equation (5.2-1) can be written as

$$R(\tau) = \bar{R}(\tau) + W(\tau) \quad (5.2-2a)$$

where $\bar{R}(\tau)$ denotes the deterministic component and $W(\tau)$ the random component of the noisy GCC ouput. For practical application, Equation (5.2-1) is usually realized via a Fast Fourier Transform (FFT).

Thus the GCC output consists of a discrete set of observations. Therefore, let Δt be the sampling time, then the discrete GCC output can be written as

$$R(n\Delta t) = \bar{R}(n\Delta t) + W(n\Delta t); \quad n = 0, \pm 1, \pm 2, \dots, \pm N/2. \quad (5.2-2b)$$

Using Equation (5.2-1), the deterministic and the random components of $R(n\Delta t)$ can be obtained. For example, taking the expected value on both sides of Equation (5.2-1), the deterministic component is

$$\bar{R}(n\Delta t) = \sum_{k=-B}^B |h_k|^2 \frac{\alpha_{1k} \alpha_{2k}^*}{\alpha_{1k}^* \alpha_{2k}} e^{j\omega_k n\Delta t}. \quad (5.2-3a)$$

But from Appendix I, we have the relation

$$\frac{\alpha_{1k} \alpha_{2k}^*}{\alpha_{1k}^* \alpha_{2k}} = \sum_{i=1}^J S_{ki} e^{-j\omega_k \tau_i} \quad (5.2-3b)$$

where τ_i is the true time delay between two sensors for target i and S_{ki} is the corresponding target discrete power spectral density.

Substituting Equation (5.2-3b) into Equation (5.2-3a) yields

$$\begin{aligned} \bar{R}(n\Delta t) &= \sum_{i=1}^J \sum_{k=-B}^B S_{ki} |h_k|^2 e^{j\omega_k (n\Delta t - \tau_i)} \\ &= \sum_{i=1}^J S_i p_i (n\Delta t - \tau_i) \end{aligned} \quad (5.2-3c)$$

where the i th target power S_i and the normalized auto-correlation are given by

$$S_i = \sum_{k=-B}^B S_{ki} \quad (5.2-3d)$$

$$\rho_i(n\Delta t - \tau_i) = \sum_{k=-B}^B (S_{ki}/S_i) |h_k|^2 e^{j\omega_k(n\Delta t - \tau_i)}. \quad (5.2-3e)$$

The covariance of the random component is given by (see Appendix I)

$$\begin{aligned} \Lambda_{nm} &= E[W(n\Delta t) W(m\Delta t) - \overline{W(n\Delta t)} \overline{W(m\Delta t)}] \\ &= \sum_{k=-B}^B |h_k|^4 \left[G_{11}(k) G_{22}(k) e^{-j\omega_k m\Delta t} + G_{12}^2(k) e^{j\omega_k m\Delta t} \right] e^{j\omega_k n\Delta t} \end{aligned} \quad (5.2-4a)$$

where $G_{11}(k)$, $G_{22}(k)$, and $G_{12}(k)$ are the discrete auto-spectra and discrete cross spectrum, respectively, given by:

$$G_{11}(k) = \overline{\alpha_{1k} \alpha_{1k}^*} = \sum_{i=1}^J S_{ki} + N_{1k} \quad (5.2-4b)$$

$$G_{22}(k) = \overline{\alpha_{2k} \alpha_{2k}^*} = \sum_{i=1}^J S_{ki} + N_{2k} \quad (5.2-4c)$$

and

$$G_{12}(k) = \frac{\alpha_{1k} \alpha_{2k}^*}{\alpha_{2k}} = \sum_{i=1}^J s_{ki} e^{-j\omega_k \tau_i} . \quad (5.2-4d)$$

Now define the $2J$ unknown parameter vector by

$$\underline{\theta} = (s_1, s_2, \dots, s_J; \tau_1, \tau_2, \dots, \tau_J)^T \quad (5.2-5a)$$

and the assumed matching function by

$$h_n(\underline{\theta}) = \sum_{i=1}^J s_i \rho_i(n\Delta t - \tau_i) , \quad (5.2-5b)$$

then the observation Equation (5.2-2b) can be written as

$$R(n\Delta t) = h_n(\underline{\theta}) + w(n\Delta t) ; \quad n = 0, \pm 1, \pm 2, \dots, \pm N/2 . \quad (5.2-5c)$$

In matrix notation, this can be written as

$$\underline{z} = \underline{h}(\underline{\theta}) + \underline{w} \quad (5.2-6a)$$

where

$$\underline{z} = [R(-N\Delta t/2), \dots, R(N\Delta t/2)]^T \quad (5.2-6b)$$

$$\underline{h}(\underline{\theta}) = [h_{-N/2}(\underline{\theta}), \dots, h_{-N/2}(\underline{\theta})]^T \quad (5.2-6c)$$

$$\underline{W} = [W(-N\Delta t/2), \dots, W(N\Delta t/2)]^T \quad (5.2-6d)$$

are $N+1$ dimensional vectors.

Note that the noise vector is zero mean with matrix covariance

$$E(\underline{W} \underline{W}^T) = \Lambda \quad (5.2-6e)$$

where the mn element of Λ is given by Equation (5.2-4a). Using an LMS error criteria, the best estimate of the unknown parameter vector $\underline{\theta}$ is obtained by minimizing the function

$$J(\underline{\theta}) = [\underline{Z} - \underline{h}(\underline{\theta})]^T [\underline{Z} - \underline{h}(\underline{\theta})] . \quad (5.2-7)$$

Thus the best estimate of $\underline{\theta}$ is given by

$$\hat{\underline{\theta}} = \underset{\underline{\theta}}{\text{Min Arg}} J(\underline{\theta}) \quad (5.2-8a)$$

or equivalently the vector null equation

$$\left. \frac{\partial J(\underline{\theta})}{\partial \underline{\theta}} \right|_{\underline{\theta} = \hat{\underline{\theta}}} = \left[\frac{\partial \underline{h}(\underline{\theta})}{\partial \underline{\theta}} \right]_{\underline{\theta} = \hat{\underline{\theta}}}^T [\underline{Z} - \underline{h}(\hat{\underline{\theta}})] = \underline{0} . \quad (5.2-8b)$$

Note that because we are trying to find a best match of the observed GCC output to an assumed reference function, the resulting estimator is appropriately called the Matched Estimator.

5.3 ESTIMATOR PERFORMANCE EVALUATION

In this section we present the multi-parameter covariance matrix bound for the post GCC multitarget processor. Rewriting the vector null equation (5.2-8b) as

$$\underline{y}(\underline{\theta}) = \left[\frac{\partial \underline{h}(\underline{\theta})}{\partial \underline{\theta}} \right]^T [\underline{z} - \underline{h}(\underline{\theta})] = \underline{0}, \quad (5.3-1)$$

the Taylor series expansion of $\underline{y}(\underline{\theta})$ about $\underline{\theta}_0$, the true parameter vector yields (ignoring the higher order terms)

$$\underline{y}(\underline{\theta}) = \underline{y}(\underline{\theta}_0) + \left. \frac{\partial \underline{y}(\underline{\theta})}{\partial \underline{\theta}} \right|_{\underline{\theta} = \underline{\theta}_0} (\underline{\theta} - \underline{\theta}_0). \quad (5.3-2a)$$

Since by definition $\underline{y}(\underline{\theta}) = \underline{0}$, we must have

$$\begin{aligned} \underline{y}(\underline{\theta}_0) &= - \left. \frac{\partial \underline{y}(\underline{\theta})}{\partial \underline{\theta}} \right|_{\underline{\theta} = \underline{\theta}_0} (\hat{\underline{\theta}} - \underline{\theta}_0) \\ &= - A(\underline{\theta}_0) \hat{\delta \underline{\theta}} \end{aligned} \quad (5.3-2b)$$

where $\hat{\delta}_{\underline{\theta}} \stackrel{\Delta}{=} (\hat{\underline{\theta}} - \underline{\theta}_0)$ and

$$\begin{aligned}
 A(\underline{\theta}_0) &= \left. \frac{\partial \underline{y}(\underline{\theta})}{\partial \underline{\theta}} \right|_{\underline{\theta} = \underline{\theta}_0} \\
 &= \left. \frac{\partial h(\underline{\theta})}{\partial \underline{\theta}} \right|_{\underline{\theta} = \underline{\theta}_0} [Z - h(\underline{\theta}_0)] - \left[\frac{\partial h(\underline{\theta})}{\partial \underline{\theta}} \right]_{\underline{\theta} = \underline{\theta}_0}^T \left[\frac{\partial h(\underline{\theta})}{\partial \underline{\theta}} \right]_{\underline{\theta} = \underline{\theta}_0} \\
 &\approx -H^T(\underline{\theta}_0) H(\underline{\theta}_0) \tag{5.3-2c}
 \end{aligned}$$

In deriving Equation (5.3-2c), it was assumed that the first term is negligible for sufficiently high SNR. Therefore, from Equation (5.3-2b), one obtains the matrix covariance equation

$$\text{COV}[\underline{y}(\underline{\theta}_0)] = A(\underline{\theta}_0) \text{COV}[\hat{\delta}_{\underline{\theta}}] A(\underline{\theta}_0)^T. \tag{5.3-2d}$$

But from Equation (5.3-1)

$$\text{COV}[\underline{y}(\underline{\theta}_0)] = H^T(\underline{\theta}_0) \Lambda H(\underline{\theta}_0). \tag{5.3-2e}$$

Therefore, the estimator's matrix covariance is

$$\text{COV}[\hat{\delta}_{\underline{\theta}}] = A^{-1}(\underline{\theta}_0) H^T(\underline{\theta}_0) \Lambda H(\underline{\theta}_0) A^{-1}(\underline{\theta}_0). \tag{5.3-3}$$

5.4 SIMULATION

A computer program was developed on the VAX-11/780 at NUSC to simulate the multitarget GCC output. For simplicity, a two-sensor, two-target environment was chosen. The GCC output observation window was set at ten times the reciprocal signal bandwidth. Both targets are assumed to have a broadband flat spectra. One thousand Monte Carlo iterations were used for each time delay separation. Simulation results are plotted along with the theoretical performance predictions.

5.4.1 Simulation Procedure

Figure 5-1 diagrams the simulation procedure. The multitarget GCC output observation vector (Equation (5.2-6a)) was generated by adding observation noise sequence with prescribed covariance to the noise-free GCC component. The noise vector was generated using the following procedure: (1) calculating the multitarget GCC covariance matrix from Equation (5.2-4a), (2) factoring the matrix into lower and upper triangular matrices using the Gramm-Schmidt orthogonalization procedure, and (3) multiplying the lower triangular matrix by a white noise vector to produce the desired correlated observation noise vector. Finally, the GCC observation vector was processed by the matched estimator.

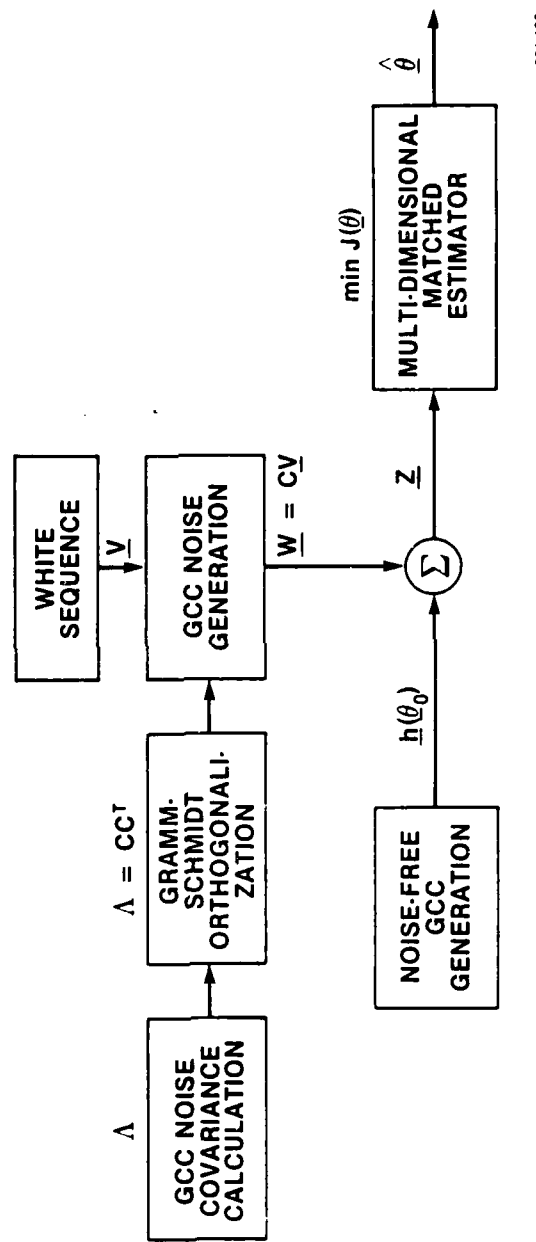


Figure 5-1. Post GCC Multitarget Processor Simulation

5.4.2 Discussion of Results

Since a detailed investigation of the matched estimator will be shown elsewhere,^{37,38} only a brief discussion of the simulation results will be presented here. Figure 5-2 shows the bias characteristics of a conventional GCC estimator; the target assumed a broadband, one-sided spectrum between 0 and B Hz while the interference assumed a broadband, one-side spectrum between $\frac{B}{2}$ and B Hz, the target strength is at 0 dB and the interference is at -1 dB. Note the large bias when targets are separated just below the reciprocal signal bandwidth. In this region, targets are not resolved with the conventional GCC estimator. Figures 5-3 and 5-4 show the normalized rms (normalized by the time delay standard deviation of target only) performance of a conventional GCC estimator, the post GCC matched estimator, and the optimum multitarget estimator as a function of time delay separation. While Figure 5-3 assumed identical broadband signal and interference spectra, Figure 5-4 assumed the interference occupied the upper half frequency band but maintained the same interference power. Note that the conventional GCC rms was clipped at a degradation ratio of 20 for time delay separation less than the reciprocal signal bandwidth. Both Figures 5-3 and 5-4 show the marked improvement of the matched estimator over the GCC estimator. Note the close performance between the matched estimator and the optimum processor.

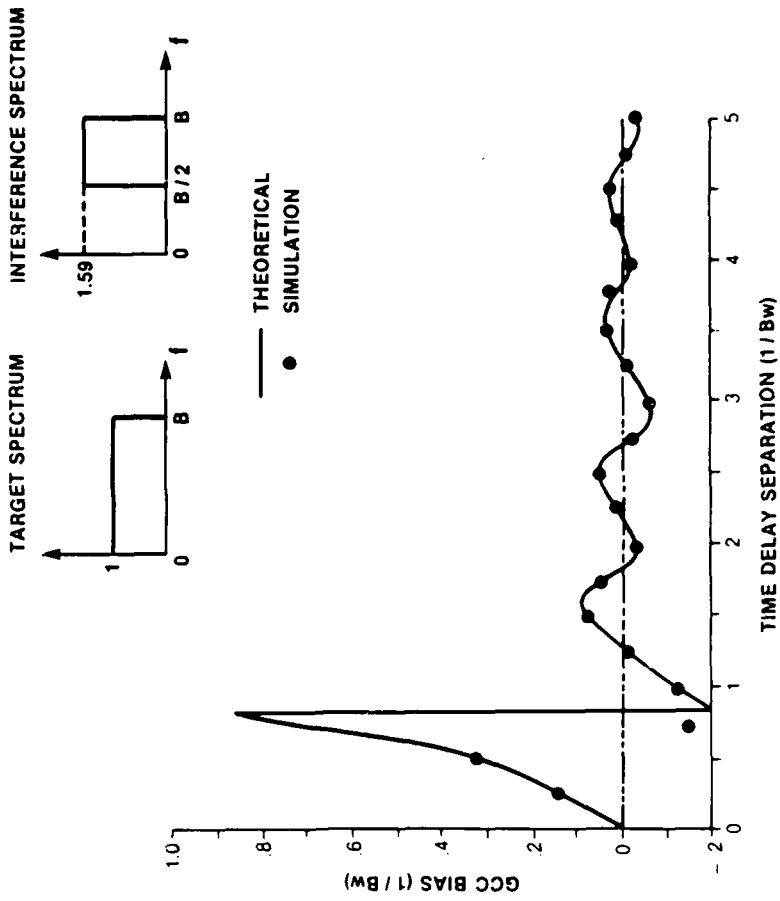


Figure 5-2. GCC Bias Versus Delay Separation (SNR = 0 dB, INR = -1 dB;
 $S:0 \rightarrow B$, $I:B/2 \rightarrow B$, $N:0 \rightarrow B$)

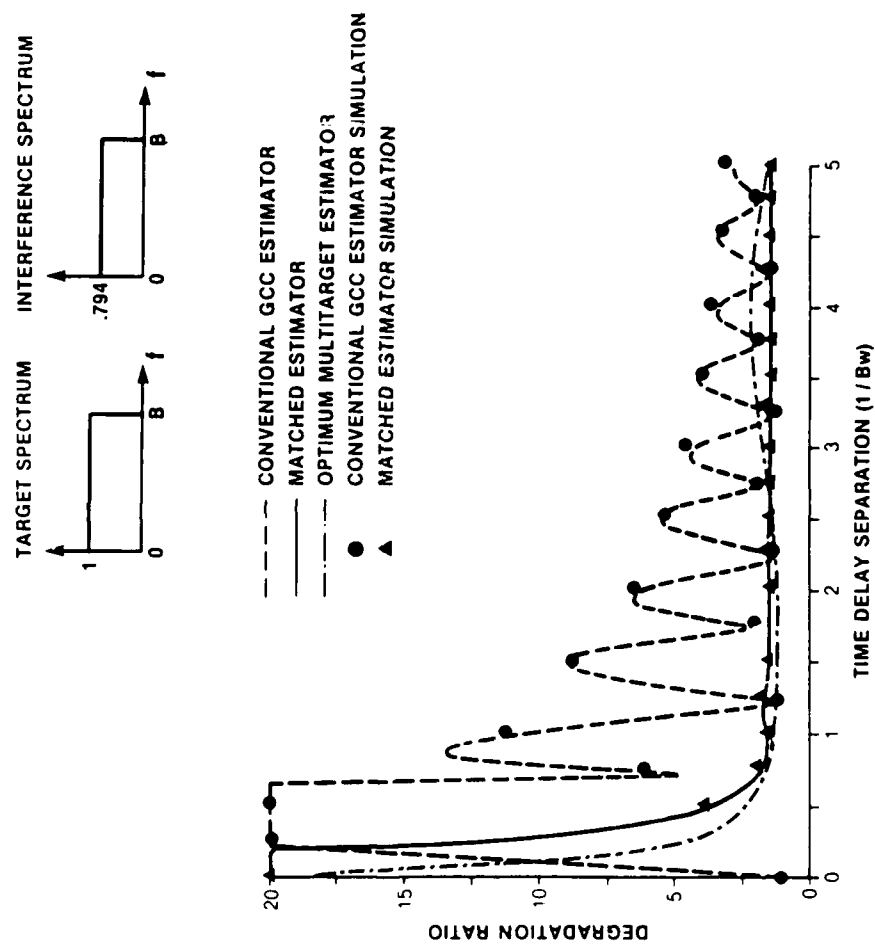


Figure 5-3. Degradation Ratio Versus Time Delay Separation (SNR = 0 dB,
INR = -1 dB; S:0 → B, I:0 → B, N:0 → B)
021.161

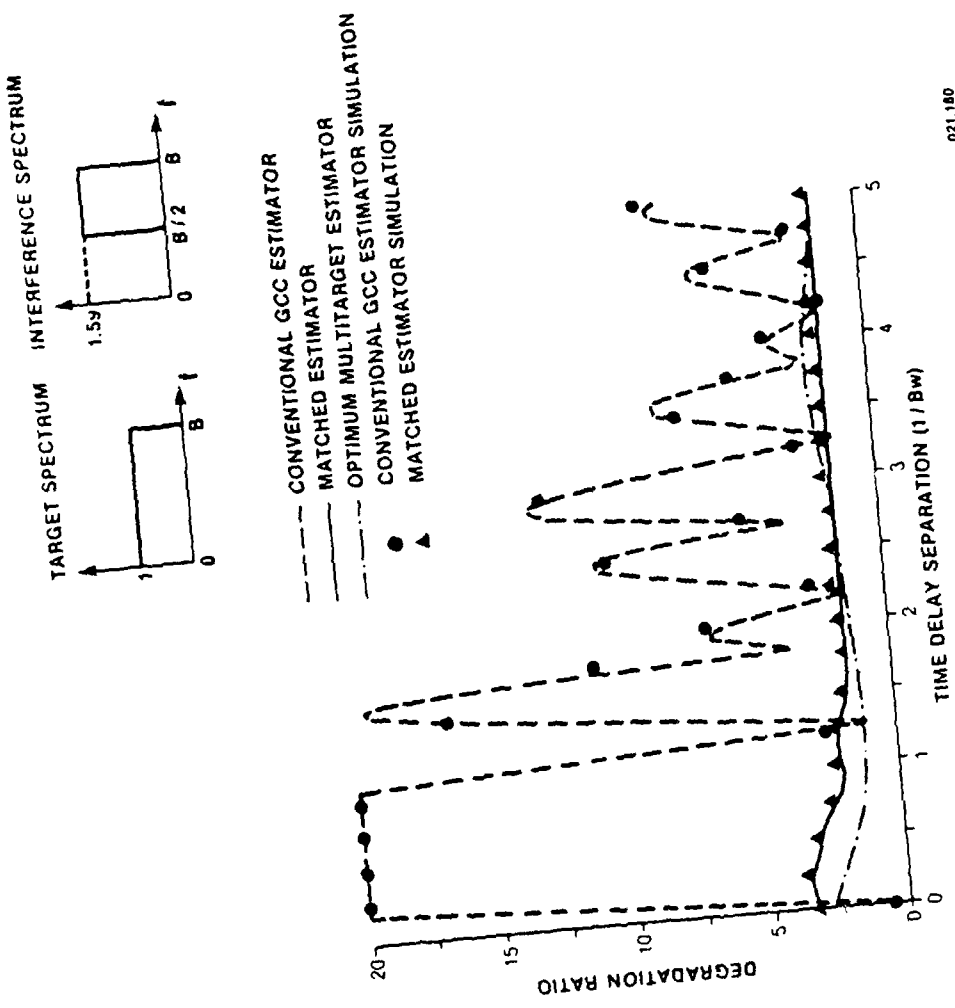


Figure 5-4. Degradation Ratio Versus Time Delay Separation ($\text{SNR} = 0 \text{ dB}$,
 $\text{INR} = -1 \text{ dB}$; $S:0 \rightarrow B$, $1:B/2 \rightarrow B$, $N:0 \rightarrow B$)

CHAPTER 6

OPTIMUM VARIABLE TIME DELAY ESTIMATION AND TRACKING

*And remember men will scorn it, 'tis original and true, and
the obloquy of newness may fall bitterly on you.*
-- SARAH WILLIAMS

6.1 INTRODUCTION

Our study on the optimum multisensor, multitarget parameter estimation thus far has assumed that all targets are stationary in space. The resulting set of observed signal waveforms yields a well-known Stationary Parameter Long Observation Time (SPLIT) process. The optimum multitarget estimator under this assumption was derived and presented in Chapter 3. Note that for a stationary parameter process, the resulting estimator (MLE) is asymptotically efficient. Thus an optimum estimator can always be found for the stationary parameter case by selecting an arbitrarily long observation window. This, however, is not necessarily true for the variable parameter case where, by increasing the observation window, it may also be necessary to increase the order of the dynamic model. In addition, the variable time delay dynamic causes an incoherent signal integration which results in a reduced signal processing gain when the stationary optimum processor is used.

In reality, targets are more likely moving than stationary; we therefore devote this and the next chapter to addressing this important problem. In our discussion we shall differentiate the estimation process from the tracking process as follows. The estimation process is an open loop, batch process whereby the best estimate of the unknown parameter is derived from T seconds of observation. On the other hand, the tracking process is a sequential process whereby the best estimate of the unknown parameter is given continuously as a function of time.

The variable time delay estimation of a single target environment has been studied by a number of researchers. For example, Knapp and Carter¹⁴ studied the optimum GCC in the presence of source motion and concluded that the optimum processor requires a time compression and expansion operation. Schultheiss and Weinstein¹⁵ studied the lower bounds on the localization errors of a moving source observed by a passive array. Chan, Riley and Plant¹⁶ investigated the estimation of nonstationary delay by modeling the time delay as a finite impulse response (FIR) process. Friedlander¹⁷ studied the joint time delay and signal spectrum estimation using an ARMA modeling approach. In this chapter we study the problem of variable time delay estimation and tracking with a strong emphasis on practical estimator realization. In addition, our formulation includes the general multisensor, multitarget environment.

This chapter is organized as follows. Section 6.2 develops the likelihood equation. Section 6.3 presents the variable time delay estimator. Section 6.4 derives the estimator performance bounds. Finally, Section 6.5 discusses the problem of variable time delay tracking.

6.2 THE LIKELIHOOD EQUATION

Let the M sensor array outputs from J moving acoustic sources be written as (see Equation (2.3-1))

$$y(t, \underline{\ell}_i) = \sum_{j=1}^J a_{ij} s_j (t + D_{ij}(t)) + n_i(t); \quad t \in [0, T] \quad (6.2-1)$$

where $i = 1, 1, \dots, M$; a_{ij} is the known signal attenuation factor and for convenience assumed unity; $D_{ij}(t)$ is the variable propagation time delay from target j to sensor i ; and $s_j(t)$ and $n_i(t)$ are the band-limited signal and noise processes with the usual assumptions of zero mean, Gaussian, time stationary, mutually uncorrelated, and spatially homogeneous. Note that it is the time dependence of the propagation delays that renders the observed waveforms non-stationary.

Now let the time delay variation over a T -second observation be modeled by a P th order Taylor polynomial:

$$D(t) = D + \dot{D}t + \dots + \frac{D^{(P)}}{P!} t^P \quad (6.2-2)$$

where $D^{(P)}$ denotes the Pth order derivative of $D(t)$ evaluated at $t = 0$.

We segment the T-second observation into N equal subintervals (Figure 6-1) and let $\Delta t = T/N$. Furthermore, let D_{MAX} be the maximum time delay rate and B be the signal bandwidth. Then from the development shown in Appendix J, we can select Δt to satisfy the relation.

$$\frac{8}{B} \leq \Delta t \leq \frac{1}{4BD_{MAX}} \quad (6.2-3a)$$

so that the resulting loss in coherence is negligible. Furthermore, the time delay variation within the Δt -second interval will be essentially linear. Therefore, using the results from Appendix J, the frequency domain representation of the observed waveform from the i th sensor and the n th interval is

$$\begin{aligned} a_{ikn} &= \frac{1}{\Delta t} \int_{(n-1)\Delta t}^{n\Delta t} y(t, \underline{\lambda}_i) e^{-j\omega_k t} dt \\ &= \frac{1}{\Delta t} \int_{(n-1)\Delta t}^{n\Delta t} \left[\sum_{j=1}^J s_j(t + D_{ij}(t)) + n_i(t) \right] e^{-j\omega_k t} dt \end{aligned}$$

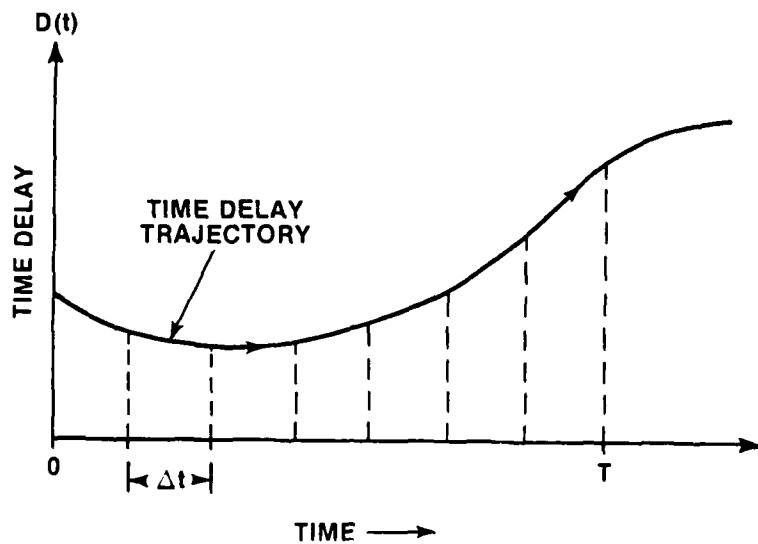
$$\approx \sum_{j=1}^J \beta_{kjn} e^{j\omega_k D_{ij}(t_n)} + \eta_{ikn}$$

$$= W_{ikn}^* \beta_{kn} + \eta_{ikn} \quad (6.2-3b)$$

where $\omega_k = 2\pi k / \Delta t$, $t_n = (n - 1/2) \Delta t$ and

$$W_{ikn}^* = \left(e^{j\omega_k D_{ij}(t_1)} \dots e^{j\omega_k D_{ij}(t_N)} \right) \quad (6.2-3c)$$

$$\beta_{kn} = (\beta_{k1n} \dots \beta_{kJn})^T. \quad (6.2-3d)$$



021.61.

Figure 6-1. Polynomial Model of Variable Time Delay

In addition, β_{kjn} and n_{ikn} are defined by the relations

$$\beta_{kjn} \triangleq \frac{1}{\Delta t} \int_{(n-1)\Delta t}^{n\Delta t} s_j(t) e^{-j\omega_k t} dt \quad (6.2-3e)$$

$$n_{ikn} \triangleq \frac{1}{\Delta t} \int_{(n-1)\Delta t}^{n\Delta t} n_i(t) e^{-j\omega_k t} dt . \quad (6.2-3f)$$

Note that $D_{ij}(t_n)$ is $D_{ij}(t)$ evaluated time t_n . When $D_{ij}(t)$ is modeled by a P th order polynomial, $D_{ij}(t_n)$ contains $P + 1$ unknown coefficients. Furthermore, β_{kjn} and n_{ikn} are zero mean, complex Gaussian variables whose covariances are given by

$$E(\beta_{kjn} \beta_{k'j'n'}^*) = \begin{cases} S_{kjn}; & \text{if } k=k', j=j', \text{ and } n=n' \\ 0; & \text{otherwise} \end{cases} \quad (6.2-3g)$$

and

$$E(n_{ikn} n_{i'k'n'}^*) = \begin{cases} N_{ikn}; & \text{if } i=i', k=k', \text{ and } n=n' \\ 0; & \text{otherwise} . \end{cases} \quad (6.2-3h)$$

Thus we have utilized the assumption that target waveform and noise waveform Fourier coefficients are uncorrelated for different targets, different frequencies, and at different observation intervals.

Now define the M sensor observation vector, $\underline{\alpha}_{kn}$, at the nth observation interval as

$$\underline{\alpha}_{kn} = (\alpha_{1kn} \alpha_{2kn} \dots \alpha_{Mkn})^T; k=1, \dots, B. \quad (6.2-4a)$$

Then one can write

$$\underline{\alpha}_{kn} = W_{kn} \underline{\beta}_{kn} + \underline{\eta}_{kn} \quad (6.2-4b)$$

where

$$W_{kn} = \begin{bmatrix} w_{1kn}^* \\ \vdots \\ w_{2kn}^* \\ \vdots \\ \cdot \\ \vdots \\ w_{Mkn}^* \end{bmatrix} \quad (6.2-4c)$$

$$\underline{\eta}_{kn} = (\eta_{1kn} \eta_{2kn} \dots \eta_{Mkn})^T. \quad (6.2-4d)$$

Note that $\underline{\alpha}_{kn}$ is a zero mean, complex Gaussian vector whose covariance matrix is

$$\begin{aligned} R_{kn} &= E(\underline{\alpha}_{kn} \underline{\alpha}_{kn}^*) \\ &= W_{kn} S_k W_{kn}^* + N_k Q_k \end{aligned} \quad (6.2-4e)$$

where it is defined as in Chapter 2 that

$$\begin{aligned} S_k &= E(\underline{\beta}_{kn} \underline{\beta}_{kn}^*) = \text{diag } \{S_{k1} \dots S_{kJ}\} \\ N_k Q_k &= E(\underline{n}_{kn} \underline{n}_{kn}^*) . \end{aligned} \quad (6.2-4f)$$

Note that S_k , N_k and Q_k are independent of the observation intervals for known signal and noise spectra.

Furthermore, writing

$$\underline{\alpha}_n = (\underline{\alpha}_{1n}^*, \underline{\alpha}_{2n}^*, \dots, \underline{\alpha}_{Bn}^*)^* \quad (6.2-5a)$$

and denoting the set of M sensors, J target, and P order polynomial unknown parameter vector as $\underline{\alpha}$, then the pdf of $\underline{\alpha}_n$ is given by

$$p(\underline{\alpha}_n | \underline{\theta}) = \pi^{-BM} \prod_{k=1}^B |\underline{R}_{kn}|^{-1} \exp\{-\underline{\alpha}_{kn}^* \underline{R}_{kn}^{-1} \underline{\alpha}_{kn}\} . \quad (6.2-5b)$$

Finally, writing

$$\underline{\alpha} = (\underline{\alpha}_1^*, \underline{\alpha}_2^*, \dots, \underline{\alpha}_N^*)^* , \quad (6.2-5c)$$

we have the pdf of the complete observation vector as

$$p(\underline{\alpha} | \underline{\theta}) = \prod_{n=1}^N p(\underline{\alpha}_n | \underline{\theta}) \quad (6.2-5d)$$

since observations are independent between intervals.

Substituting Equation (6.2-5b) into (6.2-5d) yields

$$p(\underline{\alpha}|\underline{\theta}) = \pi^{-BMN} \prod_{n=1}^N \prod_{k=1}^B |R_{kn}|^{-1} \exp\{-\alpha_{kn}^* R_{kn}^{-1} \alpha_{kn}\}. \quad (6.2-6a)$$

The corresponding log-likelihood function is

$$\begin{aligned} \Lambda(\underline{\theta}) &= \log p(\underline{\alpha}|\underline{\theta}) \\ &= -BMN \log (\pi) - \sum_{n=1}^N \sum_{k=1}^B \Lambda_{kn}(\underline{\theta}) \end{aligned} \quad (6.2-6b)$$

where

$$\Lambda_{kn}(\underline{\theta}) = \log |R_{kn}| + \alpha_{kn}^* R_{kn}^{-1} \alpha_{kn}. \quad (6.2-6c)$$

Note that Equation (6.2-6c) is a direct generalization of the development shown in Chapter 3 from a single observation interval to a multiple observation interval. The likelihood equation is given by

$$\nabla \Lambda(\underline{\theta}) = - \sum_{n=1}^N \sum_{k=1}^B \nabla \Lambda_{kn}(\underline{\theta}) = 0. \quad (6.2-6d)$$

Note that for $n = 1$, Equation (6.2-6d) reduces to Equation (3.2-11) in Chapter 3.

6.3 VARIABLE TIME DELAY ESTIMATION

We noted in the previous section that the multi-interval, multi-sensor and multitarget likelihood equation is simply a generalization of a single observation interval case. Therefore, many of the results developed in Chapter 3 are either applicable or can be generalized. In this section we examine in some detail the variable time delay estimator.

We can write

$$w_{kn} = (\underline{v}_{k1n}, \underline{v}_{k2n}, \dots, \underline{v}_{kjn}) \quad (6.3-1a)$$

in Equation (6.2-4c) where the complex column steering vector at interval n is given in accordance with Equation (3.5.1-8a) by

$$\underline{v}_{kjn} = \left(1, e^{j\omega_k U_1^T \underline{\tau}_j(t_n)}, e^{j\omega_k U_2^T \underline{\tau}_j(t_n)}, \dots, e^{j\omega_k U_{M-1}^T \underline{\tau}_j(t_n)} \right) \quad (6.3-1b)$$

where

$$\underline{\tau}_j(t_n) = (\tau_{1j}(t_n), \tau_{2j}(t_n), \dots, \tau_{M-1,j}(t_n)) \quad (6.3-1c)$$

$$\begin{aligned} \text{and } \tau_{ij}(t_n) &= D_{i+1,j}(t_n) - D_{i,i}(t_n) \\ &= \tau_{ij} + \dot{\tau}_{ij} t_n + \dots + (\tau_{ij}^{(P)}/P!) t_n^P. \end{aligned} \quad (6.3-1d)$$

Note that $\tau_{ij}(t_n)$ is the variable time delay difference between sensors i and $i + 1$ of target j , and τ_{ij} , $\dot{\tau}_{ij}$, $\ddot{\tau}_{ij}$. . . are the time delay, delay rate, and delay acceleration, etc evaluated at $t = 0$.

Now define the i th order polynomial coefficient vector for the $M - 1$ variable time delay of the j th target by

$$\underline{\tau}_j^{(i)} = (\tau_{1j}^{(i)}, \tau_{2j}^{(i)}, \dots, \tau_{M-1,j}^{(i)})^T; \quad i = 0, 1, \dots, P \\ j = 1, 2, \dots, J \quad (6.3-2a)$$

and the complete $q = 1(M-1)(P+1)$ parameter vector for M sensors, J targets, and P order polynomial by

$$\underline{\theta}^T = (\underline{\tau}_1^{(0)}, \dots, \underline{\tau}_1^{(P)}, \underline{\tau}_2^{(0)}, \dots, \underline{\tau}_2^{(P)}, \dots, \underline{\tau}_J^{(0)}, \dots, \underline{\tau}_J^{(P)}). \quad (6.3-2b)$$

Using Equations (6.2-4f) and (6.3-1a) in (6.2-4e), one can rewrite the covariance matrix R_{kn} as

$$R_{kn} = \sum_{j=1}^J S_{kj} P_{kjn} + N_k Q_k \quad (6.3-3a)$$

where we have defined as in Chapter 3 the relation

$$P_{kjn} = \underline{v}_{kjn} \underline{v}_{knj}^* \quad (6.3-3b)$$

Note the close similarity between Equations (6.3-3a) and (3.2-3c).

In fact, with minor modification, the developments presented in Chapter 3 are directly applicable. Carrying out the mathematical manipulation as shown in Section 3.5.1, the optimum estimate of the parameter vector $\underline{\theta}$ is given by (see Equation (3.5.1-7)) the simultaneous solution of

$$\begin{aligned} \frac{\partial \Lambda(\underline{\theta})}{\partial \theta_i} &= \sum_{n=1}^N \sum_{k=1}^B |\tilde{h}_{kjn}|^2 \underline{a}_{kn}^* \tilde{Q}_{kjn}^{-1} \left(\frac{\partial p_{kjn}}{\partial \theta_i} - \tilde{a}_{kjn} \frac{\partial G_{kjn}}{\partial \theta_i} p_{kjn} \right) \tilde{Q}_{kjn}^{-1} \underline{a}_{kn} \\ &\quad - \tilde{a}_{kjn} \frac{\partial G_{kjn}}{\partial \theta_i} \\ &= 0; \text{ for every } \theta_i \in \Omega_j \text{ and } j = 1, \dots, J \end{aligned} \quad (6.3-4a)$$

where Ω_j is the parameter set associated with target j defined by relation $\Omega_j = (\underline{x}_j^{(i)}; i = 0, \dots, P)$. Furthermore, the various quantities appearing in Equation (6.3-4) are defined as follows:

$$|\tilde{h}_{kjn}|^2 = \frac{s_{kj}/\tilde{N}_{kj}^2}{1 + G_{kjn} s_{kj}/\tilde{N}_{kj}} \quad (6.3-4b)$$

$$\tilde{a}_{kjn} = \tilde{N}_{kj} |\tilde{h}_{kjn}|^2 \quad (6.3-4c)$$

$$G_{kjn} = \underline{v}_{kjn}^* \tilde{Q}_{kjn}^{-1} \underline{v}_{kjn} \quad (6.3-4d)$$

$$\tilde{Q}_{kjn}^{-1} = \sum_{\substack{i=1 \\ i \neq j}}^J S_{ki} P_{kin} + N_k Q_k / \tilde{N}_{kj} \quad (6.3-4e)$$

and

$$\tilde{N}_{kj} = \sum_{\substack{i=1 \\ i \neq j}}^J S_{ki} + N_k . \quad (6.3-4f)$$

Now combining Equations (6.3-1b) and (6.3-3b), one obtains the ℓm element of the matrix P_{kjn} as

$$p_{kjn}^{\ell m} = e^{j\omega_k (\underline{U}_{\ell-1} - \underline{U}_{m-1})^T \underline{\tau}_j(t_n)} . \quad (6.3-5a)$$

Therefore, for any parameter θ_i belonging to the target j parameter set Ω_j , we have

$$\begin{aligned} \frac{\partial p_{kjn}^{\ell m}}{\partial \theta_i} &= j\omega_k (\underline{U}_{\ell-1} - \underline{U}_{m-1})^T \frac{\partial \underline{\tau}_j(t_n)}{\partial \theta_i} p_{kjn}^{\ell m} \\ &= j\omega_k \frac{\partial \Phi_n^{\ell m}}{\partial \theta_i} p_{kjn}^{\ell m} \end{aligned} \quad (6.3-5b)$$

where

$$\Phi_n^{\ell m} = (\underline{U}_{\ell-1} - \underline{U}_{m-1})^T \underline{\tau}_j(t_n) . \quad (6.3-5c)$$

Recall the definition of the vector $\underline{\tau}_j$, a column vector whose first i entries are one and the remainder are zero. Hence the derivative $\Phi_n^{\ell m}$ w.r.t. θ_i can be evaluated as follows.

Let $\theta \in \tau_{ij}^{(0)}$ (i.e., the constant delay terms), then we have

$$\frac{\partial \Phi_n^{lm}}{\partial \theta_i} = \begin{cases} 1; & \text{if } m \leq i \leq l-1 \\ -1; & \text{if } l \leq i \leq m-1 \\ 0; & \text{otherwise} \end{cases}$$

$= \Phi_i$. (6.3-5d)

This is identical to that obtained in Equation (3.5.1-8d). Furthermore, if we let $\theta_i \in \tau_{ij}^{(p)}$ (i.e., the p th derivative terms), we obtain

$$\frac{\partial \Phi_n^{lm}}{\partial \theta_i} = \begin{cases} t_n^p / p!; & \text{if } m \leq i \leq l-1 \\ -t_n^p / p!; & \text{if } l \leq i \leq m-1 \\ 0; & \text{otherwise.} \end{cases}$$
(6.3-5e)

Now let Φ_n be the matrix whose lm element is Φ_n^{lm} , then we have the following relations

$$\frac{\partial \Phi_n}{\partial \theta_i^{(p)}} = \frac{t_n^p}{p!} \frac{\partial \Phi_n}{\partial \theta_i^{(0)}} = \frac{t_n^p}{p!} \Phi_i$$
(6.3-5f)

where $\theta_i^{(p)} = \tau_{ij}^{(p)}$. Note the above relation is independent of j .

Now combining Equations (6.3-5b) and (6.3-5f), one can write

$$\frac{\partial P_{kjn}}{\partial \theta_i^{(p)}} = j\omega_k V_{kjn} \frac{\partial \Phi_n}{\partial \theta_i^{(p)}} V_{kjn}^*$$
(6.3-6a)

where V_{kjn} denotes a diagonal matrix and is related to the vector v_{kjn} by the simple relation

$$V_{kjn} = I \underline{v}_{kjn} \quad (6.3-6b)$$

where I is an $M \times M$ identity matrix.

In addition, one can write

$$\begin{aligned} \frac{\partial G_{kjn}}{\partial \underline{\theta}_i(p)} &= \frac{\partial}{\partial \underline{\theta}_i(p)} (\underline{v}_{kjn}^* \tilde{Q}_{kjn}^{-1} \underline{v}_{kjn}) \\ &= \text{tr} \left(\tilde{Q}_{kjn}^{-1} \frac{\partial P_{kjn}}{\partial \underline{\theta}_i(p)} \right) \\ &= j\omega_k \text{tr} \left(\tilde{Q}_{kjn}^{-1} V_{kjn} \frac{\partial \Phi_n}{\partial \underline{\theta}_i(p)} \underline{v}_{kjn}^* \right). \end{aligned} \quad (6.3-6c)$$

Finally, using Equations (6.3-5f), (6.3-6a), and (6.3-6c) in (6.3-4a) yields the desired form of the likelihood equation

$$\begin{aligned} \frac{\partial \Lambda(\underline{\theta})}{\partial \underline{\theta}_i(p)} &= \sum_{n=1}^N \sum_{k=1}^B j\omega_k \frac{t_n^p}{p!} \left[|\tilde{h}_{kjn}|^2 \underline{v}_{kjn}^* \tilde{Q}_{kjn}^{-1} V_{kjn} (\Phi_i - \tilde{b}_{in}^{kj} \mathbf{1}_M) \right. \\ &\quad \left. V_{kjn}^* \tilde{Q}_{kjn}^{-1} \underline{v}_{kjn} - \tilde{b}_{in}^{kj} \right] \\ &= 0; \quad i = 1, \dots, M-1 \\ p &= 0, \dots, P \\ j &= 1, \dots, J \end{aligned} \quad (6.3-7a)$$

where the bias term is given by

$$\tilde{b}_{in}^{kj} = \tilde{a}_{kjn} \operatorname{tr} (\tilde{Q}_{kjn}^{-1} V_{kjn} \Phi_i V_{kjn}^*). \quad (6.3-7b)$$

Note that by setting $N = 1$, $P = 0$, it can be readily shown that Equation (6.3-6a) reduces to Equation (3.5.1-11a), the stationary time delay, single interval case that we have studied in Chapter 3. In general, simultaneously solving the set of equations as shown in Equation (6.3-6a) yields the optimum estimate of the unknown parameter set. Optimality here assumes that our Fourier representation of the time-compressed waveform as shown in Appendix J is valid. In the following section we will examine the performance bound and the processor structure of this estimator.

6.4 PERFORMANCE BOUND AND ESTIMATOR REALIZATION

In this section we investigate the appropriate performance bound of the multisensor, multitarget variable time delay estimator. We then study the structure of the estimator for a few simple but important cases. Performance comparison is made between the variable time delay estimation and the stationary time delay estimation.

6.4.1 Variable Time Delay Performance Bound

For a sufficiently long observation time or sufficiently high SNR, an appropriate bound for the variable time delay estimator is the CRLB. The CRLB is given by

$$\text{VAR}(\underline{\theta}_i) \geq (J^{-1})_{ii} \quad (6.4.1-1a)$$

where $(\)_{ii}$ denotes the i th diagonal element of a matrix and J is the Fisher Information Matrix whose ij element is given by

$$J_{ij} \triangleq E\left(\frac{\partial^2 \Lambda(\underline{\theta})}{\partial \theta_i \partial \theta_j}\right); \quad \begin{matrix} i = 1, \dots, q \\ j = 1, \dots, q \end{matrix} \quad (6.4.1-1b)$$

where $\Lambda(\underline{\theta})$ is the log-likelihood function given by Equation (6.2-6b).

Using Equation (6.2-6b) and carrying out the same mathematical manipulations shown in Section 3.4, one obtains

$$J_{ij} = \sum_{n=1}^N \sum_{k=1}^B \text{tr} \left(- \frac{\partial R_{kn}^{-1}}{\partial \theta_i} \frac{\partial R_{kn}}{\partial \theta_j} \right) \Bigg|_{\underline{\theta} = \underline{\theta}_0} \quad (6.4.1-2a)$$

where the observation covariance matrix is given in Equation (6.3-3a) and the partial derivatives are given by

$$\frac{\partial R_{kn}}{\partial \theta_j} = S_{kj} \frac{\partial P_{kjn}}{\partial \theta_j} \quad (6.4.1-2b)$$

$$\frac{\partial R_{kn}^{-1}}{\partial \theta_i} = -|h_{kjn}|^2 \tilde{Q}_{kjn}^{-1} \left(\frac{\partial P_{kjn}}{\partial \theta_i} - \tilde{a}_{kjn} \frac{\partial G_{kjn}}{\partial \theta_i} P_{kjn} \right) \tilde{Q}_{kjn}^{-1}. \quad (6.4.1-2c)$$

6.4.2 Estimator Realization

In this section we study the structure of the variable time delay estimator for a number of simple but important cases. We are working primarily with Equations (6.3-6a) and (6.4.1-2).

6.4.2.1 Case 1: One Target and Two Sensors with Delay Rate

(J = 1, M = 2, p = 1, N ≥ 2). For convenience we assume $Q_k = I$; i.e., the noise processes are equal in power and uncorrelated between sensors. The unknown parameter vector is $\underline{\theta} = (\tau, \dot{\tau})^T$. The variable time delay is given by

$$\tau(t_n) = \tau + \dot{\tau} t_n \quad (6.4.2-1a)$$

where

$$t_n = (n - \frac{1}{2}) \Delta t; \quad n = 1, \dots, N. \quad (6.4.2-1b)$$

The steering vector at t_n is $\underline{v}_{kn} = \begin{pmatrix} 1 & e^{j\omega_k \tau(t_n)} \end{pmatrix}$. In addition, the following relations can be verified easily using Equations (6.3-4b) to (6.3-4f) (suppressing the j index for simplicity).

$$\tilde{Q}_{kn}^{-1} = Q_k^{-1} = I \quad (6.4.2-1c)$$

$$G_{kn} = v_{kn}^* \tilde{Q}_{kn}^{-1} v_{kn} = 2 \quad (6.4.2-1d)$$

$$|\tilde{h}_{kn}|^2 = \frac{s_k/N_k^2}{1 + 2 s_k/N_k} \triangleq |h_k|^2 \quad (6.4.2-1e)$$

$$\tilde{a}_{kn} = N_k |\tilde{h}_{kn}|^2 \triangleq \tilde{a}_k \quad (6.4.2-1f)$$

$$\Phi_1 = \begin{bmatrix} 0 & -1 \\ 1 & 0 \end{bmatrix}; v_{kn} = \begin{bmatrix} 1 & 0 \\ 0 & e^{j\omega_k \tau(t_n)} \end{bmatrix} \quad (6.4.2-1g)$$

and the bias term is zero since

$$\begin{aligned} \tilde{b}_n^k &= \tilde{a}_{kn} \operatorname{tr}(\tilde{Q}_{kn}^{-1} v_{kn} \Phi_1 v_{kn}^*) \\ &= 0. \end{aligned} \quad (6.4.2-1h)$$

Hence, letting $\underline{\theta}_1^{(0)} = \tau$, $\underline{\theta}_1^{(1)} = \dot{\tau}$ in Equation (6.3-6a) and using the relations shown from Equation (6.4.2-1c) to (6.4.2-1h) yields the likelihood equation for the optimum estimate of τ and $\dot{\tau}$. They are given as follows:

$$\frac{\partial \Lambda(\underline{\theta})}{\partial \tau} = \sum_{n=1}^N \sum_{k=1}^B j\omega_k |h_k|^2 \underline{a}_{kn}^* v_{kn} \Phi_1 v_{kn}^* \underline{a}_{kn} = 0 \quad (6.4.2-2a)$$

$$\frac{\partial \Lambda(\theta)}{\partial t} = \sum_{n=1}^N \sum_{k=1}^B j\omega_k t_n |h_k|^2 \underline{\alpha}_{kn}^* v_{kn} \Phi_1 v_{kn}^* \underline{\alpha}_{kn} = 0 . \quad (6.4.2-2b)$$

The above equations can be further simplified by noting that

$$\begin{aligned} v_{kn} \Phi_1 v_{kn}^* &= \begin{bmatrix} 1 & 0 \\ 0 & e^{j\omega_k \tau(t_n)} \end{bmatrix} \begin{bmatrix} 0 & -1 \\ 1 & 0 \end{bmatrix} \begin{bmatrix} 1 & 0 \\ 0 & e^{-j\omega_k \tau(t_n)} \end{bmatrix} \\ &= \begin{bmatrix} 0 & -e^{-j\omega_k \tau(t_n)} \\ e^{j\omega_k \tau(t_n)} & 0 \end{bmatrix} \end{aligned} \quad (6.4.2-2c)$$

and writing

$$\underline{\alpha}_{kn} = \begin{bmatrix} \alpha_{1kn} \\ \alpha_{2kn} \end{bmatrix} \quad (6.4.2-2d)$$

so that

$$\underline{\alpha}_{kn}^* v_{kn} \Phi_1 v_{kn}^* \underline{\alpha}_{kn} = \alpha_{1kn}^* \alpha_{2kn}^* e^{j\omega_k \tau(t_n)} - \alpha_{1kn}^* \alpha_{2kn} e^{-j\omega_k \tau(t_n)} \quad (6.4.2-2e)$$

Using Equation (6.4.2-2e), the likelihood equation can be rewritten as

$$\begin{aligned}
 \frac{\partial \Lambda(\tau, \dot{\tau})}{\partial \tau} &= \sum_{k=-B}^B \sum_{n=1}^N j\omega_k |h_k|^2 \alpha_{1kn} \alpha_{2kn}^* e^{j\omega_k(\tau + \dot{\tau}t_n)} \\
 &= \frac{\partial}{\partial \tau} \sum_{k=-B}^B \sum_{n=1}^N |h_k|^2 \alpha_{1kn} \alpha_{2kn}^* e^{j\omega_k(\tau + \dot{\tau}t_n)} \\
 &= \frac{\partial}{\partial \tau} R(\tau, \dot{\tau}) \\
 &= 0 . \tag{6.4.2-3a}
 \end{aligned}$$

where $R(\tau, \dot{\tau})$ is generally called the broadband ambiguity function and is given by

$$R(\tau, \dot{\tau}) = \sum_{k=-B}^B \sum_{n=1}^N |h_k|^2 \alpha_{1kn} \alpha_{2kn}^* e^{j\omega_k(\tau + \dot{\tau}t_n)} . \tag{6.4.2-3b}$$

Similarly, we have

$$\frac{\partial \Lambda(\tau, \dot{\tau})}{\partial \dot{\tau}} = \frac{\partial}{\partial \dot{\tau}} R(\tau, \dot{\tau}) = 0 . \tag{6.4.2-3c}$$

Thus the optimum estimate of $\tau, \dot{\tau}$ is given by the pair $(\hat{\tau}, \hat{\dot{\tau}})$ which peaks the ambiguity function $R(\tau, \dot{\tau})$. If the frequency samples are sufficiently dense, then the broadband ambiguity function can be written as

$$R(\tau, t) = \frac{1}{2\pi} \int_{-B}^B \sum_{n=1}^N a_{1n}(\omega) a_{2n}^*(\omega) |h(\omega)|^2 e^{j\omega(\tau+it_n)} d\omega . \quad (6.4.2-4)$$

Figure 6-2 diagrams one possible implementation of this processor.

Note that frequency samples from each subinterval are phase-compensated and then summed. Note the similarity between Figures 6-2 and 3-2.

We next examine the performance bound of this estimator. The parameters of interest are $\theta_1 = \tau$ and $\theta_2 = t$. The covariance matrix can be evaluated using Equation (6.4.2-2). The detail of the derivation is given in Appendix K. The main results are given below:

$$\text{VAR}(\hat{\tau}) = \left[\frac{2\pi(4N^2 - 1)}{N^2 - 1} \right] \frac{1}{\lambda T} \quad (6.4.2-5a)$$

$$\text{VAR}(\hat{t}) = \left[\frac{24\pi N^2}{N^2 - 1} \right] \frac{1}{\lambda T^3} \quad (6.4.2-5b)$$

and

$$\text{COV}(\hat{\tau}, \hat{t}) = - \left[\frac{12\pi N^2}{N^2 - 1} \right] \frac{1}{\lambda T^2} \quad (6.4.2-5c)$$

where

$$\lambda = \frac{2\pi}{\Delta t} \sum_{k=-B}^B \omega_k^2 \frac{S_k^2/N_k^2}{1 + 2 S_k/N_k} \quad (6.4.2-5d)$$

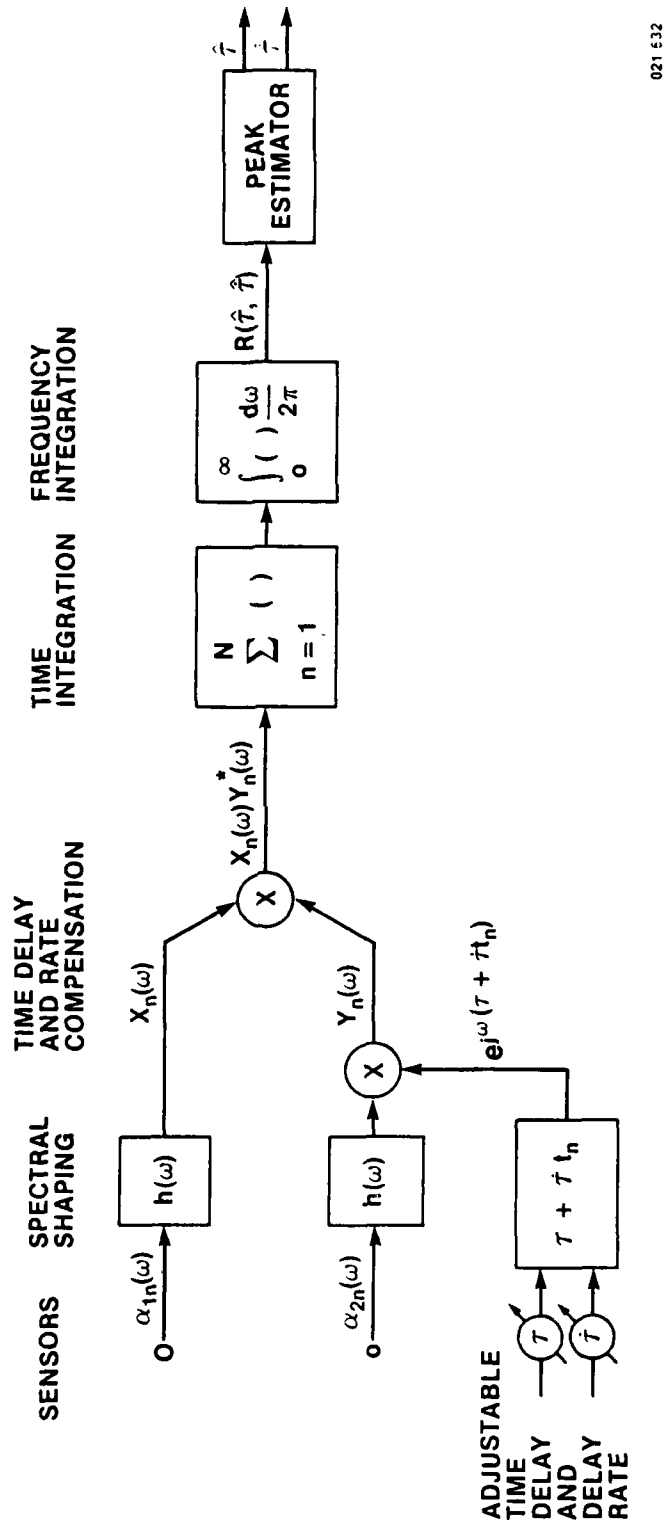


Figure 6-2. Two-Sensor, One-Target Time Delay Doppler Processor

$$= \int_{-B}^B \omega^2 \frac{S^2(\omega)/N^2(\omega)}{1 + 2 \frac{S(\omega)/N(\omega)}{S^2(\omega)/N^2(\omega)}} d\omega . \quad (6.4.2-5e)$$

Note that the above equations indicate that the number of observation subintervals, N , must be equal to or greater than two for the resulting estimate to be meaningful. Note that the estimates, $\hat{\tau}$ and \hat{t} , allow the time delay to be estimated at any point within the observation interval $[0, T]$. Thus at any time $t \in [0, T]$, the estimated time delay is given by

$$\hat{\tau}(t) = \hat{\tau} + \hat{t} t; \quad t \in [0, T] . \quad (6.4.2-6)$$

Since $\hat{\tau}$, \hat{t} are unbiased, $\hat{\tau}(t)$ is also unbiased. Furthermore, the variance of the resulting estimate is

$$\begin{aligned} \text{VAR}(\hat{\tau}(t)) &= \text{VAR}(\hat{\tau}) + t^2 \text{VAR}(\hat{t}) + 2t \text{COV}(\hat{\tau}, \hat{t}) \\ &= \left[\frac{8\pi N^2}{(N^2 - 1)\lambda T} \right] \left[\left(1 - \frac{1}{4N^2} \right) - 3\left(\frac{t}{T}\right) + 3\left(\frac{t}{T}\right)^2 \right] \end{aligned} \quad (6.4.2-7)$$

where Equations (6.4.2-5a) to (6.4.2-5c) have been used.

Note that $\text{VAR}(\hat{\tau}(t))$ is quadratic in t . It is easy to verify that the variance is minimum at $t = \frac{T}{2}$; i.e., the midpoint of the observation interval. Finally, if N is substantially greater than one, then Equation (6.4.2-7) can be approximated by

$$\hat{\text{VAR}}(\tau(t)) \approx \left[\frac{8\pi}{\lambda T} \right] \left[1 - 3\left(\frac{t}{T}\right) + 3\left(\frac{t}{T}\right)^2 \right] \quad (6.4.2-8a)$$

and when evaluated at the midpoint of the interval, Equation (6.4.2-7) yields the minimum variance

$$\hat{\text{VAR}}\left(\tau\left(\frac{T}{2}\right)\right) = \frac{2\pi}{\lambda T}. \quad (6.4.2-8b)$$

This is equal exactly to the CRLS for the stationary target case (see Equation (3.5.1-16a)).

Thus one can conclude that the presence of time delay rate (or doppler) degrades the performance of time delay estimate w.r.t. the stationary time delay case. Therefore, defining the Doppler Degradation Ratio (DDR) as the ratio of the time delay variance of the variable time delay case to that of the stationary time case, one obtains, by using Equations (6.4.2-7) and (6.4.2-8b), the following:

$$\begin{aligned} \text{DDR} &= \frac{\hat{\text{VAR}}(\tau(t))}{\hat{\text{VAR}}\left(\tau\left(\frac{T}{2}\right)\right)} \\ &= \left(\frac{4N^2}{N^2 - 1} \right) \left[\left(1 - \frac{1}{4N^2} \right) - 3\left(\frac{t}{T}\right) + 3\left(\frac{t}{T}\right)^2 \right]. \end{aligned} \quad (6.4.2-9a)$$

For $N \gg 1$, we have the following approximation:

$$\text{DDR} \approx 4 \left[1 - 3\left(\frac{t}{T}\right) + 3\left(\frac{t}{T}\right)^2 \right]. \quad (6.4.2-9b)$$

AD-A129 805

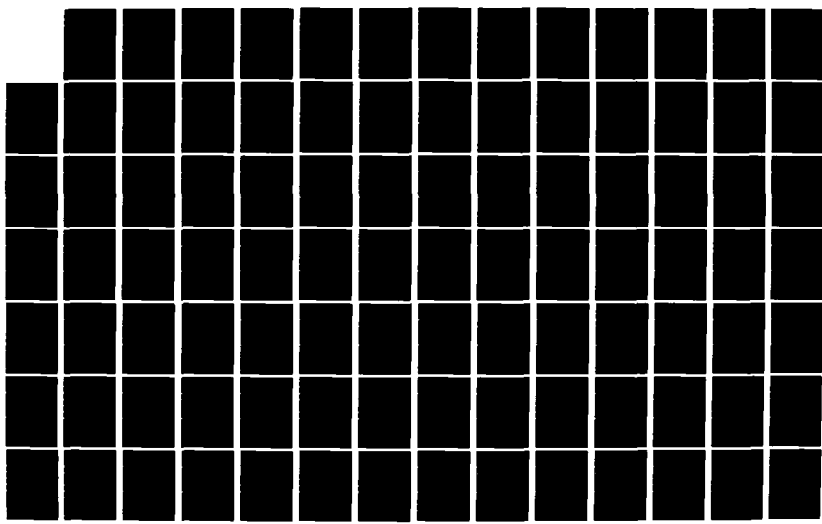
OPTIMUM MULTISENSOR MULTITARGET LOCALIZATION AND
TRACKING(U) NAVAL UNDERWATER SYSTEMS CENTER NEW LONDON
CT NEW LONDON LAB L C NG 87 JUN 83 NUSC-TR-6931

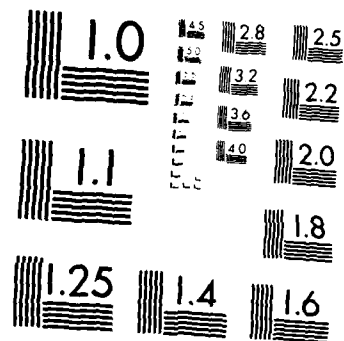
3/4

UNCLASSIFIED

F/G 12/1

NL





MICROCOPY RESOLUTION TEST CHART
NATIONAL BUREAU OF STANDARDS 1963

On the other hand, if the stationary processor is used directly over T seconds of observation in the presence of time delay doppler, the question is what would be the resulting performance of the time delay estimate. We note in Appendix J that time delay doppler causes an effective additional phase shift and signal attenuation on the resulting Fourier coefficient representation. In the development presented in Section 6.2, we accounted for the additional time delay but not the signal attenuation. The reason was that by subdividing the T -second observation into smaller subintervals, the resulting loss in signal coherence is negligible. However, if we attempt to process the T -second observation without subdivision, the loss in signal coherence must be accounted for. This can be accomplished as follows and the resulting performance bound is easily obtained.

Let \dot{D}_1 and \dot{D}_2 be the propagation time delay rates as observed by sensors 1 and 2, respectively. Then the Fourier representation of the observation is given by

$$\tilde{\alpha}_{1k} = \beta_k a_1 e^{j\omega_k \dot{D}_1 (\frac{T}{2})} + \eta_{1k} \quad (6.4.2-10a)$$

$$\tilde{\alpha}_{2k} = \beta_k a_2 e^{j\omega_k \dot{D}_2 (\frac{T}{2})} + \eta_{2k}; \quad k = 1, \dots, B \quad (6.4.2-10b)$$

where a_1 and a_2 are the signal attenuation coefficients given, respectively, by $a_1 = \text{sinc}(\omega_k \dot{D}_1 \frac{T}{2})$ and $a_2 = \text{sinc}(\omega_k \dot{D}_2 \frac{T}{2})$,

where $\text{sinc}(\cdot) = \frac{\sin(\cdot)}{(\cdot)}$ (see Appendix J). Hence writing Equations (6.4.2-10a) and (6.4.2-10b) in vector notation yields

$$\tilde{\underline{\alpha}}_k = \beta_k \tilde{\underline{v}}_k + \underline{n}_k; \quad k = 1, \dots, B \quad (6.4.2-11a)$$

where the steering vector \underline{v}_k is given by

$$\tilde{\underline{v}}_k = \begin{pmatrix} a_1 e^{j\omega_k D_1(\frac{T}{2})} & a_2 e^{j\omega_k D_2(\frac{T}{2})} \end{pmatrix}^T. \quad (6.4.2-11b)$$

The observation covariance matrix is

$$\begin{aligned} \tilde{\underline{R}}_k &= E(\tilde{\underline{\alpha}}_k \tilde{\underline{\alpha}}_k^*) \\ &= S_k \tilde{\underline{p}}_k + N_k Q_k \end{aligned} \quad (6.4.2-12a)$$

where

$$\tilde{\underline{p}}_k = \tilde{\underline{v}}_k \tilde{\underline{v}}_k^* = \tilde{\underline{v}}_k \underline{l}_2 \tilde{\underline{v}}_k^*. \quad (6.4.2-12b)$$

Note that \underline{l}_2 is a 2×2 matrix of one and the diagonal matrix $\tilde{\underline{v}}_k$ is defined by the relation $\tilde{\underline{v}}_k = I \underline{v}_k$. The parameter of interest is the time delay τ defined by the relation $\tau = D_2(\frac{T}{2}) - D_1(\frac{T}{2})$. The variance of the stationary time delay estimate is given by (see Equation (3.5.1-15a)).

$$\text{VAR}_S(\hat{\tau}) \geq \left[\sum_{k=1}^B \text{tr} \left(-\frac{\partial \tilde{R}_k^{-1}}{\partial \tau} \frac{\partial \tilde{R}_k}{\partial \tau} \right) \right]^{-1}. \quad (6.4.2-13a)$$

Following the procedure shown in Section 3.5.1, we obtain

$$\begin{aligned} \text{tr} \left(-\frac{\partial \tilde{R}_k^{-1}}{\partial \tau} \frac{\partial \tilde{R}_k}{\partial \tau} \right) &= -\omega_k^2 |h_k|^2 s_k \text{tr}(\tilde{V}_k \Phi_1^2 \tilde{V}_k^*) \\ &= (a_1^2 + a_2^2) \omega_k^2 |h_k|^2 s_k \end{aligned} \quad (6.4.2-13b)$$

since it can be verified that

$$\text{tr}(\tilde{V}_k \Phi_1^2 \tilde{V}_k^*) = -(a_1^2 + a_2^2). \quad (6.4.2-13c)$$

Substituting Equation (6.4.2-13b) in (6.4.2-13a) yields

$$\begin{aligned} \text{VAR}_S(\hat{\tau}) &\geq \left[\sum_{k=1}^B (a_1^2 + a_2^2) \omega_k^2 \frac{s_k^2/N_k^2}{1 + 2 s_k^2/N_k} \right]^{-1} \\ &\doteq \frac{2\pi}{\tilde{\lambda} T} \end{aligned} \quad (6.4.2-14a)$$

where

$$\tilde{\lambda} = \sum_{k=-B}^B \left(\frac{a_1^2 + a_2^2}{2} \right) \omega_k^2 \frac{s_k^2/N_k^2}{1 + 2 s_k^2/N_k} \frac{2\pi}{T}$$

$$= \int_{-B}^B \overline{a^2} \omega^2 \frac{S^2(\omega)/N^2(\omega)}{1 + 2 S(\omega)/N(\omega)} d\omega \quad (6.4.2-14b)$$

and

$$\overline{a^2} \triangleq \frac{1}{2} \left[\text{sinc}^2(\omega D_1 \frac{T}{2}) + \text{sinc}^2(\omega D_2 \frac{T}{2}) \right]. \quad (6.4.2-14c)$$

Hence the DDR (i.e., the ratio of Equation (6.4.2-14a) to (6.4.2-8b)) is

$$\begin{aligned} \text{DDR} &= \frac{\text{VAR}_s(\hat{\tau})}{\text{VAR}(\hat{\tau}(\frac{T}{2}))} \\ &= \frac{\lambda}{\tilde{\lambda}} \\ &\geq 1. \end{aligned} \quad (6.4.2-15)$$

since $\tilde{\lambda} \leq \lambda$. Assuming $D = D_1 = D_2$, Figure 6-3 shows the DDR for the variable delay approach and the stationary time delay processor approach.

6.4.2.2 Case 2: One Target and Two Sensors with Variable Time Delay ($J = 1, M = 2, p = P, N > 2$). In Section 6.4.2.1 we studied the one-target, two-sensor case with linear time delay rate. The studies on the performance bound showed that the variance of the estimates improve with T for time delay and T^3 for time delay rate. Therefore,

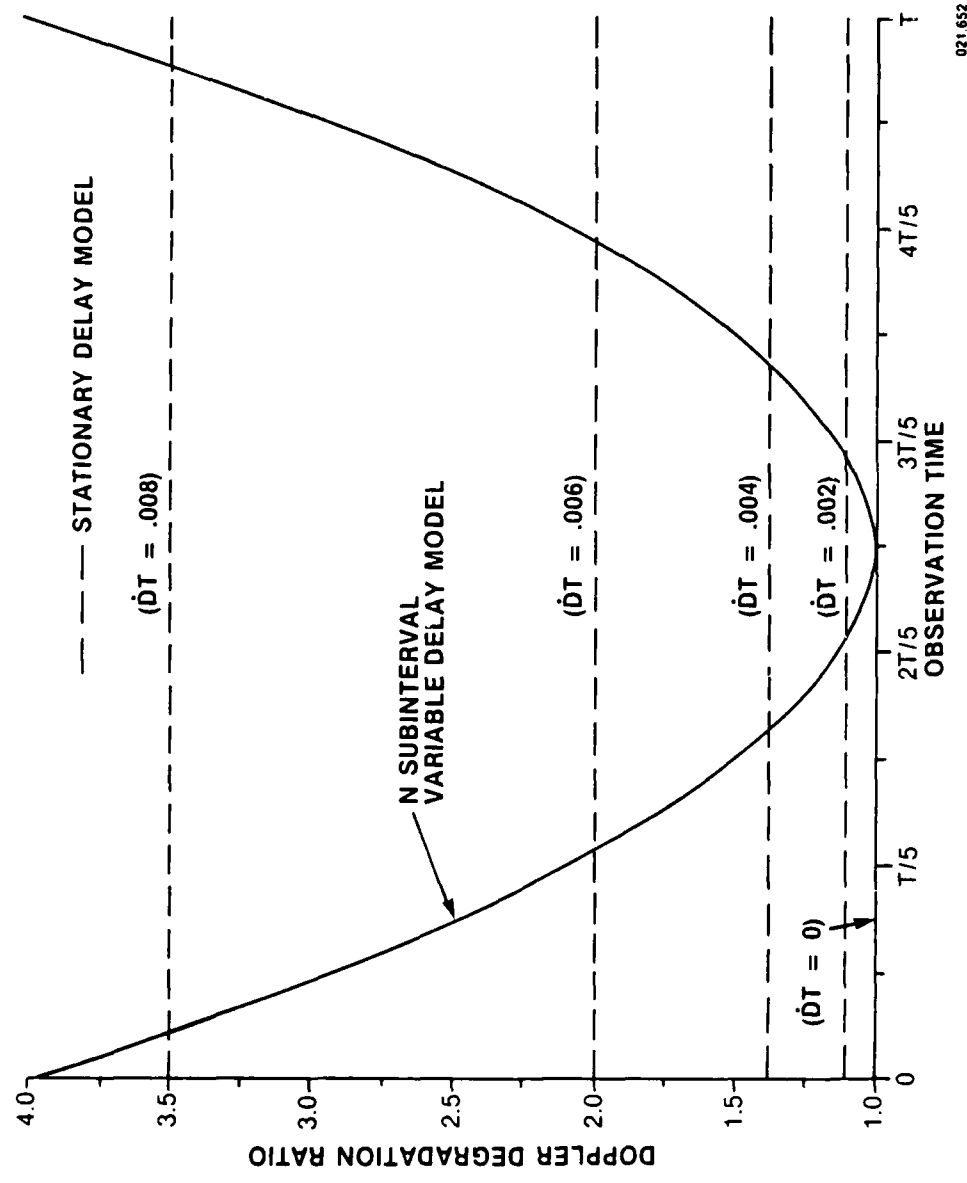


Figure 6-3. Doppler Degradation Ratio for Variable Delay Model and Stationary Delay Model

021652

increasing the observation time improves the estimates. However, increasing the observation time will also be likely to increase the order of the model. In this section, we extend the study to a more general case where the variable time delay is modeled by a Pth order polynomial in time.

Let the variable time delay function be modeled as

$$\begin{aligned}\tau(t) &= \tau + \dot{\tau}t + \dots + \frac{\tau^{(P)}}{P!} t^P \\ &= \underline{h}^T(t) \underline{\epsilon}\end{aligned}\quad (6.4.2-16a)$$

where

$$\underline{h}(t) = (1 \ t \ t^2/2 \dots t^P/P!)^T \quad (6.4.2-16b)$$

and $\underline{\epsilon}$ is the parameter vector given by

$$\underline{\epsilon} = (\tau \ \dot{\tau} \ \ddot{\tau} \ \dots \ \tau^{(P)})^T. \quad (6.4.2-16c)$$

Using Equation (6.3-7a), the likelihood equations consist of solving $P + 1$ simultaneous equations given by (the subscript j has been suppressed for notational simplicity since $j = 1$)

$$\frac{\partial \Lambda(\underline{\epsilon})}{\partial \tau^{(p)}} = \sum_{n=1}^N \sum_{k=1}^B j \omega_k \left(\frac{t_n^p}{p!} \right) |h_k|^2 \alpha_{kn}^* v_{kn} \Phi_1 v_{kn}^* \alpha_{kn} = 0 \quad (6.4.2-17)$$

for $p = 0, 1, \dots, P$.

Using Equation (6.4.2-2e), Equation (6.4.2-17) can be simplified to

$$\begin{aligned}
 \frac{\partial \Lambda(\underline{\theta})}{\partial \tau(p)} &= \sum_{k=-B}^B \sum_{n=1}^N j\omega_k \left(\frac{t_n^p}{p!} \right) |h_k|^2 \alpha_{1kn} \alpha_{2kn}^* e^{j\omega_k \tau(t_n)} \\
 &= \frac{\partial}{\partial \tau(p)} \sum_{k=-B}^B \sum_{n=1}^N |h_k|^2 \alpha_{1kn} \alpha_{2kn}^* e^{j\omega_k h^T(t_n) \underline{\theta}} \\
 &= 0
 \end{aligned} \tag{6.4.2-18}$$

for $p = 0, 1, \dots, P$ and $t_n = (n - \frac{1}{2}) \Delta t$.

Note that although $\tau(t)$ is P th order over the observation interval T , Δt was chosen so that the variation of time delay is nearly linear over Δt . Hence, results derived in Appendix J are applicable. A signal processor which realizes Equation (6.4.2-18) is given in Figure 6-4. Note the close similarity between Figures 6-4 and 6-2.

We next examine the performance bound of this estimator.

Using the results from Section 6.4.1, the ij element of the Fisher Information Matrix is

$$J_{ij} = \sum_{n=1}^N \sum_{k=1}^B \text{tr} \left(- \frac{\partial R_{kn}^{-1}}{\partial \theta_i} \frac{\partial R_{kn}}{\partial \theta_j} \right)$$

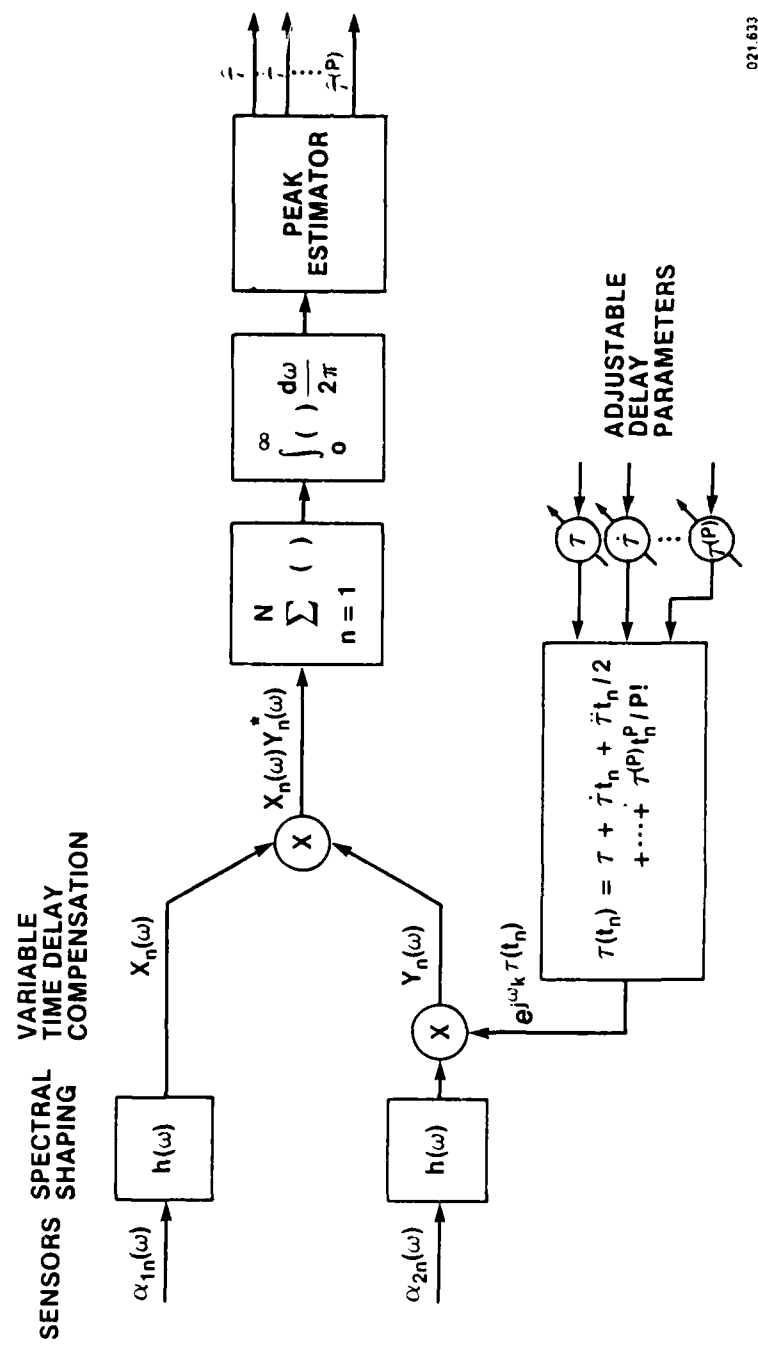


Figure 6-4. Two-Sensor, One-Target Variable Time Delay Processor

$$= \sum_{n=1}^N \sum_{k=1}^B \text{tr} \left(- \frac{\partial R_{kn}^{-1}}{\partial \tau^{(i-1)}} \frac{\partial R_{kn}}{\partial \tau^{(j-1)}} \right). \quad (6.4.2-19a)$$

Now utilizing Equations (6.3-5f), (6.3-6a), and the relation

$$R_{kn} = S_k P_{kn} + N_k Q_k, \quad (6.4.2-19b)$$

one obtains

$$\frac{\partial R_{kn}}{\partial \tau^{(i)}} = S_k \frac{\partial P_{kn}}{\partial \tau^{(i)}} = j\omega_k \left(\frac{t_n^i}{i!} \right) v_{kn} \phi_1 v_{kn}^* \quad (6.4.2-19c)$$

$$\begin{aligned} \frac{\partial R_{kn}^{-1}}{\partial \tau^{(i)}} &= -|h_k|^2 Q_k^{-1} \frac{\partial P_{kn}}{\partial \tau^{(i)}} Q_k^{-1} \\ &= -j\omega_k \left(\frac{t_n^i}{i!} \right) |h_k|^2 v_{kn} \phi_1 v_{kn}^* \end{aligned} \quad (6.4.2-19d)$$

where $Q_k = I$, i.e., noise processes, are uncorrelated and

$$|h_k|^2 = \frac{S_k/N_k^2}{1 + 2 S_k/N_k} \quad (6.4.2-19e)$$

$$v_{kn} = \begin{bmatrix} 1 & 0 \\ 0 & e^{j\omega_k \tau(t_n)} \end{bmatrix}. \quad (6.4.2-19f)$$

Substituting Equations (6.4.2-19c) and (6.4.2-19d) in (6.4.2-19a) yields

$$\begin{aligned}
 J_{ij} &= -\sum_{n=1}^N \sum_{k=1}^B \omega_k^2 \left[\frac{t_n^{i+j-2}}{(i-1)! (j-1)!} \right] |h_k|^2 s_k \operatorname{tr}(v_{kn} \phi_1^2 v_{kn}^*) \\
 &= C_{ij} \sum_{k=-B}^B \omega_k^2 \frac{s_k^2/N_k^2}{1 + 2 \frac{s_k^2/N_k^2}{s_k^2/N_k}} \\
 &= C_{ij} \lambda \frac{\Delta t}{2\pi} \tag{6.4.2-20a}
 \end{aligned}$$

where λ is as given in Equation (6.4.2-5d) and C_{ij} is defined by

$$C_{ij} = \sum_{n=1}^N \frac{t_n^{i+j-2}}{(i-1)! (j-1)!} \cdot \tag{6.4.2-20b}$$

Let C be a matrix whose ij element is C_{ij} , then it can be shown that

$$C = H^T H \tag{6.4.2-21a}$$

where H is an $N \times (P+1)$ matrix given by

$$H = \begin{bmatrix} 1 & t_1 & t_1^2/2 & \dots & t_1^P/P! \\ 1 & t_2 & t_2^2/2 & \dots & t_2^P/P! \\ \vdots & \ddots & \ddots & \ddots & \ddots \\ \vdots & \ddots & \ddots & \ddots & \ddots \\ 1 & t_N & t_N^2/2 & \dots & t_N^P/P! \end{bmatrix} \cdot \tag{6.4.2-21b}$$

Note that the matrix H relates the N subinterval midpoint time delay to the parameter vector of interest. Namely,

$$\underline{\tau} = H \underline{\theta} \quad (6.4.2-21c)$$

where the vector $\underline{\tau}$ is defined by

$$\underline{\tau} = (\tau(t_1) \ \tau(t_2) \ \dots \ \tau(t_N))^T. \quad (6.4.2-21d)$$

Therefore, using Equation (6.4.2-20a) the covariance matrix of the parameter vector $\underline{\theta}$ is bounded below by

$$\begin{aligned} \text{COV}(\underline{\theta}) &\geq J^{-1} \\ &\geq \frac{2\pi N(H^T H)^{-1}}{\lambda T}. \end{aligned} \quad (6.4.2-22)$$

For $p = 1$, Equation (6.4.2-22) reduces to Equations (6.4.2-5a), (6.4.2-5b), and (6.4.2-5c).

Furthermore, if $\hat{\underline{\theta}}$ is the estimated parameter vector, then the estimated time delay at any time within the interval $[0, T]$ is (see Equation (6.4.2-16a)).

$$\hat{\tau}(t) = \underline{h}^T(t) \hat{\underline{\theta}}. \quad (6.4.2-23)$$

Hence, the variance of the resulting time delay estimate is

$$\begin{aligned} \text{VAR}(\hat{\tau}(t)) &= \underline{h}^T(t) \text{ COV}(\hat{\underline{\theta}}) \underline{h}(t) \\ &= \frac{2\pi N \underline{h}^T(t) (H^T H)^{-1} \underline{h}(t)}{\lambda T} . \end{aligned} \quad (6.4.2-24)$$

6.4.2.3 Case 3: One Target and Three Sensors with Variable Time

Delay ($J = 1, M = 3, p = P, N \geq 2$). We studied the problem of estimating localization parameters of a stationary target in Section 3.5.2. We discussed at length the rationale for the two-step approach; i.e., first estimate the time delay between sensor arrays and then map the estimated time delays to the localization parameters via the target array geometry. We studied the optimum multisensor time delay processor and examined the resulting estimator performance bound. In this section we extend our investigation to the moving target case. Our immediate concern, however, is on the two-variable time delay estimation from a three-sensor array.

Let the two variable time delays (see Section 3.5.2) be modeled by a P th order polynomial as

$$\begin{aligned} \tau_1(t) &= \tau_1 + \dot{\tau}_1 t + \dots + (\tau_1^{(P)}/P!) t^P \\ &= \underline{h}^T(t) \underline{\theta}_1 \end{aligned} \quad (6.4.2-25a)$$

$$\begin{aligned}\tau_2(t) &= \tau_2 + \dot{\tau}_2 t + \dots + (\tau_2^{(p)}/p!) t^p \\ &= \underline{h}^T(t) \underline{\theta}_2\end{aligned}\quad (6.4.2-25b)$$

where

$$\underline{h}(t) = (1 \ t \ t^2/2 \ \dots \ t^p/p!)^T \quad (6.4.2-25c)$$

$$\underline{\theta}_i = (\tau_i \ \dot{\tau}_i \ \ddot{\tau}_i \ \dots \ \tau_i^{(p)})^T; \quad i = 1, 2 \quad (6.4.2-25d)$$

and the $2(p+1)$ parameter vector of interest is

$$\underline{\theta} = (\underline{\theta}_1^T \ \underline{\theta}_2^T)^T. \quad (6.4.2-25e)$$

Note that, $\underline{\theta}_i$, the i th element of $\underline{\theta}$ is given by

$$\theta_i = \begin{cases} \tau_1^{(i-1)}; & \text{if } i \leq p+1 \\ \tau_2^{(i-p-2)}; & \text{if } i > p+1 \end{cases} \quad (6.4.2-25f)$$

for $i = 1, 2, \dots, 2(p+1)$.

From Equation (6.3-6a) the likelihood equations are

$$\frac{\partial \Lambda(\underline{\theta})}{\partial \theta_i} = \frac{\partial \Lambda(\underline{\theta})}{\partial \tau_1^{(i-1)}}$$

$$\begin{aligned}
 &= \sum_{n=1}^N \sum_{k=1}^B j\omega_k \frac{t_n^{(i-1)}}{(i-1)!} |h_k|^2 \underline{\alpha}_{kn}^* v_{kn} \Phi_1 v_{kn}^* \underline{\alpha}_{kn} \\
 &= 0 . \tag{6.4.2-26a}
 \end{aligned}$$

for $i \leq P + 1$; and

$$\begin{aligned}
 \frac{\partial \Lambda(\underline{\theta})}{\partial \theta_i} &= \frac{\partial \Lambda(\underline{\theta})}{\partial \tau_2^{(i-P-2)}} \\
 &= \sum_{n=1}^N \sum_{k=1}^B j\omega_k \frac{t_n^{(i-P-2)}}{(i-P-2)!} |h_k|^2 \underline{\alpha}_{kn}^* v_{kn} \Phi_2 v_{kn}^* \underline{\alpha}_{kn} \\
 &= 0 \tag{6.4.2-26b}
 \end{aligned}$$

for $i > P + 1$.

Now using Equations (3.5.1-8d), (3.5.2-3) and (3.5.2-6c), the matrices V_{kn} , Φ_1 and Φ_2 are given by

$$V_{kn} = \text{diag} \begin{bmatrix} e^{-j\omega_k \tau_1(t_n)} & 1 & e^{j\omega_k \tau_2(t_n)} \end{bmatrix} \tag{6.4.2-26c}$$

$$\Phi_1 = \begin{bmatrix} 0 & -1 & -1 \\ 1 & 0 & 0 \\ 1 & 0 & 0 \end{bmatrix} \tag{6.4.2-26d}$$

$$\Phi_2 = \begin{bmatrix} 0 & 0 & -1 \\ 0 & 0 & -1 \\ 1 & 1 & 0 \end{bmatrix} \quad (6.4.2-26e)$$

and

$$|h_k|^2 = \frac{S_k/N_k^2}{1 + 3 S_k/N_k} . \quad (6.4.2-26f)$$

Therefore, the following relations can be shown:

$$\underline{\alpha}_{kn}^* V_{kn} \Phi_1 V_{kn} \underline{\alpha}_{kn} = A_{kn} - A_{kn}^*, \quad (6.4.2-27a)$$

where

$$A_{kn} = \alpha_{1kn} \alpha_{2kn}^* e^{j\omega_k \tau_1(t_n)} + \alpha_{1kn} \alpha_{3kn}^* e^{j\omega_k (\tau_1(t_n) + \tau_2(t_n))} \quad (6.4.2-27b)$$

and

$$\underline{\alpha}_{kn}^* V_{kn} \Phi_2 V_{kn}^* \underline{\alpha}_{kn} = B_{kn} - B_{kn}^* \quad (6.4.2-27c)$$

where

$$B_{kn} = \alpha_{1kn} \alpha_{3kn}^* e^{j\omega_k (\tau_1(t_n) + \tau_2(t_n))} + \alpha_{2kn} \alpha_{3kn}^* e^{j\omega_k \tau_2(t_n)} . \quad (6.4.2-27d)$$

Thus substituting Equations (6.4.2-27a) to (6.4.2-27d) in Equations (6.4.2-26a) and (6.4.2-26b) yields the set of simplified likelihood equations

$$\begin{aligned} \frac{\partial \Lambda(\underline{\theta})}{\partial \tau_1^{(i-1)}} &= \frac{\partial}{\partial \tau_1^{(i-1)}} \sum_{k=-B}^B \sum_{n=1}^N |h_k|^2 \left(\alpha_{1kn} \alpha_{2kn}^* e^{j\omega_k \tau_1(t_n)} \right. \\ &\quad \left. + \alpha_{1kn} \alpha_{3kn}^* e^{j\omega_k (\tau_1(t_n) + \tau_2(t_n))} \right) \\ &= 0; \text{ for } i = 1, \dots, P+1 \end{aligned} \quad (6.4.2-28a)$$

and

$$\begin{aligned} \frac{\partial \Lambda(\underline{\theta})}{\partial \tau_2^{(i-P-2)}} &= \frac{\partial}{\partial \tau_2^{(i-P-2)}} \sum_{k=-B}^B \sum_{n=1}^N |h_k|^2 \left(\alpha_{2kn} \alpha_{3kn}^* e^{j\omega_k \tau_2(t_n)} \right. \\ &\quad \left. + \alpha_{1kn} \alpha_{3kn}^* e^{j\omega_k (\tau_1(t_n) + \tau_2(t_n))} \right) \\ &= 0; \text{ for } i = P+2, \dots, 2P. \end{aligned} \quad (6.4.2-28b)$$

The above two sets of equations can be combined into one as follows. We note that $\alpha_{2kn} \alpha_{3kn}^* e^{j\omega_k \tau_2(t_n)}$ is not a function of $\tau_1^{(i-1)}$ for $i = 1, \dots, P+1$ and that $\alpha_{1kn} \alpha_{2kn}^* e^{j\omega_k \tau_1(t_n)}$ is not a function of $\tau_2^{(i-P-2)}$ for $i = P+2, \dots, 2P$. Therefore, we can add these two terms, respectively, to Equations (6.4.2-28a) and

(6.4.2-28b). Now we can define the $2(P + 1)$ parameter ambiguity function by

$$\begin{aligned}
 R(\underline{\theta}) = & \sum_{k=-B}^B \sum_{n=1}^N |h_k|^2 \left(\alpha_{1kn} \alpha_{2kn}^* e^{j\omega_k \tau_1(t_n)} \right. \\
 & + \alpha_{2kn} \alpha_{3kn}^* e^{j\omega_k \tau_2(t_n)} \\
 & \left. + \alpha_{1kn} \alpha_{3kn}^* e^{j\omega_k (\tau_1(t_n) + \tau_2(t_n))} \right). \tag{6.4.2-29}
 \end{aligned}$$

Therefore, combining Equations (6.4.2-28a), (6.4.2-28b) and (6.4.2-29), we find that the optimum estimate of $\underline{\theta}$ is given by $\hat{\underline{\theta}}$ which peaks the ambiguity function $R(\underline{\theta})$, or equivalently the corresponding null of $\partial R(\underline{\theta})/\partial \theta_i$; or more specifically one can write

$$\frac{\partial R(\underline{\theta})}{\partial \theta_i} = 0; \text{ for } i = 1, 2, \dots, 2P \tag{6.4.2-30}$$

where θ_i is as given in Equation (6.4.2-25f).

We next derive the performance bound of this estimator. From Equation (6.4.1-2), the ij element of the Fisher Information Matrix is

$$J_{ij} = \sum_{n=1}^N \sum_{k=1}^B \text{tr} \left(-\frac{\partial R_{kn}^{-1}}{\partial \theta_i} \frac{\partial R_{kn}}{\partial \theta_j} \right); \begin{matrix} i = 1, \dots, 2(P+1) \\ j = 1, \dots, 2(P+1) \end{matrix} \quad (6.4.2-31a)$$

$$= \begin{cases} J_{ij}^{(11)} & ; \text{ if } i \leq P+1, j \leq P+1 \\ J_{ij}^{(12)} & ; \text{ if } i \leq P+1, j > P+1 \\ J_{ij}^{(21)} & ; \text{ if } i > P+1, j \leq P+1 \\ J_{ij}^{(22)} & ; \text{ if } i > P+1, j > P+1 . \end{cases} \quad (6.4.2-31b)$$

Thus the Fisher Information Matrix can be partitioned into four sub-matrices as

$$J = \begin{bmatrix} J^{(11)} & | & J^{(12)} \\ \hline \cdots & + & \cdots \\ J^{(21)} & | & J^{(22)} \end{bmatrix} \quad (6.4.2-31c)$$

Using Equations (6.4.2-25f) and (6.4.2-31b), and the procedures shown in Section (6.4.2.2), elements of each submatrix can be evaluated as follows:

$$J_{ij}^{(11)} = \sum_{n=1}^N \sum_{k=1}^B \text{tr} \left(-\frac{\partial R_{kn}^{-1}}{\partial \tau_1^{(i-1)}} \frac{\partial R_{kn}}{\partial \tau_1^{(j-1)}} \right)$$

$$\begin{aligned}
 &= - \sum_{n=1}^N \sum_{k=1}^B \omega_k^2 \frac{t_n^{i+j-2}}{(i-1)! (j-1)!} |h_k|^2 s_k \operatorname{tr}(v_{kn} \phi_1^2 v_{kn}^*) \\
 &= C_{ij}^{(11)} \sum_{k=-B}^B \omega_k^2 \frac{s_k^2/N_k^2}{1 + 3 s_k/N_k} \\
 &= C_{ij}^{(11)} \lambda_3 \frac{\Delta t}{\pi} \tag{6.4.2-32a}
 \end{aligned}$$

where

$$\operatorname{tr}(v_{kn} \phi_1^2 v_{kn}^*) = -4 \tag{6.4.2-32b}$$

$$C_{ij}^{(11)} = \sum_{n=1}^N \frac{t_n^{i+j-2}}{(i-1)! (j-1)!} \tag{6.4.2-32c}$$

$$\begin{aligned}
 \lambda_3 &= \frac{2\pi}{\Delta t} \sum_{k=-B}^B \omega_k^2 \frac{s_k^2/N_k^2}{1 + 3 s_k/N_k} \\
 &\approx \int_{-B}^B \omega_2^2 \frac{S(\omega)^2/N(\omega)^2}{1 + 3 S(\omega)/N(\omega)} \cdot \tag{6.4.2-32d}
 \end{aligned}$$

Furthermore, let $C^{(11)}$ be a square matrix whose ij element is $C_{ij}^{(11)}$, then it can be shown that

$$C^{(11)} = H_1^T H_1 \tag{6.4.2-32e}$$

where H_1 is an $N \times (P + 1)$ matrix given by

$$H = \begin{bmatrix} 1 & t_1 & t_1^2/2 & \dots & t_1^P/P! \\ 1 & t_2 & t_2^2/2 & \dots & t_2^P/P! \\ \vdots & \vdots & \vdots & \ddots & \vdots \\ 1 & t_N & t_N^2/2 & \dots & t_N^P/P! \end{bmatrix}. \quad (6.4.2-32f)$$

Hence, one can write

$$J^{(11)} = (H^T H) \lambda_3 \frac{\Delta t}{\pi}. \quad (6.4.2-32g)$$

Similarly, one obtains

$$\begin{aligned} J_{ij}^{(22)} &= \sum_{n=1}^N \sum_{k=1}^B \operatorname{tr} \left(- \frac{\partial R_{kn}^{-1}}{\partial \tau_2^{(i-P-2)}} \frac{\partial R_{kn}}{\partial \tau_2^{(j-P-2)}} \right) \\ &= - \sum_{n=1}^N \sum_{k=1}^B \omega_k^2 \left[\frac{t_n^{(i+j-2(P+1))}}{(i-P-2)! (j-P-2)!} \right] |h_k|^2 s_k \operatorname{tr}(v_{kn} \Phi_2^2 v_{kn}^*) \\ &= C_{ij}^{(22)} \lambda_3 \frac{\Delta t}{\pi} \end{aligned} \quad (6.4.2-33a)$$

where

$$c_{ij}^{(22)} = \sum_{n=1}^N \frac{t_n^{i+j-2(p+1)}}{(i-p-2)! (j-p-2)!}$$

$$= c_{i'j'}^{(11)} \quad (6.4.2-33b)$$

where $i' = i - p - 1$ and $j' = j - p - 1$.

Thus if $C^{(22)}$ is a matrix whose ij element is given by $c_{ij}^{(22)}$, then one can write

$$C^{(22)} = C^{(11)}$$

$$= H^T H. \quad (6.4.2-33c)$$

Therefore, one can also write

$$J^{(22)} = J^{(11)}. \quad (6.4.2-33d)$$

Finally, we note that since J must be symmetric, we have

$$J^{(21)} = (J^{(12)})^T. \quad (6.4.2-34)$$

The submatrix $J^{(12)}$ can be evaluated as follows:

$$J_{ij}^{(12)} = \sum_{n=1}^N \sum_{k=1}^B \text{tr} \left(-\frac{\partial R_{kn}^{-1}}{\partial \tau_2^{(i-1)}} \frac{\partial R_{kn}}{\partial \tau_2^{(j-p-2)}} \right) \quad (6.4.2-35a)$$

where

$$\begin{aligned} -\frac{\partial R_{kn}^{-1}}{\partial \tau_1^{(i-1)}} &= |h_k|^2 \frac{\partial P_{kn}}{\partial \tau_1^{(i-1)}} \\ &= j\omega_k \left[\frac{t_n^{i-1}}{(i-1)!} \right] |h_k|^2 v_{kn} \Phi_1 v_{kn}^* \end{aligned} \quad (6.4.2-35b)$$

$$\begin{aligned} \frac{\partial R_{kn}}{\partial \tau_2^{(j-p-2)}} &= S_k \frac{\partial P_{kn}}{\partial \tau_2^{(j-p-2)}} \\ &= j\omega_k \left[\frac{t_n^{j-p-2}}{(j-p-2)!} \right] v_{kn} \Phi_2 v_{kn}^* . \end{aligned} \quad (6.4.2-35c)$$

Hence one can write

$$\begin{aligned} J_{ij}^{(12)} &= -\sum_{n=1}^N \sum_{k=1}^B \omega_k^2 \frac{t_n^{i+j-p-3}}{(i-1)! (j-p-2)!} |h_k|^2 S_k \text{tr}(v_{kn} \Phi_1 \Phi_2 v_{kn}^*) \\ &= C_{ij}^{(12)} \lambda_3 \frac{\Delta t}{2\pi} \end{aligned} \quad (6.4.2-35d)$$

since $\text{tr}(v_{kn} \Phi_1 \Phi_2 v_{kn}^*) = -2$.

Now

$$C_{ij}^{(12)} = C_{ij}^{(11)}$$

where $j' = j - p - 1$. We can also write $C^{(12)}$, the matrix whose ij element is $C_{ij}^{(12)}$, as

$$C^{(12)} = H^T H. \quad (6.4.2-35e)$$

Finally, the submatrix $J^{(12)}$ is given by

$$J^{(12)} = (H^T H) \lambda_3 \frac{\Delta t}{2\pi}. \quad (6.4.2-35f)$$

Thus combining Equations (6.4.2-32g), (6.4.2-33a), and (6.4.2-35f), the Fisher Information matrix is

$$J = A \lambda_3 \frac{T}{2\pi N} \quad (6.4.2-36a)$$

where the relation $T = N\Delta t$ has been used and the matrix A is given by

$$A = \begin{bmatrix} 2H^T H & | & H^T H \\ \hline \cdots & + & \cdots \\ H^T H & | & 2H^T H \end{bmatrix}. \quad (6.4.2-36b)$$

Therefore, the covariance bound is

$$\begin{aligned} \text{COV}(\hat{\theta}) &\geq J^{-1} \\ &\geq \left(\frac{2\pi N}{\lambda_3 T} \right) A^{-1} \end{aligned} \quad (6.4.2-37a)$$

$$\geq A^{-1} \left(2 \sum_{k=1}^B \omega_k^2 \frac{s_k^2/N_k^2}{1 + 3 s_k^2/N_k^2} \right)^{-1}. \quad (6.4.2-37b)$$

Note for a fixed time delay with one observation interval, we have $H = 1$, and Equation (6.4.2-37b) is easily shown to be identical to Equation (C-24a) for the three-sensor array case.

Note that if $\hat{\underline{e}} = (\hat{\underline{e}}_1 \ \hat{\underline{e}}_2)^T$ is the estimate obtained from solving Equation (6.4.2-30), then the time delay estimates at any point within the interval $[0, T]$ are given by

$$\begin{bmatrix} \hat{\tau}_1(t) \\ \hat{\tau}_2(t) \end{bmatrix} = \begin{bmatrix} \underline{h}^T(t) & | & \underline{0}^T \\ \hline & | & | \\ \underline{0}^T & | & \underline{h}^T(t) \end{bmatrix} \begin{bmatrix} \hat{\underline{e}}_1 \\ \hat{\underline{e}}_2 \end{bmatrix} \quad (6.4.2-38a)$$

and the matrix covariance is

$$\text{COV} \begin{bmatrix} \hat{\tau}_1(t) \\ \hat{\tau}_2(t) \end{bmatrix} = \begin{bmatrix} \underline{h}^T(t) & | & \underline{0}^T \\ \hline & | & | \\ \underline{0}^T & | & \underline{h}^T(t) \end{bmatrix} \text{COV } (\hat{\underline{e}}) \begin{bmatrix} \underline{h}(t) & | & \underline{0} \\ \hline & | & | \\ \underline{0} & | & \underline{h}(t) \end{bmatrix}. \quad (6.4.2-38b)$$

6.5 VARIABLE TIME DELAY TRACKING

In the previous sections, we studied the problem of variable time delay estimation using the following procedure:

1. modeling the time delay variation over a T -second observation interval by a P th order polynomial,
2. partitioning the observation interval into N equal subintervals,
3. obtaining the Fourier representation of the observed waveforms for each subinterval, and
4. estimating the polynomial coefficients from the combined observation vector of each subinterval.

A criterion in selecting N was presented. It was shown in Appendix J that when N satisfies this constraint, the resulting loss of signal coherence due to time delay rate is minimal. Furthermore, when this constraint is satisfied, the time delay variation over each subinterval is essentially linear.

If targets are to be tracked over a time interval which is considerably longer than T seconds, then the above mentioned procedure

need modification. There are two possible approaches: (1) increase T to accommodate the total observation interval by increasing the order of the polynomial, or (2) select a suitable choice of a fixed observation window and the order of the polynomial; as time increases, the fixed-length observation window and the assumed polynomial model will also move in time. A major drawback of the first approach is the solution delay. One must wait until the end of the observation interval before one can start the estimation procedure. For many real-time applications, this kind of solution delay is unacceptable. Therefore, our major emphasis in this section is on the second approach where observations from a T -second sliding window will be used for parameter estimation. Furthermore, we will study the recursive sequential nature of the algorithm which incorporates estimates from the previous cycle.

6.5.1 Sequential Fixed-Interval Time Delay Tracking

Consider a simple two-sensor case with observed variable time delay. Note that the general multisensor, multitarget case can be similarly treated with more complicated notation. Figure 6-5 illustrates the problem of our interest. Suppose that time delay variation over an observation interval $[0, T]$ can be modeled by a P th order polynomial. Thus one can write the time delay as

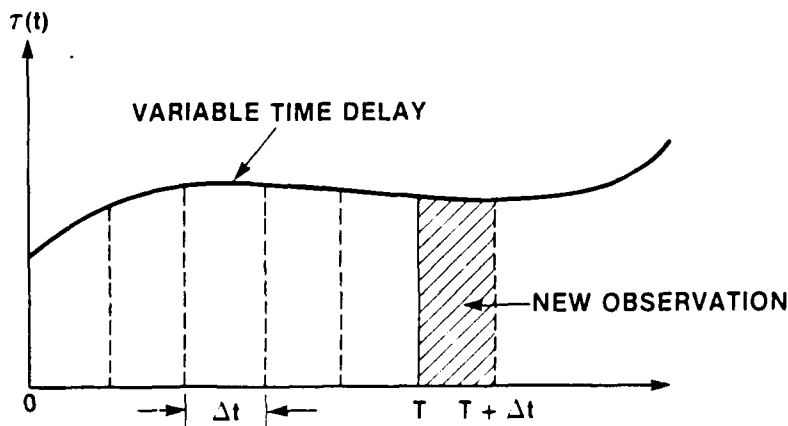
$$\begin{aligned}\tau_0(t) &= \tau_0 + \dot{\tau}_0 t + \frac{\ddot{\tau}_0 t^2}{2} + \dots + \frac{\tau_0^{(P)} t^P}{P!} \\ &= \underline{h}^T(t) \underline{\epsilon}_0\end{aligned}\quad (6.5-1a)$$

where

$$\underline{h}^T(t) = (1 \ t \ t^2/2 \ \dots \ t^P/P!) \quad (6.5-1b)$$

$$\underline{\epsilon}_0 = (\tau_0 \ \dot{\tau}_0 \ \ddot{\tau}_0 \ \dots \ \tau_0^{(P)})^T. \quad (6.5-1c)$$

Note that the subscripts denote the time at which the polynomial coefficients are evaluated.



021 650

Figure 6-5. Sequential Fixed-Interval Time Delay Tracking

Assume that there are N subintervals and let $\underline{\alpha}_n$, $n = 1, 2, \dots$ be the observation vector of Fourier coefficients for each subinterval. Then the best estimate of $\underline{\theta}_0$ is obtained by maximizing the density function $p(\underline{\alpha}_N \underline{\alpha}_{N-1} \dots \underline{\alpha}_1 | \underline{\theta}_0)$ as discussed in the previous sections. Now suppose a new observation vector $\underline{\alpha}_{N+1}$ is available. Again we wish to estimate $\underline{\theta}_1$ over the interval $[\Delta t, T + \Delta t]$. Now suppose the best estimate of $\underline{\theta}_1$ is found and a new observation vector $\underline{\alpha}_{N+2}$ is available, what is the best procedure in estimating $\underline{\theta}_2$ over the interval $[2\Delta t, T + 2\Delta t]$. Here we study this fixed-interval recursive time delay tracking algorithm in some detail.

First we write the parameter vector $\underline{\theta}_n$ as

$$\underline{\theta}_n = (\tau_n \dot{\tau}_n \ddot{\tau}_n \dots \tau_n^{(P)})^T \quad (6.5-2a)$$

so that the time delay variation over the interval $[n\Delta t, T + n\Delta t]$ can be written as

$$\tau_n(t) = \tau_n + \dot{\tau}_n(t - n\Delta t) + \dots + \tau_n^{(P)}(t - n\Delta t)^P / P! \quad (6.5-2b)$$

Furthermore, denoting the time-dependent state vector $\underline{\theta}_n(t)$ as

$$\underline{\theta}_n(t) = (\tau_n(t) \dot{\tau}_n(t) \dots \tau_n^{(P)})^T, \quad (6.5-2c)$$

then from Equation (6.5-2b) one obtains the state propagation equation

$$\underline{e}_n(t) = H(t - n\Delta t)\underline{e}_n \quad (6.5-3a)$$

where

$$H(t) = \begin{bmatrix} 1 & t & t^2/2 & \dots & t^p/p! \\ 0 & 1 & t & \dots & t^{p-1}/(p-1)! \\ 0 & 0 & 1 & \dots & t^{p-2}/(p-2)! \\ \vdots & \vdots & \vdots & \ddots & \vdots \\ \vdots & \vdots & \vdots & \ddots & \vdots \\ \vdots & \vdots & \vdots & \ddots & \vdots \\ 0 & 0 & 0 & \dots & 1 \end{bmatrix} \quad (6.5-3b)$$

Assume that the best estimate of \underline{e}_0 is $\hat{\underline{e}}_0$ obtained using methods discussed in Sections 6.3 and 6.4. In addition, let $M_0 = \text{COV}(\hat{\underline{e}}_0)$ be the covariance matrix. Now consider the problem of estimating \underline{e}_1 from the observation set $(\hat{\underline{e}}_0, \underline{a}_2, \underline{a}_3, \dots, \underline{a}_{N+1})$. We shall consider a Maximum A Posterior (MAP) estimate obtained by maximizing the a posteriori density function $p(\underline{e}_1 | \hat{\underline{e}}_0, \underline{a}_2, \underline{a}_3, \dots, \underline{a}_{N+1})$. But one can write

$$p(\underline{e}_1 | \hat{\underline{e}}_0, \underline{a}_2, \dots, \underline{a}_{N+1}) = \frac{p(\underline{a}_2, \dots, \underline{a}_{N+1} | \underline{e}_1, \hat{\underline{e}}_0) p(\underline{e}_1 | \hat{\underline{e}}_0)}{p(\hat{\underline{e}}_0, \underline{a}_2, \dots, \underline{a}_{N+1})}. \quad (6.5-4a)$$

However, maximizing the left-hand side of Equation (6.5-4a) w.r.t. \underline{e}_1 is the same as maximizing the numerator on the right-hand side of Equation (6.5-4a) since the denominator is not a function of \underline{e}_1 .

Furthermore, the set of observations $(\underline{\alpha}_2, \underline{\alpha}_3, \dots, \underline{\alpha}_{N+1})$ does not depend on $\hat{\underline{e}}_0$. Hence the quantity one wants to maximize is

$$L(\underline{\alpha}_1) = \log\{p(\underline{\alpha}_2, \dots, \underline{\alpha}_{N+1} | \underline{\alpha}_1) p(\underline{\alpha}_1 | \hat{\underline{e}}_0)\}. \quad (6.5-4b)$$

Now from Equation (6.2-6a), we obtain

$$p(\underline{\alpha}_2, \dots, \underline{\alpha}_{N+1} | \underline{\alpha}_1) = \pi^{-2BN} \prod_{n=2}^{N+1} \prod_{k=1}^B |R_{kn}|^{-1} \exp\{-\underline{\alpha}_{kn}^* R_{kn}^{-1} \underline{\alpha}_{kn}\}. \quad (6.5-4c)$$

But from Equation (6.5-3a), the best estimate of $\underline{\alpha}_1$ in the absence of new observation is

$$\hat{\underline{e}}_0(\Delta t) = H \hat{\underline{e}}_0 \quad (6.5-4d)$$

where $H = H(\Delta t)$. Since the change of the state over one subinterval will be small, we model $\underline{\alpha}_1$ by the relation

$$\underline{\alpha}_1 = H \hat{\underline{e}}_0 + \underline{e}_1 \quad (6.5-4e)$$

where \underline{e}_1 is a random Gaussian error vector with mean $E(\underline{e}_1) = \underline{0}$, and covariance $E(\underline{e}_1 \underline{e}_1^T) = E_1$. Thus using Equation (6.5-4e), one can write.

$$p(\underline{\alpha}_1 | \hat{\underline{e}}_0) = (2\pi)^{-(P+1)/2} |P_1|^{-1/2} \exp\{-\frac{1}{2}(\underline{\alpha}_1 - \hat{\underline{e}}_1)^T P_1^{-1} (\underline{\alpha}_1 - \hat{\underline{e}}_1)\} \quad (6.5-4f)$$

where

$$\tilde{\underline{\theta}}_1 = E(\underline{\theta}_1 | \hat{\underline{\theta}}_0) = H \hat{\underline{\theta}}_0 \quad (6.5-4g)$$

$$\begin{aligned} P_1 &= E[(\underline{\theta}_1 - \tilde{\underline{\theta}}_1)(\underline{\theta}_1 - \tilde{\underline{\theta}}_1)^T] \\ &= H M_0 H^T + E_1. \end{aligned} \quad (6.5-4h)$$

Substituting Equations (6.5-4c) and (6.5-4f.) in (6.5-4b) and simplifying, then the maximum of $L(\underline{\theta}_1)$ is obtained by solving the set of necessary and sufficient conditions

$$\frac{\partial L(\underline{\theta}_1)}{\partial \underline{\theta}_1} = \frac{\partial \Lambda(\underline{\theta}_1)}{\partial \underline{\theta}_1} - P_1^{-1} (\underline{\theta}_1 - \tilde{\underline{\theta}}_1) = 0 \quad (6.5-5a)$$

$$\frac{\partial^2 L(\underline{\theta}_1)}{\partial \underline{\theta}_1^2} < 0 \quad (6.5-5b)$$

where

$$\Lambda(\underline{\theta}_1) = - \sum_{n=2}^{N+1} \sum_{k=1}^B \Lambda_{kn}(\underline{\theta}_1) \quad (6.5-5c)$$

and

$$\Lambda_{kn}(\underline{\theta}_1) = \log |R_{kn}| + \underline{\alpha}_{kn}^* R_{kn}^{-1} \underline{\alpha}_{kn} \quad (6.5-5d)$$

as was defined in Equation (6.2-6c).

By repeated application of steps from Equations (6.5-4a) to (6.5-5d), one obtains the necessary conditions for the estimate of the state vector $\underline{\theta}_i$ at $t = i \Delta t$ as

$$\frac{\partial L(\underline{\theta}_i)}{\partial \underline{\theta}_i} = \frac{\partial \Lambda(\underline{\theta}_i)}{\partial \underline{\theta}_i} - P_i^{-1} (\underline{\theta}_i - \tilde{\underline{\theta}}_i) = 0 \quad (6.5-6a)$$

$$\frac{\partial^2 L(\underline{\theta}_i)}{\partial \underline{\theta}_i^2} < 0 \quad (6.5-6b)$$

for $i = 0, 1, 2, \dots$.

where

$$\Lambda(\underline{\theta}_i) = - \sum_{n=i+1}^{N+i-1} \sum_{k=1}^B \Lambda_{kn}(\underline{\theta}_i) \quad (6.5-6c)$$

$$\Lambda_{kn}(\underline{\theta}_i) = \log |R_{kn}| + \underline{\alpha}_{kn}^* R_{kn}^{-1} \underline{\alpha}_{kn} \quad (6.5-6d)$$

$$\underline{\theta}_i = H \hat{\underline{\theta}}_{i-1} + \underline{\epsilon}_i \quad (6.5-6e)$$

$$\tilde{\underline{\theta}}_i = E(\underline{\theta}_i | \hat{\underline{\theta}}_{i-1}) = H \hat{\underline{\theta}}_{i-1} \quad (6.5-6f)$$

$$\begin{aligned} P_i &= E[(\underline{\theta}_i - \tilde{\underline{\theta}}_i)(\underline{\theta}_i - \tilde{\underline{\theta}}_i)^T] \\ &= H M_{i-1} H^T + \Sigma_i \end{aligned} \quad (6.5-6g)$$

and furthermore

$$\Sigma_i = E(\underline{e}_i \underline{e}_i^T) \quad (6.5-6h)$$

and

$$\Sigma_i = \text{COV}(\hat{\underline{e}}_i). \quad (6.5-6i)$$

Note that in Equation (6.5-6a), since $\tilde{\underline{e}}_i \approx \hat{\underline{e}}_i$, $\Lambda(\underline{e}_i)$ can be linearized about $\tilde{\underline{e}}_i$ to yield

$$\frac{\partial \Lambda(\underline{e}_i)}{\partial \underline{e}_i} = \underline{f}(\tilde{\underline{e}}_i) + \left(\frac{\partial \underline{f}^T(\tilde{\underline{e}}_i)}{\partial \underline{e}_i} - P_i^{-1} \right) (\underline{e}_i - \tilde{\underline{e}}_i) = 0 \quad (6.5-7a)$$

or solving yields

$$\hat{\underline{e}}_i = \tilde{\underline{e}}_i - J^{-1}(\tilde{\underline{e}}_i) \underline{f}(\tilde{\underline{e}}_i) \quad (6.5-7b)$$

where

$$J(\tilde{\underline{e}}_i) = \frac{\partial \underline{f}(\tilde{\underline{e}}_i)}{\partial \underline{e}_i} - P_i^{-1} \quad (6.5-7c)$$

$$\underline{f}(\tilde{\underline{e}}_i) = \frac{\partial \Lambda(\underline{e}_i)}{\partial \underline{e}_i} \Bigg|_{\underline{e}_i = \tilde{\underline{e}}_i} \quad (6.5-7d)$$

$$\frac{\partial \underline{f}^T(\tilde{\underline{e}}_i)}{\partial \underline{e}_i} = \frac{\partial^2 \Lambda(\underline{e}_i)}{\partial \underline{e}_i^2} \Bigg|_{\underline{e}_i = \tilde{\underline{e}}_i} \quad (6.5-7e)$$

which is known as the Hessian.³⁹

Finally, using Equation (6.5-5c) and results from Section 3.3, we obtain the following explicit expressions for the first and second vector derivative of $\Lambda(\underline{\theta}_i)$ w.r.t. $\underline{\theta}_i$.

$$\begin{aligned} \frac{\partial \Lambda(\underline{\theta}_i)}{\partial \underline{\theta}_i} &= - \sum_{n=i+1}^{N+i-1} \sum_{k=1}^B \frac{\partial \Lambda_{kn}(\underline{\theta}_i)}{\partial \underline{\theta}_i} \\ &= - \sum_{n=i+1}^{N+i-1} \sum_{k=1}^B \left[\text{tr} \left(R_{kn}^{-1} \frac{\partial R_k}{\partial \underline{\theta}_i} \right) + \underline{\alpha}_{kn}^* \frac{\partial R_{kn}^{-1}}{\partial \underline{\theta}_i} \underline{\alpha}_{kn} \right] \end{aligned} \quad (6.5-7f)$$

and

$$\begin{aligned} \frac{\partial^2 \Lambda(\underline{\theta}_i)}{\partial \underline{\theta}_i \partial \underline{\theta}_j} &= - \sum_{n=i+1}^{N+i-1} \sum_{k=1}^B \frac{\partial^2 \Lambda_{kn}(\underline{\theta}_i)}{\partial \underline{\theta}_i \partial \underline{\theta}_j} \\ &= \sum_{n=i+1}^{N+i-1} \sum_{k=1}^B \left[\text{tr} \left(R_{kn}^{-1} \frac{\partial R_{kn}}{\partial \underline{\theta}_i} R_{kn}^{-1} \frac{\partial R_{kn}}{\partial \underline{\theta}_j} \right) - \text{tr} \left(R_{kn}^{-1} \frac{\partial^2 R_{kn}}{\partial \underline{\theta}_i \partial \underline{\theta}_j} \right) \right. \\ &\quad \left. - \underline{\alpha}_{kn}^* \frac{\partial^2 R_{kn}^{-1}}{\partial \underline{\theta}_i \partial \underline{\theta}_j} \underline{\alpha}_{kn} \right] \end{aligned} \quad (6.5-7g)$$

where $\underline{\theta}_i$, $\underline{\theta}_j$ are the i , j element of the vector $\underline{\theta}_i$.

Lastly, if $\hat{\underline{\theta}}_n$ is the estimate at the instant $t = n\Delta t$, then from Equation (6.5-3a), the best estimate of $\hat{\underline{\theta}}_n$ at any time inside the interval $[n\Delta t, (n+N)\Delta t]$ is

$$\hat{e}_n(t) = H(t - n\Delta t) \hat{e}_n \quad (6.5-8a)$$

and the covariance is

$$\text{COV}(\hat{e}_n(t)) = H(t - n\Delta t) \text{COV}(\hat{e}_n) H^T(t - n\Delta t). \quad (6.5-8b)$$

CHAPTER 7

OPTIMUM VARIABLE LOCALIZATION PARAMETER ESTIMATION AND TRACKING

Render unto man the things which are man's and unto the computer the things which are the computer's.
-- NORBERT WEINER

7.1 INTRODUCTION

We have studied in some detail in Chapter 6 the problem of multisensor, multitarget variable time delay estimation and tracking. Since the ultimate objective is to estimate and track the localization parameters (e.g., target range and bearing), we therefore devote this chapter to addressing this important issue. The approach that we are undertaking is very similar to the stationary parameter case we have studied in Section 3.5.2, where for a multisensor array, the stationary target range and bearing are obtained by a geometric mapping from estimated time delays. Thus for the variable localization parameter case, our approach is to estimate the variable parameters by a geometric mapping from estimated time delays and time delay rates, where the latter are obtained using techniques presented in Chapter 6. The choice of a two-step (or indirect) approach to the variable localization parameter case is determined by the same set of arguments presented for the stationary parameter case. The pertinent arguments have been discussed in Section 3.5.2.

The study on passive estimation and tracking of variable target parameters has received considerable interest in the literature. Most of the early studies have been concentrated on the single target and single sensor array. However, the extension to a multitarget, multisensor environment has received increasing attention. The complexity of this problem increases rapidly as the number of targets and sensors increases. There are two notably different approaches in attacking this problem. The first approach starts from the target dynamic tracking filter (or data processor) and attempts to model the measurement processes. One theory which has received considerable attention recently is the Joint Probability Data Association Filter (JPDAF) discussed by Bar-Shalom,¹⁸ Bar-Shalom and Tse,¹⁹ and Fortmann, Bar-Shalom and Scheffe.²⁰ Here the measurements assume a probabilistic model. An underlying assumption for this approach is that the signal processor which produces the measurements cannot be modified to account for the multitarget problem. Thus one must rely on modeling the measurements. In fact, using a linear superposition assumption, Ng and Bar-Shalom presented a model of unresolved measurement for multitarget tracking.^{21,22} However, for this approach the inability to change the signal processor is a major limitation in obtaining a satisfactory solution to the actual problem. In fact, the intimate relation between the signal processor and the data processor designs was pointed out by Fortmann, Bar-Shalom and Scheffe.²⁰ They showed that the selected parameter in the signal processor directly affects the performance of the tracking filter. Or more generally, given a particular target-sensor environment, the

structure of the signal processor and its relationship with the data processor will ultimately determine the overall performance of the system.

The second approach, on the other hand, starts the investigation from the signal processor. Here one finds that the signal processing gain increases in proportion to time. However, by increasing the processing time, one can no longer assume a SPLIT process, which is the basic assumption used in many existing signal processor designs. Typically, one finds that under a target motion assumption, a signal processor must estimate both the static and motion parameters. Failure to compensate for the parameter dynamic will result in a substantial loss in coherent integration. Consequently, it negates the very purpose of long-time integration. Studies in this approach are notably pursued by Carter and Abraham²³ in estimating source motion from time delay and time compression measurement. Also, Schultheiss and Weinstein evaluated the CRLB of estimating the differential Doppler shift.¹⁵ Moura and Baggeroer investigated the problem of space-time tracking by a passive observer.²⁴ These studies, however, deal only with the single target (or source) problem.

The approach being undertaken in this chapter can be considered as an extension of the second approach. However, we address a more general problem and we do not limit the parameter dynamic to a simple rate variation. In addition, we also discuss the tracking methodology. In short, it is strongly believed that the two approaches

mentioned above will ultimately converge and result in an integrated signal-data processor. The integrated processor will combine the signal processor and the data processor in such a manner as to achieve the best possible processor structure. It should be pointed out that the study on the relationship between digital signal processing (used in signal processor design) and control and estimation theory (used in data processor design) was first discussed by Willsky.⁴⁰ It is hoped that our study in this chapter will help advance the concept of integrated signal-data processor design.

This chapter is organized as follows. Section 7.2 discusses the methodology in variable localization parameter estimation and Section 7.3 investigates the problem of localization parameter tracking. Finally, in Section 7.4 we present our approach to target state estimation and tracking.

7.2 VARIABLE LOCALIZATION PARAMETER ESTIMATION

Our approach to variable localization parameter estimation is the following:

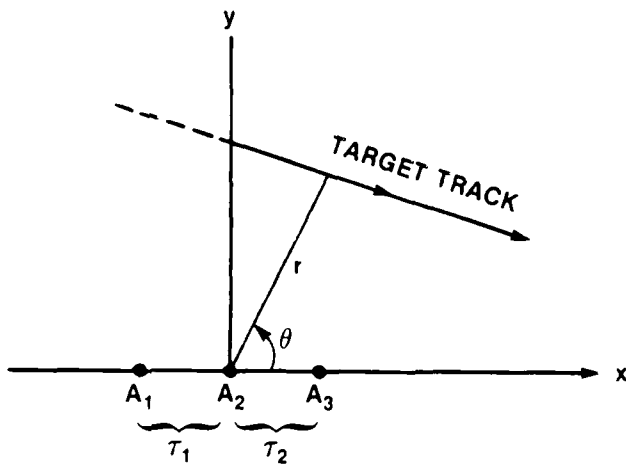
1. Apply the optimum multisensor, multitarget variable time delay estimator as presented in Chapter 6;
2. Evaluate the time delay estimate at any desired time within the observation interval $[0, T]$; and

3. Map the time delay estimate to the localization parameters (range and bearing) using the target sensor geometry.

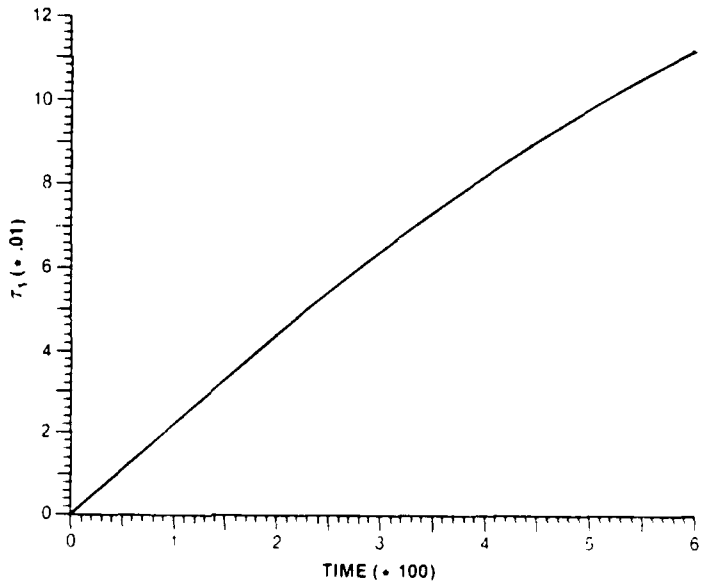
For the purpose of demonstration, consider a single target, three-sensor array system shown in Figure 7-1a and 7-1b. Figure 7-1a shows a target travelling at a constant course and speed. (Note this assumption is unnecessary for the approach discussed here.) Figure 7-1b, on the other hand, shows a typical time delay variation as a function of time over a 10-minute interval. Note that over this interval the time delay variation can be modeled adequately by a second order polynomial. For a smaller observation interval (e.g., 5 minutes), it can easily be modeled by a first order polynomial.

To illustrate our procedure, we assume that the observation interval is $[0, T]$, where $T = 5$ minutes. Thus at the end of the 5-minute interval, we want to know the target range and bearing. Our procedure is as follows. First, we partition the interval $[0, T]$ into N equal subintervals, where N is chosen according to Equation (6.2-3). We next apply the variable time delay estimator as discussed in Section 6.4.2.3. Let the resulting estimated time delays at time $t \in [0, T]$ be given by (see Equation 6.4.2-38a))

$$\begin{bmatrix} \hat{\tau}_1(t) \\ \hat{\tau}_2(t) \end{bmatrix} = \begin{bmatrix} \underline{h}^T(t) & | & \underline{0}^T \\ \hline \underline{0}^T & | & \underline{h}^T(t) \end{bmatrix} \begin{bmatrix} \hat{\theta}_1 \\ \hat{\theta}_2 \end{bmatrix} \quad (7.2-1)$$



a. TARGET SENSOR ARRAYS GEOMETRY



b. TIME DELAY VARIATION AS A FUNCTION OF TIME

021.612

Figure 7-1. Single Target, Three-Sensor Array Variable Localization Parameter Estimation

where $\underline{h}(t)$, $\hat{\theta}_1$, and $\hat{\theta}_2$ are defined accordingly in Section 6.4.2.3.

We next map the estimated time delays to range and bearing using Equations (D-10a) and (D-10b). Hence we obtain

$$\hat{B}(t) = -\sin^{-1} \left(\frac{C}{2L} (\hat{\tau}_1(t) + \hat{\tau}_2(t)) \right) \quad (7.2-2a)$$

$$\hat{R}(t) = \frac{L^2}{C} \left(\frac{\cos^2 \hat{B}(t)}{\hat{\tau}_2(t) - \hat{\tau}_1(t)} \right) \quad (7.2-2b)$$

where L is the interarray separation and C is the propagation speed of the medium.

We next evaluate the performance bound of the localization parameters about the true values. Let $R(t)$, $B(t)$ be the true range and bearing, then from Equation (G-8) in Appendix G, one obtains

$$\text{VAR}(\hat{B}(t)) = \frac{1}{2} \left(\frac{C}{L \cos B(t)} \right)^2 \left[\text{VAR}(\hat{\tau}_1(t)) + \text{COV}(\hat{\tau}_1(t), \hat{\tau}_2(t)) \right] \quad (7.2-3a)$$

$$\text{VAR}(\hat{R}(t)) = 2C^2 \left(\frac{R(t)}{L \cos B(t)} \right)^4 \left[\text{VAR}(\hat{\tau}_1(t)) - \text{COV}(\hat{\tau}_1(t), \hat{\tau}_2(t)) \right]. \quad (7.2-3b)$$

But from Equations (6.4.2-38a and b), we have

$$\text{COV} \begin{bmatrix} \hat{\tau}_1(t) \\ \hat{\tau}_2(t) \end{bmatrix} = \begin{bmatrix} \underline{h}^T(t) & | & \underline{0}^T \\ \hline \underline{0}^T & | & \underline{h}^T(t) \end{bmatrix} \text{COV}(\underline{\epsilon}) \begin{bmatrix} \underline{h}(t) & | & \underline{0} \\ \hline \underline{0} & | & \underline{h}(t) \end{bmatrix} \quad (7.2-4a)$$

and from Equation (6.4.2-37b) we have

$$\text{COV}(\underline{\epsilon}) = A^{-1} \left[2 \sum_{k=1}^B \omega_k^2 \frac{s_k^2/N_k^2}{1 + 3 s_k^2/N_k^2} \right]^{-1} \quad (7.2-4b)$$

where A is given in Equation (6.4.2-36b). Now writing A as

$$A = \begin{bmatrix} 2\Lambda & | & \Lambda \\ \hline \Lambda & | & 2\Lambda \end{bmatrix} \quad (7.2-4c)$$

where $\Lambda = H^T H$, and using the well known relation in matrix algebra

$$\begin{bmatrix} B & | & C \\ \hline D & | & E \end{bmatrix}^{-1} = \begin{bmatrix} (B - CE^{-1}D)^{-1} & | & -B^{-1}C(E - DB^{-1}C)^{-1} \\ \hline -E^{-1}D(B - CE^{-1}D)^{-1} & | & (E - DB^{-1}C)^{-1} \end{bmatrix}, \quad (7.2-4d)$$

the matrix inverse of A is given by

$$A^{-1} = \frac{2}{3} \begin{bmatrix} \Lambda^{-1} & | & -\frac{1}{2}\Lambda^{-1} \\ \hline -\frac{1}{2}\Lambda^{-1} & | & \Lambda^{-1} \end{bmatrix}. \quad (7.2-4e)$$

Substituting Equations (7.2-4b) and (7.2-4e) in (7.2-4a) yields

$$\text{COV} \begin{bmatrix} \hat{\tau}_1(t) \\ \hat{\tau}_2(t) \end{bmatrix} = \begin{bmatrix} \underline{h}^T(t)\Lambda^{-1}\underline{h}(t) & -\frac{1}{2}\underline{h}^T(t)\Lambda^{-1}\underline{h}(t) \\ -\frac{1}{2}\underline{h}^T(t)\Lambda^{-1}\underline{h}(t) & \underline{h}^T(t)\Lambda^{-1}\underline{h}(t) \end{bmatrix}$$

$$\left[3 \sum_{k=1}^B \omega_k^2 \frac{S_k^2/N_k^2}{1 + 3 S_k^2/N_k^2} \right]^{-1} \quad (7.2-5)$$

Finally, using Equation (7.2-5) in (7.2-3a) and (7.2-3b) yields the desired expressions

$$\text{VAR}(\hat{B}(t)) = \frac{1}{4} \left(\frac{c}{L \cos B(t)} \right)^2 \left[\underline{h}^T(t)\Lambda^{-1}\underline{h}(t) \right] \text{VAR}(\hat{\tau}_1) \quad (7.2-6a)$$

$$\text{VAR}(\hat{R}(t)) = 3c^2 \left(\frac{R(t)}{L \cos B(t)} \right)^2 \left[\underline{h}^T(t)\Lambda^{-1}\underline{h}(t) \right] \text{VAR}(\hat{\tau}_1) \quad (7.2-6b)$$

where

$$\text{VAR}(\hat{\tau}_1) = 3 \left\{ \sum_{k=1}^B \omega_k^2 \frac{S_k^2/N_k^2}{1 + 3 S_k^2/N_k^2} \right\}^{-1}; \quad \omega_k = \frac{2\pi}{\Delta t} \quad (7.2-6c)$$

is the variance of an optimum time delay estimate from a three-sensor array (see Equation (C-26), Appendix C).

Now let $\text{VAR}_s(\hat{B})$ and $\text{VAR}_s(\hat{R})$ denote the bearing and range variance for the stationary target case. Then from Appendix G Equations (G-15) and (G-16), we obtain

$$\frac{\text{VAR}(\hat{B}(t))}{\text{VAR}_s(\hat{B})} = \begin{bmatrix} \cos B(0) \\ \cos B(t) \end{bmatrix} \begin{bmatrix} \underline{h}^T(t) \Lambda^{-1} \underline{h}(t) \end{bmatrix} N \quad (7.2-7a)$$

$$\frac{\text{VAR}(\hat{R}(t))}{\text{VAR}_s(\hat{R})} = \begin{bmatrix} R(t) \cos B(0) \\ R(0) \cos B(t) \end{bmatrix} \begin{bmatrix} \underline{h}^T(t) \Lambda^{-1} \underline{h}(t) \end{bmatrix} N \quad (7.2-7b)$$

where $B(0) = B(t=0)$, $R(0) = R(t=0)$, and $N = \frac{T}{\Delta t}$.

Note that if time delays are stationary, then the right-hand sides of Equation (7.2-7a) and (7.2-7b) are unity. Since we have $B(t) = B(0)$, $R(t) = R(0)$, $\underline{h}(t) = 1$, $H^T = [1 1 \dots 1]$, so

$$\underline{h}^T(t) \Lambda^{-1} \underline{h}(t) N = (H^T H)^{-1} N = 1. \quad (7.2-7c)$$

Thus, as expected, the performance of the variable parameter case reduces to the stationary performance case.

We next examine the localization performance when time delays can be modeled by a first order polynomial in time. Thus using the definition shown in Equations (6.4.2-5c) and (6.4.2-32f) we obtain

$$\Lambda = H^T H = \begin{bmatrix} 1 & 1 & \dots & 1 \\ t_1 & t_2 & \dots & t_N \end{bmatrix} \begin{bmatrix} 1 & t_1 \\ 1 & t_2 \\ \vdots & \vdots \\ 1 & t_N \end{bmatrix}$$

$$= \begin{bmatrix} N & \sum_{i=1}^N t_i \\ \sum_{i=1}^N t_i & \sum_{i=1}^N t_i^2 \end{bmatrix} \quad (7.2-8a)$$

Hence one obtains after some algebraic manipulation

$$\underline{h}^T(t) \Lambda^{-1} \underline{h}(t) = \frac{Nt^2 - 2t \sum_{i=1}^N t_i + \sum_{i=1}^N t_i^2}{\left(N \sum_{i=1}^N t_i^2 \right) - \left(\sum_{i=1}^N t_i \right)^2}$$

$$= \frac{t^2 - 2t \bar{t} + \bar{t}^2}{N (\bar{t}^2 - \bar{t}^2)} \quad (7.2-8b)$$

where

$$\bar{t} = \frac{1}{N} \sum_{i=1}^N t_i = \frac{N \Delta t}{2} \quad (7.2-8c)$$

$$\bar{t}^2 = \frac{1}{N} \sum_{i=1}^N t_i^2 = (4N^2 - 1) \frac{\Delta t^2}{12} \quad (7.2-8d)$$

and

$$\bar{t}^2 - \bar{t}^2 = \frac{(N^2 - 1)}{12} \Delta t^2 . \quad (7.2-8e)$$

Note that Equation (7.2-8b) has a minimum at $t_{\min} = \bar{t}$; i.e., at the midpoint of the observation interval. At $t = \bar{t}$, Equation (7.2-8b) reduces to

$$\underline{h}^T(\bar{t}) \Lambda^{-1} \underline{h}(\bar{t}) = \frac{1}{N}. \quad (7.2-8f)$$

Now substituting Equation (7.2-8b) in (7.2-7a and b) yields

$$\frac{\text{VAR}(\hat{B}(t))}{\text{VAR}_s(B)} = \left[\frac{\cos B(0)}{\cos B(t)} \right] \left[\frac{t^2 - 2t \bar{t} + \bar{t}^2}{(\bar{t}^2 - t^2)} \right] \quad (7.2-9a)$$

$$\frac{\text{VAR}(\hat{R}(t))}{\text{VAR}_s(R)} = \left[\frac{R(t) \cos B(0)}{R(0) \cos B(t)} \right] \left[\frac{t^2 - 2t \bar{t} + \bar{t}^2}{(\bar{t}^2 - t^2)} \right] \quad (7.2-9b)$$

Thus from Equations (7.2-9a and b) one concludes in general that the performance of the localization parameter estimates for the variable parameter case degrades w.r.t. the stationary parameter case. The degradation, however, is minimal at the midpoint of the interval.

In the examples that we have considered thus far, we discussed only the single target localization parameter estimation. The multi-target case, in theory, presents no insurmountable difficulties because our approach relies primarily on the time delay processor. All localization parameters are obtained via a geometric mapping from time delay measurements.

7.3 VARIABLE LOCALIZATION PARAMETER TRACKING

Our approach to variable localization parameter tracking is mechanized via a geometric mapping from time delay estimates obtained from the variable time delay tracking processor. In particular, we employ the method of sequential fixed-interval time delay tracking as presented in Section 6.5.1.

Recall from Section 6.5.1 that the method employs a T-second sliding window over the incoming signal waveform. Over the T-second interval an appropriate variable time delay model is used. A state vector consisting of the time delay and its higher order derivates is evaluated at the beginning of the T-second window. This parameter state vector is estimated sequentially at every $\Delta t = \frac{T}{N}$ seconds and the estimate is obtained based on the current T-second observation and the previous estimate. Knowledge of the time delay state vector at any point allows the estimated time delay to be evaluated at any other point. In particular, one can evaluate at the most current observation subinterval. Thus let $\hat{\theta}_n$ be the estimated time delay state vector for the one-target, three-sensor case. Then one can write

$$\hat{\theta}_n = \begin{bmatrix} \hat{\theta}_{n1} \\ \hat{\theta}_{n2} \end{bmatrix} \quad (7.3-1a)$$

where

$$\hat{\theta}_{ni} = (\tau_{ni} \quad \ddot{\tau}_{ni} \quad \dots \quad \tau_{ni}^{(p)})^T ; \quad i = 1, 2 . \quad (7.3-1b)$$

Therefore, the time delay estimates at $t = T + n\Delta t$ are

$$\hat{\tau}_{ni}(T) = h^T(T) \hat{\theta}_{ni} ; \quad i = 1, 2 . \quad (7.3-2)$$

Therefore, the estimated range and bearing at the most recent observation interval are (using Equations (7.2-2a and b))

$$\hat{B}_n(T) = -\sin^{-1} \left[\frac{C}{2L} (\hat{\tau}_{n1}(T) + \hat{\tau}_{n2}(T)) \right] \quad (7.3-3a)$$

$$\hat{R}_n(T) = \frac{L^2}{C} \left(\frac{\cos^2 \hat{B}_n(T)}{\hat{\tau}_{n2}(T) - \hat{\tau}_{n1}(T)} \right) \quad (7.3-3b)$$

for $n = 1, 2 \dots$

7.4 TARGET STATE ESTIMATION AND TRACKING

In the previous sections we considered the problem of estimation and tracking target localization parameters. In this section we briefly study a method of target state estimation and tracking.

The state of a target is defined by the target's location and velocity components. Thus the target state vector consists of a target's location and velocity vectors. Therefore, target state estimation and tracking is concerned with simultaneously estimating and tracking a target's location and velocity components.

In the literature, the problems of target state estimation have been well treated. The usual approach is to formulate the problem in such a way as to yield a Kalman filter-type solution. For example, the target motion is modeled by a dynamic equation of the form

$$\underline{x}_{n+1} = \underline{f}(\underline{x}_n) + G \underline{w}_n ; \quad n = 0, 1, \dots \quad (7.4-1a)$$

where \underline{x}_n is the target state at time $t = (n + 1)\Delta t$, $\underline{f}(\underline{x}_n)$ is a vector function of the state, G is a matrix, and \underline{w}_n is a process noise vector. The best estimate of the state $\hat{\underline{x}}_n$ is sought subject to a measurement equation of the form

$$\underline{z}_n = \underline{h}(\underline{x}_n) + \underline{v}_n \quad (7.4-1b)$$

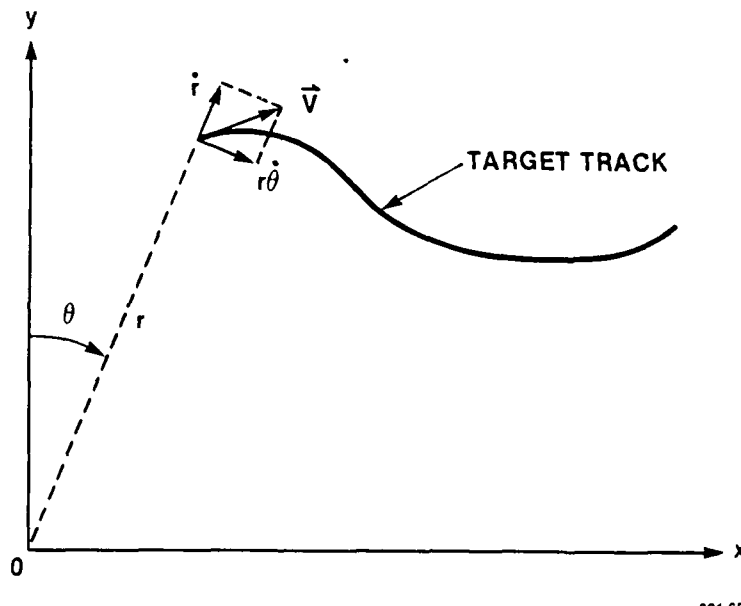
where \underline{z}_n is the measurement vector consisting of time delays, range, bearing or frequency, etc; $\underline{h}(\underline{x}_n)$ is a vector function relating the measurement to the state; and \underline{v}_n represents the measurement noise vector.

When $f(\cdot)$ and $h(\cdot)$ are linear and the noise processes are Gaussian, Equations (7.4-1a and b) are solved optimally by the celebrated Kalman filter. When either $f(\cdot)$ or $h(\cdot)$ is nonlinear, which is usually the case for target state estimation and tracking, an Extended Kalman Filter (EKF) is used where all nonlinearities are linearized about the best state estimate. However, the EKF is no longer the optimum solution and, in fact, convergence can no longer be guaranteed (see Gelb⁴¹). The general continuous time equivalence of Equations (7.4-1a and b) was studied by Kushner and Stratonovich.⁴² While assuming only a Gaussian noise process, Kushner and Stratonovich derived a partial differential equation governing the time-dependent state's probability density function (see McGarty⁴²).

We mentioned earlier that the EKF linearized all nonlinear functions about the best estimate of the state. This linearization is probably adequate for small process and measurement noises. However, we are interested in a low SNR environment where the signal processor is required to have a long integration time such that the effect of target dynamics must be considered. Under this assumption, we present a method of target state estimation and tracking from the signal processor viewpoint. Thus our approach is to estimate the target's localization and motion parameters from the estimated variable time delay processor.

7.4.1 Target State Estimation

We are interested in estimating the target state (for example, range, bearing, range rate, and bearing rate) over a T-second observation. In this approach, we do not require the target to travel on a constant course and speed as is usually the model assumed by the Kalman filter formulation. But instead, we assume that the variable time delay due to target motion can be modeled by a finite order polynomial in time. Therefore, the variable time delay processor discussed in Section 6.3 is applicable. Figure 7-2 shows the target geometry and the appropriate state variables.



021.651

Figure 7-2. Geometry of Target State Estimation

Let the target state variable in the polar coordinate be represented by

$$\underline{v}_P = (r, \theta, \dot{r}, \dot{\theta})^T \quad (7.4-2a)$$

and in the rectangular coordinate by

$$\underline{y}_R = (x, y, \dot{x}, \dot{y})^T. \quad (7.4-2b)$$

Note that there exists a unique mapping between the two state variable representations. Let the mapping operator $T()$ be defined such that

$$\underline{y}_R = T(\underline{v}_P) \quad (7.4-2c)$$

and

$$\underline{v}_P = T^{-1}(\underline{y}_R). \quad (7.4-2d)$$

Now from Appendix D, we have the geometric relations between time delay measurements and the localization parameters;

$$r = f_1(\tau_1, \tau_2) \quad (7.4-3a)$$

$$\theta = f_2(\tau_1, \tau_2) \quad (7.4-3b)$$

where $f_1()$ and $f_2()$ are given in Equations (D-8a) and (D-8b).

Therefore, one can write the range rate and bearing rate as

$$\begin{aligned}\dot{r} &= \frac{\partial f_1}{\partial \tau_1} \dot{\tau}_1 + \frac{\partial f_1}{\partial \tau_2} \dot{\tau}_2 \\ &= f_3(\tau_1, \tau_2, \dot{\tau}_1, \dot{\tau}_2)\end{aligned}\quad (7.4-3c)$$

$$\begin{aligned}\dot{\theta} &= \frac{\partial f_2}{\partial \tau_1} \dot{\tau}_1 + \frac{\partial f_2}{\partial \tau_2} \dot{\tau}_2 \\ &= f_4(\tau_1, \tau_2, \dot{\tau}_1, \dot{\tau}_2).\end{aligned}\quad (7.4-3d)$$

We can define the partial time delay vector \underline{x} by

$$\underline{x} \stackrel{\Delta}{=} (\tau_1 \ \tau_2 \ \dot{\tau}_1 \ \dot{\tau}_2)^T. \quad (7.4-3e)$$

Then the target state vector can be related to the partial time delay vector \underline{x} by

$$\underline{y}_p = \underline{f}(\underline{x}) \quad (7.4-3f)$$

where

$$\underline{f}(\) = (f_1(\) \ f_2(\) \ f_3(\) \ f_4(\))^T. \quad (7.4-3g)$$

Therefore, the best estimate $\hat{\underline{y}}_p$ is given by

$$\hat{\underline{y}}_p = \underline{f}(\hat{\underline{x}}) \quad (7.4-4a)$$

and the covariance of this estimate is given by

$$\text{COV}(\hat{\underline{Y}}_P) = F \text{ COV}(\hat{\underline{X}}) F^{-1} \quad (7.4-4b)$$

where the matrix F is given by

$$F = \frac{\partial f}{\partial \underline{X}} \text{ (evaluated at some desired } \underline{X}^*) \quad (7.4-4c)$$

The partial time delay vector \underline{X} can be obtained using results from Section 6.4.2.3. Thus from Equations (6.4.2-25a and b), we have the vector $\underline{X}(t)$; i.e., the vector \underline{X} evaluated at any time $t \in [0, T]$ is given by

$$\begin{aligned} \underline{X}(t) &= \begin{bmatrix} \underline{h}^T(t) & | & \underline{0}^T \\ \hline \underline{0}^T & + & \dot{\underline{h}}^T(t) \\ \hline \underline{h}^T(t) & | & \underline{0}^T \\ \hline \underline{0}^T & | & \dot{\underline{h}}^T(t) \end{bmatrix} \begin{bmatrix} \underline{e}_1 \\ \underline{e}_2 \end{bmatrix} \\ &= h(t) \underline{e} \end{aligned} \quad (7.4-5a)$$

where $\underline{e} = [\underline{e}_1 \ \underline{e}_2]^T$ is the time delay state vector at time $t = 0$, and $\dot{\underline{h}}(t)$ is the derivative of $\underline{h}(t)$ w.r.t. the time variable.

Hence, the best estimate of $\underline{X}(t)$ is given by

$$\hat{\underline{X}}(t) = h(t) \hat{\underline{e}} \quad (7.4-5b)$$

and the covariance of $\hat{x}(t)$ is given by

$$\text{COV}(\hat{x}(t)) = h(t) \text{COV}(\hat{\theta}) h^T(t) \quad (7.4-5c)$$

where $\text{COV}(\hat{\theta})$ is given in Equation (6.4.2-37b).

Thus by estimating the time delays and the delay rates, the target state vector can also be estimated. Finally, the performance bound can also be evaluated at any point within the observation interval.

7.4.2 Target State Tracking

Our approach to target state tracking is to extend the results in variable localization parameter tracking to include the target motion parameters. Again we use the sequential fixed-interval time delay tracking processor discussed in Section 6.5.1.

Here we assume that the time delay tracking processor yields the time delay state vector $\hat{\theta}_n$ at $t = n\Delta t$. Therefore, from Equation (7.4-5a), the best estimate of $x_n(T)$ at time $t = T + n\Delta t$ is given by

$$\hat{x}_n(T) = h(T) \hat{\theta}_n. \quad (7.4-6a)$$

Therefore, replacing \hat{x} by $\hat{x}_n(T)$ in Equation (7.4-4a) yields the target state estimate as a function of time, namely

$$\hat{y}_p(\tilde{t}_n) = f(\hat{x}_n(T)) \quad (7.4-6b)$$

where $\tilde{t}_n = T + n\Delta t$ is the time of the most recent observation subinterval.

CHAPTER 8

SUMMARY, CONCLUSIONS, AND RECOMMENDATIONS

Behind an able man there are always other able men. -- (Chinese Proverb)

We have studied in detail the methodologies of optimum signal processing for passive time delay estimation in a multisensor, multitarget environment. Our investigations were motivated by (1) the inherent inability of the existing time delay estimator to resolve estimation bias in a multitarget environment, and (2) the apparent lack of research and understanding in this area. In the literature, the studies of interference were confined to studying the effect of interference on the existing processor and the methods of interference suppression. The location or direction of interference was usually assumed known. Our study as presented here, however, treats the interference as another target of interest.

We pointed out that the traditional approach is optimum for a single target only. In the multitarget environment, the existing approach is biased due to the inherent mismatch between the single target signal processor design and the multitarget operating environment. We argue that for a high performance sonar system, it is

important to have an unbiased processor since measurement bias cannot be easily removed with further post-estimator processing.

The optimum multisensor, multitarget time delay processor is derived from a Maximum Likelihood viewpoint. The actual processor is obtained by reducing the likelihood equation via straightforward but somewhat tedious manipulations to the simplest form. The general multisensor, multitarget processor is applied to a two-sensor, one-target case. The resulting processor is shown to be identical to the GCC studied by Knapp and Carter.¹ We next studied the two-sensor, two-target problem. We showed the optimum two-sensor, two-target processor and presented the CRLB. We then extended our study to address the estimation of localization parameters. Much of our attention had been spent on the discussion of a basic three-sensor ranging array. We showed that for passive ranging and directional finding, an optimum processor is the focus beamformer which yields a direct estimate of range and bearing. We argued that an alternate approach is to measure the inter-sensor time delay and then geometrically map the time delay measurements to the corresponding ranges and bearings.

The focus beamformer approach can be called the one-step approach, whereas the alternate time delay approach can be called the two-step approach. It was shown in Section 3.5.2 that both approaches yield identical performance in terms of the CRLB. However, there are major differences between the two approaches:

(1) the focus beamformer requires searching over a range/ bearing space of a correlation function which is asymmetric with respect to the range and bearing variables; on the other hand, any correlation over the time delay variables is always symmetrical; (2) for tracking purposes, the focus beamformer approach requires a two-dimensional error detector design whereas the time delay approach can be implemented using two one-dimensional error detectors; and (3) arguing from the Law of Large Numbers, both approaches yield Gaussian measurement noise. However, for the time delay approach, the resulting range and bearing estimates could be biased and have non-Gaussian statistics if a direct non-linear geometric mapping from time delay measurements is used. For a practical implementation, the two-step time delay approach is preferred because the symmetry of the correlation function over the time delay variables yields simple and efficient tracking logic. This is especially advantageous for a low SNR environment where the increased smoothing time required (to make the estimator efficient) can be achieved via a simple feedback design. Finally, for the three-sensor ranging array, the potential bias and non-Gaussian statistics can be minimized if mapping to intermediate variables is used instead of range and bearing; for example, mapping to cosine bearing and inverse range since they are linearly related to time delay measurements.

We also investigated the general optimum inter-sensor time delay vector estimator. Our study showed that given M sensors, the

M-1 time delay can be obtained with M-1 correlators. This is in marked contrast with Hahn's approach²⁵ where a total $M(M-1)\frac{1}{2}$ correlations are required. In addition, we presented a simple expression of the CRLB of time delay vector estimation under a single target assumption. Finally, in our study of the three-sensor ranging array, we pointed out the improved performance of the optimum formulation versus the conventional approach.

We stated that one of the strongest assumptions we made in studying the optimum time delay processor is the assumption of known target power spectrum. Therefore, we briefly addressed the problem of power spectral estimation. We studied the optimum spectral estimator for the two-sensor, one-target case and the two-sensor, two-target case. We briefly studied the problem of joint time delay and spectral estimation. A somewhat surprising result is that time delay estimates and spectral estimates are uncorrelated. This implies that the joint time delay/spectral estimation does not degrade the resulting estimator performance when assuming either is known. Furthermore, we found that while the time delay CRLB decreases as the inverse of observation time, the power spectral CRLB decreases as the inverse square of observation time.

We next addressed the problem of practical implementation of the optimum multisensor, multitarget time delay processor. We

noted that one approach is to assume a weak signal in noise environment. Here the intricate structure of the optimum multisensor, multitarget time delay processor is drastically reduced to a manageable form. We also discussed a single target assumption approach as a suboptimal processor in a multitarget environment. We provided a numerical illustration of the single target processor behavior in the presence of interference. Performance of the single target processor was compared to the optimum multitarget processor. We noted that in the presence of interference, the single target processor, in general, was biased and had a larger variance except when the target interference time delay separation is small; i.e., less than a correlation pulse width. Within this region, however, the optimum multitarget processor has a variance which grows without bound as the separation decreases for the case of identical signal and interference spectrum. This reflected the inappropriateness of using a multitarget formulation in a single (merged) target environment.

In a multisensor, multitarget environment, an optimum processor remains optimum so long as the actual number of sensors and targets matches the number assumed in the optimum processor design. A mismatch in either the number of targets (addressed in this study) or the number of sensors (caused perhaps by element failure) will automatically degrade the processor performance. Therefore, a key element in using the optimum multitarget processor is the correct detection of the number of targets.

The optimum multisensor, multitarget processors which we have derived, studied and discussed thus far were based on the assumption of a SPLIT process. This assumption is difficult to satisfy for a more general moving target environment. Therefore, we further refined our study to account for the effects of target motion.

The approach we have taken was to model the time delay motion by a finite order polynominal in time and partition the observation interval into N equal subintervals. It was shown that in order for the time-compressed waveform to be Fourier representable, N must satisfy a certain constraint. When this assumption is valid, one can again express the multisensor, multitarget, multi-interval observation in terms of a multi-dimensional Fourier coefficient vector. The result of using an MLE approach yielded the multisensor, multitarget variable time delay processor. This processor provided an estimate of the time delay and its higher order derivatives at any time within the observation interval. It was shown that for time delay estimate, the minimum variance always occurs at the midpoint of the observation interval.

The time delay processors we have discussed thus far are batched processor; i.e., one must wait until the end of a T -second observation before one starts any computations. In many applications, this T -second solution delay is not acceptable. Therefore, we have investigated and proposed a sequential fixed-interval time

delay processor. This processor obtains its current estimate by utilizing the most current subinterval observation and the prior estimates. We obtained an expression for the covariance calculation.

We next addressed the problem of variable localization parameter estimation and tracking. Our approach was similar to the stationary parameter case. We first estimated the time delay trajectory using the variable time delay processor. Localization parameters were then obtained via a geometric mapping from the time delay estimate. For target state estimation where we are interested in both the target position and velocity components, the mapping function utilized both time delay and time delay rate estimates.

Although we have studied a very broad area covering technical issues in signal processor design, parameter estimation and target state estimation and tracking, there are many questions, however, which remain unanswered. Therefore, we suggest them as topics for further investigation.

Our study presented here concentrated on the multisensor multitarget signal processing. However, closely related to the multitarget situation is the multipath environment encountered in many underwater sonar signal processing situations. Since multipath signals are correlated, one cannot simplify the signal

processor as we did for the multitarget case, where target signals are rightfully assumed uncorrelated. Thus, in terms of signal processor design, the multipath processor is somewhat more complex w.r.t. the multitarget processor.

The post correlator matched estimator we have studied assumes a known signal and interference power spectra. However, knowledge of the target spectrum is seldom exact. Therefore, it is important to investigate the robustness of the estimator when a mismatch exists .

Finally, our approach to localization parameter estimation and tracking, or more generally, target state estimation and tracking, starts from a signal processing design viewpoint. Traditional approaches are mostly formulated in terms of a Kalman filter. Therefore, it will be of utmost interest to compare the performance of these two approaches in terms of solution accuracy, computation requirements, effects of maneuvering target handling capability, and tracking threshold.

APPENDIX A
DEFINITION OF COMPLEX GAUSSIAN PROBABILITY DENSITY FUNCTION (pdf)

This appendix briefly describes the meaning of a complex Gaussian probability density function (pdf). A thorough treatment of this subject can be found in Goodman.⁴³

Let $X(t)$ be a zero mean wide-sense stationary white Gaussian random process with correlation function $E[X(t) X(\tau)] = \sigma^2 \delta(t - \tau)$, then its Fourier coefficients from a T-second observation are given by

$$\begin{aligned} X_k &= \frac{1}{T} \int_0^T X(t) e^{-j\omega_k t} dt \\ &= I_k - j Q_k ; \quad k = 1, 2, \dots, 8 \end{aligned} \quad (A-1)$$

where I_k and Q_k are known as the in-phase and quadrature phase components. It can be easily verified that I_k and Q_k are Gaussian distributed with the following statistics:

$$E(I_k) = E(Q_k) = E(I_k Q_k) = 0 \quad (A-2a)$$

$$E(I_k^2) = E(Q_k^2) = \frac{\sigma^2}{2T} . \quad (A-2b)$$

Let $\underline{Z}_k = (I_k \ Q_k)^T$, then the bivariate real Gaussian pdf of \underline{Z}_k is given by

$$P(\underline{Z}_k) = (2\pi)^{-1} |R_k|^{-\frac{1}{2}} \exp\left\{-\frac{1}{2} \underline{Z}_k^T R_k^{-1} \underline{Z}_k\right\} \quad (A-3a)$$

where

$$\underline{R}_k \triangleq E(\underline{z}_k \underline{z}_k^T) = \frac{1}{2T} \begin{bmatrix} \sigma^2 & 0 \\ 0 & \sigma^2 \end{bmatrix} \quad (A-3b)$$

Now a complex Gaussian uni-variate pdf of x_k is defined by

$$P(x_k) = \pi^{-1} |c_k|^{-1} \exp\{-x_k^* c_k^{-1} x_k\} \quad (A-4a)$$

where

$$c_k = E(x_k x_k^*) = \sigma^2/T. \quad (A-4b)$$

It is straightforward to verify that $|R_k|^{-\frac{1}{2}} = 2|c_k|^{-1}$ and $x_k^* c_k^{-1} x_k = \underline{z}_k^T R_k^{-1} \underline{z}_k / 2$, hence one can write

$$P(x_k) = P(\underline{z}_k) = (\pi\sigma^2)^{-1} \exp\left\{-\frac{\underline{z}_k^T R_k^{-1} \underline{z}_k}{2\sigma^2}\right\}. \quad (A-5)$$

Therefore, in general let \underline{x} be a complex Gaussian B -dimensional vector such that

$$\underline{x} = \underline{I} - j \underline{Q} \quad (A-6a)$$

with

$$E(\underline{I} \underline{I}^T) = E(\underline{Q} \underline{Q}^T) = V/2 \quad (A-6b)$$

$$E(\underline{I} \underline{Q}^T) = -E(\underline{Q} \underline{I}^T) = -W/2. \quad (A-6c)$$

Now define a $2B$ -dimensional real vector as

$$\underline{z} = (\underline{I}^T \underline{Q}^T)^T. \quad (A-7)$$

Then it can be shown that $P(\underline{X})$ is a complex Gaussian pdf defined by

$$P(\underline{X}) = P(\underline{Z}) = \pi^{-B} |c|^{-1} \exp\{-\underline{x}^* c^{-1} \underline{x}\} \quad (A-8)$$

where

$$c = E(\underline{X} \ \underline{X}^*) = V + j W. \quad (A-9)$$

APPENDIX B

CALCULATION OF CRAMER-RAO LOWER BOUND FOR TWO-SENSOR, TWO-TARGET CASE

This appendix calculates the Cramer-Rao Lower Bound (CRLB) for the two-sensor, two-target case. Using Equations (3.4-1) and (3.4-5), the CRLB of the time delay estimates are:

$$\text{VAR}(\hat{\tau}_i) \geq [J^{-1}]_{ii} ; \quad i = 1, 2 . \quad (\text{B-1})$$

Now the symmetric Fisher's Information matrix J can be written as

$$J^{-1} = \begin{bmatrix} J_{11} & J_{12} \\ J_{21} & J_{22} \end{bmatrix}^{-1} = \frac{1}{(J_{11}J_{22} - J_{12}^2)} \begin{bmatrix} J_{22} & -J_{12} \\ -J_{12} & J_{11} \end{bmatrix} .$$

Therefore

$$\text{VAR}(\hat{\tau}_i) \geq \frac{1}{(1 - M_{12}^2)} \frac{1}{J_{ii}} ; \quad i = 1, 2 \quad (\text{B-2})$$

where

$$M_{12} = \frac{J_{12}}{(J_{11} J_{22})^{\frac{1}{2}}}$$

is defined as the coefficient of mutual dependence. The quantities J_{ij} are defined by Equation (3.4-5) as:

$$J_{ij} = \sum_{k=1}^B \operatorname{tr} \left(-\frac{\partial R_k^{-1}}{\partial \tau_i} \frac{\partial R_k}{\partial \tau_j} \right); \quad \begin{matrix} i = 1, 2 \\ j = 1, 2 \end{matrix} \quad (B-3)$$

In what follows, we present a detailed calculation of the quantity J_{ij} . Using the relations given in Equations (3.2-6) and (3.5.1-4a); i.e.,

$$R_k = S_{k1} P_{k1} + S_{k2} P_{k2} + N_k I \quad (B-4)$$

and

$$-\frac{\partial R_k^{-1}}{\partial \tau_i} = |\tilde{h}_{ki}|^2 \tilde{Q}_{ki}^{-1} \left(\frac{\partial P_{ki}}{\partial \tau_i} - \tilde{a}_{ki} \frac{\partial G_{ki}}{\partial \tau_i} P_{ki} \right) \tilde{Q}_{ki}^{-1}; \quad i = 1, 2 \quad (B-5)$$

we obtain

$$\begin{aligned} \operatorname{tr} \left(-\frac{\partial R_k^{-1}}{\partial \tau_i} \frac{\partial R_k}{\partial \tau_j} \right) &= S_{kj} |\tilde{h}_{ki}|^2 \left[\operatorname{tr} \left(\tilde{Q}_{ki}^{-1} \frac{\partial P_{ki}}{\partial \tau_i} \tilde{Q}_{ki}^{-1} \frac{\partial P_{kj}}{\partial \tau_j} \right) \right. \\ &\quad \left. - \tilde{a}_{ki} \frac{\partial G_{ki}}{\partial \tau_i} \operatorname{tr} \left(\tilde{Q}_{ki}^{-1} P_{ki} \tilde{Q}_{ki}^{-1} \frac{\partial P_{kj}}{\partial \tau_j} \right) \right]. \end{aligned} \quad (B-6)$$

The trace of the quantities inside the parentheses can be evaluated as follows. From Equation (3.2-7c), we find

$$\tilde{Q}_{k1}^{-1} = \tilde{N}_{k1} (S_{k2} P_{k2} + N_k I)^{-1}$$

$$\begin{aligned}
 &= \frac{\tilde{N}_{k1}}{N_k} \left[I - \frac{S_{k2}/N_k}{I + 2 S_{k2}/N_k} P_{k2} \right] \\
 &= \frac{\tilde{N}_{k1}}{N_k} \begin{bmatrix} 1 - a_{k2} & -a_{k2} e^{-j\omega_k \tau_2} \\ -a_{k2} e^{j\omega_k \tau_2} & 1 - a_{k2} \end{bmatrix} \tag{B-7}
 \end{aligned}$$

where

$$a_{k2} = \frac{S_{k2}/N_k}{I + 2 S_{k2}/N_k} \tag{B-8}$$

and similarly

$$\tilde{Q}_{k2}^{-1} = \frac{\tilde{N}_{k2}}{N_k} \begin{bmatrix} 1 - a_{k1} & -a_{k1} e^{-j\omega_k \tau_1} \\ -a_{k1} e^{j\omega_k \tau_1} & 1 - a_{k1} \end{bmatrix} \tag{B-9}$$

where

$$a_{k1} = \frac{S_{k1}/N_k}{I + 2 S_{k1}/N_k} \tag{B-10}$$

Note that \tilde{Q}_{ki}^{-1} is a Hermitian matrix with identical diagonal elements. Therefore, letting

$$\tilde{Q}_{ki}^{-1} = \begin{bmatrix} q_{11}^i & q_{12}^i \\ q_{12}^{i*} & q_{11}^i \end{bmatrix}$$

we have

$$\begin{aligned} \tilde{Q}_{ki} \frac{\partial P_{kj}}{\partial \tau_j} &= j\omega_k \begin{bmatrix} q_{11}^i & q_{12}^i \\ q_{12}^{i*} & q_{11}^i \end{bmatrix} \begin{bmatrix} 0 & -e^{-j\omega_k \tau_j} \\ e^{j\omega_k \tau_j} & 0 \end{bmatrix} \\ &= j\omega_k \begin{bmatrix} q_{12}^i e^{j\omega_k \tau_j} & -q_{11}^i e^{-j\omega_k \tau_j} \\ q_{11}^i e^{j\omega_k \tau_j} & -q_{12}^{i*} e^{-j\omega_k \tau_j} \end{bmatrix} \end{aligned} \quad (B-11)$$

and after some algebraic manipulation, we obtain from Equation (B-11)

$$\tilde{Q}_{ki}^{-1} \frac{\partial P_{ki}}{\partial \tau_i} \tilde{Q}_{ki}^{-1} \frac{\partial P_{kj}}{\partial \tau_j} = -\omega_k^2 \begin{bmatrix} A_{11}^{ij} & A_{12}^{ij} \\ A_{12}^{ij*} & A_{11}^{ij*} \end{bmatrix} \quad (B-12)$$

where

$$A_{11}^{ij} = (q_{12}^i)^2 e^{j\omega_k(\tau_i + \tau_j)} - (q_{11}^i)^2 e^{-j\omega_k(\tau_i - \tau_j)}$$

$$A_{12}^{ij} = (q_{11}^i) \left[q_{12}^i e^{j\omega_k(\tau_i + \tau_j)} - q_{12}^{i*} e^{-j\omega_k(\tau_i - \tau_j)} \right].$$

Thus

$$\begin{aligned} \text{tr} \left(\tilde{Q}_{ki}^{-1} \frac{\partial p_{ki}}{\partial \tau_i} \tilde{Q}_{kj}^{-1} \frac{\partial p_{kj}}{\partial \tau_j} \right) &= -\omega_k^2 (A_{11}^{ij} + A_{11}^{ij*}) \\ &= -2\omega_k^2 \operatorname{Re} \{ A_{11}^{ij} \} \end{aligned} \quad (\text{B-13})$$

where $\operatorname{Re} \{ \}$ denotes the real part.

Now using Equations (B-7) and (B-8), we obtain

$$\begin{aligned} \text{tr} \left[\left(\tilde{Q}_{k1}^{-1} \frac{\partial p_{k1}}{\partial \tau_1} \right)^2 \right] &= 2\omega_k^2 \left(\frac{\tilde{N}_{k1}}{N_k} \right)^2 (1 - a_{k2})^2 \\ &\quad \left[1 - \frac{a_{k2}^2}{(1 - a_{k2})^2} \cos 2\omega_k \Delta_{12} \right] \end{aligned} \quad (\text{B-14a})$$

$$\begin{aligned} \text{tr} \left[\left(\tilde{Q}_{k2}^{-1} \frac{\partial p_{k2}}{\partial \tau_2} \right)^2 \right] &= 2\omega_k^2 \left(\frac{\tilde{N}_{k2}}{N_k} \right)^2 (1 - a_{k1})^2 \\ &\quad \left[1 - \frac{a_{k2}^2}{(1 - a_{k1})^2} \cos 2\omega_k \Delta_{12} \right] \end{aligned} \quad (\text{B-14b})$$

$$\text{tr} \left(\tilde{Q}_{k1}^{-1} \frac{\partial p_{k1}}{\partial \tau_1} \tilde{Q}_{k2}^{-1} \frac{\partial p_{k2}}{\partial \tau_2} \right) = 2\omega_k^2 \left(\frac{\tilde{N}_{k1}}{N_k} \right)^2 (1 - 2a_{k2}) \cos \omega_k \Delta_{12} \quad (\text{B-14c})$$

where

$$\Delta_{12} \triangleq \tau_1 - \tau_2$$

is the time delay separation.

On the other hand, we have

$$\begin{aligned}
 \tilde{Q}_{k1}^{-1} P_{ki} &= \begin{bmatrix} q_{11}^i & q_{12}^i \\ q_{12}^{i*} & q_{11}^i \end{bmatrix} \begin{bmatrix} 1 & e^{-j\omega_k \tau_i} \\ e^{j\omega_k \tau_i} & 1 \end{bmatrix} \\
 &= \begin{bmatrix} q_{11}^i + q_{12}^i e^{j\omega_k \tau_i} & q_{11}^i e^{-j\omega_k \tau_i} + q_{12}^i \\ q_{12}^{i*} + q_{11}^i e^{j\omega_k \tau_i} & q_{12}^{i*} e^{-j\omega_k \tau_i} + q_{11}^i \end{bmatrix} \\
 &= \begin{bmatrix} B_{11}^i & B_{12}^i \\ B_{12}^i & B_{11}^{i*} \end{bmatrix} . \quad (B-15)
 \end{aligned}$$

Thus combining Equations (B-11) and (B-15) we obtain

$$\begin{aligned}
 \text{tr}\left(\tilde{Q}_{ki}^{-1} P_{ki} \tilde{Q}_{ki}^{-1} \frac{\partial P_{kj}}{\partial \tau_j}\right) &= j\omega_k \text{tr} \left\{ \begin{bmatrix} B_{11}^i & B_{12}^i \\ B_{12}^{i*} & B_{11}^{i*} \end{bmatrix} \right. \\
 &\quad \left. \begin{bmatrix} q_{12}^i e^{j\omega_k \tau_j} - q_{11}^i e^{-j\omega_k \tau_j} \\ q_{11}^i e^{j\omega_k \tau_j} - q_{12}^{i*} e^{-j\omega_k \tau_j} \end{bmatrix} \right\} \\
 &= j\omega_k \left[(B_{11}^i q_{12}^i + B_{12}^i q_{11}^i) e^{j\omega_k \tau_j} \right. \\
 &\quad \left. - (B_{12}^{i*} q_{11}^i + B_{11}^{i*} q_{12}^i) e^{-j\omega_k \tau_j} \right] \\
 &= j\omega_k [C_{ij} - C_{ij}^*] \\
 &= -2\omega_k \text{Im}\{C_{ij}\} \tag{B-16}
 \end{aligned}$$

where

$$\begin{aligned}
 C_{ij} &\triangleq (B_{11}^i q_{12}^i + B_{12}^i q_{11}^i) e^{j\omega_k \tau_j} \\
 &= (q_{11}^i)^2 e^{-j\omega_k \Delta_{ij}} + (q_{12}^i)^2 e^{j\omega_k \sigma_{ij}} + 2 q_{11}^i q_{12}^i e^{j\omega_k \tau_j}, \tag{B-17}
 \end{aligned}$$

$\text{Im} \{ \}$ denotes the imaginary part,

$$\text{and } \Delta_{ij} \triangleq \tau_i - \tau_j ; \quad \sigma_{ij} \triangleq \tau_i + \tau_j .$$

Now from Equations (B-7) and (B-8), the following are obtained:

$$c_{11} = \left(\frac{\tilde{N}_{k1}}{N_k} \right)^2 (1 - a_{k2})^2 \left(1 - \frac{a_{k2}}{1 - a_{k2}} e^{j\omega_k \Delta_{12}} \right)^2 \quad (\text{B-18a})$$

$$c_{22} = \left(\frac{\tilde{N}_{k2}}{N_k} \right)^2 (1 - a_{k1})^2 \left(1 - \frac{a_{k1}}{1 - a_{k1}} e^{j\omega_k \Delta_{21}} \right)^2 \quad (\text{B-18b})$$

and

$$c_{12} = \left(\frac{\tilde{N}_{k1}}{N_k} \right)^2 (1 - a_{k2})^2 \left(1 - \frac{a_{k2}}{1 - a_{k2}} e^{j\omega_k \Delta_{12}} \right)^2 e^{-j\omega_k \Delta_{12}}. \quad (\text{B-18c})$$

Now substituting Equations (B-18a-c) into (B-16) yields

$$\text{tr} \left(\tilde{Q}_{k1}^{-1} P_{k1} \tilde{Q}_{k1}^{-1} \frac{\partial P_{k1}}{\partial \tau_1} \right) = 2\omega_k \left(\frac{\tilde{N}_{k1}}{N_k} \right)^2 a_{k2} (1 - a_{k2})$$

$$\left(2 \sin \omega_k \Delta_{12} - \frac{a_{k2}}{1 - a_{k2}} \sin 2\omega_k \Delta_{12} \right)$$

(B-19a)

$$\text{tr} \left(\tilde{Q}_{k2}^{-1} P_{k2} \tilde{Q}_{k2}^{-1} \frac{\partial P_{k2}}{\partial \tau_2} \right) = 2\omega_k \left(\frac{\tilde{N}_{k2}}{N_k} \right)^2 a_{k1} (1 - a_{k1})$$

$$\left(2 \sin \omega_k \Delta_{12} - \frac{a_{k2}}{1 - a_{k2}} \sin 2\omega_k \Delta_{12} \right)$$

(B-19b)

and

$$\text{tr} \left(\tilde{Q}_{k1}^{-1} P_{k1} \tilde{Q}_{k1}^{-1} \frac{\partial P_{k1}}{\partial \tau_2} \right) = 2\omega_k \left(\frac{\tilde{N}_{k1}}{N_k} \right)^2 (1 - 2a_{k2}) 2 \sin \omega_k \Delta_{12} . \quad (\text{B-19c})$$

In addition, from Equations (3.5.1-5b) and (B-11), we have

$$\begin{aligned} \frac{\partial G_{ki}}{\partial \tau_i} &= \text{tr} \left(\tilde{Q}_{ki}^{-1} \frac{\partial P_{ki}}{\partial \tau_i} \right) \\ &= j\omega_k \left(q_{12}^i e^{j\omega_k \tau_i} - q_{12}^{i*} e^{-j\omega_k \tau_i} \right) \end{aligned} \quad (\text{B-20})$$

and for $i = 1$

$$\frac{\partial G_{k1}}{\partial \tau_1} = 2\omega_k a_{k2} \left(\frac{\tilde{N}_{k1}}{N_k} \right) \sin \omega_k \Delta_{12} . \quad (\text{B-21})$$

Finally, substituting Equations (B-14a-c), (B-18a-c) and (B-19a-c) into (B-6) we find:

$$\begin{aligned} \text{tr}\left(-\frac{\partial R_k^{-1}}{\partial \tau_1} \frac{\partial R_k}{\partial \tau_1}\right) &= S_{k1} |h_{k1}|^2 \left\{ \text{tr} \left[\left(\tilde{Q}_{k1}^{-1} \frac{\partial P_{k1}}{\partial \tau_1} \right)^2 \right] \right. \\ &\quad \left. - \tilde{a}_{k1} \frac{\partial G_{k1}}{\partial \tau_1} \text{tr} \left(\tilde{Q}_{k1}^{-1} P_{k1} \tilde{Q}_{k1}^{-1} \frac{\partial P_{k1}}{\partial \tau_1} \right) \right\} \\ &= 2\omega_k^2 S_{k1} |h_{k1}|^2 \left(\frac{\tilde{N}_{k1}}{N_k} \right)^2 (1 - a_{k2})^2 \gamma_1 \end{aligned} \quad (\text{B-22a})$$

where

$$\begin{aligned} \gamma_1 = \left\{ 1 - E_1 \cos 2\omega_k \Delta_{12} - E_2 \sin^2 \omega_k \Delta_{12} \right. \\ \left. + E_3 (\sin \omega_k \Delta_{12}) (\sin 2\omega_k \Delta_{12}) \right\} \end{aligned} \quad (\text{B-22b})$$

with

$$E_1 = \frac{a_{k2}^2}{(1 - a_{k2})^2} \quad (\text{B-22c})$$

$$E_2 = 4 \tilde{a}_{k1} (1 - a_{k2}) \left(\frac{\tilde{N}_{k1}}{N_k} \right) E_1 \quad (\text{B-22d})$$

$$E_3 = \frac{2 \tilde{a}_{k1} a_{k2}^3}{(1 - a_{k2})^2} \left(\frac{\tilde{N}_{k1}}{N_k} \right). \quad (\text{B-22e})$$

Similarly, we have

$$\text{tr} \left(-\frac{\partial R_k^{-1}}{\partial \tau_2} \frac{\partial R_k}{\partial \tau_2} \right) = 2\omega_k^2 s_{k2} |h_{k2}|^2 \left(\frac{\tilde{N}_{k2}}{N_k} \right) (1 - a_{k1})^2 \gamma_2 \quad (\text{B-23})$$

where γ_2 is obtained by exchanging indices between 1 and 2 from γ_1 . Finally, the cross term is

$$\begin{aligned} \text{tr} \left(-\frac{\partial R_k^{-1}}{\partial \tau_1} \frac{\partial R_k}{\partial \tau_2} \right) &= s_{k2} |h_{k1}|^2 \left\{ \text{tr} \left(\tilde{Q}_{k1}^{-1} \frac{\partial P_{k1}}{\partial \tau_1} \tilde{Q}_{k1}^{-1} \frac{\partial P_{k2}}{\partial \tau_2} \right) \right. \\ &\quad \left. - \tilde{a}_{k1} \frac{\partial G_{k1}}{\partial \tau_1} \text{tr} \left(\tilde{Q}_{k1}^{-1} P_{k1} \tilde{Q}_{k1}^{-1} \frac{\partial P_{k2}}{\partial \tau_2} \right) \right\} \\ &= 2\omega_k^2 s_{k2} |h_{k1}|^2 (1 - 2 a_{k2}) \left(\frac{\tilde{N}_{k1}}{N_k} \right)^2 \gamma_{12} \quad (\text{B-24a}) \end{aligned}$$

where

$$\gamma_{12} = \cos \omega_k \Delta_{12} - 2 \tilde{a}_{k1} a_{k2} \left(\frac{\tilde{N}_{k1}}{N_k} \right) \sin^2 \omega_k \Delta_{12}. \quad (\text{B-24b})$$

Thus, the elements of the Fisher's Information matrix are:

$$J_{11} = 2 \sum_{k=1}^B \omega_k^2 s_{k1} |h_{k1}|^2 \left(\frac{\tilde{N}_{k1}}{N_k} \right)^2 (1 - a_{k2})^2 \gamma_1 \quad (\text{B-25a})$$

$$J_{12} = 2 \sum_{k=1}^B \omega_k^2 s_{k2} |h_{k1}|^2 \left(\frac{\tilde{N}_{k1}}{N_k} \right)^2 (1 - 2a_{k2}) \gamma_{12} \quad (B-25b)$$

$$J_{22} = 2 \sum_{k=1}^B \omega_k^2 s_{k2} |h_{k2}|^2 \left(\frac{\tilde{N}_{k2}}{N_k} \right)^2 (1 - a_{k1})^2 \gamma_2. \quad (B-25c)$$

Using the definition of $|h_{ki}|^2$, N_{ki} and a_{ki} in Equations (3.5.1-4b), (3.5.1-2c), (B-8), and (B-10), Equations (B-25a-c) can be expressed in integral form for a sufficiently long observation time T as follows:

$$J_{11} = \frac{T}{\pi} \int_0^\infty \omega^2 \left(\frac{s_1^2/N^2}{1 + G_1 s_1/(s_2 + N)} \right) \left(\frac{1 + s_2/N}{1 + 2 s_2/N} \right)^2 \gamma_1 d\omega \quad (B-26a)$$

$$J_{12} = \frac{T}{\pi} \int_0^\infty \omega^2 \left(\frac{s_1 s_2/N^2}{1 + G_1 s_1/(s_2 + N)} \right) \left(\frac{1}{1 + 2 s_2/N} \right) \gamma_{12} d\omega \quad (B-26b)$$

and

$$J_{22} = \frac{T}{\pi} \int_0^\infty \omega^2 \left(\frac{s_2^2/N^2}{1 + G_2 s_2/(s_1 + N)} \right) \left(\frac{1 + s_1/N}{1 + 2 s_1/N} \right)^2 \gamma_2 d\omega. \quad (B-26c)$$

where

$$G_1 = (1 + s_2/N) \left[2 - \left(\frac{s_2/N}{1 + 2 s_2/N} \right) |1 + e^{-j\omega\Delta_{12}}|^2 \right] \quad (B-26d)$$

$$G_2 = (1 + S_1/N) \left[2 - \left(\frac{S_1/N}{1 + 2 S_1/N} \right) |1 + e^{j\omega\Delta_{12}}|^2 \right] \quad (B-26e)$$

A somewhat simpler expression for γ_1 , γ_{12} , and γ_2 can be obtained as follows. From Equation (B-22a-e) we obtain

$$\epsilon_1 = \frac{a_{k2}^2}{(1 - a_{k2})^2} = \frac{\left(\frac{S_2/N}{1 + 2 S_2/N} \right)^2}{\left(\frac{1 + S_2/N}{1 + 2 S_2/N} \right)^2} = \left(\frac{S_2/N}{1 + S_2/N} \right)^2 \quad (B-27a)$$

$$\epsilon_2 = 4 \tilde{a}_{k1} (1 - a_{k2}) \left(\frac{\tilde{N}_{k1}}{N_k} \right) \epsilon_1 = w_1 \epsilon_1 \quad (B-27b)$$

where

$$w_1 = 4 \left[\frac{S_1/N}{1 + G_1 S_1/(S_2 + N)} \right] \left[\frac{1 + S_2/N}{1 + 2 S_2/N} \right] \quad (B-27c)$$

and

$$\epsilon_3 = \frac{2 \tilde{a}_{k1} a_{k2}^3}{(1 - a_{k2})^2} \left(\frac{\tilde{N}_{k1}}{N_k} \right) = 2 \tilde{a}_{k1} a_{k2} \left(\frac{\tilde{N}_{k1}}{N_k} \right) \epsilon_1 = w_2 \epsilon_1 \quad (B-27d)$$

where

$$w_2 = 2 \left[\frac{S_1/N}{1 + G_1 S_1/(S_2 + N)} \right] \left[\frac{S_2/N}{1 + 2 S_2/N} \right]. \quad (B-27e)$$

Hence Equation (B-22b) can be written as

$$\begin{aligned}\gamma_1 &= 1 - E_1 \left(\cos 2\omega_k \Delta_{12} + w_1 \sin^2 \omega_k \Delta_{12} - w_2 \sin \omega_k \Delta_{12} \sin 2\omega_k \Delta_{12} \right) \\ &= 1 - E_1 \sum_{n=0}^3 A_n \cos^n \omega_k \Delta_{12}\end{aligned}\quad (\text{B-28a})$$

where

$$A_0 = 4 \left[\frac{S_1/N}{1 + G_1 S_1/(S_2 + N)} \right] \left[\frac{1 + S_2/N}{1 + 2 S_2/N} \right] - 1 \quad (\text{B-28b})$$

$$A_1 = -4 \left[\frac{S_1/N}{1 + G_1 S_1/(S_2 + N)} \right] \left[\frac{S_2/N}{1 + 2 S_2/N} \right]$$

$$A_2 = 1 - A_0$$

$$A_3 = -A_1 .$$

Similarly, one obtains

$$\gamma_2 = 1 - E_2 \sum_{n=0}^3 B_n \cos^n \omega_k \Delta_{12} \quad (\text{B-28c})$$

where

$$B_0 = 4 \left[\frac{S_2/N}{1 + G_2 S_2/(S_1 + N)} \right] \left[\frac{1 + S_1/N}{1 + 2 S_1/N} \right] - 1 \quad (B-28d)$$

$$B_1 = -4 \left[\frac{S_2/N}{1 + G_2 S_2/(S_1 + N)} \right] \left[\frac{S_1/N}{1 + 2 S_1/N} \right]$$

$$B_2 = 1 - B_0$$

$$B_3 = -B_1$$

Finally, from Equation (B-24b)

$$\gamma_{12} = \cos \omega_k \Delta_{12} - 2 \left[\frac{S_1/N}{1 + G_1 S_1/(S_2 + N)} \right] \left[\frac{S_2/N}{1 + 2 S_2/N} \right] \sin^2 \omega_k \Delta_{12}. \quad (B-28e)$$

APPENDIX C

CRAMER-RAO LOWER BOUND OF TIME DELAY ESTIMATION FROM MULTISENSOR ARRAY

In general, the Cramer-Rao Lower Bound (CRLB) is given by

$$\text{VAR}(\hat{\theta}_i) \geq [J^{-1}]_{ii} \quad (C-1)$$

where J is the Fisher Information matrix whose ij element is defined by (Equation (3.4-5)).

$$J_{ij} = \sum_{k=1}^B \text{tr} \left(-\frac{\partial R_k^{-1}}{\partial \theta_i} \frac{\partial R_k}{\partial \theta_j} \right). \quad (C-2)$$

Under the assumptions of (1) single target, (2) spatially incoherent noise processes and (3) identical sensor array noise power spectrum, the CRLB can be evaluated easily.

From Equations (3.5.1-2) and (3.5.1-4) we obtain

$$R_k = S_k P_k + N_k Q_k, \quad (C-3)$$

where $N_k Q_k = N_k I$ using assumptions (2) and (3), and the relation

$$-\frac{\partial R_k^{-1}}{\partial \theta_i} = |h_k|^2 \frac{\partial P_k}{\partial \theta_i}, \quad (C-4)$$

where

$$|h_k|^2 = \frac{S_k/N_k^2}{1 + M S_k/N_k} \quad (C-5)$$

and M is the number of available sensors.

From Equations (3.5.1-10b) one obtains

$$\frac{\partial P_k}{\partial \theta_i} = j\omega_k V_k \frac{\partial \Phi}{\partial \theta_i} V_k^* \quad (C-6)$$

where V_k , the steering matrix, is given by

$$V_k = \text{diag} \left\{ e^{j\omega_k D_1}, e^{j\omega_k D_2}, \dots, e^{j\omega_k D_M} \right\} \quad (C-7)$$

and the mn element of the matrix $\frac{\partial \Phi}{\partial \theta_i}$ is

$$\left(\frac{\partial \Phi}{\partial \theta_i} \right)_{mn} = \frac{\partial}{\partial \theta_i} (D_m - D_n) . \quad (C-8)$$

Now since

$$\frac{\partial R_k}{\partial \theta_j} = S_k \frac{\partial P_k}{\partial \theta_j} \quad (C-9)$$

from Equation (C-3) and using Equation (C-4) in Equation (C-2), one obtains the expression

$$\begin{aligned} \text{tr} \left(-\frac{\partial R_k^{-1}}{\partial \theta_i} \frac{\partial R_k}{\partial \theta_j} \right) &= S_k |h_k|^2 \text{tr} \left(\frac{\partial P_k}{\partial \theta_i} \frac{\partial P_k}{\partial \theta_j} \right) \\ &= -S_k |h_k|^2 \omega_k^2 \text{tr} \left(v_k \frac{\partial \Phi}{\partial \theta_i} v_k^* v_k \frac{\partial \Phi}{\partial \theta_j} v_k^* \right). \quad (\text{C-10}) \end{aligned}$$

Now using the relation $v_k^* v_k = I$ and $\text{tr}(AB) = \text{tr}(BA)$, Equation (C-10) becomes

$$\text{tr} \left(-\frac{\partial R_k^{-1}}{\partial \theta_i} \frac{\partial R_k}{\partial \theta_j} \right) = -S_k |h_k|^2 \omega_k^2 \text{tr} \left(\frac{\partial \Phi}{\partial \theta_i} \frac{\partial \Phi}{\partial \theta_j} \right). \quad (\text{C-11})$$

Therefore

$$\begin{aligned} J_{ij} &= -\sum_{k=1}^B S_k |h_k|^2 \omega_k^2 \text{tr} \left(\frac{\partial \Phi}{\partial \theta_i} \frac{\partial \Phi}{\partial \theta_j} \right) \\ &= -\text{tr} \left(\frac{\partial \Phi}{\partial \theta_i} \frac{\partial \Phi}{\partial \theta_j} \right) \sum_{k=1}^B \omega_k^2 \frac{S_k^2 / N_k^2}{I + M S_k / N_k}. \quad (\text{C-12}) \end{aligned}$$

Knowing J_{ij} 's for all i and j , Equation (C-1) can be used to calculate the CRLB. Using Equations (C-1) and (C-12), we shall establish the following relation.

Given M sensors under a single target, spatially incoherent and spectrally identically distributed noise environment, the CRLB for the incremental time delay are identical and equal to

$$\text{VAR}(\hat{\tau}_i) \geq \left[M \sum_{k=1}^B \omega_k^2 \left(\frac{s_k^2/n_k^2}{1 + M s_k^2/n_k^2} \right) \right]^{-1} ; \quad i = 1, 2, \dots, M-1 . \quad (\text{C-13a})$$

Furthermore, denote the time delay between any two sensors by D, then

$$\text{VAR}(\hat{D}_{ML}) = \text{VAR}(\hat{\tau}_i) \text{ for all } i. \quad (\text{C-13b})$$

Thus, Equation (C-13a) implies that under optimal signal processing, the time delay estimation between any two sensors improves when the number of sensors is increased.

We shall establish Equations (C-13a) and (C-13b) through the following intermediate steps:

- (1) Let τ_i, τ_j be any two elements of the incremental time delay vector, then

$$\text{tr} \left(\frac{\partial \Phi}{\partial \tau_i} \frac{\partial \Phi}{\partial \tau_j} \right) = \begin{cases} -2 i (M-j) & ; j \geq i \\ -2 j (M-i) & ; i \geq j \end{cases} . \quad (\text{C-14})$$

(2)

$$\begin{aligned} \text{VAR}(\hat{\tau}_i) &\geq [J^{-1}]_{ii} \\ &\geq \left[M \sum_{k=1}^B \omega_k^2 \left(\frac{s_k^2/n_k^2}{1 + M s_k^2/n_k} \right) \right]^{-1} \\ &\quad ; \text{ for } i = 1, 2, \dots, M-1 . \end{aligned}$$

(C-15)

(3) Define $D_{mn} = D_m - D_n$, and $t_i = D_{i+1} - D_i$; then

$$\text{VAR}(\hat{D}_{mn}) = \text{VAR}(\hat{\tau}_i) \text{ for all } m, n, \text{ and } i. \quad (\text{C-16})$$

From Equation (C-8), the mn element of the matrix Φ is given by

$$\Phi^{mn} = \{D_{mn}\} . \quad (\text{C-17})$$

Therefore, the matrix Φ can be written as

$$\Phi = \begin{bmatrix} 0 & -\tau_1 & -(\tau_1 + \tau_2) & \dots & \dots & \dots & -\sum_{i=1}^{M-1} \tau_i \\ \tau_1 & 0 & -\tau_2 & \dots & \dots & \dots & -\sum_{i=1}^{M-2} \tau_i \\ (\tau_1 + \tau_2) & -\tau_2 & 0 & \dots & \dots & \dots & \dots \\ \dots & \dots & \dots & \dots & \dots & \dots & \dots \\ \dots & \dots & \dots & \dots & \dots & \dots & \dots \\ \dots & \dots & \dots & \dots & \dots & \dots & -\tau_{M-1} \\ \sum_{i=1}^{M-1} \tau_i & \sum_{i=1}^{M-2} \tau_i & \dots & \dots & \dots & \tau_{M-1} & 0 \end{bmatrix}.$$

(C-18)

Note that Φ is a skew symmetric matrix (i.e., $\Phi = -\Phi^T$); all elements in the main diagonal are zeros; the incremental time delays occupy the first diagonal; and that any elements above the first diagonal can be obtained by summing the elements to the left and below.

Now it can be verified that

$$\frac{\partial \Phi}{\partial \tau_i} = \begin{bmatrix} 0_{ixi} & | & -1_{ix(M-i)} \\ \hline 1_{(M-i)xi} & | & 0_{(M-i)x(M-i)} \end{bmatrix} \quad (C-19)$$

where 0_{ixi} denotes an $i \times i$ matrix of 0's and $1_{(M-i)xi}$ denotes an $(M-i) \times i$ matrix of 1's.

Therefore, for $j \geq i$, we have

$$\text{tr} \left(\frac{\partial \Phi}{\partial \tau_i} \frac{\partial \Phi}{\partial \tau_j} \right) = \text{tr} \left\{ \begin{bmatrix} A_{jxj} & | & -B_{jx(M-j)} \\ \hline B^T & | & 0_{(M-j)x(M-j)} \end{bmatrix} \right. \\ \left. \begin{bmatrix} 0_{jxj} & | & -1_{jx(M-j)} \\ \hline 1_{(M-j)xj} & | & 0_{(M-j)x(M-j)} \end{bmatrix} \right\} \quad (C-20a)$$

where

$$A_{jxj} = \begin{bmatrix} 0_{ixi} & | & -1_{ix(j-i)} \\ \hline 1_{(j-1)xi} & | & 0_{(j-i)x(j-i)} \end{bmatrix} \quad (C-20b)$$

$$B_{jx(M-j)} = \begin{bmatrix} -1_{ix(M-j)} \\ \vdots \\ 0_{(j-i)x(M-j)} \end{bmatrix}. \quad (C-20c)$$

Thus, using Equations (C-20b) and (C-20c) in Equation (C-20a) and carrying out the necessary matrix operation, one finds

$$\text{tr} \left(\frac{\partial \Phi}{\partial \tau_i} \frac{\partial \Phi}{\partial \tau_j} \right) = -2i(m-j) \quad ; \quad j \geq i \quad (C-21a)$$

and by symmetry argument, we obtain

$$\text{tr} \left(\frac{\partial \Phi}{\partial \tau_i} \frac{\partial \Phi}{\partial \tau_j} \right) = -2j(m-i) \quad ; \quad i \geq j. \quad (C-21b)$$

This proves Equation (C-14).

Next we want to show Equation (C-15).

Combining Equations (C-2), (C-5), (C-12) and (C-14), we obtain

$$J = \left[2 \sum_{k=1}^B \omega_k^2 \left(\frac{s_k^2/n_k^2}{I + M s_k^2/n_k} \right) \right] A \quad (C-22)$$

where A is a matrix given by

$$A = \begin{bmatrix} (M-1) & (M-2) & \dots & 1 \\ (M-2) & 2(M-2) & \dots & 2 \\ \cdot & \cdot & \cdot & \cdot \\ \cdot & \cdot & \cdot & \cdot \\ \cdot & \cdot & \cdot & \cdot \\ 1 & 2 & \dots & (M-1) \end{bmatrix} = \begin{cases} i(M-j) & ; j \geq i \\ j(M-i) & ; i \geq j \end{cases} . \quad (C-23)$$

Thus the inverse of J is

$$J^{-1} = A^{-1} \left[2 \sum_{k=1}^B \omega_k^2 \left(\frac{s_k^2/n_k^2}{1 + M s_k^2/n_k} \right) \right]^{-1} \quad (C-24a)$$

and therefore the diagonal elements of J^{-1} are

$$[J^{-1}]_{ii} = [A^{-1}]_{ii} \left[2 \sum_{k=1}^B \omega_k^2 \left(\frac{s_k^2/n_k^2}{1 + M s_k^2/n_k} \right) \right]^{-1} ;$$

$i = 1, 2, \dots, M-1 .$

(C-24b)

By inspection, the matrix A^{-1} is given by the $M \times M$ matrix

$$A^{-1} = \frac{1}{M} \begin{bmatrix} 2 & -1 & & & \\ -1 & 2 & -1 & 0 & \\ & -1 & 2 & -1 & \\ & & 0 & -1 & 2 \end{bmatrix} \quad (C-25a)$$

or the ij element is given by

$$A_{ij}^{-1} = \begin{cases} \frac{2}{M}; & i = j \\ -\frac{1}{M}; & |i-j| = 1 \\ 0; & |i-j| > 1 \end{cases} \quad (C-25b)$$

This can be verified by a direct multiplication to show that $A^{-1}A = I$. Therefore, using Equation (C-25b) in Equations (C-24b) and (C-15) yields the desired result:

$$\begin{aligned} \text{VAR}(\hat{\epsilon}_i) &\geq [J^{-1}]_{ii} \\ &\geq \left[M \sum_{k=1}^B \omega_k^2 \left(\frac{s_k^2/N_k^2}{1 + M s_k^2/N_k} \right) \right]^{-1}. \end{aligned} \quad (C-26)$$

This proves Equation (C-15).

It is easy to see that

$$\text{COV}(\hat{\tau}_i, \hat{\tau}_j) = \begin{cases} -\text{VAR}(\hat{\tau}_i)/2 & ; \text{ if } |i-j| = 1 \\ 0 & ; \text{ if } |i-j| > 1 \end{cases} . \quad (\text{C-27})$$

Finally writing

$$D_{mn} = \sum_{i=n}^{m-1} \tau_i \quad (\text{C-28})$$

as the time delay between sensors n and m , the maximum likelihood estimation (MLE) of D_{mn} is linearly related to the MLE of τ_i . Hence, the variance of \hat{D}_{mn} is given by

$$\text{VAR}(\hat{D}_{mn}) = \sum_{i=n}^{m-1} \sum_{j=n}^{m-1} E[\hat{\tau}_i \hat{\tau}_j] . \quad (\text{C-29})$$

Using Equations (C-26) and (C-27) in (C-19) yields

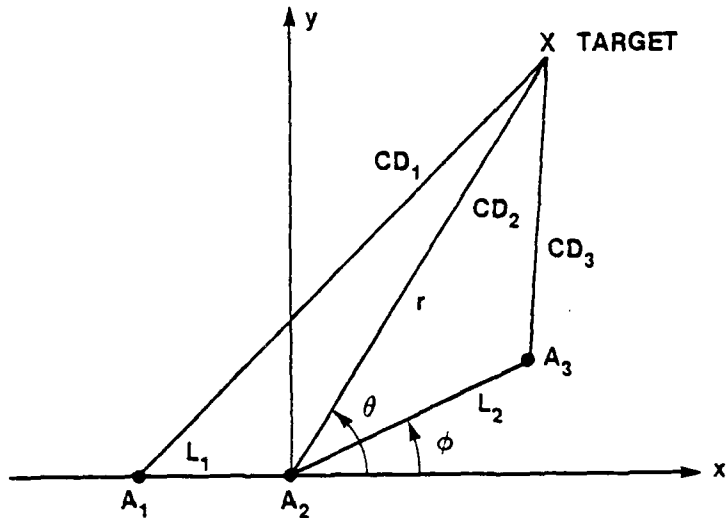
$$\begin{aligned} \text{VAR}(\hat{D}_{mn}) &= (m-n) \text{VAR}(\hat{\tau}_i) - (m-n-1) \text{VAR}(\hat{\tau}_i) \\ &= \text{VAR}(\hat{\tau}_i) . \end{aligned} \quad (\text{C-30})$$

Thus the optimum MLE of time delay between any two sensors yields the same Cramer-Rao Lower Bound.

APPENDIX D
FUNCTIONAL RELATIONSHIPS BETWEEN TARGET LOCATION VECTOR AND
MEASURED TIME DELAY VECTOR

This appendix develops the two-dimensional mathematical relationships between target location parameters and time delay parameters of a general three-sensor array.

Figure D-1 shows the general array and target geometry. In principle, measurement of time delays between sensors A_1 , A_2 and A_2 , A_3 provides the necessary set of relations to obtain target range and bearing. Using the Law of Cosine, these relationships can be obtained as



018.953

Figure D-1. A General Three-Sensor Passive Ranging Array System

$$\tau_1 = D_2 - D_1$$

$$= \frac{r - \sqrt{r^2 + L_1^2 + 2rL_1 \cos \theta}}{c} \quad (D-1a)$$

and

$$\begin{aligned} \tau_2 &= D_3 - D_2 \\ &= \frac{\sqrt{r^2 + L_2^2 - 2rL_2 \cos(\theta - \phi)} - r}{c} \end{aligned} \quad (D-1b)$$

where D_i , $i = 1, 2$ and 3 are the propagation time delays and ϕ is the offset angle of one sensor with respect to the baseline formed by the remaining two sensors.

For the case where $r \gg L_1$, and $r \gg L_2$, Equations (D-1a) and (D-1b) become

$$\begin{aligned} \tau_1 &= \frac{r}{c} \left\{ 1 - \left[1 + \left(\frac{L_1}{r} \right)^2 + 2 \left(\frac{L_1}{r} \right) \cos \theta \right]^{1/2} \right\} \\ &\approx \frac{r}{c} \left\{ 1 - \left[1 + \frac{1}{2} \left(\frac{L_1}{r} \right)^2 + \left(\frac{L_1}{r} \right) \cos \theta - \frac{1}{2} \left(\frac{L_1}{r} \right)^2 \cos^2 \theta \right] \right\} \\ &\approx -\frac{L_1}{c} \cos \theta - \frac{L_1^2 \sin^2 \theta}{2rc} \end{aligned} \quad (D-2a)$$

and similarly

$$\tau_2 \approx -\frac{L_2}{c} \cos \theta + \frac{L_2^2 \sin^2 \theta}{2rc} . \quad (D-2b)$$

However, the exact expressions for the location parameters as a function of time delays can be found using Equations (D-1a) and (D-1b) as follows.

RD-A129 885

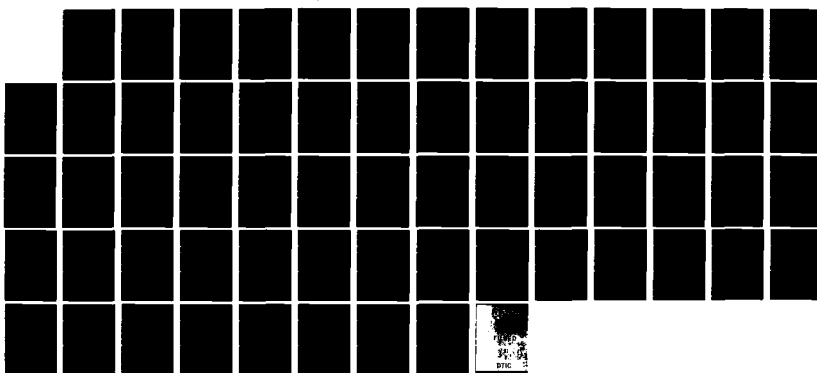
OPTIMUM MULTISENSOR MULTITARGET LOCALIZATION AND
TRACKING(U) NAVAL UNDERWATER SYSTEMS CENTER NEW LONDON
CT NEW LONDON LAB L C NG 07 JUN 83 NUSC-TR-6931

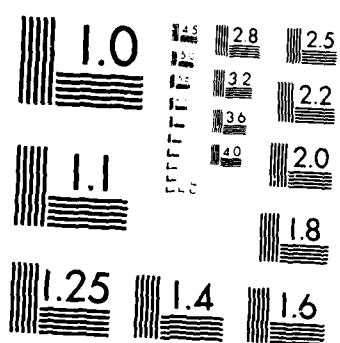
4/4

UNCLASSIFIED

F/G 12/1

NL





MICROCOPY RESOLUTION TEST CHART
NATIONAL BUREAU OF STANDARDS 1963 A

After rearranging, squaring and simplifying, Equations (D-1a) and (D-1b) reduce to

$$\left\{ \begin{array}{l} (c\tau_1)^2 - L_1^2 = 2r(c\tau_1 + L_1 \cos \theta) \end{array} \right. \quad (D-3a)$$

$$\left\{ \begin{array}{l} (c\tau_2)^2 - L_2^2 = -2r(c\tau_2 + L_2 \cos(\theta - \phi)) . \end{array} \right. \quad (D-3b)$$

We first solve for θ , the bearing and then solve for r , the range. Dividing Equations (D-3a) and (D-3b) yields

$$\frac{c\tau_1 + L_1 \cos \theta}{c\tau_2 + L_2 \cos(\theta - \phi)} = - \frac{(c\tau_1)^2 - L_1^2}{(c\tau_2)^2 - L_2^2} = -k \quad (D-4a)$$

so one can write

$$L_1 \cos \theta + KL_2 \cos(\theta - \phi) = -(c\tau_1 + Kc\tau_2) \quad (D-4b)$$

and from which one obtains

$$\theta = \xi + \cos^{-1} \left(- \frac{c\tau_1 + Kc\tau_2}{A} \right) \quad (D-5a)$$

where

$$A \sin \xi = KL_2 \sin \phi$$

$$A \cos \xi = L_1 + KL_2 \cos \phi . \quad (D-5b)$$

Therefore, from Equation (D-5a), one obtains

$$\begin{aligned}\cos \theta &= \cos \left[\xi + \cos^{-1} \left(-\frac{c\tau_1 + Kc\tau_2}{A} \right) \right] \\ &= \frac{(c\tau_1 + Kc\tau_2)(L_1 + KL_2 \cos \phi)}{A^2} \\ &\quad - \frac{\sqrt{A^2 - (c\tau_1 + Kc\tau_2)^2}}{A^2} KL_2 \sin \phi\end{aligned}\tag{D-5c}$$

where

$$\begin{aligned}A^2 &= (L_1 + KL_2 \cos \phi)^2 + (KL_2 \sin \phi)^2 \\ &= (L_1 + KL_2)^2 (1 - \alpha)\end{aligned}\tag{D-5d}$$

where

$$\alpha = \frac{2KL_1 L_2 (1 - \cos \phi)}{(L_1 + KL_2)^2}.\tag{D-5e}$$

Now substituting Equation (D-5c) into (D-3a), one obtains the range solution as

$$\begin{aligned}r &= \frac{(c\tau_1)^2 - L_1^2}{2(c\tau_1 + L_1 \cos \theta)} \\ &= \frac{[(c\tau_1)^2 - L_1^2](L_1 + KL_2)(1 - \alpha)}{2\{c\tau_1(L_1 + KL_2)(1 - \alpha) - L_1(c\tau_1 + Kc\tau_2)(1 - \beta) - \xi\}}\end{aligned}\tag{D-6a}$$

where

$$\xi = \sqrt{1 - \alpha - \gamma^2} KL_1 L_2 \sin \phi$$

where

$$\beta = \frac{KL_2(1 - \cos \phi)}{L_1 + KL_2} \quad (D-6b)$$

$$\gamma = \frac{c\tau_1 + Kc\tau_2}{L_1 + KL_2} \quad . \quad (D-6c)$$

From the relation (D-4a)

$$K = \left(\frac{L_1}{L_2}\right)^2 \frac{1 - \left(\frac{c\tau_1}{L_1}\right)^2}{1 - \left(\frac{c\tau_2}{L_2}\right)^2} \quad (D-6d)$$

Equation (D-6) can be simplified to

$$r = \frac{L_1 \left[1 - \left(\frac{c\tau_1}{L_1}\right)^2 + L_2 \left(1 - \left(\frac{c\tau_2}{L_2}\right)^2 \right) \right]}{2 \left[\left(\frac{c\tau_2}{L_2}\right) - \left(\frac{c\tau_1}{L_1}\right) + \Gamma(\phi) \right]} (1 - \alpha) \quad (D-7a)$$

where

$$\Gamma(\phi) = \frac{c\tau_1}{KL_2} (\alpha - \beta) + \left[\left(\frac{c\tau_1}{L_1}\right) \alpha - \left(\frac{c\tau_2}{L_2}\right) \beta \right] + \sqrt{1 - \alpha - \gamma^2} \sin \phi \quad (D-7b)$$

is a function of the offset angle ϕ .

Now further algebraic manipulation shows that

$$\begin{aligned} \frac{c\tau_1}{KL_2} (\alpha - \beta) &= \frac{c\tau_1}{KL_2} \left[\frac{2KL_1L_2(1 - \cos \phi)}{(L_1 + KL_2)^2} - \frac{KL_2(1 - \cos \phi)}{L_1 + KL_2} \right] \\ &= \left(\frac{L_1 - KL_2}{L_1 + KL_2} \right) (1 - \cos \phi) c\tau_1 \end{aligned} \quad (D-7c)$$

and

$$\begin{aligned} \left(\frac{c\tau_1}{L_1} \right) \alpha - \left(\frac{c\tau_2}{L_2} \right) \beta &= \frac{c\tau_1 2KL_2(1 - \cos \phi)}{(L_1 + KL_2)^2} - \frac{c\tau_2 K(1 - \cos \phi)}{(L_1 + KL_2)} \\ &= \frac{K(1 - \cos \phi)}{(L_1 + KL_2)^2} [2L_2 c\tau_1 - c\tau_2(L_1 + KL_2)] . \end{aligned} \quad (D-7d)$$

Combining Equations (D-7c) and (D-7d) yields

$$\begin{aligned} \left(\frac{c\tau_1}{L_1} \right) (\alpha - \beta) + \left(\frac{c\tau_1}{L_1} \right) \alpha - \left(\frac{c\tau_2}{L_2} \right) \beta \\ &= \frac{1 - \cos \phi}{(L_1 + KL_2)^2} [c\tau_1(L_1 - KL_2) + 2KL_2 c\tau_1 - Kc\tau_2(L_1 + KL_2)] \\ &= \frac{1 - \cos \phi}{(L_1 + KL_2)^2} (L_1 + KL_2) (c\tau_1 - Kc\tau_2) \\ &= \frac{c\tau_1 - Kc\tau_2}{L_1 + KL_2} (1 - \cos \phi) . \end{aligned} \quad (D-7e)$$

Thus Equation (D-7b) becomes

$$\Gamma(\phi) = \frac{c\tau_1 - Kc\tau_2}{L_1 + KL_2} (1 - \cos \phi) + \sqrt{1 - \alpha - \gamma^2} \sin \phi. \quad (D-7f)$$

Note for a colinear array system (i.e., $\phi = 0$), we have $\alpha = 0$, $\Gamma(0) = 0$, and the range and bearing equations are given by

$$r = \frac{L_1 \left[1 - \left(\frac{c\tau_1}{L_1} \right)^2 \right] + L_2 \left[1 - \left(\frac{c\tau_2}{L_2} \right)^2 \right]}{2 \left[\left(\frac{c\tau_2}{L_2} \right) - \left(\frac{c\tau_1}{L_1} \right) \right]} \quad (D-8a)$$

and

$$\theta = \cos^{-1} \left(- \frac{c\tau_1 + Kc\tau_2}{L_1 + KL_2} \right). \quad (D-8b)$$

In addition for $L_1 = L_2 = L$ and $r \gg L_1$, using Equations (D-2a) and (D-2b), it can be shown that

$$\theta = \cos^{-1} \left[- \frac{c(\tau_1 + \tau_2)}{2L} \right] \quad (D-9a)$$

$$r = \frac{L^2 \sin^2 \theta}{c(\tau_2 - \tau_1)}. \quad (D-9b)$$

If θ is defined w.r.t. the broadside direction, Equations (D-9a) and (D-9b) can be written as

$$\theta = -\sin^{-1} \left[\frac{c}{2L} (\tau_1 + \tau_2) \right] \quad (D-10a)$$

$$r = \frac{L^2}{c} \frac{\cos^2 \theta}{(\tau_2 - \tau_1)} \quad (D-10b)$$

APPENDIX E

STATISTICAL CORRELATION BETWEEN TIME DELAY ESTIMATES WITH COMMON INPUT CHANNEL

If time delay estimates are obtained from two Generalized Cross-Correlators (GCC) whose inputs contain a common noise channel (Figure E-1), then the resulting time delay estimates are correlated. This appendix calculates the resulting correlation from a frequency domain approach.

Let the frequency domain (Fourier) representation of a T-second observation of waveforms from sensor array A_1 , A_2 , and A_3 with signal propagation delays D_1 , D_2 and D_3 , respectively, be written as:

$$\alpha_{1k} = \beta_k e^{j\omega_k D_1} + n_{1k} \quad . \quad (E-1a)$$

$$\alpha_{2k} = \beta_k e^{j\omega_k D_2} + n_{2k} \quad (E-1b)$$

$$\alpha_{3k} = \beta_k e^{j\omega_k D_3} + n_{3k} ; \quad k = 1, 2, \dots, B \quad (E-1c)$$

with $S_k = E(\beta_k \beta_k^*)$ and $N_{ik} = E(n_{ik} n_{ik}^*)$ for all i as the discrete signal and noise power spectra, respectively, at frequency $\omega_k = 2\pi k/T$. For convenience we assume that interarray noise processes are uncorrelated. The time delay $\tau_1 = D_2 - D_1$ and $\tau_2 = D_3 - D_2$ can be obtained by seeking the null of the GCC functions (Equation (3.5.1-14c)).

$$f_1(\tau_1) = \sum_{k=-B}^B j\omega_k h_{1k}^* h_{2k}^* \alpha_{1k}^* \alpha_{2k}^* e^{j\omega_k \tau_1} \quad (E-2a)$$

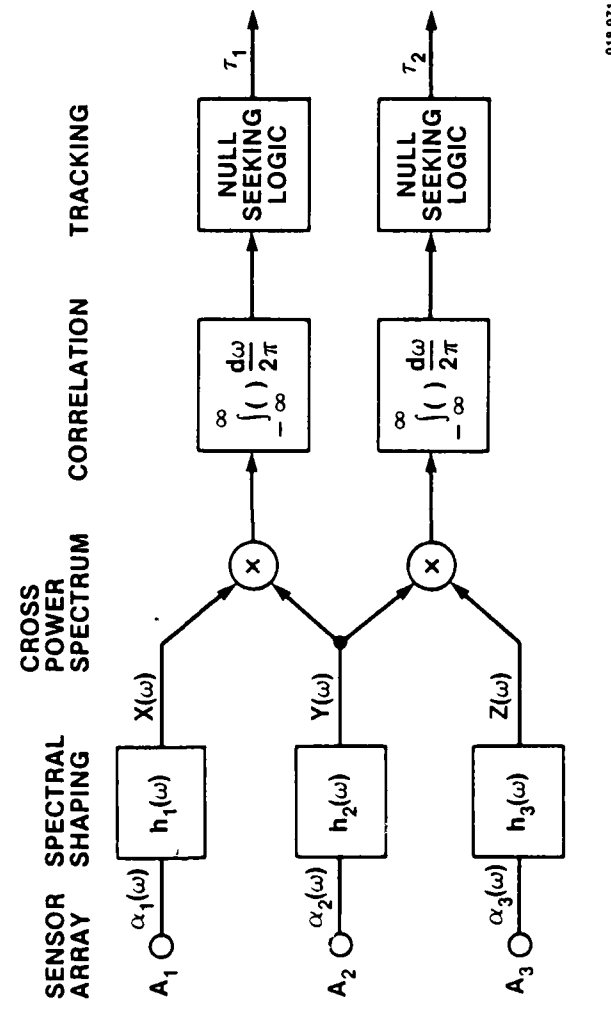


Figure E-1. Generalized Cross Correlator Pair with Common Input Channel

and

$$f_2(\tau_2) = \sum_{k=-B}^B j\omega_k h_{2k}^* h_{3k} \alpha_{2k} \alpha_{3k}^* e^{j\omega_k \tau_2} \quad (E-2b)$$

where B is the uppermost frequency of either the signal or the noise and h_{ik} is the frequency shaping filter whose frequency response is

$$|h_{ik}|^2 = \frac{S_k/N_{ik}^2}{1 + 2 S_k/N_{ik}} . \quad (E-2c)$$

Let $\hat{\tau}_1$ and $\hat{\tau}_2$ be the estimated time delay, then the quantity of interest is the covariance between $\hat{\tau}_1$ and $\hat{\tau}_2$; i.e., $\text{COV}(\hat{\tau}_1, \hat{\tau}_2)$. The Taylor series expansion of $f_1(\tau_1)$ and $f_2(\tau_2)$ about the true time delay τ_1^0 and τ_2^0 yields

$$f_1(\tau_1) = f_1(\tau_1^0) + \left. \frac{\partial f_1(\tau_1)}{\partial \tau_1} \right|_{\tau_1 = \tau_1^0} (\tau_1 - \tau_1^0) + \dots \quad (E-3a)$$

and

$$f_2(\tau_2) = f_2(\tau_2^0) + \left. \frac{\partial f_2(\tau_2)}{\partial \tau_2} \right|_{\tau_2 = \tau_2^0} (\tau_2 - \tau_2^0) + \dots . \quad (E-3b)$$

Neglecting the higher order terms (small error assumption) and setting $f_1(\tau_1) = f_2(\tau_2) = 0$ in Equations (E-3a) and (E-3b), one obtains

$$-f_1(\tau_1^0) = \frac{\partial f_1(\tau_1^0)}{\partial \tau_1} (\tau_1 - \tau_1^0) \quad (E-4a)$$

$$-f_2(\tau_2^0) = \frac{\partial f_2(\tau_2^0)}{\partial \tau_2} (\tau_2 - \tau_2^0) . \quad (E-4b)$$

We shall make the following assumptions as a result of a long observation time process: (1) the expected value of the derivative is equal to the derivative of the expected value, and (2) the derivative is uncorrelated with time delay. Then from Equations (E-4a) and (E-4b), one obtains

$$\overline{-f_1^0} = \overline{\frac{\partial f_1^0}{\partial \tau_1}} \overline{(\tau_1 - \tau_1^0)} \quad (E-5a)$$

$$\overline{-f_2^0} = \overline{\frac{\partial f_2^0}{\partial \tau_2}} \overline{(\tau_2 - \tau_2^0)} \quad (E-5b)$$

where for simplicity we denote the expected values of $f_1(\tau_1^0)$ and $f_2(\tau_2^0)$ by f_1^0 and f_2^0 . Thus, the product of the means is

$$\overline{f_1^0} \overline{f_2^0} = \overline{\frac{\partial f_1^0}{\partial \tau_1}} \overline{\frac{\partial f_2^0}{\partial \tau_2}} \overline{(\tau_1 - \tau_1^0)} \overline{(\tau_2 - \tau_2^0)} . \quad (E-6)$$

On the other hand, the mean of the product is

$$\overline{f_1^0 f_2^0} = \overline{\frac{\partial f_1^0}{\partial \tau_1}} \overline{\frac{\partial f_2^0}{\partial \tau_2}} \overline{(\tau_1 - \tau_1^0)(\tau_2 - \tau_2^0)} . \quad (E-7)$$

Therefore, the covariance is

$$\text{COV}(\hat{\tau}_1, \hat{\tau}_2) = \overline{(\tau_1 - \tau_1^0)(\tau_2 - \tau_2^0)} - \overline{(\tau_1 - \tau_1^0)} \overline{(\tau_2 - \tau_2^0)}$$

$$= \frac{\overline{f_1^0 f_2^0} - \overline{f_1^0} \overline{f_2^0}}{\left(\overline{\frac{\partial f_1^0}{\partial \tau_1}} \overline{\frac{\partial f_2^0}{\partial \tau_2}} \right)} . \quad (E-8)$$

From Equations (E-2a) and (E-2b), the quantities in Equation (E-8) can be evaluated as follows.

$$\overline{\frac{\partial f_1^0}{\partial \tau_1}} = \sum_{k=-B}^B (j\omega_k)^2 h_{1k} h_{2k}^* s_k \quad (E-9a)$$

$$\overline{\frac{\partial f_2^0}{\partial \tau_2}} = \sum_{k=-B}^B (j\omega_k)^2 h_{2k} h_{3k}^* s_k \quad (E-9b)$$

$$\overline{f_1^0} = \sum_{k=-B}^B j\omega_k h_{1k} h_{2k}^* s_k \quad (E-9c)$$

$$\overline{f_2^0} = \sum_{k=-B}^B j\omega_k h_{2k} h_{3k}^* s_k \quad (E-9d)$$

and

$$\begin{aligned} \overline{f_1^0 f_2^0} &= \sum_{k=-B}^B \sum_{l=-B}^B (j\omega_k)(j\omega_l) h_{1k} h_{2k}^* h_{2l} h_{3l}^* \\ &\quad \overline{a_{1k}^* a_{2k}^* a_{2l}^* a_{3l}^*} e^{j(\omega_k \tau_1^0 + \omega_l \tau_2^0)} . \end{aligned} \quad (E-10)$$

But

$$\begin{aligned} \overline{a_{1k}^* a_{2k}^* a_{2l}^* a_{3l}^*} &= \overline{a_{1k}^* a_{2k}^* a_{2l}^* a_{3l}^*} + \overline{a_{1k}^* a_{2l}^* a_{2k}^* a_{3l}^*} \\ &\quad + \overline{a_{1k}^* a_{3l}^* a_{2k}^* a_{2l}^*} \\ &= S_k^2 e^{-j(\omega_k \tau_1^0 + \omega_l \tau_2^0)} + S_k^2 e^{-j\omega_k (\tau_1^0 + \tau_2^0)} \delta_{k+l} \\ &\quad + S_k (S_k + N_{2k}) e^{-j\omega_k (\tau_1^0 + \tau_2^0)} \delta_{k-l} , \end{aligned} \quad (E-11)$$

where $\delta_{k-\ell}$ is the Kronecker delta defined by $\delta_{k-\ell} = 1$ if $k = \ell$; and $\delta_{k-\ell} = 0$ if $k \neq \ell$.

Now substituting Equation (E-11) into Equation (E-10) yields:

$$\begin{aligned}
 \overline{f_1^0 f_2^0} &= \sum_{k=-B}^B \sum_{\ell=-B}^B (j\omega_k) (j\omega_\ell) h_{1k} h_{2k}^* h_{2\ell} h_{3\ell}^* s_k^2 \\
 &\quad + \sum_{k=-B}^B \omega_k^2 h_{1k} h_{3k}^* |h_{2k}|^2 s_k^2 \\
 &\quad - \sum_{k=-B}^B \omega_k^2 h_{1k} h_{3k}^* |h_{2k}|^2 s_k (s_k + n_{2k}) \\
 &= \left(\sum_{k=-B}^B j\omega_k h_{1k} h_{2k}^* s_k \right) \left(\sum_{k=-B}^B j\omega_k h_{2k} h_{3k}^* s_k \right) \\
 &\quad - \sum_{k=-B}^B \omega_k^2 h_{1k} h_{3k}^* |h_{2k}|^2 s_k n_{2k} \\
 &= \overline{f_1^0} \overline{f_2^0} - \sum_{k=-B}^B \omega_k^2 h_{1k} h_{3k}^* |h_{2k}|^2 s_k n_{2k} . \tag{E-12}
 \end{aligned}$$

Finally, using Equations (E-9a) through (E-12) in Equation (E-8) yields

$$\text{COV}(\hat{\tau}_1, \hat{\tau}_2) = \frac{-\sum_{k=-B}^B \omega_k^2 h_{1k} h_{3k}^* |h_{2k}|^2 S_k N_{2k}}{\left(\sum_{k=-B}^B \omega_k^2 h_{1k} h_{2k}^* S_k \right) \left(\sum_{k=-B}^B \omega_k^2 h_{2k} h_{3k}^* S_k \right)} . \quad (\text{E-13})$$

Equation (E-13) can also be expressed in continuous frequency domain as

$$\text{COV}(\hat{\tau}_1, \hat{\tau}_2) = -\frac{2\pi}{T} \frac{\int_0^B \omega^2 h_1(\omega) h_3^*(\omega) |h_2(\omega)|^2 S(\omega) N_2(\omega) d\omega}{\int_0^B \omega^2 h_1 h_2^*(\omega) S(\omega) d\omega \int_0^B \omega^2 h_2(\omega) h_3^*(\omega) S(\omega) d\omega} . \quad (\text{E-14})$$

Note that if either the definition of τ_1 or τ_2 is reversed, the sign in Equation (E-13) and (E-14) is also reversed.

Finally, it can also be shown similarly that the variances of the estimates are given by:

$$\text{VAR}(\hat{\tau}_1) = \frac{\overline{f_1^0}^2 - \overline{f_1^0}^2}{\left(\frac{\partial f_1^0}{\partial \tau_1} \right)^2}$$

$$\begin{aligned}
 &= \frac{\sum_{k=-B}^B \omega_k^2 |h_{1k}|^2 |h_{2k}|^2 [S_k(N_{1k} + N_{2k}) + N_{1k} N_{2k}]}{\left(\sum_{k=-B}^B \omega_k^2 h_{1k} h_{2k}^* S_k \right)^2} \\
 &= \frac{2\pi}{T} \frac{\int_0^B \omega^2 |h_1(\omega)|^2 |h_2(\omega)|^2 [S(N_1 + N_2) + N_1 N_2] d\omega}{\left(\int_0^B \omega^2 h_1(\omega) h_2^*(\omega) S(\omega) d\omega \right)^2} . \quad (\text{E-15})
 \end{aligned}$$

Similarly, one obtains

$$\text{VAR}(\hat{\tau}_2) = \frac{2\pi}{T} \frac{\int_0^B \omega^2 |h_2(\omega)|^2 |h_3(\omega)|^2 [S(N_2 + N_3) + N_2 N_3] d\omega}{\left(\int_0^B \omega^2 h_2(\omega) h_3^*(\omega) S(\omega) d\omega \right)^2} . \quad (\text{E-16})$$

A substantial simplification can be obtained for the case of bandlimited flat signal and noise power spectra.

Let

$$S(\omega) = \begin{cases} S & \text{if } \omega_1 \leq \omega \leq \omega_2 \\ 0 & \text{otherwise} \end{cases}$$

$$N_i(\omega) = \begin{cases} N & \text{if } \omega_1 \leq \omega \leq \omega_2 \text{ and for all } i \\ 0 & \text{otherwise} \end{cases}$$

be the signal and the noise power spectra and assume identical frequency spectral filters for all channels, then the covariance expression of Equation (E-14) reduces to

$$\begin{aligned} \text{COV}(\hat{\tau}_1, \hat{\tau}_2) &= -\frac{2\pi}{T} \left(\frac{S}{N} \int_0^B \omega^2 d\omega \right)^{-1} \\ &= -\frac{2\pi}{T} \left[\left(\frac{2}{3} \right) \left(\frac{S}{N} \right) (\omega_2^3 - \omega_1^3) \right]^{-1} \end{aligned} \quad (\text{E-17})$$

and the variances reduce to

$$\begin{aligned}
 \text{VAR}(\hat{\tau}_1) &= \text{VAR}(\hat{\tau}_2) \\
 &= \frac{2\pi}{T} \left[\frac{(S/N)^2}{1 + 2 S/N} \int_0^B \omega^2 d\omega \right]^{-1} \\
 &= \frac{2\pi}{T} \left[\frac{2 (S/N)^2}{3(1 + 2 S/N)} (\omega_2^3 - \omega_1^3) \right]^{-1} . \tag{E-18}
 \end{aligned}$$

Comparison between Equations (E-18) and (E-17) shows that

$$\text{COV}(\hat{\tau}_1, \hat{\tau}_2) = - \frac{S/N}{1 + 2 S/N} \text{VAR}(\hat{\tau}_1) . \tag{E-19}$$

APPENDIX F
DERIVATION OF EQUATION (3.5.2-7a)

From Equation (3.5.2-7a) we have

$$\frac{\partial \Lambda}{\partial r}(r, \theta) = \sum_{k=1}^B j\omega_k |h_k|^2 v_k^* v_k \frac{\partial \Phi}{\partial r} v_k^* v_k . \quad (F-1)$$

Using the relation

$$\frac{\partial \Phi}{\partial r} = \frac{\partial \Phi}{\partial \tau_1} \frac{\partial \tau_1}{\partial r} + \frac{\partial \Phi}{\partial \tau_2} \frac{\partial \tau_2}{\partial r} \quad (F-2)$$

and Equation (3.5.1-10a-c)

$$\frac{\partial}{\partial \tau_i} (v_k l_M v_k^*) = j\omega_k v_k \frac{\partial \Phi}{\partial \tau_i} v_k^* \quad (F-3)$$

in Equation (F-1) yields

$$\begin{aligned} \frac{\partial \Lambda(r, \theta)}{\partial r} &= \left\{ \sum_{k=1}^B j\omega_k |h_k|^2 v_k^* v_k \frac{\partial \Phi}{\partial \tau_1} v_k^* v_k \right\} \frac{\partial \tau_1}{\partial r} \\ &\quad + \left\{ \sum_{k=1}^B j\omega_k |h_k|^2 v_k^* v_k \frac{\partial \Phi}{\partial \tau_2} v_k^* v_k \right\} \frac{\partial \tau_2}{\partial r} \\ &= \frac{\partial}{\partial \tau_1} \left\{ \sum_{k=1}^B |h_k|^2 v_k^* v_k l_M v_k^* v_k \right\} \frac{\partial \tau_1}{\partial r} \end{aligned}$$

$$+ \frac{\partial}{\partial \tau_2} \left\{ \sum_{k=1}^B |h_k|^2 \alpha_k^* v_k l_M v_k^* \alpha_k \right\} \frac{\partial \tau_2}{\partial r}$$

$$= \frac{\partial}{\partial r} \sum_{k=1}^B |h_k|^2 \alpha_k^* v_k l_M v_k^* \alpha_k . \quad (F-4)$$

But

$$\begin{aligned} v_k l_M v_k^* &= \begin{bmatrix} e^{-j\omega_k \tau_1} & 0 & 0 \\ 0 & 1 & 0 \\ 0 & 0 & e^{-j\omega_k \tau_2} \end{bmatrix} \begin{bmatrix} 1 & 1 & 1 \\ 1 & 1 & 1 \\ 1 & 1 & 1 \end{bmatrix} \begin{bmatrix} e^{j\omega_k \tau_1} & 0 & 0 \\ 0 & 1 & 0 \\ 0 & 0 & e^{j\omega_k \tau_2} \end{bmatrix} \\ &= \begin{bmatrix} 1 & e^{-j\omega_k \tau_1} & e^{-j\omega_k (\tau_1 + \tau_2)} \\ e^{j\omega_k \tau_1} & 1 & e^{-j\omega_k \tau_2} \\ e^{j\omega_k (\tau_1 + \tau_2)} & e^{j\omega_k \tau_2} & 1 \end{bmatrix} \quad (F-5) \end{aligned}$$

and

$$\begin{aligned} \alpha_k^* v_k l_M v_k^* \alpha_k &= \left\{ |\alpha_{1k}|^2 + |\alpha_{2k}|^2 + |\alpha_{3k}|^2 \right\} \\ &\quad + \left\{ (\alpha_{2k}^* \alpha_{1k} e^{j\omega_k \tau_1}) + (\alpha_{2k}^* \alpha_{1k} e^{j\omega_k \tau_1})^* \right\} \end{aligned}$$

$$\begin{aligned}
& + \left\{ (\alpha_{3k}^* \alpha_{2k} e^{j\omega_k \tau_2}) + (\alpha_{3k}^* \alpha_{2k} e^{j\omega_k \tau_2})^* \right\} \\
& + \left\{ (\alpha_{3k}^* \alpha_{1k} e^{j\omega_k (\tau_1 + \tau_2)}) + (\alpha_{3k}^* \alpha_{1k} e^{j\omega_k (\tau_1 + \tau_2)})^* \right\}. \\
\end{aligned} \tag{F-6}$$

Now using the fact that the first term in Equation (F-6) is not parameter-dependent and that quantities in the parentheses are conjugate symmetric, Equation (F-4) can be rewritten as

$$\begin{aligned}
\frac{\partial \Lambda(r, \theta)}{\partial r} &= \frac{\partial}{\partial r} \sum_{k=-B}^B |h_k|^2 \left\{ \alpha_{2k}^* \alpha_{1k} e^{j\omega_k \tau_1} + \alpha_{3k}^* \alpha_{2k} e^{j\omega_k \tau_2} \right. \\
&\quad \left. + \alpha_{3k}^* \alpha_{1k} e^{j\omega_k (\tau_1 + \tau_2)} \right\} \\
&= \frac{T}{2\pi} \frac{\partial}{\partial r} \int_{-\infty}^{\infty} |h(\omega)|^2 G(\omega; \tau_1, \tau_2) d\omega
\end{aligned} \tag{F-7}$$

where

$$\begin{aligned}
G(\omega; \tau_1, \tau_2) &= T \left[(\alpha_{2k}^* \alpha_{1k}) e^{j\omega_k \tau_1} + (\alpha_{3k}^* \alpha_{2k}) e^{j\omega_k \tau_2} \right. \\
&\quad \left. + (\alpha_{3k}^* \alpha_{1k}^*) e^{j\omega_k (\tau_1 + \tau_2)} \right].
\end{aligned} \tag{F-8}$$

APPENDIX G
CALCULATION OF LOCALIZATION UNCERTAINTY FROM THREE-SENSOR ARRAYS

This appendix calculates the localization uncertainty based on a two inter-array time delay measurement.

From Equations (D-10a) and D-10b), the approximate ($r \gg L$) time delays to range and bearing relation are given by

$$\theta = -\sin^{-1} \left\{ \frac{c}{2L} (\tau_1 + \tau_2) \right\} \quad (G-1)$$

$$r = \frac{L^2}{c} \frac{\cos^2 \theta}{(\tau_2 - \tau_1)} \quad (G-2)$$

where c is the speed of sound, and L is the inter-array separation.

Letting $\underline{Y} = (\theta, r)^T$, $\underline{X} = (\tau_1, \tau_2)$, Equations (G-1) and (G-2) can be written as

$$\underline{Y} = \underline{f}(\underline{X}) \quad (G-3)$$

where $\underline{f}(\underline{X}) = (f_1(\underline{X}), f_2(\underline{X}))^T$ is the vector function defined according to Equations (G-1) and (G-2). Let \underline{Y}^* and \underline{X}^* be the nominal values, $\delta\underline{Y}$ and $\delta\underline{X}$ be the deviations from the nominal; then a first-order expansion about the nominal (R, B) yields

$$\delta\underline{Y} = \frac{\partial \underline{f}}{\partial \underline{X}} \delta\underline{X} \quad (G-4)$$

where it is defined that

$$\begin{aligned} \frac{\partial f^*}{\partial \underline{x}} &= \begin{bmatrix} \frac{\partial f_1^*}{\partial \theta} & \frac{\partial f_1^*}{\partial r} \\ \frac{\partial f_2^*}{\partial \theta} & \frac{\partial f_2^*}{\partial r} \end{bmatrix} \\ &= \begin{bmatrix} a & a \\ b & -b \end{bmatrix} \end{aligned} \quad (G-5a)$$

where

$$a = -\frac{c}{2L \cos B} \quad (G-5b)$$

$$b = \frac{R^2 c}{L^2 \cos^2 B} \quad (G-5c)$$

since $R \gg L$.

Now post-multiplying Equation (G-4) by its transpose and taking the expected value yields the desired covariance relations:

$$\text{COV}(\underline{y}) = \left(\frac{\partial f^*}{\partial \underline{x}} \right) \text{COV}(\underline{x}) \left(\frac{\partial f^*}{\partial \underline{x}} \right)^T. \quad (G-6)$$

Let

$$\text{COV}(\underline{x}) = \begin{bmatrix} \sigma_{11}^2 & \sigma_{12}^2 \\ \sigma_{12}^2 & \sigma_{11}^2 \end{bmatrix} \quad (G-7)$$

then

$$\begin{aligned} \text{COV}(\underline{Y}) &= \begin{bmatrix} a & a \\ b & -b \end{bmatrix} \begin{bmatrix} \sigma_{11}^2 & \sigma_{12}^2 \\ \sigma_{12}^2 & \sigma_{11}^2 \end{bmatrix} \begin{bmatrix} a & b \\ a & -b \end{bmatrix} \\ &= \begin{bmatrix} 2(\sigma_{11}^2 + \sigma_{12}^2)a^2 & 0 \\ 0 & 2(\sigma_{11}^2 - \sigma_{12}^2)b^2 \end{bmatrix} \quad (G-8) \end{aligned}$$

and the determinant of $\text{COV}(\underline{Y})$ is

$$|\text{COV}(\underline{Y})| = 4 a^2 b^2 (\sigma_{11}^4 - \sigma_{12}^4) \quad (G-9)$$

The area of the one-sigma error ellipse is

$$\begin{aligned} S &= \pi |\text{COV}(\underline{Y})|^{\frac{1}{2}} \\ &= -2 ab \pi \sqrt{\sigma_{11}^4 - \sigma_{12}^4} \\ &= \frac{\pi (Rc)^2}{L^3 \cos^3 B} \sqrt{\sigma_{11}^4 - \sigma_{12}^4} \quad (G-10) \end{aligned}$$

The time delay covariance matrix for the optimum approach is
(see Equation (3.5.2-16d))

$$P_0 = \begin{bmatrix} 1 & -\frac{1}{2} \\ -\frac{1}{2} & 1 \end{bmatrix} \text{VAR}(\hat{\tau}_1) \quad (G-11)$$

and the conventional is

$$P_c = \begin{bmatrix} 1 & -\frac{S/N}{1+2S/N} \\ -\frac{S/N}{1+2S/N} & 1 \end{bmatrix} \text{VAR}_c(\hat{\tau}_1) . \quad (G-12)$$

Thus the corresponding area is

$$S_0 = \sqrt{\frac{3}{4}} \frac{\pi(Rc)^2}{L^3 \cos^3 B} \text{VAR}(\hat{\tau}) \quad (G-13)$$

and

$$S_c = \frac{\pi(Rc)^2}{L^3 \cos^3 B} \frac{\sqrt{(1 + 3 S/N)(1 + S/N)}}{(1 + 2 S/N)} \text{VAR}_c(\hat{\tau}_1) \quad (G-14)$$

where $\text{VAR}(\hat{\tau}_1)$ and $\text{VAR}_c(\hat{\tau}_1)$ are the estimated time delay variances of the optimum and the conventional processors, respectively.

Finally, from Equations (G-8) and (G-11), the optimum range and bearing variance expressions are given by

$$\begin{aligned} \text{VAR}(\hat{B}) &= 2(\sigma_{11}^2 + \sigma_{12}^2) a^2 \\ &= \frac{1}{4} \left(\frac{c}{L \cos B} \right)^2 \text{VAR}(\hat{\tau}_1) \end{aligned} \quad (\text{G-15})$$

$$\begin{aligned} \text{VAR}(\hat{R}) &= 2(\sigma_{11}^2 - \sigma_{12}^2) b^2 \\ &= 3c^2 \left(\frac{R}{L \cos B} \right)^4 \text{VAR}(\hat{\tau}_1) \end{aligned} \quad (\text{G-16})$$

and from Equations (G-8) and (G-12), the conventional range and bearing variance expressions are:

$$\text{VAR}_C(\hat{B}) = \frac{1}{2} \left(\frac{c}{L \cos B} \right)^2 \left(\frac{1 + S/N}{1 + 2 S/N} \right) \text{VAR}_C(\hat{\tau}_1) \quad (\text{G-17a})$$

$$\text{VAR}_C(\hat{R}) = 2c^2 \left(\frac{R}{L \cos B} \right)^4 \left(\frac{1 + 3 S/N}{1 + 2 S/N} \right) \text{VAR}_C(\hat{\tau}_1). \quad (\text{G-17b})$$

Using the relation given in Equation (3.5.2-16c),

$$\frac{\text{VAR}(\hat{\tau}_1)}{\text{VAR}_C(\hat{\tau}_1)} = \frac{2}{3} \left(\frac{1 + 3 S/N}{1 + 2 S/N} \right),$$

the conventional range and bearing variance equation can also be expressed as:

$$\begin{aligned} \text{VAR}_C(\hat{B}) &= \frac{3}{4} \left(\frac{c}{L \cos B} \right)^2 \left(\frac{1 + S/N}{1 + 3 S/N} \right) \text{VAR}(\hat{\tau}_1) \\ &= 3 \left(\frac{1 + S/N}{1 + 3 S/N} \right) \text{VAR}(\hat{B}) \end{aligned} \quad (\text{G-18})$$

and

$$\text{VAR}_c(\hat{R}) = 3c^2 \left(\frac{R}{L \cos B} \right)^4 \text{VAR}(\hat{\tau}_1)$$
$$= \text{VAR}(R) . \quad (\text{G-19})$$

Equations (G-18) and (G-19) show that for estimating range, the conventional approach and the optimal approach have identical variance. On the other hand for estimating bearing, the conventional yields a variance which is three times the optimum at low SNR environment.

APPENDIX H
GCC STATISTICAL PERFORMANCE IN THE PRESENCE OF INTERFERENCE

This appendix develops the appropriate expressions for the bias and variance of the time delay estimate from a Generalized Cross-Correlator (GCC) in the presence of interference.

Let the frequency domain representation of a T-second observation of waveforms from two-sensor arrays, A_1 and A_2 , in the presence of J targets be written as:

$$a_{1k} = \underline{v}_{1k} \underline{\beta}_k + n_{1k} \quad (H-1a)$$

$$a_{2k} = \underline{v}_{2k} \underline{\beta}_k + n_{2k}; \quad k=1, 2, \dots, B \quad (H-1b)$$

where B is the highest frequency components of the signal or the noise processes; n_{1k} and n_{2k} are the Fourier components of the noise processes at frequency $\omega_k = 2\pi k/T$. In addition, the complex vectors $\underline{\beta}_k$, \underline{v}_{1k} and \underline{v}_{2k} are defined by

$$\underline{v}_{ik} = [e^{j\omega_k D_{i1}}, e^{j\omega_k D_{i2}}, \dots, e^{j\omega_k D_{iJ}}]; i = 1, 2 \quad (H-1c)$$

and

$$\underline{\beta}_k = [\beta_{k1}, \beta_{k2}, \dots, \beta_{kJ}]^T \quad (H-1d)$$

where D_{ij} is the propagation time delay from target j to sensor i and β_{kj} is the Fourier component of the signal spectrum of target j. For convenience, it is assumed that both the signal and noise processes are zero mean and mutually uncorrelated. Thus, we have the relations for the discrete signal and noise power spectra

$$\overline{B_{ki} B_{kj}^*} = \begin{cases} S_{kj}; & \text{if } i = j \\ 0; & \text{if } i \neq j \end{cases} \quad (\text{H-2a})$$

and

$$\overline{n_{ik} n_{jk}^*} = \begin{cases} N_k; & \text{if } i = j \\ 0; & \text{if } i \neq j \end{cases} \quad (\text{H-2b})$$

where $(\bar{\cdot})$ denotes the expected value.

Without loss of generality, let target $j = 1$ be the target of interest, then the best estimate of $\tau_1 = D_{21} - D_{11}$ from a GCC (see Equation (3.5.1-14b)) is to seek the null of the equation:

$$f(\tau) = \sum_{k=-B}^B j\omega_k |h_k|^2 \alpha_{1k} \alpha_{2k}^* e^{j\omega_k \tau} = 0 \quad (\text{H-3a})$$

where $|h_k|^2$, given by

$$|h_k|^2 = \frac{S_{k1}/N_k^2}{1 + 2 S_{k1}/N_k}, \quad (\text{H-3b})$$

is the optimum spectral shaping filter for a single target environment. Because of the observation noise, Equation (H-3) is a stochastic algebraic equation. On average, however, the mean of the estimate must satisfy the equation

$$\bar{f}(\tau) = \sum_{k=-B}^B j\omega_k |h_k|^2 \overline{\alpha_{1k} \alpha_{2k}^*} e^{j\omega_k \tau} = 0. \quad (\text{H-4a})$$

But from Equations (H-1a) and (H-1b), one obtains

$$\begin{aligned} \overline{\alpha_{1k} \alpha_{2k}^*} &= \underline{v}_{1k} \tilde{S}_k \underline{v}_{2k}^* \\ &= \sum_{j=1}^J S_{kj} e^{-j\omega_k \tau_j} \end{aligned} \quad (\text{H-4b})$$

where

$$\tau_j = D_{2j} - D_{1j} \quad (\text{H-4c})$$

is the actual time delay difference between sensor array A_1 and A_2 of target j and

$$\begin{aligned} \tilde{S}_k &= \overline{\underline{B}_k \underline{B}_k^*} \\ &= \text{diag}\{S_{k1}, S_{k2}, \dots, S_{kJ}\} \end{aligned} \quad (\text{H-4d})$$

is a diagonal signal spectral matrix. Therefore, the mean estimate must satisfy the equation

$$\overline{f(\tau)} = \sum_{k=-B}^B j\omega_k |h_k|^2 \underline{v}_{1k} \tilde{S}_k \underline{v}_{2k}^* e^{j\omega_k \tau} = 0 \quad (\text{H-5a})$$

or using Equation (H-4b), we have

$$\overline{f(\tau)} = \sum_{j=1}^J \sum_{k=-B}^B j\omega_k |h_k|^2 S_{kj} e^{j\omega_k (\tau - \tau_j)} = 0. \quad (\text{H-5b})$$

Equation (H-5b) can be manipulated to yield

$$\bar{f}(\tau) = \frac{\partial}{\partial \tau} \sum_{j=1}^J R_j(\tau - \tau_j) = 0 \quad (H-5c)$$

where

$$R_j(\tau) \triangleq \sum_{k=-B}^B |h_k|^2 s_{kj} e^{j\omega_k \tau} \quad (H-5d)$$

is the auto-correlation of target j .

Denoting the total power for target j by

$$P_j = \sum_{k=-B}^B S_{kj}, \quad (H-6a)$$

the total received power by the sensor array as

$$P = \sum_{j=1}^J P_j + N; \quad N = \sum_{k=-B}^B N_k, \quad (H-6b)$$

and the normalized total correlation by

$$\rho(\tau) \triangleq \frac{\bar{f}(\tau)}{P}, \quad (H-6c)$$

then Equation (H-5c) can be rewritten as

$$\rho(\tau) = \sum_{j=1}^J a_j \frac{\partial}{\partial \tau} \rho_j(\tau - \tau_j) = 0 \quad (H-7a)$$

where

$$a_j = P_j/P \quad (H-7b)$$

and

$$\rho_j(\tau) = R_j(\tau)/P_j. \quad (H-7c)$$

In general, Equation (H-7a) must be solved numerically; however, for the case in which the interference is close to the true target of interest, then one can write

$$\rho_j(\tau - \tau_j) \approx \rho_j(0) + \rho'_j(0)(\tau - \tau_j) + \frac{\rho''_j(0)}{2} (\tau - \tau_j)^2 \quad (H-8a)$$

where $\rho'_j(0)$ and $\rho''_j(0)$ denote the first and second derivative.

But

$$\rho'_j(0) = \left(\sum_{k=-B}^B j\omega_k |h_k|^2 S_{kj} \right) / P_j = 0 \quad (H-8b)$$

and

$$\begin{aligned} \rho''_j(0) &= - \left(\sum_{k=-B}^B \omega_k^2 |h_k|^2 S_{kj} \right) / P_j \\ &= - \left(\frac{T}{\pi} \int_0^B \omega_k^2 |h_k|^2 S_j(\omega) d\omega \right) / P_j \\ &= -W_j / P_j \end{aligned} \quad (H-8c)$$

$$= - \frac{\tau(S_j/N)(S_1/N)}{\pi P_j(1 + 2 S_1/N)} \int_{\omega_1}^{\omega_2} \omega^2 d\omega \quad (H-8d)$$

where in the last equation the signals and noise are assumed flat and bandlimited.

Therefore, using Equation (H-8a) in Equation (H-7a) yields

$$\sum_{j=1}^J a_j \rho_j''(0)(\tau - \tau_j) = 0 .$$

Thus, the mean estimate of τ_1 is

$$\begin{aligned} \hat{\tau}_1 &= \left(\sum_{j=1}^J a_j \rho_j''(0) \tau_j \right) \left(\sum_{j=1}^J a_j \rho_j''(0) \right)^{-1} \\ &= \left(\sum_{j=1}^J w_j \tau_j \right) \left(\sum_{j=1}^J w_j \right)^{-1} \end{aligned} \quad (H-8e)$$

where

$$w_j = \frac{\tau}{\pi} \int_0^B \omega^2 |h(\omega)|^2 S_j(\omega) d\omega . \quad (H-8f)$$

Now using Equations (H-8e) and (H-7b) in Equation (H-8d) yields

$$\hat{\tau}_1 = \left[\sum_{j=1}^J (S_j/N) \tau_j \right] \left[\sum_{j=1}^J (S_j/N) \right]^{-1} \quad (H-9)$$

Thus, the time delay estimate from a second expansion of the correlation function is a weighted linear combination of time delays from every target. For the two-target case, let the signal of interest be $S_1 = S$, interference $S_2 = I$, then Equation (H-9) yields

$$\hat{\tau}_1 = \frac{S}{S+I} \tau_1 + \frac{I}{S+I} \tau_2 . \quad (\text{H-10})$$

The bias in general is

$$\begin{aligned} b_1 &= \hat{\tau}_1 - \tau_1 \\ &= \left[\sum_{j=1}^J (S_j/N)(\tau_j - \tau_1) \right] \left[\sum_{j=1}^J (S_j/N) \right]^{-1} \end{aligned} \quad (\text{H-11})$$

and for the two-target case

$$b_1 = \frac{1}{I+S/I} (\tau_2 - \tau_1) . \quad (\text{H-12})$$

We next derive the expression for the variance. Using the linearization procedure, it is easy to verify that the resulting variance of the time delay estimate from seeking the null of the function $f(\tau)$ is given by

$$\text{VAR}(\hat{\tau}_1) = \frac{\overline{f(\hat{\tau}_1)}^2}{\left(\frac{\partial \overline{f(\hat{\tau}_1)}}{\partial \tau} \right)^2} \quad (\text{H-13a})$$

where $\hat{\tau}_1$ is chosen such that

$$\overline{f(\hat{\tau}_1)} = \sum_{k=-B}^B j\omega_k |h_k|^2 \overline{a_{1k}^* a_{2k}^*} e^{j\omega_k \hat{\tau}_1} = 0 . \quad (\text{H-13b})$$

But from Equation (H-3a) and (H-5a-d), we have

$$\overline{\hat{f}(\tau_1)^2} = \sum_{k=-B}^B \sum_{\ell=-B}^B (j\omega_k)(j\omega_\ell) |h_k|^2 |h_\ell|^2 \frac{\overline{a_{1k} a_{2k}^* a_{1\ell} a_{2\ell}^*}}{e^{j(\omega_k + \omega_\ell)\hat{\tau}_1}} \quad (H-14a)$$

and

$$\overline{\frac{\partial \hat{f}(\tau_1)}{\partial \tau}} = \sum_{k=-B}^B (j\omega_k)^2 |h_k|^2 \overline{a_{1k} a_{2k}^*} e^{j\omega_k \hat{\tau}_1}. \quad (H-14b)$$

Now using the following relations

$$\overline{a_{1k} a_{2k}^*} = \underline{v}_{1k} \tilde{s}_k \underline{v}_{2k} = \sum_{j=1}^J s_{kj} e^{-j\omega_k \tau_j} \quad (H-15a)$$

$$\begin{aligned} \overline{a_{1k} a_{2k}^* a_{1\ell} a_{2\ell}^*} &= \overline{a_{1k} a_{2k}^*} \overline{a_{1\ell} a_{2\ell}^*} + \overline{a_{1k} a_{1\ell}} \overline{a_{2k}^* a_{2\ell}^*} \\ &\quad + \overline{a_{1k} a_{2\ell}^*} \overline{a_{2k}^* a_{1\ell}} \\ &= \overline{a_{1k} a_{2k}^*} \overline{a_{1\ell} a_{2\ell}^*} + (\underline{v}_{1k} \tilde{s}_k \underline{v}_{2k}^* + n_k)^2 \delta_{k+\ell} \\ &\quad + (\underline{v}_{1k} \tilde{s}_k \underline{v}_{2k}^*)^2 \delta_{k-\ell} \end{aligned} \quad (H-15b)$$

Equations (H-14a) and (H-14b) can be simplified to

$$\overline{f(\tau_1)^2} = \sum_{k=-B}^B \omega_k^2 |h_k|^4 \left\{ (\underline{v}_{1k} \tilde{s}_k \underline{v}_{1k}^* + N_k)^2 - (\underline{v}_{1k} \tilde{s}_k \underline{v}_{2k}^* e^{j\omega_k \hat{\tau}_1})^2 \right\} \quad (H-16a)$$

$$\frac{\partial \overline{f(\tau_1)}}{\partial \tau} = - \sum_{k=-B}^B \omega_k^2 |h_k|^2 \underline{v}_{1k} \tilde{s}_k \underline{v}_{2k}^* e^{j\omega_k \hat{\tau}_1}. \quad (H-16b)$$

Substituting Equations (H-16a) and (H-16b) in (H-13a) yields the desired expression for the variance of the $\hat{\tau}_1$ estimate:

$$\text{VAR}(\hat{\tau}_1) = \frac{\sum_{k=-B}^B \omega_k^2 |h_k|^4 \left\{ (\underline{v}_{1k} \tilde{s}_k \underline{v}_{1k}^* + N_k)^2 - (\underline{v}_{1k} \tilde{s}_k \underline{v}_{2k}^* e^{j\omega_k \hat{\tau}_1})^2 \right\}}{\left[\sum_{k=-B}^B \omega_k^2 |h_k|^2 (\underline{v}_{1k} \tilde{s}_k \underline{v}_{2k}^* e^{j\omega_k \hat{\tau}_1}) \right]^2} \quad (H-17a)$$

$$= \frac{2\pi}{T} \frac{\int_B \omega^2 |h|^4 \left[(\underline{v}_1 \tilde{s} \underline{v}_1^* + N)^2 - (\underline{v}_1 \tilde{s} \underline{v}_2^* e^{j\omega \hat{\tau}_1})^2 \right] d\omega}{\left(\int_B \omega^2 |h|^2 \underline{v}_1 \tilde{s} \underline{v}_2^* e^{j\omega \hat{\tau}_1} d\omega \right)^2} \quad (H-17b)$$

Recall that

$$\underline{v}_1 \tilde{s} \underline{v}_1^* + N = N + \sum_j s_j \quad (H-18a)$$

$$\underline{v}_1 \tilde{s} \underline{v}_2^* e^{j\omega \hat{\tau}_1} = \sum_j s_j e^{j\omega \Delta_j} \quad (\text{H-18b})$$

where $\Delta_j \stackrel{\Delta}{=} \hat{\tau}_1 - \tau_j$, then Equation (H-17b) can be rewritten as

$$\text{VAR}(\hat{\tau}_1) = \frac{2\pi}{T} \frac{\int \left(N + \sum_j s_j \right)^2 - \left(\sum_j s_j e^{j\omega \Delta_j} \right)^2 \omega^2 |h|^4 d\omega}{\left[\int \left(\sum_j s_j e^{j\omega \Delta_j} \right) \omega^2 |h|^2 d\omega \right]^2} \quad (\text{H-19})$$

For the special case where

$$s_j(\omega) = \begin{cases} s_j; & \omega_1 \leq \omega \leq \omega_2 \text{ and } -\omega_2 \leq \omega \leq -\omega_1 \\ 0; & \text{otherwise} \end{cases}$$

$$N(\omega) = \begin{cases} N; & \omega_1 \leq \omega \leq \omega_2 \text{ and } -\omega_2 \leq \omega \leq -\omega_1 \\ 0; & \text{otherwise} \end{cases}$$

Equation (H-19) reduces to

$$\text{VAR}(\hat{\tau}_1) = \frac{2\pi}{T} \frac{\left(N + \sum_j s_j \right)^2 R(0) - \sum_i \sum_j s_i s_j R(\Delta_i + \Delta_j)}{\left(\sum_j s_j R(\Delta_j) \right)^2}$$

$$= \frac{2\pi}{T} \left[\frac{1 - \sum_i \sum_j a_i a_j \rho(\Delta_i + \Delta_j)}{2 \left(\sum_j a_j \rho(\Delta_j) \right)^2} \right] R^{-1}(0) \quad (H-20a)$$

where

$$a_i = S_i \left(N + \sum_j S_j \right)^{-1} \quad (H-20b)$$

$$R(\tau) = \int_{\omega_1}^{\omega_2} \omega^2 \cos \omega \tau d\omega \quad (H-20c)$$

$$\rho(\tau) = R(\tau)/R(0) \quad (H-20d)$$

$$= \begin{cases} 1 ; \text{ if } \tau = 0 \\ \frac{1}{R(0)} \left[\frac{2\omega \cos \omega \tau + (\omega \tau)^2}{\tau^2} - \frac{2}{\tau^3} \sin \omega \tau \right] \Big|_{\omega_1}^{\omega_2} ; \text{ if } \tau \neq 0. \end{cases} \quad (H-20e)$$

For the two-target case, Equation (H-20) becomes

$$\text{VAR}(\hat{\tau}_1) = \frac{\pi}{T} \left\{ \frac{1 - [a_1^2 \rho(2\Delta_1) + a_2^2 \rho(2\Delta_2) + 2a_1 a_2 \rho(\Delta_1 + \Delta_2)]}{2[a_1 \rho(\Delta_1) + a_2 \rho(\Delta_2)]^2} \right\} R^{-1}(0). \quad (H-21a)$$

Note that

$$a_1 = \frac{S/N}{I + S/N + I/N} \quad (H-21b)$$

$$a_2 = \frac{I/N}{I + S/N + I/N} \quad (H-21c)$$

where we have let $S_1 = S$, $S_2 = I$ be the signal and the interference power spectrum, respectively. If the interference is far away from the target in time delay, Equation (H-21) becomes

$$\begin{aligned} \text{VAR}_{\infty}(\hat{\tau}_1) &= \lim_{\substack{\Delta_1 \rightarrow 0 \\ \Delta_2 \rightarrow \infty}} \text{VAR}(\hat{\tau}_1) \\ &= \frac{2\pi}{T} \left(\frac{1 - a_1^2}{2a_1^2} \right) R^{-1}(0). \end{aligned} \quad (H-22)$$

Therefore, the normalized variance is

$$\begin{aligned} \frac{\text{VAR}(\hat{\tau}_1)}{\text{VAR}_{\infty}(\hat{\tau}_1)} &= \left(\frac{a_1^2}{1 - a_1^2} \right) \\ &\quad \left[\frac{1 - (a_1^2 \rho(2\Delta_1) + a_2^2 \rho(2\Delta_2) + 2a_1 a_2 \rho(\Delta_1 + \Delta_2))}{2(a_1 \rho(\Delta_1) + a_2 \rho(\Delta_2))} \right]. \end{aligned} \quad (H-23)$$

Appendix I

CALCULATION OF MULTITARGET GENERALIZED CROSS-CORRELATION COVARIANCE

The calculation of the covariance matrix resulting from discrete observation of the Generalized Cross-Correlation (GCC) function in the presence of multitarget interference is presented. The results presented here are obtained from a frequency domain formulation.

Let the noisy observed waveforms from two sensors in the presence of J targets be represented by

$$y_1(t) = \sum_{i=1}^J s_i(t) + n_1(t) \quad (I-1)$$

$$y_2(t) = \sum_{i=1}^J s_i(t + D_i) + n_2(t) \quad (I-2)$$

where $s_i(t)$ is the ith target signal waveform and $n_1(t)$, $n_2(t)$ are the noise processes. It is assumed that signals and noises are zero mean, mutually uncorrelated, band-limited Gaussian processes.

Let the waveforms be sampled at a sampling rate of Δt seconds such that $T = N \Delta t$ seconds of the waveforms are observed. Discrete Fourier transforms of Equations (I-1) and (I-2) yield the equivalent frequency domain representation as

$$\alpha_{1k} = \sum_{i=1}^J \beta_{ki} + n_{1k} \quad (I-3)$$

$$\alpha_{2k} = \sum_{i=1}^J \beta_{ki} e^{j\omega_k D_i} + \eta_{2k} \quad (I-4)$$

where

$$\omega_k = 2\pi k/T$$

$$\alpha_{lk} = \frac{1}{N} \sum_{n=1}^N y_l(n\Delta t) e^{-j(2\pi nk/N)} ; \quad l = 1, 2 \quad (I-5)$$

$$\beta_{ki} = \frac{1}{N} \sum_{n=1}^N s_i(n\Delta t) e^{-j(2\pi nk/N)} ; \quad i = 1, 2, \dots, J \quad (I-6)$$

and

$$\eta_{lk} = \frac{1}{N} \sum_{n=1}^N \eta_l(n\Delta t) e^{-j(2\pi nk/N)} ; \quad l = 1, 2 . \quad (I-7)$$

The GCC is obtained from the following:

$$R(\tau) = \sum_{k=-B}^B \alpha_{lk} \alpha_{2k}^* |H_k|^2 e^{j\omega_k \tau} \quad (I-8)$$

where $|H_k|^2$ is the spectral shaping filter.

Equation (I-8) is usually implemented via inverse FFT. Consequently, discrete observations of the GCC $R(\tau)$, $R(n\Delta t)$, are obtained. For simplicity, let $R(n) = R(n\Delta t)$, then we can write

$$R(n) = \sum_{k=-B}^B \alpha_{1k} \alpha_{2k}^* |H_k|^2 e^{j(2\pi nk/N)} . \quad (I-9)$$

We are interested in the auto covariance of $R(n)$ and $R(m)$, Λ_{nm} , for any n and m . In general, one can write

$$\Lambda_{nm} = \overline{R(n) R(m)} - \overline{R(n)} \overline{R(m)} . \quad (I-10)$$

Now substituting Equation (I-9) into (I-10) and simplifying yields

$$\Lambda_{nm} = \sum_{k=-B}^B \sum_{l=-B}^B \left\{ \left(\overline{\alpha_{1k} \alpha_{2k}^* \alpha_{1l} \alpha_{2l}^*} - \overline{\alpha_{1k} \alpha_{2k}^*} \overline{\alpha_{1l} \alpha_{2l}^*} \right) \right. \\ \left. |H_k|^2 |H_l|^2 e^{j(2\pi/N)(kn+lm)} \right\} \quad (I-11)$$

Since α_{ik} for all i and k are zero mean complex Gaussian random variables uncorrelated for different frequency ω_k , one can write (using the fourth order product moment formula)

$$\overline{\alpha_{1k} \alpha_{2k}^* \alpha_{1l} \alpha_{2l}^*} = \overline{\alpha_{1k} \alpha_{2k}^*} \overline{\alpha_{1l} \alpha_{2l}^*} + \overline{\alpha_{1k} \alpha_{1l}} \overline{\alpha_{2k}^* \alpha_{2l}^*} + \\ \overline{\alpha_{1k} \alpha_{2l}^*} \overline{\alpha_{2k}^* \alpha_{1l}} . \quad (I-12)$$

Substituting Equation (I-12) into (I-11) yields

$$\Lambda_{nm} = \sum_{k=-B}^B \sum_{\ell=-B}^B \left\{ \left(\overline{\alpha_{1k} \alpha_{1\ell}} \overline{\alpha_{2k}^* \alpha_{2\ell}^*} + \overline{\alpha_{1k}^* \alpha_{2\ell}^*} \overline{\alpha_{2k}^* \alpha_{1\ell}} \right) |H_k|^2 |H_\ell|^2 e^{j(2\pi/N)(kn+\ell m)} \right\}. \quad (I-13)$$

Now using Equations (I-3) and (I-4), the quantities inside the parentheses in (I-13) can be evaluated as follows:

$$\overline{\alpha_{1k} \alpha_{1\ell}} \overline{\alpha_{2k}^* \alpha_{2\ell}^*} = \left(\sum_{i=1}^J S_{ki} + N_{1k} \right) \left(\sum_{i=1}^J S_{ki} + N_{2k} \right) \delta_{k+\ell} \quad (I-14)$$

$$\overline{\alpha_{1k}^* \alpha_{2\ell}^*} \overline{\alpha_{2k}^* \alpha_{1\ell}} = \left(\sum_{i=1}^J S_{ki} e^{-j\omega_k D_i} \right)^2 \delta_{k-\ell} \quad (I-15)$$

where $S_{ki} = \overline{\beta_{ki}^2}$, $N_{1k} = \overline{n_{1k}^2}$, and $N_{2k} = \overline{n_{2k}^2}$.

Finally, substituting Equations (I-14) and (I-15) into (I-13) yields

$$\begin{aligned} \Lambda_{nm} &= \sum_{k=-B}^B \left\{ \left(\sum_{i=1}^J S_{ki} + N_{1k} \right) \left(\sum_{i=1}^J S_{ki} + N_{2k} \right) \right\} |H_k|^4 e^{j(2\pi k/N)(n-m)} \\ &\quad + \sum_{k=-B}^B \left(\sum_{i=1}^J S_{ki} e^{-j\omega_k D_i} \right)^2 |H_k|^4 e^{j(2\pi k/N)(n+m)}. \end{aligned} \quad (I-16)$$

For a single target case with identical noise power spectral density, Equation (I-16) yields

$$\begin{aligned}
 \Lambda_{nm}^{(1)} &= \sum_{k=-B}^B \left\{ (S_k + N_k)^2 e^{j(2\pi k/N)(n-m)} \right. \\
 &\quad \left. + S_k^2 e^{-j2\omega_k D} e^{j(2\pi k/N)(n-m)} \right\} |H_k|^4 \\
 &= \sum_{k=-B}^B (S_k^2 + 2S_k N_k + N_k^2) |H_k|^4 e^{j(2\pi k/N)(n-m)} \\
 &\quad + \sum_{k=-B}^B |H_k|^4 S_k^2 e^{j(2\pi k/N)(n+m-2D/\Delta t)} \tag{I-17}
 \end{aligned}$$

$$\begin{aligned}
 &\approx \frac{T}{2\pi} \left\{ \int_{-B}^B (S^2 + 2SN + N^2) |H|^4 e^{j\omega(n-m)\Delta t} d\omega \right. \\
 &\quad \left. + \int_{-B}^B |H|^4 S^2 e^{j\omega((n+m)\Delta t - 2D)} d\omega \right\} \tag{I-18}
 \end{aligned}$$

where S , N , and H denote the continuous power spectra.

For the case of uniform spectral shaping, i.e., $|H|^2 = 1$, we obtain

$$\Lambda_{nm}^{(1)} = \rho_{SS}(n-m) + 2\rho_{SN}(n-m) + \rho_{NN}(n-m) + \rho_{SS}[(n+m) - 2D/\Delta t] \tag{I-19}$$

where if $\Phi_{XX}(\omega)$ is the power spectrum of X , then $\rho_{XX}(\tau)$ is given by

$$\rho_{XX}(\tau) = \frac{T}{2\pi} \int_{-B}^B \Phi_{XX}^2(\omega) e^{j\omega\tau} d\omega. \quad (I-20)$$

For a two-target case with equal noise power spectra, Equation (I-16) reduces to:

$$\begin{aligned} \Lambda_{nm}^{(2)} &= \sum_{k=-B}^B (s_{k1} + s_{k2} + n_k)^2 |H_k|^4 e^{j(2\pi k/N)(n-m)} \\ &\quad + \sum_{k=-B}^B (s_{k1} e^{-j\omega_k D_1} + s_{k2} e^{-j\omega_k D_2})^2 |H_k|^4 e^{j(2\pi k/N)(n+m)} \\ &\quad (I-21) \end{aligned}$$

$$\begin{aligned} &= \sum_{k=-B}^B |H_k|^4 \left\{ [s_{k1}^2 + s_{k2}^2 + n_k^2 + 2(s_{k1}s_{k2} + s_{k1}n_k + s_{k2}n_k)] \right. \\ &\quad e^{j(2\pi k/N)(n-m)} + \left[s_{k1}^2 e^{-j2\omega_k D_1} \right. \\ &\quad \left. + 2s_{k1}s_{k2} e^{-j\omega_k (D_1+D_2)} \right. \\ &\quad \left. + s_{k2}^2 e^{-j2\omega_k D_2} \right] e^{j(2\pi k/N)(n+m)} \left. \right\}. \quad (I-22) \end{aligned}$$

Hence the continuous approximation is given by

$$\Lambda_{nm}^{(2)} \approx \frac{T}{2\pi} \int_{-B}^B |H|^4 \left\{ [S_1^2 + S_2^2 + N^2 + 2(S_1 S_2 + S_1 N + S_2 N)] e^{j\omega(n-m)\Delta t} \right. \\ \left. + [S_1^2 e^{-j2\omega D_1} + 2S_1 S_2 e^{-j\omega(D_1+D_2)} + S_2^2 e^{-j2\omega D_2}] \right. \\ \left. e^{j\omega(n+m)\Delta t} \right\} d\omega . \quad (I-23)$$

Now for uniform spectral shading $|H|^2 = 1$ and using the definition of Equation (I-20) in (I-23) yields

$$\Lambda_{nm}^{(2)} = \rho_{S_1 S_1}(n - m) + \rho_{S_2 S_2}(n - m) + \rho_{NN}(n - m) \\ + 2[\rho_{S_1 S_2}(n - m) + \rho_{S_1 N}(n - m) + \rho_{S_2 N}(n - m)] \\ + \rho_{S_1 S_2} [(n + M) - 2D_1/\Delta t] + 2\rho_{S_1 S_2} [(n + M) - (D_1 + D_2)/\Delta t] \\ + \rho_{S_2 S_2} [(n + M) - 2D_2/\Delta t] . \quad (I-24)$$

APPENDIX J
FOURIER REPRESENTATION OF A TIME-COMPRESSED WAVEFORM

If a signal waveform, $s(t)$, emitted by a moving target is observed by a stationary (or moving) sensor array, the observed signal waveform is compressed if the target is closing or is expanded if the target is opening. Let the propagation delay from target to sensor vary linearly with time such that

$$D(t) = D + \dot{D}t \quad (J-1)$$

where D is the initial delay and \dot{D} is the delay rate. Note that $\dot{D} = \frac{V}{C}$ where V is the relative velocity along the line of sound (LOS) and C is the propagation speed of the medium. Because of the time-varying delay, the observed waveform at the sensor array output is $s(t + D(t))$. In this appendix, we develop an appropriate frequency domain representation of this waveform.

Let $s(t)$ be a zero mean, band-limited, Gaussian process, then $s(t)$ can be represented in terms of Fourier expansion by

$$s(t) = \sum_{k=-B}^{B} \alpha_k e^{j\omega_k t} \quad (J-2)$$

where

$$\alpha_k = \frac{1}{T} \int_0^T s(t) e^{-j\omega_k t} dt, \quad (J-3)$$

$\omega_k = (2\pi k)\frac{1}{T}$, T is the observation interval, and B is the bandwidth.

Now for the time-compressed waveform, let $\tilde{\alpha}_k$ be the corresponding Fourier coefficients. One can then write

$$\tilde{\alpha}_k = \frac{1}{T} \int_0^T s(t + D(t)) e^{-j\omega_k t} dt. \quad (J-4)$$

But from Equation (J-2), one obtains

$$\begin{aligned} s(t + D(t)) &= \sum_{\ell=-B}^B \alpha_\ell e^{j\omega_\ell(t+D(t))} \\ &= \sum_{\ell=-B}^B \alpha_\ell e^{j\omega_\ell(\beta t + D)} \end{aligned} \quad (J-5)$$

where Equation (J-1) has been used and that we have defined

$$\beta = 1 + \frac{V}{C}$$

as the time compression ratio.

Substituting Equation (J-5) into (J-4) and interchanging the summation and the integration operation yields

$$\tilde{\alpha}_k = \sum_{\ell=-B}^B \alpha_\ell e^{j\omega_\ell D} \left[\frac{1}{T} \int_0^T e^{j(\beta\omega_\ell - \omega_k)t} dt \right]. \quad (J-7)$$

It can be shown that

$$\begin{aligned}
 & \frac{1}{T} \int_0^T e^{j(\beta\omega_l - \omega_k)t} dt \\
 &= e^{j(\beta\omega_l - \omega_k)\frac{T}{2}} \left(\frac{\sin(\beta\omega_l - \omega_k)\frac{T}{2}}{(\beta\omega_l - \omega_k)\frac{T}{2}} \right) \\
 &= \begin{cases} \text{sinc}(\theta_k) e^{-j\theta_k}; & \text{if } l = k \\ 0; & \text{if } l \neq k \text{ and } \beta \approx 1 \end{cases} \quad (J-8)
 \end{aligned}$$

where

$$\theta_k = \frac{\omega_k VT}{2C} \quad (J-9)$$

and $\text{sinc}() = \frac{\sin()}{()}$.

Therefore, substituting Equation (J-8) into (J-7) yields

$$\begin{aligned}
 \tilde{\alpha}_k &= \left[\text{sinc}(\theta_k) e^{j\omega_k(D + \frac{VT}{2C})} \right] \alpha_k \\
 &= \left[\text{sinc}(\theta_k) e^{j\omega_k D(\frac{T}{2})} \right] \alpha_k. \quad (J-10)
 \end{aligned}$$

Thus Equation (J-10) shows that the effects of time compression on the Fourier coefficients are: (1) an effective time delay evaluated at the midpoint of the processing interval; and (2) an effective coherent reduction in signal amplitude which is a function of the net change in time delay over the same interval. Thus if coherence is to be maintained such that $1 \geq \text{sinc}(\theta_k) \geq 0.9$ for

all frequency ω_k , then the following condition must be satisfied; namely, T must be chosen such that

$$T \leq \frac{1}{4DB} \quad (J-11)$$

where D is the time delay rate and B is the signal bandwidth as defined earlier.

On the other hand, if Fourier coefficients are to be uncorrelated, it can be shown²⁹ that T must be chosen such that

$$T \geq \frac{8}{B} . \quad (J-12)$$

Combining Equations (J-11) and (J-12) yields the desired constraint

$$8 \leq BT \leq \frac{1}{4D} . \quad (J-13)$$

Thus when the observation interval T satisfies Equation (J-13), the time-compressed Fourier coefficients are given by Equation (J-10) and adjacent Fourier coefficients are uncorrelated.

APPENDIX K

VARIABLE TIME DELAY CRAMER-RAO LOWER BOUND FOR TWO-SENSOR, ONE-TARGET CASE

The time delay variation is assumed linear. Therefore, the parameter vector is $\underline{\theta} = (\tau, \dot{\tau})^T$. In general, the Cramer-Rao Lower Bound (CRLB) is given for the two-parameter case by

$$\text{VAR}(\theta_i) \geq \frac{1}{(1 - M_{12}^2)} \frac{1}{J_{ii}} ; \quad i = 1, 2 \quad (K-1)$$

where M_{12} is the coefficient of mutual dependence given by

$$M_{12} = \frac{J_{12}}{(J_{11} J_{12})^{1/2}} \quad (K-2)$$

and J_{ij} is given by (see Equation (6.4.1-2))

$$J_{ij} = \sum_{n=1}^N \sum_{k=1}^B \text{tr} \left(- \frac{\partial R_{kn}^{-1}}{\partial \theta_i} \frac{\partial R_{kn}}{\partial \theta_j} \right)_{\underline{\theta} = \underline{\theta}_0} . \quad (K-3)$$

For the two-sensor, one-target case, the covariance matrix R_{kn} is given by

$$R_{kn} = S_k P_{kn} + N_k Q_k \quad (K-4)$$

where $Q_k = I$ for the reason given in Section 6.4.2 and

$$P_{kn} = V_{kn} 1_M V_{kn}^* \quad (K-5)$$

with

$$v_{kn} = \begin{bmatrix} 1 & 0 \\ 0 & e^{j\omega_k(\tau+it_n)} \end{bmatrix} . \quad (K-6)$$

Now using Equation (6.3-6a), it can be shown that

$$\frac{\partial R_{kn}}{\partial \tau} = S_k \frac{\partial P_{kn}}{\partial \tau} = j\omega_k S_k v_{kn} \Phi_1 v_{kn}^* \quad (K-7)$$

$$\frac{\partial R_{kn}}{\partial t} = S_k \frac{\partial P_{kn}}{\partial t} = j\omega_k S_k t_n v_{kn} \Phi_1 v_{kn}^* \quad (K-8)$$

and from the relation (see Equation (3.5.1-4a))

$$\frac{\partial R_{kn}^{-1}}{\partial \theta_i} = -|h_k|^2 Q_k^{-1} \left(\frac{\partial P_{kn}}{\partial \theta_i} - a_{kn}^2 \frac{\partial G_{kn}}{\partial \theta_i} P_{kn} \right) Q_k^{-1} \quad (K-9)$$

where

$$|h_k|^2 = \frac{S_k/N_k^2}{1 + 2S_k/N_k} \quad (K-10a)$$

$$\frac{\partial G_{kn}}{\partial \theta_i} = \frac{\partial}{\partial \theta_i} (V_{kn}^* Q_k^{-1} V_{kn}) = 0 . \quad (K-10b)$$

One obtains the following derivatives:

$$\frac{\partial R_{kn}^{-1}}{\partial \tau} = -j\omega_k |h_k|^2 v_{kn} \phi_1 v_{kn}^* \quad (K-11)$$

$$\frac{\partial \dot{R}_{kn}^{-1}}{\partial \tau} = -j\omega_k t_n |h_k|^2 v_{kn} \phi_1 v_{kn}^* . \quad (K-12)$$

Hence, combining Equations (K-3), K-7), (K-8), (K-11), and (K-12), one obtains

$$\begin{aligned} J_{11} &= \sum_{n=1}^N \sum_{k=1}^B \text{tr} \left(-\frac{\partial R_{kn}^{-1}}{\partial \tau} \frac{\partial R_{kn}}{\partial \tau} \right) \\ &= -\sum_{n=1}^N \sum_{k=1}^B \omega_k^2 |h_k|^2 s_k \text{tr}(v_{kn} \phi_1^2 v_{kn}^*) \\ &= 2N \sum_{k=1}^B \omega_k^2 |h_k|^2 s_k \end{aligned} \quad (K-13)$$

since $\text{tr}(v_{kn} \phi_1^2 v_{kn}^*) = -2$.

Similarly, one obtains

$$\begin{aligned} J_{12} &= \sum_{n=1}^N \sum_{k=1}^B \text{tr} \left(-\frac{\partial R_{kn}^{-1}}{\partial \tau} \frac{\partial \dot{R}_{kn}^{-1}}{\partial \tau} \right) \\ &= -\sum_{n=1}^N \sum_{k=1}^B \omega_k^2 |h_k|^2 s_k t_n \text{tr}(v_{kn} \phi_1^2 v_{kn}^*) \end{aligned}$$

$$= \left(2 \sum_{n=1}^N t_n \right) \sum_{k=1}^B \omega_k^2 |h_k|^2 s_k . \quad (K-14)$$

where $t_n = (n - \frac{1}{2})\Delta t$ is as defined in Section 6.4.2.

The J_{22} term can also be obtained as

$$\begin{aligned} J_{22} &= \sum_{n=1}^N \sum_{k=1}^B \text{tr} \left(- \frac{\partial R_{kn}^{-1}}{\partial \tau} \frac{\partial R_{kn}}{\partial \tau} \right) \\ &= - \sum_{n=1}^N \sum_{k=1}^B \omega_k^2 |h_k|^2 s_k t_n^2 \text{tr}(v_{kn} \phi_1^2 v_{kn}^*) \\ &= \left(2 \sum_{n=1}^N t_n^2 \right) \sum_{k=1}^B \omega_k^2 |h_k|^2 s_k . \end{aligned} \quad (K-15)$$

Thus using Equations (K-13), (K-14), and (K-15), the Fisher Information matrix J is given by

$$\begin{aligned} J &= \begin{bmatrix} J_{11} & J_{12} \\ J_{12} & J_{22} \end{bmatrix} \\ &= \begin{bmatrix} N & \sum_{n=1}^N t_n \\ \sum_{n=1}^N t_n & \sum_{n=1}^N t_n^2 \end{bmatrix} \sum_{k=1}^B 2\omega_k^2 |h_k|^2 s_k . \end{aligned} \quad (K-16)$$

Thus the coefficient of mutual dependence is

$$\begin{aligned}
 M_{12}^2 &= \frac{J_{12}^2}{J_{11} J_{22}} \\
 &= \frac{\left(\sum_{n=1}^N t_n \right)^2}{N \sum_{n=1}^N t_n^2} \\
 &= \frac{(\Delta t N^2/2)^2}{\Delta t^2 N^2 (4N^2 - 1)/12} \\
 &= \frac{3N^2}{4N^2 - 1}. \tag{K-17}
 \end{aligned}$$

Therefore, the variance and covariance of the parameter vector is

$$\begin{aligned}
 \text{VAR}(\hat{\tau}) &= \frac{1}{1 - M_{12}^2} \frac{1}{J_{11}} \\
 &= \left(\frac{4N^2 - 1}{N^2 - 1} \right) \left(2N \sum_{k=1}^B \omega_k^2 \frac{s_k^2/N_k^2}{1 + 2s_k/N_k} \right)^{-1} \tag{K-18a}
 \end{aligned}$$

$$\dot{=} \frac{2\pi(4N^2 - 1)}{N^2 - 1} \left(2T \int_0^\infty \omega^2 \frac{S^2(\omega)/N^2(\omega)}{1 + 2S(\omega)/N(\omega)} d\omega \right)^{-1} \quad (K-18b)$$

where $\dot{=}$ denotes the continuous frequency approximation and $T = N\Delta t$.

Similarly, we obtain

$$VAR(\tau) = \frac{1}{1 - M_{12}^2} \frac{1}{J_{22}}$$

$$= \left(\frac{4N^2 - 1}{N^2 - 1} \right) \frac{\left(2 \sum_{k=1}^B \omega_k^2 \frac{S_k^2/N_k^2}{1 + 2S_k/N_k} \right)^{-1}}{\sum_{n=1}^N t_n^2}$$

$$= \left(\frac{4N^2 - 1}{N^2 - 1} \right) \left[\frac{12}{(4N^2 - 1)N \Delta t^2} \right] \left(2 \sum_{k=1}^B \omega_k^2 \frac{S_k^2/N_k^2}{1 + 2S_k/N_k} \right)^{-1}$$

$$= \left[\frac{12}{(N^2 - 1)N \Delta t^2} \right] \left(2 \sum_{k=1}^B \omega_k^2 \frac{S_k^2/N_k^2}{1 + 2S_k/N_k} \right)^{-1} \quad (K-19a)$$

$$\dot{=} \left[\frac{12(2\pi)N^2}{N^2 - 1} \right] \left[2T^3 \int_0^\infty \omega^2 \frac{S^2(\omega)/N^2(\omega)}{1 + 2S(\omega)/N(\omega)} d\omega \right]^{-1} \quad (K-19b)$$

and finally, the covariance is

$$\begin{aligned}
 \text{COV}(\tau, \dot{\tau}) &= -\frac{J_{12}}{J_{11} J_{22} - J_{12}^2} \\
 &= -\left(\frac{M_{12}^2}{1 - M_{12}^2}\right) \frac{1}{J_{12}} \\
 &= -\left(\frac{3N^2}{N^2 - 1}\right) \frac{\left(2 \sum_{k=1}^B \omega_k^2 \frac{S_k^2/N_k^2}{1 + 2S_k/N_k}\right)^{-1}}{\sum_{n=1}^N t_n} \\
 &= -\left(\frac{3N^2}{N^2 - 1}\right) \left(\frac{2}{N^2 \Delta t}\right) \left(2 \sum_{k=1}^B \omega_k^2 \frac{S_k^2/N_k^2}{1 + 2S_k/N_k}\right)^{-1} \\
 &= -\left[\frac{6}{(N^2 - 1)\Delta t}\right] \left(2 \sum_{k=1}^B \omega_k^2 \frac{S_k^2/N_k^2}{1 + 2S_k/N_k}\right)^{-1} \quad (\text{K-20a})
 \end{aligned}$$

$$= -\left[\frac{6(2\pi)N^2}{N^2 - 1}\right] \left[2T^2 \int_0^\infty \omega^2 \frac{S^2(\omega)/N^2(\omega)}{1 + 2S(\omega)/N(\omega)}\right]^{-1} \quad (\text{K-20b})$$

Note that Equations (K-18), (K-19), and (K-20) indicate that for $N = 1$, the variances and covariance are unbounded. Thus for a meaningful joint estimation of τ and $\dot{\tau}$, the number of observation intervals must be equal or greater than two.

REFERENCES

1. C. H. Knapp and G. C. Carter, "The Generalized Correlation Method for Estimation of Time Delay," IEEE Transactions on ASSP, Vol ASSP-24, August 1976, pp 320-327.
2. G. C. Carter, "IEEE Special Issue on 'Time Delay Estimation,'" IEEE Transactions on ASSP, Vol ASSP-29(3), June 1981.
3. W. R. Hahn and S. A. Tretter, "Optimum Processing for Delay-Vector Estimation in Passive Signal Arrays," IEEE Transactions on Information Theory, Vol IT-19(5), September 1973, pp 608-614.
4. J. C. Hassab and R. E. Boucher, "Optimum Estimation of Time-Delay by a Generalized Correlator," IEEE Transactions on ASSP, Vol ASSP-27 (4), August 1979, pp 373-380.
5. F. Scheweppe, "Sensor Array Data Processing for Multiple Signal Source," IEEE Transactions on Information Theory, Vol IT-14(2), March 1968, pp 294-305.
6. P. M. Schultheiss, "Passive Sonar Detection in the Presence of Interference," JASA Vol 43(3), 1968, pp 418-425.
7. V. C. Anderson and P. Rudnick, "Rejection of a Coherent Signal Arrival at an Array," JASA (Vol 45(2), 1969, pp 406-410.
8. J. Capon, "High Resolution Frequency Wavenumber Spectrum Analysis," Proceedings of the IEEE, Vol 57(8), August 1969, pp 1408-1418.
9. B. D. Steinberg, "A Proposed Approach for Increasing the Azimuthal Resolution of HF Radar," IEEE Transactions on Antenna and Propagation, Vol AP-20(5), September 1972, pp 613-618.
10. H. Cox, "Resolving Power and Sensitivity to Mismatch of Optimum Array Processor," JASA (Vol 54(3), 1973, pp 771-785.
11. T. P. McGarty, "The Effect of Interfering Signals on the Performance of Angle of Arrival Estimates," IEEE Transactions on Aerospace and Electronic Systems, Vol AES-10(1), January 1974, pp 70-77.
12. A. J. Rockmore and N. J. Bershad, "Nearfield Discrimination Capabilities of a Linear Array," JASA (Vol 58(3), September 1975, pp 684-692.

13. N. Owsley and G. Swope, "Time Delay Estimation in a Sensor Array," IEEE Transactions on ASSP, Vol ASSP-29(3), June 1981.
14. C. Knapp and G. C. Carter, "Estimation of Time Delay in the Presence of Source or Receiver Motion," JASA (Vol 61, No. 6, June 1977, pp 1545-1549).
15. P. M. Schultheiss and E. Weinstein, "Estimation of Differential Doppler Shifts," JASA (Vol 66, No. 5, November 1979, pp 1412-1419).
16. Y. T. Chan, Riley, J. M., and Plant, J. B., "Modeling of Time Delay and Its Application to Estimation of Nonstationary Delays," IEEE Transactions on Acoustic, Speech and Signal Processing, Vol ASSP-29, No. 3, June 1981.
17. B. Friedlander, "An ARMA Modeling Approach to Multitarget Tracking," Proceedings of the 19th IEEE Conference on Decision and Control, December 1980.
18. Y. Bar-Shalom, "Tracking Methods in a Multitarget Environment," IEEE Transactions on Automatic Control, Vol AC-23, August 1978, pp 618-626.
19. Y. Bar-Shalom, and E. Tse, "Tracking in a Cluttered Environment with Probabilistic Data Association," Automatica, Vol 11, September 1975, pp 451-460.
20. T. E. Fortmann, Bar-Shalom, Y. and Scheffe, M., "Multitarget Tracking Using Joint Probabilistic Data Association," Proceedings of the 1980 IEEE Conference on Decision and Control, Albuquerque, New Mexico, December 1980.
21. L. C. Ng and Y. Bar-Shalom, "Modeling of Unresolved Measurements for Multitarget Tracking," Proceedings of the 1981 IEEE Ocean Conference, Boston, Massachusetts, September 1981.
22. L. C. Ng and Y. Bar-Shalom, "Modeling of Unresolved Detections for Tracking of Neighboring Targets," University of Connecticut Technical Report EECS-System-80-8, September 1980.
23. G. C. Carter and P. B. Abraham, "Estimation of Source Motion from Time Delay and Time Compression Measurement," JASA (Vol 67(3), March 1980, pp 830-832).
24. J. M. Moura and A. B. Baggeroer, "Passive System Theory with Narrow Band and Linear Constraints: Part 1," IEEE Journal of Oceanic Engineering, Vol OE-3(1), January 1978, pp 5-13.
25. W. R. Hahn, "Optimum Signal Processing for Passive Range and Bearing Estimation," JASA (Vol 58(1), July 1975, pp 201-207).

26. A. M. Yaglom, "Theory of Stationary Random Functions," Prentice-Hall, 1962.
27. V. H. MacDonald and P. M. Schultheiss, "Optimum Passive Bearing Estimation in a Spatially Incoherent Noise Environment," JASA (Vol 46(1), 1969, pp 37-43.
28. A. J. Rockmore, "Space-Time Signal Processing," Dept of E.E., U.S. Naval Postgraduate School, June 1979.
29. W. S. Hodgkiss and L. W. Nolte, "Covariance Between Fourier Coefficient Representing the Time Waveforms Observed From An Array of Sensors," JASA (Vol 59(3), March 1976, pp 582-590.
30. J. Capon, "Application of Detection and Estimation Theory to Large Array Seismology," Proceedings of the IEEE, Vol 58(5), May 1970, pp 760-770.
31. A. E. Bryson and Y. C. Ho, "Applied Optimal Control," Blaisdell, 1969.
32. H. Van Trees, "Detection, Estimation and Modulation Theory," Part I, Wiley, 1968.
33. W. J. Bangs, "Array Processing with Generalized Beamformers," Ph.D Thesis, Yale University, September 1971.
34. W. J. Bangs and P. M. Schultheiss, "Space-Time Processing for Optimal Parameter Estimation," Proceedings of NATO Advanced Study Institute on Signal Processing, University of Technology, Loughborough, U. K., August - September 1972.
35. G. C. Carter, "Time Delay Estimation," NUSC TR 5335, Naval Underwater Systems Center, 9 April 1976.
36. T. P. McGarty, "Azimuth Elevation Estimation Performance of a Spatially Dispersive Channel," IEEE Transactions on Aerospace and Electronic Systems, Vol AES-10(1), January 1974, pp 58-69.
37. W. K. Fischer, and L. C. Ng, "Improved Multitarget Time Delay Estimation: Matched Filter Approach," NUSC Technical Report (in preparation).
38. W. K. Fischer, and L. C. Ng, "Improved Time Delay Estimation in the Presence of Interference," Proceedings of the IEEE, 1983 ICASSP, April 1983.
39. A. P. Sage and J. L. Melsa, "Estimation Theory with Applications to Communications and Control," McGraw-Hill, 1971.

40. A. S. Willsky, "Relationships Between Digital Signal Processing and Control and Estimation Theory," Proceedings of the IEEE, Vol. 66 (9), September 1978.
41. A. Gelb, "Applied Optimal Estimation," The MIT Press, 1974.
42. T. P. McGarty, "Stochastic Systems and State Estimation," John Wiley and Sons, 1974.
43. N. R. Goodman, "Statistical Analysis Based on a Certain Multivariate Complex Gaussian Distribution (An Introduction)," Ann. Math. Stat. 34, 1963, pp 152-157.

INITIAL DISTRIBUTION LIST

Addressee	No. of Copies
ASN (RE&S)	1
OUSDR&E (Research & Advanced Technology)	2
Deputy USDR&E (Research & Advanced Technology)	1
OASN DAS (Research & Advanced Technology)	1
ONR, ONR-100, -200, -203, -411 (James Smith, S. Wegman), -425	6
CNO, OP-098, -96	2
CNM, MAT-05, SP-20	2
DIA, DT-2C	1
NAVAL SURFACE WEAPONS CENTER, WHITE OAK LABORATORY	1
NRL	1
NRL, USRD	1
NAVELECSYSCOM, ELEX 03	1
NAVSEASYSCOM, SEA-63Z41, -63D (R. Cockerill), PMS-409 (Dr. R. Snuggs, CAPT Sparks, CAPT Bolka)	5
NOSC, Code 6565 (Library)	2
DTNSRDC, Carderock	1
NUWES, San Diego	1
NUWES, Hawaii	1
NISC	1
NAVPGSCOL	1
NAVMARCOL	1
NETC	1
CENTER FOR NAVAL ANALYSES (ACQUISITION UNIT)	1
DTIC	12
DARPA	1
NOAA/ERL	1
NATIONAL RESEARCH COUNCIL	1
WEAPON SYSTEM EVALUATION GROUP	1
WOODS HOLE OCEANOGRAPHIC INSTITUTION	1
ARL, UNIV OF TEXAS	1
MARINE PHYSICAL LAB, SCRIPPS	1
Herbert Gish, Bolt Beranek and Newman, 50 Moulton St., Cambridge, MA 02138	1
Prof. Louis Scharf, Dept. of Electrical Engineering, Colorado State Univ., Fort Collins, CO 80523	1
Prof. Donald Tufts, Dept. of Electrical Engineering, Univ. of Rhode Island, Kingston, RI 02881	1
C. Hindman, TRW, Defense & Space Systems Group, One Space Park, Redondo Beach, CA 90278	1
Prof. P. M. Schultheiss, Dept. of Electrical Engineering, P.O. Box 2157, Yale University, 15 Prospect St., New Haven, CT 06520	1
Prof. Y. T. Chan, Dept. of Electrical Engineering, Royal Military College, Kingston, Ontario, Canada K7L 2W3	1
Frank W. Symons, Applied Research Laboratory, Penn State University, P.O. Box 30, State College, PA 16801	1
Donald G. Childers, Dept. of Electrical Engineering, University of Florida, Gainesville, FL 32611	1
Prof. Y. Bar-Shalom, E.E. Dept., University of Connecticut, Storrs, CT 06268	1

INITIAL DISTRIBUTION LIST (Cont'd)

Addressee	No. of Copies
Dr. Carl Wenk, Analysis & Technology, Inc., North Stonington, CT 06359	1
Dr. C. Y. Chong, AI & DS, 201 San Antonio Circle, Suite 286, Mountain View, CA 94040	1
Prof. A. A. Willsky, LIDS, MIT, Cambridge, MA 02211	1
Drs. B. Friedlander and A. Rockmore, Systems Control Technology, Palo Alto, CA 94304	2
Prof. Thomas Kailath, Dept. of Electrical Engineering, Stanford University, Stanford, CA 94305	1

END

FILMED